

**INVESTIGATIONS OF KINETIC ASPECTS IN
NITROXIDE-MEDIATED RADICAL POLYMERIZATION OF
STYRENE**

By

Afsaneh Nabifar

A thesis
presented to the University of Waterloo
in fulfillment of the
thesis requirement of the degree of
Master of Applied Science
in
Chemical Engineering

Waterloo, Ontario, Canada, 2007

© Afsaneh Nabifar, 2007

I hereby declare that I am the sole author of this thesis. This is a true copy of the thesis, including any required final revisions, as accepted by my examiners. I understand that my thesis may be made electronically available to the public.

Afsaneh Nabifar

Abstract

An experimental and modeling investigation of nitroxide-mediated radical polymerization (NMRP) of styrene using 2,2,6,6-tetramethyl-1-piperidinyloxy (TEMPO) as controller is presented. The objective was to examine the effect of temperature, controller to initiator molar ratio, and initiation mode on conversion, molecular weight and polydispersity development, and also to generate a source of reliable experimental data for parameter estimation and further model validation purposes.

Polymerizations with a bimolecular initiator (Benzoyl Peroxide; BPO) were carried out at 120 and 130°C, with TEMPO/BPO molar ratios of 0.9 to 1.5. The effects of temperature and TEMPO/BPO ratio on polydispersity, molecular weight averages and conversion (rate) were studied. Results indicate that increasing temperature increases the rate of polymerization while the decrease in molecular weights is only slight. It was also observed that increasing the ratio of TEMPO/BPO decreased both the rate of polymerization and molecular weights.

To investigate the contribution of thermal self-initiation in NMRP of styrene, thermal NMRP of styrene with TEMPO in the absence of initiator was carried out at 120 and 130°C. The results were compared with regular thermal polymerization of styrene and NMRP of styrene in the presence of BPO. It was observed that although the thermal polymerization of styrene can be controlled to some extent in the presence of TEMPO to provide lower polydispersity polystyrene, the polymerization was never as controlled as that obtained by a BPO initiated NMRP. Additional experiments were conducted with a unimolecular initiator and compared to the corresponding bimolecular system with the same level of nitroxide at 120°C, to gain additional insight on the advantages and disadvantages of each system.

In addition, the importance of diffusion-controlled (DC) effects on the bimolecular NMRP of styrene was assessed experimentally by creating conditions where DC effects may be present from the outset. The results were corroborated by mathematical modeling and it was concluded that DC-effects are weak in the NMRP of styrene, even in the presence of “worst case scenario” conditions created.

Finally, a mathematical (mechanistic) model based on a detailed reaction mechanism for bimolecular NMRP of styrene was presented and the predicted profiles of monomer conversion, molecular weight averages and polydispersity were compared with experimental data. Comparisons suggest that the present understanding of the reaction system is still inconclusive, either because of inaccuracy in values of kinetic rate constants used or because of some possible side reactions taking place in the polymerization system that are not included in the model. This was somewhat surprising, given that papers on controlled radical polymerization, and NMRP in particular, have clearly dominated the scientific polymer literature in the last fifteen years or so.

Acknowledgements

Keep “Ithaka” always in mind

Arriving there is what you’re destined for

But don’t hurry the journey at all

Better if it lasts for years,

So you’re old by the time you reach the island,

Wealthy with all you’ve gained on the way...

From “Ithaka” by Constantine P. Cavafy

I entered the University of Waterloo to get a degree, but what I gained is not only a degree but experience, knowledge, friendship and hopefully wisdom. A lot of people helped me and supported me to reach my goal; I would like to acknowledge their contributions and offer my gratitude.

First, a special thanks to my supervisor, Professor Alexander Penlidis, for his invaluable guidance and support in both my academic and personal life. I believe I have been extremely lucky to have him as my mentor. I consider him not only as a supervisor but also as a father figure who guided me and helped me to adapt myself to the new environment and the culture of Canada. Many thanks also goes to Professor Neil McManus for his help and support and also for sharing his vast laboratory experience with me. I have learned a lot from our many discussions. I would also like to express my appreciation to Professor Eduardo Vivaldo-Lima of UNAM, Mexico, for his generosity of patience in answering my many questions.

My sincere gratitude goes out to my old lab mates, Dr. Matthew Scolah and Ramin Khesareh for their patience with me and for training me in the lab; and Joy Cheng for her constant encouragement. Many thanks to my friends, Nafiseh Dadgostar, Paula Kruger, Alejandro Salinger, Milen Pavlov, Julia Kraus and in particular Dr. Jeremy Barbay, who supported me along the way with good humor and love.

I am extremely grateful for the support of my family. I would like to thank my brothers for their financial and moral support. Special thanks to my dear sister, Azadeh Nabifar, and her

husband, Hossien Shahkarami, without whose generosity and determination I wouldn't be able to come to Canada. Finally, and most importantly, I would like to thank the dearest person in my life, my mom, for dedicating her life to us and being both a mother and a father to our family.

TABLE OF CONTENTS

Abstract.....	iii
Acknowledgements.....	v
List of Figures.....	ix
List of Tables.....	xiv
CHAPTER 1 – INTRODUCTION.....	1
CHAPTER 2 – LITERATURE BACKGROUND.....	4
2.1 Controlled Radical Polymerization (CRP).....	4
2.1.1 Basic Requirements.....	5
2.1.2 Typical Features.....	7
2.1.3 Comparison with Regular Free Radical Polymerization (FRP).....	10
2.1.4 Approaches towards Controlled Radical Polymerization.....	15
2.1.5 Overview of Materials Made by CRP Methods.....	18
2.1.6 Material Applications.....	19
2.2 Nitroxide-Mediated Radical Polymerization (NMRP).....	20
2.2.1 Background and Historical Perspective.....	20
2.2.2 Types of Initiators in Nitroxide-Mediated Radical Polymerization.....	24
2.2.2.1 Bimolecular Initiator.....	24
2.2.2.2 Unimolecular Initiator.....	24
2.2.3 Kinetics Features.....	25
2.2.3.1 Persistent Radical Effect (PRE).....	26
2.2.3.2 Descriptive Equations.....	27
2.2.4 Applications and Future Perspective.....	30
2.2.4.1 Development of New Nitroxides.....	30
2.2.4.2 Manufacturing Issues.....	32
2.3 References.....	34
CHAPTER 3 – EXPERIMENTAL METHODS.....	41
3.1 Reagent Purification.....	41
3.2 Polymer Synthesis.....	41
3.3 Polymer Characterization.....	41
3.3.1 Gravimetry.....	41
3.3.2 Size Exclusion Chromatography.....	42
3.4 References.....	43
CHAPTER 4 – RESULTS AND DISCUSSION.....	44
4.1 Design and Summary of Experiments.....	44
4.2 Typical Styrene Reaction Profiles in NMRP.....	46
4.3 Bimolecular NMRP.....	49
4.3.1 Effect of [TEMPO]/[BPO] Ratio.....	51
4.3.2 Effect of Temperature.....	69

4.4 Contribution of Thermal Self-Initiation of Styrene	76
4.4.1 Polymerization of Styrene	77
4.4.2 Polymerization of Styrene with TEMPO	80
4.5 Unimolecular NMRP	93
4.5.1 Comparison with Bimolecular Mode.....	95
4.5.2 Comparison with Thermal Self-initiation of Styrene	99
4.6 Other Aspects.....	100
4.6.1 Side Reactions.....	100
4.6.2 Significance of Gel Effect.....	102
4.7 References.....	106
 CHAPTER 5 – MATHEMATICAL MODELING	 110
5.1 Reaction Scheme and General Considerations	111
5.2 Overall Mass (Molar) Balances and Moment Equations.....	114
5.3 Comparison of Simulated Profiles and Experimental Data	117
5.4 References.....	127
 CHAPTER 6 – CONCLUSIONS AND RECOMMENDATIONS.....	 129
6.1 Concluding Remarks	129
6.2 Recommendations for Future Work	133
6.3 References.....	135
 APPENDIX A – TABLES OF RAW DATA	 137
 APPENDIX B – COMPLEMENTARY FIGURES	 150

LIST OF FIGURES

Figure 2.1 Areas contributing to development of CRP	5
Figure 2.2 A general CRP equilibrium between dormant and active species.....	6
Figure 2.3 First order kinetic plot for controlled radical polymerization	8
Figure 2.4 Molecular weight outcomes from an ideal controlled radical polymerization (LRP)	8
Figure 2.5 Size exclusion chromatographs of polystyrene samples. Curve A: polystyrene made by regular radical polymerization (PDI = 2), Curve B: a SEC 'standard' polystyrene made by anionic polymerization (PDI = 1.1), Curve C: polystyrene made by NMRP (PDI = 1.1)	9
Figure 2.6 General polymer chain structure from controlled radical polymerizations ^[4]	10
Figure 2.7 General structures for chain transfer agents used in RAFT polymerizations. Y = activating/stabilizing group of thiocarbonyl, R = radical leaving group	18
Figure 2.8 Examples of the variety of polymer structures made by CRP techniques ^[4]	18
Figure 2.9 Reversible activation, deactivation reaction in NMRP	20
Figure 2.10 Georges' approach to NMRP using bimolecular initiation.....	22
Figure 2.11 Unimolecular initiation approach in NMRP	25
Figure 2.12 Concentration of active radicals (R), stable radicals (X), dormant species (R-X), polymer chains (P) and monomer (M) vs. time for a controlled radical polymerization initiated by homolysis of an initiator (R-X) ^[44]	27
Figure 2.13 Structure of TEMPO-based nitroxides in NMRP.....	31
Figure 2.14 Structures of DTBN and DEPN	31
Figure 2.15 Structure of piperidinyl-N-oxyl radical (1) and corresponding alkoxyamines (2, 3)	32
Figure 4.1 Monomer conversion vs. time for NMRP of styrene at 120°C and R = [TEMPO]/[BPO] = 1.1 (Run #2)	47
Figure 4.2 First order rate plot for NMRP of styrene at 120°C and R= [TEMPO]/[BPO] = 1.1	47
Figure 4.3 Average molecular weights and polydispersity vs. conversion for NMRP of styrene at 120°C and R= [TEMPO]/[BPO] = 1.1.....	48
Figure 4.4 Bimolecular NMRP of styrene in the presence of TEMPO and BPO.....	50
Figure 4.6 Simulated concentrations of: living radicals (a), dead polymer (b), and dormant radicals (c) vs. conversion for [TEMPO]/[BPO] = 0.9 and 1.1 at T = 120°C	52
Figure 4.7 Effect of [TEMPO]/[BPO] ratio (R), on weight average molecular weights in NMRP of styrene at 120°C	54
Figure 4.8 Effect of [TEMPO]/[BPO] ratio on number average molecular weights in NMRP of styrene at 120°C.....	54
Figure 4.9 Effect of [TEMPO]/[BPO] ratio on polydispersity in NMRP of styrene at 120°C..	55
Figure 4.10 Effect of [TEMPO]/[BPO] ratio (R), on rate of polymerization in NMRP of styrene at 120°C	56

Figure 4.11 Simulated concentrations of: free TEMPO (a), living radicals (b), and dormant radicals (c) vs. conversion for $[\text{TEMPO}]/[\text{BPO}] = 1.1$ and 1.5 at $T = 120^\circ\text{C}$	57
Figure 4.12 Effect of $[\text{TEMPO}]/[\text{BPO}]$ ratio on number average molecular weights in NMRP of styrene at 120°C	58
Figure 4.13 Effect of $[\text{TEMPO}]/[\text{BPO}]$ ratio on weight average molecular weights in NMRP of styrene at 120°C	59
Figure 4.14 Effect of $[\text{TEMPO}]/[\text{BPO}]$ ratio on polydispersity in NMRP of styrene at 120°C	59
Figure 4.15 Effect of $[\text{TEMPO}]/[\text{BPO}]$ ratio on polymerization rate at 120°C	60
Figure 4.16 Effect of $[\text{TEMPO}]/[\text{BPO}]$ ratio on number average molecular weight at 120°C	61
Figure 4.17 Effect of $[\text{TEMPO}]/[\text{BPO}]$ ratio on weight average molecular weight at 120°C	61
Figure 4.18 Effect of $[\text{TEMPO}]/[\text{BPO}]$ ratio on polydispersity, PDI, at 120°C	62
Figure 4.19 Effect of $[\text{TEMPO}]/[\text{BPO}]$ ratio on polymerization rate at 130°C	63
Figure 4.20 Effect of $[\text{TEMPO}]/[\text{BPO}]$ ratio on number average molecular weight at 130°C	64
Figure 4.21 Effect of $[\text{TEMPO}]/[\text{BPO}]$ ratio on weight average molecular weight at 130°C	64
Figure 4.22 Effect of $[\text{TEMPO}]/[\text{BPO}]$ ratio on polydispersity, PDI, at 130°C	65
Figure 4.23 Semilog plot of conversion with polymerization time (a), Polydispersity plotted as a function of conversion (b), Polymer molecular weights (M_n and M_w) versus conversion (c, d) for bulk polymerization of styrene with $[\text{TEMPO}]/[\text{BPO}] = 1.1$ and 1.3 , $T = 125^\circ\text{C}$ ^[6, 8]	66
Figure 4.24 Polydispersity as a function of the $[\text{TEMPO}]/[\text{BPO}]$ ratio for NMRP of styrene: a) after 5 hrs at 135°C ^[2] , b) at 50% conversion at 120°C , c) at 50% conversion at 130°C	67
Figure 4.25 Effect of temperature on rate of polymerization at a) $[\text{TEMPO}]/[\text{BPO}] = 0.9$ b) $[\text{TEMPO}]/[\text{BPO}] = 1.1$	69
Figure 4.26 Effect of temperature on rate of polymerization at $[\text{TEMPO}]/[\text{BPO}] = 1.1$ ^[8]	70
Figure 4.27 Effect of temperature on a) number average molecular weight and b) weight average molecular weight at $[\text{TEMPO}]/[\text{BPO}] = 0.9$	70
Figure 4.28 Effect of temperature on a) number average molecular weight and b) weight average molecular weight at $[\text{TEMPO}]/[\text{BPO}] = 1.1$	71
Figure 4.29 Effect of temperature on RLPAC at $[\text{TEMPO}]/[\text{BPO}] = 0.9$	72
Figure 4.30 Effect of temperature on RLPAC at $[\text{TEMPO}]/[\text{BPO}] = 1.1$	72
Figure 4.31 Effect of temperature on polydispersity at a) $[\text{TEMPO}]/[\text{BPO}] = 0.9$ and b) $[\text{TEMPO}]/[\text{BPO}] = 1.1$	73
Figure 4.32 Effect of temperature on polydispersity at $[\text{TEMPO}]/[\text{BPO}] = 1.1$ ^[6]	74
Figure 4.33 Thermal self-initiation of styrene.....	77
Figure 4.34 Monomer conversion vs. time for thermal self-initiation of styrene at $T = 120$ and 130°C	78
Figure 4.35 Average molecular weights and polydispersity vs. conversion for thermal self-initiation of styrene at a) $T = 130^\circ\text{C}$, b) $T = 120^\circ\text{C}$	79
Figure 4.36 Main kinetic scheme for thermal polymerization of styrene with TEMPO ^[30]	83
Figure 4.37 Monomer conversion vs. time for: a) thermal polymerization of styrene in the presence of TEMPO with $[\text{TEMPO}]_0 = 0.0396\text{ M}$ b) thermal styrene, at 130°C	84

Figure 4.38 Average molecular weights and polydispersity vs. conversion for thermal polymerization of styrene in the presence of TEMPO at 130°C and $[\text{TEMPO}]_0 = 0.0396 \text{ M}$..	86
Figure 4.39 Comparison of SEC Chromatograms for a) Styrene thermal polymerization b) Styrene thermal polymerization in the presence of TEMPO, at 50% conversion and 130°C ...	87
Figure 4.40 Degenerative transfer process for bulk polymerization of styrene in presence of TEMPO ^[27]	88
Figure 4.41 Comparison between thermal NMRP and NMRP with $[\text{TEMPO}]/[\text{BPO}] = 1.1$ at 130°C and $[\text{TEMPO}]_0 = 0.0396 \text{ M}$	89
Figure 4.42 Comparison of SEC Chromatograms for a) thermal NMRP b) NMRP with BPO, at 50% conversion and 130°C	90
Figure 4.43 Effect of temperature on nitroxide-mediated thermal polymerization of styrene, $[\text{TEMPO}]_0 = 0.0396 \text{ M}$	91
Figure 4.44 SEC Chromatographs for the polymerization of styrene at 120 °C in the presence of PS-TEMPO adduct: a) the precursor adduct; b) the product after 3hrs c) 8hrs d) 60hrs	94
Figure 4.45 Comparison of conversion vs. time plots for the polymerization of styrene at 120 °C using the unimolecular initiator (\blacktriangle) and a bimolecular system $[\text{TEMPO}]/[\text{BPO}] = 1.1$ (\circ)	95
Figure 4.46 Comparison of the number average molecular weights (a) and weight average molecular weights (b) for unimolecular and bimolecular initiators	97
Figure 4.47 Comparison of polydispersity vs. conversion for bimolecular and unimolecular initiating systems	97
Figure 4.48 First order kinetic plots for unimolecular NMRP (\blacksquare), bimolecular NMRP (\circ) and thermal self-self initiation of styrene (Δ)	99
Figure 4.49 Decomposition of dormant species (alkoxyamine) in NMRP of styrene ^[39]	100
Figure 4.50 Promoted dissociation of benzoyl peroxide by TEMPO in the presence of styrene ^[35]	101
Figure 4.51 Effect of addition of prepolymer (5%) on rate of polymerization and number average molecular weights in NMRP of styrene at 130 °C, $\text{TEMPO}/\text{BPO} = 1.1$ and $[\text{BPO}]_0 = 0.036 \text{ M}$	105
Figure 4.52 Comparison of experimental data and model predictions of conversion versus time for NMRP of styrene at 120 °C, $\text{TEMPO}/\text{BPO} = 1.1$ and $[\text{BPO}]_0 = 0.0192 \text{ M}$, 45% prepolymer with $M_n = 17,400$	105
Figure 5.1 Comparison of experimental data and model predictions of conversion vs. time, at 120 °C and $[\text{TEMPO}]/[\text{BPO}] = 1.1$	118
Figure 5.2 Comparison of experimental data and model predictions of number average molecular weight vs. conversion, at 120 °C and $[\text{TEMPO}]/[\text{BPO}] = 1.1$	119
Figure 5.3 Comparison of experimental data and model predictions of polydispersity vs. conversion, at 120 °C and $[\text{TEMPO}]/[\text{BPO}] = 1.1$	119
Figure 5.4 a) Simulated concentration of nitroxyl radicals vs. conversion, b) Simulated concentrations of dead, dormant and living radicals vs. conversion, for NMRP of styrene at 120 and $[\text{TEMPO}]/[\text{BPO}] = 1.1$	121

Figure 5.5 Effect of [TEMPO]/[BPO] ratio on polymerization rate at 120 °C; comparison of experimental data and model predictions	122
Figure 5.6 Effect of [TEMPO]/[BPO] ratio on number average molecular weight at 120 °C; comparison of experimental data and model predictions	122
Figure 5.7 Effect of [TEMPO]/[BPO] ratio on polydispersity at 120 °C; comparison of experimental data and model predictions	124
Figure 5.8 Effect of [TEMPO]/[BPO] on simulated profiles of a) Nitroxyl radical, b) Living species, c) Dormant Species, and d) Dead species for NMRP of styrene at 120°C	126
Figure 6.1 %conversion, molecular weights and polydispersity versus TEMPO/BPO ratio after 10 hrs; T = 120°C	131
Figure 6.2 Molecular weights, polydispersity and time versus TEMPO/BPO ratio at 50% conversion; T = 120°C.....	132
Figure B.1 Effect of decreasing TEMPO/BPO ratio on first order plot in NMRP of styrene at 120°C	150
Figure B.2 Monomer conversion vs. time for NMRP of styrene at 120°C and [TEMPO]/[BPO] = 0.9 (Run #1).....	150
Figure B.3 First order rate plot for NMRP of styrene at 120°C and [TEMPO]/[BPO] = 0.9 .	151
Figure B.4 Average molecular weights and polydispersity vs. conversion for NMRP of styrene at 120°C and [TEMPO]/[BPO] = 0.9	151
Figure B.5 Effect of increasing TEMPO/BPO ratio on first order plot in NMRP of styrene at 120°C.....	152
Figure B.6 Monomer conversion vs. time for NMRP of styrene at 120°C and [TEMPO]/[BPO] = 1.5 (Run #4).....	152
Figure B.7 First order rate plot for NMRP of styrene at 120°C and [TEMPO]/[BPO] = 1.5 .	153
Figure B.8 Average molecular weights and polydispersity vs. conversion for NMRP of styrene at 120°C and [TEMPO]/[BPO] = 1.5	153
Figure B.9 Effect of [TEMPO]/[BPO] ratio on first order plot in NMRP of styrene at 120°C	154
Figure B.10 Monomer conversion vs. time for NMRP of styrene at 120°C and [TEMPO]/[BPO] = 1.2 (Run #3).....	154
Figure B.11 First order rate plot for NMRP of styrene at 120°C and [TEMPO]/[BPO] = 1.2	155
Figure B.12 Average molecular weights and polydispersity vs. conversion for NMRP of styrene at 120°C and [TEMPO]/[BPO] = 1.2.....	155
Figure B.13 Monomer conversion vs. time for NMRP of styrene at 130°C and [TEMPO]/[BPO] = 0.9 (Run #8).....	156
Figure B.14 Average molecular weights and polydispersity vs. conversion for NMRP of styrene at 130°C and [TEMPO]/[BPO] = 0.9.....	156
Figure B.15 Monomer conversion vs. time for NMRP of styrene at 130°C and [TEMPO]/[BPO] = 1.1 (Run #9).....	157
Figure B.16 Average molecular weights and polydispersity vs. conversion for NMRP of styrene at 130°C and [TEMPO]/[BPO] = 1.1	157

Figure B.17 Monomer conversion vs. time for NMRP of styrene at 130°C and [TEMPO]/[BPO] = 1.3 (Run #10)	158
Figure B.18 Average molecular weights vs. conversion for NMRP of styrene at 130°C and [TEMPO]/[BPO] = 1.3	158
Figure B.19 Polydispersity vs. conversion for NMRP of styrene at 130°C and [TEMPO]/[BPO] = 1.3	159
Figure B.20 Polydispersity as a function of the TEMPO/BPO ratio for NMRP of styrene a) after 10 hrs,	159
b) after 20hrs at 120°C	159
Figure B.21 Polydispersity as a function of the TEMPO/BPO ratio for NMRP of styrene a) after 8 hrs,	160
b) after 30hrs at 130°C	160
Figure B.22 Monomer conversion vs. time for thermal polymerization of styrene in the presence of TEMPO at 120°C and [TEMPO] ₀ = 0.0396 M (compared to experimental work from Saldivar-Guerra et al. [30])	160
Figure B.23 Average molecular weights and polydispersity vs. conversion for thermal polymerization of styrene in the presence of TEMPO at 120°C and [TEMPO] ₀ = 0.0396 M	161
Figure B.24 Monomer conversion vs. time for: a) thermal polymerization of styrene in the presence of TEMPO with [TEMPO] ₀ = 0.0396 M b) thermal styrene, at 120°C	161
Figure B.25 Comparison of SEC Chromatograms for a) Styrene thermal polymerization b) Styrene thermal polymerization in the presence of TEMPO, at 35% conversion and 120°C.	162
Figure B.26 Rate of polymerization presented as first order plot; comparison between thermal NMRP and NMRP with [TEMPO]/[BPO] = 1.1 at 120°C and [TEMPO] ₀ = 0.0396 M.....	162
Figure B.27 Number average molecular weights (a) and polydispersities (b) vs. conversion; Comparison between thermal NMRP and NMRP with [TEMPO]/[BPO] = 1.1 at 120°C and [TEMPO] ₀ = 0.0396 M	163
Figure B.28 Effect of [TEMPO]/[BPO] ratio on polymerization rate at 130 °C; comparison of experimental data and model predictions	163
Figure B.29 Effect of [TEMPO]/[BPO] ratio on number average molecular weight at 130 °C; comparison of experimental data and model predictions	164
Figure B.30 Effect of [TEMPO]/[BPO] ratio on polydispersity at 130 °C; comparison of experimental data and model predictions	164

LIST OF TABLES

Table 2.1 Comparison between FRP and CRP	14
Table 2.2 Some ATRP system components.....	16
Table 2.3 Significant contributions to NMRP	23
Table 2.4 Manufacturing issues in NMRP.....	33
Table 4.1 Summary of experimental runs.....	45
Table 5.1 Pioneering papers on modeling of NMRP.....	110
Table 5.2 General mechanism for NMRP kinetics ^[8]	112
Table 5.3 Kinetic rate constants for the monomolecular and bimolecular NMRP processes (T [K] and R [cal mol ⁻¹ K ⁻¹]) ^[12]	113
Table 5.4 Physical properties.....	114
Table A.1 Raw Data for Experiment #1	137
Table A.2 GPC replicates for Experiment #1	137
Table A.3 Raw Data for Experiment #2	138
Table A.4 Replicate Run for Experiment #2	138
Table A.5 Raw data for Experiment # 3	139
Table A.6 GPC replicates for Experiment #3	139
Table A.7 Raw data for Experiment # 4	140
Table A.8 GPC replicates for Experiment #4	140
Table A.9 Raw data for complementary run for Experiment # 4	140
Table A.10 Raw data for Experiment # 5	141
Table A.11 Raw data for Experiment # 6	142
Table A.12 GPC replicates for Experiment #6.....	142
Table A.13 Replicate Run for Experiment #6	142
Table A.14 Raw data for Experiment # 7	143
Table A.15 Replicate Run for Experiment #7	143
Table A.16 Raw data for Experiment #8	144
Table A.17 GPC replicates for Experiment #8.....	144
Table A.18 Raw data for Experiment #9	145
Table A.19 Replicate Run for Experiment #9	145
Table A.20 Raw data for Experiment #10	146
Table A.21 GPC replicates for Experiment #10.....	146
Table A.22 Replicate Run for Experiment #10	146
Table A.23 Raw data for Experiment #11	147
Table A.24 Raw data for Experiment #12	148
Table A.25 GPC replicates for Experiment #12.....	148
Table A.26 Replicate Run for Experiment #12	148

CHAPTER 1 – INTRODUCTION

Controlled radical polymerization (CRP) is one of the most rapidly developing areas of polymer science. The versatility, synthetic ease and the ability to produce novel polymer structures (block and gradient copolymers; star, comb, and hyperbranched architectures) are perhaps the main reasons for the increased academic (and potentially industrial) interest.

Nitroxide-mediated radical polymerization (NMRP) is one of the three currently most popular approaches towards controlled radical polymerization. Polymeric materials synthesized by NMRP can be used as coatings, adhesives, surfactants, dispersants, lubricants, gels, additives and thermoplastic elastomers, as well as materials for biomedical applications. Recently, it has been reported that block copolymers synthesized by NMRP are finding their first industrial use as dispersants in the area of pigments (See Table 2.1 in Chapter 2).

The literature on NMRP is extensive and growing. The polymer chemistry and other kinetic/mechanistic aspects of NMRP are nowadays considered relatively well understood. Detailed kinetic models that describe polymerization rate and molecular weight development are available in the literature. However, it is somewhat surprising that although NMRP is considered relatively well understood, there are still no detailed/reliable experimental studies, conducted over a range of reaction conditions, to validate/support mathematical models.

In this work, our attention has concentrated on the NMRP of styrene using 2,2,6,6-tetramethyl-1-piperidinyloxy (TEMPO) as controller. The objectives were to:

- Investigate the effect of different polymerization conditions such as different temperatures (120, 130 °C), different controller to initiator molar ratios, and different initiating systems (bimolecular, unimolecular and thermally initiated), on conversion (rate), molecular weights and polydispersity.
- Generate a source of reliable experimental data for validation and improvement of a mechanistic mathematical model. This mathematical model, with the enhanced experimental information included via updated parameter values, will subsequently guide

mechanistic model-based non-linear experimental design schemes, which can further shed light on the most uncertain parts of our process understanding.

In Chapter 2, a brief review of the nature of controlled radical polymerization (CRP) is given including basic requirements, typical features, materials that can be made through this method and their applications. Furthermore, CRP is compared with regular free radical polymerization and the mechanisms of different variants of CRP are described briefly. In subsequent sections, nitroxide-mediated radical polymerization (NMRP) is discussed in more detail and a brief historical perspective, kinetic features and applications of NMRP are presented. In addition, different initiating mechanisms in NMRP are described.

The experimental techniques used to study nitroxide-mediated radical polymerization of styrene are described in Chapter 3 and the methods employed in characterizing the polymer samples are briefly discussed.

In Chapter 4, results from the experimental part are presented and discussed. The experimental plan is summarized in Table 4.1 and typical profiles for nitroxide-mediated radical polymerization of styrene are presented. The performance of bimolecular NMRP is evaluated based on rate of polymerization, molecular weight and polydispersity values under different operating conditions (different controller to initiator ratio, and different polymerization temperature). The contribution of thermal self-initiation in NMRP of styrene is examined next; the results are further compared to regular thermal polymerization of styrene and the cases with added initiator (bimolecular and unimolecular). The performance of unimolecular NMRP is subsequently examined and further compared with the bimolecular counterpart. Finally, several important aspects of NMRP, occurrence of side reactions and importance of diffusion-controlled (DC) effects are discussed.

The reaction scheme, general considerations, overall mass balances and moment equations for the development of a mechanistic mathematical model for NMRP of styrene are given in Chapter 5. In addition, the mathematical model is validated with the experimental data described in Chapter 4. The analysis in Chapter 5 relies heavily on the mechanistic model

development efforts of Vivaldo-Lima's group (and subsequent efforts from Lona's group; for detailed referencing of these efforts see Chapter 5).

Concluding remarks are made in Chapter 6 along with a presentation of interesting extensions to this work. The thesis includes two appendices. Appendix A contains tables of the raw data used for the figures of Chapter 4, whereas Appendix B contains complementary figures that were kept out of the main text for the sake of brevity. Each chapter has its own reference section and all symbols used in the text are explained upon first use.

CHAPTER 2 – LITERATURE BACKGROUND

2.1 Controlled Radical Polymerization (CRP)

In order to improve the performance of polymeric materials and broaden their application ranges, synthesis of polymers with controlled composition/molecular architecture (and for some specific applications, narrow molecular weight distribution) has become an attractive area in polymer research.

Well defined polymers with precisely controlled structures are accessible by ionic living polymerization (anionic and cationic). However, ionic polymerizations have several practical disadvantages. Growing carbonium ion or carbonions are extremely reactive toward traces of oxygen, water, or carbon dioxide. Therefore, the polymerization system should be essentially devoid of these impurities. Even when the concentration of these impurities is at levels of parts per million, they can affect the polymerization. Therefore, these systems require great care in purification and drying of solvent and monomers, and in handling the initiator solution. The polymerization temperature is another disadvantage for living ionic polymerizations. High reaction temperatures are not suitable and the optimum temperature range is very low (varying from -20 to -78 °C) [1]. Another limitation is due to the incompatibility of the growing polymer chain-end (anion or cation) with numerous functional groups and certain monomer families [2].

Regular free radical polymerization, on the other hand, can be applied to polymerization of many monomers under relatively mild reaction conditions (compared to ionic polymerization). For instance, polymerization can be performed in water (e.g., emulsion or other aqueous polymerizations), and in the presence of trace amounts of impurities (e.g., oxygen, additives). In addition, polymerization can be conducted over a wide temperature range (-80 to 250 °C). The main drawback of regular free radical systems is that they have not been able to offer the same degree of control over polymer structure and functionality as do ionic systems. For example, polydispersities (a measure of the width of the molecular weight distribution) are

usually higher, and chain end-groups are determined by random events in regular free radical polymerization in comparison to what can be achieved through ionic polymerizations.

By retaining the advantages of regular radical polymerization and adopting concepts from ionic polymerization, controlled radical polymerization can produce materials with a well-defined microstructure (molecular architecture) and low polydispersity under mild conditions with minimal requirements for purification of monomer or solvent (Figure 2.1). In addition, the emergence of controlled radical polymerization techniques offers a route to synthesize new high-value products for specialty applications like block and graft copolymers which are (almost) inaccessible via regular free radical polymerization.

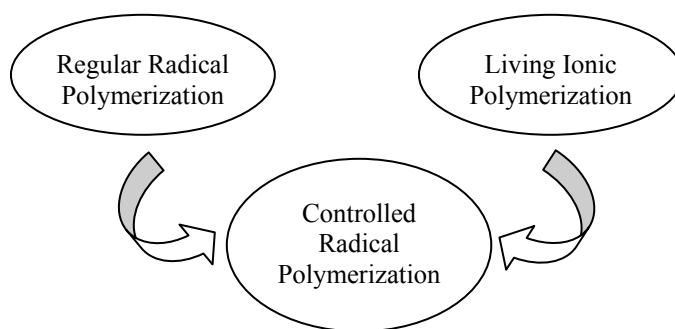


Figure 2.1 Areas contributing to development of CRP

2.1.1 Basic Requirements

Controlled radical polymerization is a family of promising techniques for the synthesis of macromolecules with well-defined molecular weight, low polydispersities (often close to unity) and various architectures under mild conditions from 20 to 140°C, with minimal requirements for purification of monomers and solvents. A common feature of the variants of CRP is the existence of an equilibrium between active free radicals and dormant species [3]. The exchange between active radicals and dormant species allows slow but simultaneous growth of all chains while keeping the concentration of radicals low enough to minimize termination.

The core reaction in CRP systems is shown in Figure 2.2. The dormant species (R_n-X) undergoes homolytic bond breakage, either by heating or by a more complex process of

activation by some added reagent, to produce one active and one stable free radical (See Eq. 2.1). k_a and k_d are activation and deactivation rate constants, respectively. The active radical ($R_n\bullet$) propagates in the presence of monomer (M) (See Eq. 2.2). The corresponding propagating radical can either be deactivated by the stable radical ($X\bullet$) or terminate with other growing radicals (See Eq. 2.3).

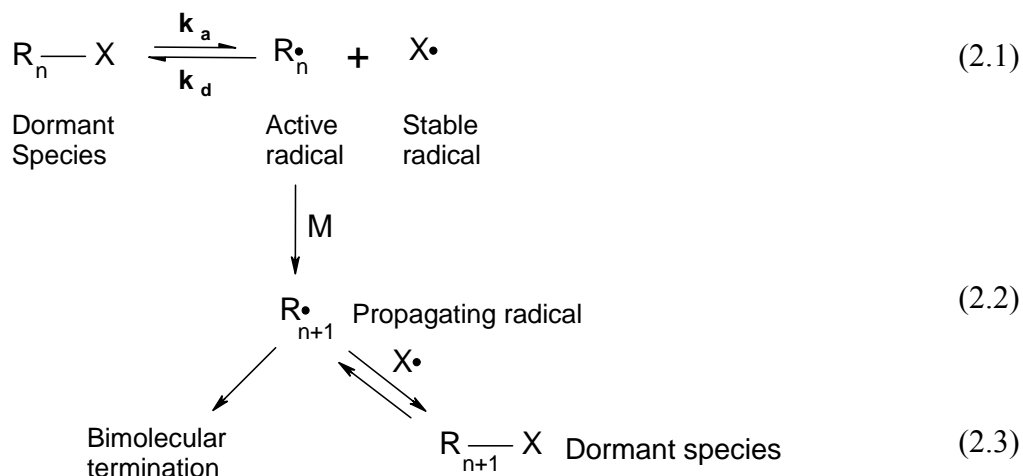


Figure 2.2 A general CRP equilibrium between dormant and active species

In order to achieve controlled conditions, the following three prerequisites should be satisfied:

1. Fast and quantitative initiation compared to propagation.
2. Small contribution of chain breaking reactions like termination and transfer reactions.
3. Fast exchange between active and dormant species.

The initiator should decompose at once or in a very short time period so that all propagating radicals grow for the same time interval (“lifetime”), therefore yielding polymer chains that are virtually of the same chain length. This means that the chains would have the same degree of polymerization (DP), and thus their distribution will have a low polydispersity. This is what happens during a living ionic polymerization since ions do not react with each other. However, in typical radical systems, the rate of radical-radical termination is high. In other words, radical lifetimes are short, and polymer chains are born, grow and die within approximately 1s; during these time-frames it is not possible to gain low polydispersity and desirable chain end functionality.

In order to use radical intermediates in a living type of polymerization it is necessary to keep the concentration of growing chains (chains that have the potential to grow, therefore including both active and dormant species) at an appropriate level, somewhere around 10^{-4} to 10^{-1} M, while keeping the active radical concentration low, preferably less than 10^{-8} M [4]. As a result, the rate of bimolecular termination will be drastically reduced (rate of termination= $k_t [R\bullet]^2$, where k_t is an overall termination rate constant and $[R\bullet]$ is the total (active) radical concentration). The common approach to achieve this is to cap the end of each active radical with a non-radical moiety (stable radical) that can easily be removed to yield back a radical (See Eq. 2.1). Ideally, the majority of chains at any given moment are in the dormant stage (capped by the stable radical). A small concentration ($\sim 10^{-7}$ to 10^{-9} M) may have a propagating radical located at the chain end (in active state). Furthermore, the stable radical is labile enough to allow the dormant chains to become active, and the same stable radical is able to react with an active chain to render it dormant. In this way, a fast equilibrium is established between dormant and active chains, with the capping group mediating the concentration of each chain type (See Eq. 2.1). The identity of the stable radical $X\bullet$ is critical to the success of controlled radical procedures. Ideal stable free radicals do not react with each other, and do not initiate polymerization.

The use of a capping group itself is not sufficient to gain low polydispersity. The exchange between dormant and active species (the equilibrium reaction) must not only favor the dormant species but also be fast [5]. In other words, the stable radical must leave and rejoin the active radical at a rate that is fast enough to allow only a few propagation steps in each activation cycle. If both activation and deactivation are fast relative to propagation, then the polymer radicals will grow in an incremental fashion, and if all the chains are initiated at the same time the resulting chains should have low polydispersities. Thus, exchange dynamics are very important in attaining control over molecular weights and polydispersities.

2.1.2 Typical Features

The ideal CRP is achieved if all chains are initiated immediately at the start of polymerization and if termination and other side reactions are negligible. This ideal system has the following features:

- Linear kinetic plot in semi-logarithmic coordinates ($\ln [M]_0/[M]$ vs. time) for an isothermal batch reactor ($[M]_0$: concentration of monomer at time 0; $[M]$: concentration of monomer at time t). With instantaneous initiation and no termination, the total radical concentration remains constant during polymerization, and this results in a linear trend in $\ln [M]_0/[M]$ vs. time, as shown in Figure 2.3. Curvature indicates deviation from the ideal situation caused by slow initiation, loss of radicals by termination, or other side reactions.

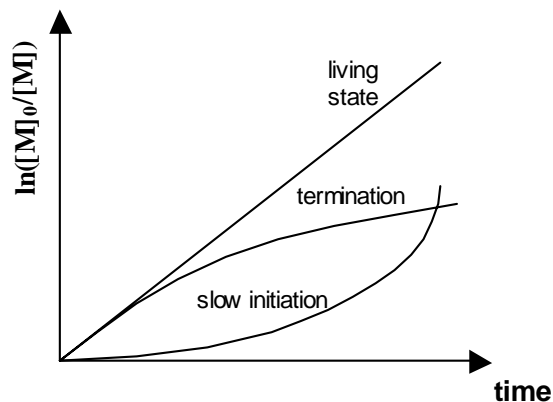


Figure 2.3 First order kinetic plot for controlled radical polymerization

- Average molecular weights increase linearly with conversion which is quite different from regular radical polymerization (FRP) in which high molecular weights are produced right from the outset (See Figure 2.4). Ideally, controlled systems lead to polymers with degrees of polymerization (DP: number of monomer repeat units in a chain) predetermined by the ratio of the concentration of consumed monomer to the introduced initiator ($DP_n = \Delta[M]/[I]_0$).

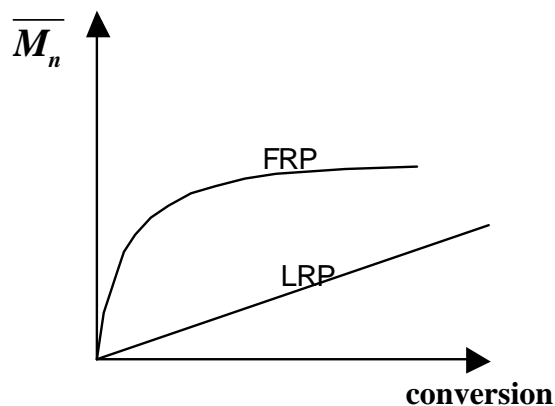


Figure 2.4 Molecular weight outcomes from an ideal controlled radical polymerization (LRP)

- Polydispersity (PDI), the ratio of the weight average to number average molecular weight (M_w/M_n), for an ideal CRP system follows the features of a Poisson distribution, such that $PDI = DP_w/DP_n = (1+1/DP_n)$ [3]. For real CRP systems, PDI is hopefully less than 1.5 (the lowest limit for a conventional radical polymerization).

Figure 2.5 (drawn from our experimental work) shows an example of size exclusion chromatography (SEC) data of polystyrene made by nitroxide-mediated radical polymerization (NMRP) (Curve C) compared to polystyrene made by anionic polymerization (Curve B) and regular radical polymerization (Curve A). Clearly the polystyrene made by NMRP has a much narrower molecular weight distribution (MWD), and hence lower polydispersity, than the sample made by regular radical polymerization. The polydispersity of the NMRP sample is very close to the one made by anionic polymerization (chromatography “standard”).

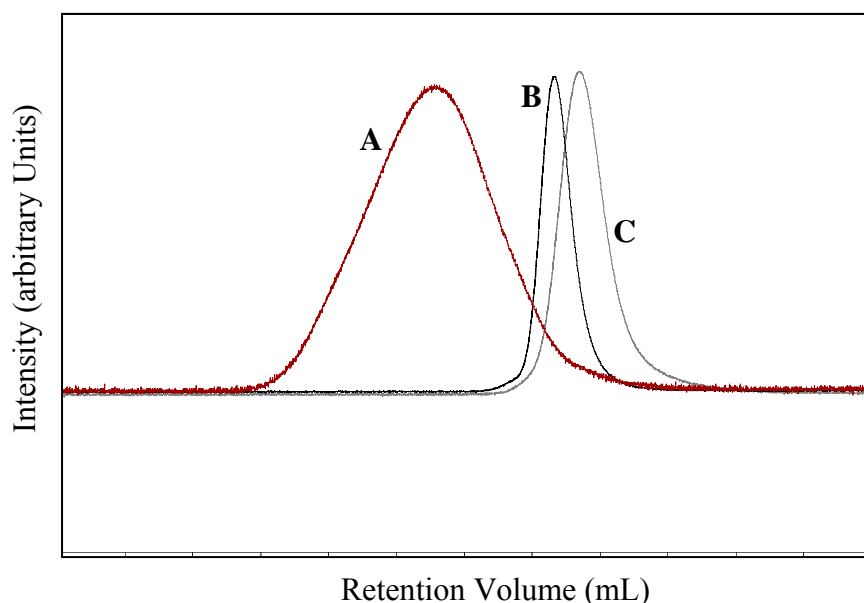


Figure 2.5 Size exclusion chromatographs of polystyrene samples. Curve A: polystyrene made by regular radical polymerization (PDI = 2), Curve B: a SEC 'standard' polystyrene made by anionic polymerization (PDI = 1.1), Curve C: polystyrene made by NMRP (PDI = 1.1)

- CRP polymerizations have the ability to produce polymers with functional end-groups, either at the initiator end (I_n) or the terminal end (X) (Figure 2.6). Y can be any substituent like phenyl, chloride, etc. Also, functionality can be potentially placed in other key

segments of the polymer chain. Chemical functionality plays a large role in the polymer's final properties and adds flexibility for post-polymerization/modification reactions to be performed (e.g., cross-linking or curing). Functional end-groups on polymers produced using CRP may be used to grow a second polymer chain from it, thereby producing block copolymers [4].

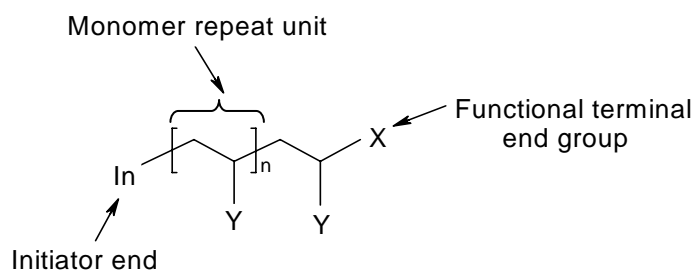


Figure 2.6 General polymer chain structure from controlled radical polymerizations [4]

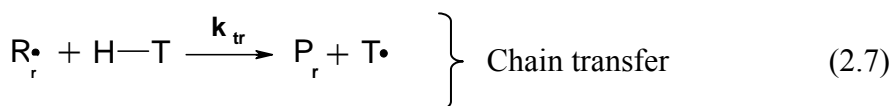
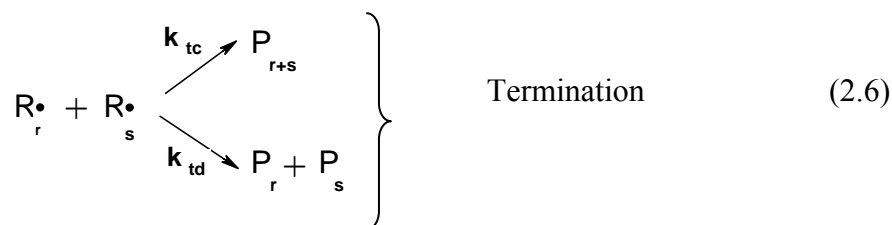
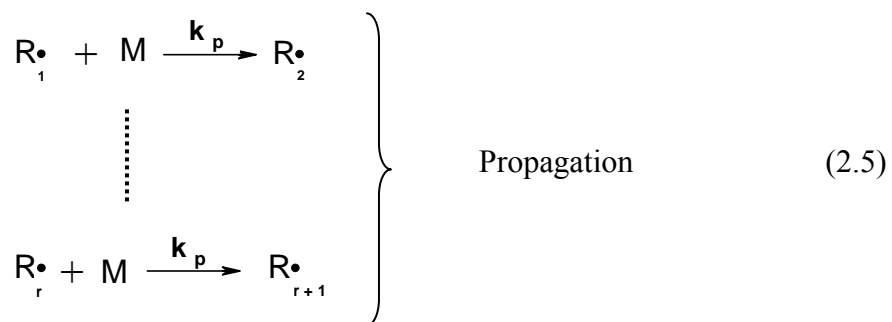
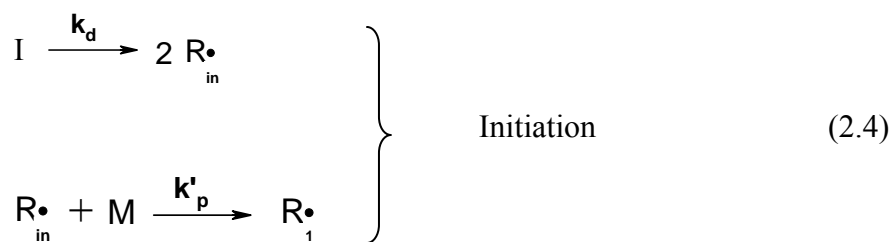
2.1.3 Comparison with Regular Free Radical Polymerization (FRP)

Since controlled radical polymerization involves the elementary radical reactions found in regular free radical polymerization (FRP), it is necessary to grasp the underlying mechanisms of FRP first, in order to be able to understand the CRP mechanism and compare the two systems together.

FRP consists (at a minimum) of three main steps: initiation, propagation and termination, in addition to a fourth step, chain transfer (to a small molecule) [6]. The first step is initiation which is composed of two processes: generation of primary radicals ($R_{\bullet in}$) and reaction of these radicals with monomer to produce radicals of chain length unity ($R_{\bullet 1}$) (See Eq. 2.4). Typical initiators (peroxides, azo compounds, etc.) are used at concentrations between 0.01-1 mol %.

The next step is propagation, the repeated addition of the alkene monomer molecules to the radical species ($R_{\bullet r}$) (See Eq. 2.5). Each propagation (chain growth) reaction results in a polymer chain that is one repeat unit longer. Thus the propagation reaction is repeated over and over, and the chain grows longer and longer. The propagation rate constant is considered to be chain length independent, with typical values of $k_p \approx 10^{3\pm 1} M^{-1} s^{-1}$.

At some point, the propagating polymer radical stops growing and terminates. Termination with the annihilation of the radical centers occurs by a bimolecular reaction between two radicals. Two radicals can terminate either by coupling (k_{tc}) or disproportionation (k_{td}) with rate constant $k_t > 10^7 \text{ M}^{-1} \text{ s}^{-1}$ (See Eq. 2.6). Rate coefficients of termination are chain length and conversion dependent.



Chain transfer (to a small molecule) is a reaction in which growth of a radical is stopped via abstraction of a labile hydrogen atom from a small molecule T (See Eq. 2.7). It results in the radical centre being transferred to another molecule (e.g. monomer, solvent, chain transfer agent), the radical itself becomes a dead polymer molecule, and thus growth is stopped. However, because the radical is transferred to another molecule that can further re-initiate and

subsequently propagate, the overall radical concentration is not reduced and therefore chain transfer is not formally a chain terminating reaction as Eq. 2.6.

In regular radical polymerization, a key point to note is that all four main steps (initiation, propagation, termination and transfer) occur concurrently. In particular, initiation is required throughout the polymerization in order to maintain a relatively constant (steady state) radical concentration, since radical species are always terminating. The total time it takes for a chain to be initiated, propagate, and then terminate is of the order of seconds. The time taken to consume all of the monomer normally ranges from minutes to many hours. Thus, to react all of the monomer one must continually supply new radicals to the reaction. This is achieved by choosing an initiator that decomposes into radicals throughout the reaction.

This has a number of consequences. Firstly, high molecular weight materials form very early on in the reaction. However, chains that are produced early in the reaction are likely to have a different degree of polymerization compared with those produced later in the reaction because of the variation in reactant concentrations and rate constants. This means that the molecular weight distribution (MWD) of the final polymer will contain a wide range of DPs. The normal measure of the width of the MWD, the polydispersity (PDI), is the ratio of the weight average to number average molecular weight (M_w/M_n). In a regular free radical polymerization, it can be shown that the minimum PDI that can be obtained is 1.5 [6]. In most cases, however, the polydispersity is greater than this, often being in the range of 2 to 3, or even higher.

Another consequence of continuous initiation and termination is almost no control over chain end-groups. For example, one end-group may be an initiator fragment that comes from initiator decomposition; another could be an unsaturated vinyl group (double bond) due to termination through disproportionation. During the radical life time (1s) it is very hard to add a special terminating agent to produce end functional polymers. Thus producing polymers with controlled architecture is constrained.

CRP closely resembles regular free radical systems. The basic underlying mechanism is the same, yet there are some distinct differences. The concept of exchange between active and dormant species (See Eq. 2.1) has provided a convenient tool for controlled radical polymerizations to produce materials with low polydispersity and controlled structure. Table

2.1 compares some of the key characteristics of regular and controlled free radical polymerization.

Table 2.1 Comparison between FRP and CRP

Characteristics	Regular Radical Polymerization (FRP)	Controlled Radical Polymerization (CRP)
Initiation/ radical generation	slow and fast (depending on the half- life of the chosen initiator)	preferably fast (initiator decomposes at once or in a very short period of time)
Propagation	fast (monomer is added every ~ 1ms)	slow (monomer is added every ~ 1min)
Transfer reactions	present	negligible
Termination	>99% of chains are essentially dead	portion of irreversibly terminated chains <10%
Activation/deactivation reaction	absent	most important reaction that differentiates CRP from FRP
Radical lifetime	< 1s	>1hr
Rate of polymerization	fast (% conversion per hour ~ 10-20 %)	slow (% conversion per hour ~ 1-2 %)
Polydispersity	>>> 1.5	~ 1.1 - 1.3
Molecular weights (MW) *	≈ 100,000 -300,000 gr/mol	≈ 30,000 gr/mol
Diffusional effects for k_t	significant	negligible
Diffusional effects for k_p & f	can become significant at high conversion (T_g effects)	negligible
Concentration of growing chains	$10^{-7} - 10^{-9}$ M	$10^{-4} - 10^{-1}$ M
Degree of control over molecular architecture	weak	good
Share in overall market (as of 2007)	> 70%	negligible
Industrial applications (as of 2007)	Wide/ diverse	slowly appearing **
Availability	early 1900's till now	early to mid 80's till now

* These are typical molecular weights that can be achieved; of course higher MWs can be obtained in emulsion polymerization and lower MW can be produced in the presence of transfer agents.

** There is a report showing that Ciba Specialty Chemicals have started commercializing acrylic block copolymers produced via CRP [7].

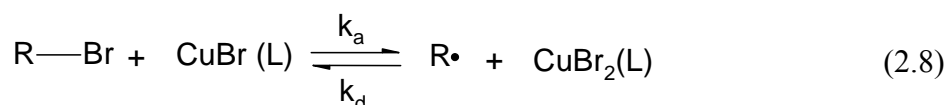
2.1.4 Approaches towards Controlled Radical Polymerization

There are several approaches to controlled radical polymerization. All of these approaches employ some sort of dynamic equilibrium between growing free radicals and various types of dormant species. The exchange process is at the very core of the CRP methods and can be approached in several ways depending on the structure of the dormant and deactivating species, the presence of a catalyst and the particular chemistry and mechanism of the exchange.

Currently three methods appear to be most efficient and may lead to commercial applications:

- **Atom Transfer Radical Polymerization (ATRP)**
- **Nitroxide-Mediated Radical Polymerization (NMRP)**
- **Reversible Addition-Fragmentation Transfer (RAFT)**

Since 1995 (the year of the independent discoveries of ATRP by Matyjaszewski et al. [8] and Sawamoto et al. [9]) the technical literature on ATRP has been growing very rapidly. Radical generation in ATRP involves an organic halide undergoing a reversible redox process catalyzed by a transition metal compound such as cuprous halide [10]. Eq. 2.8 shows the general mechanism of ATRP system catalyzed with copper bromide (CuBr (L)). The system consists of an initiator that has an easily transferable halide atom (R–Br) and a catalyst. The catalyst (or activator) is a lower oxidation state metal halide (CuBr (L)) with a suitable ligand (L). Polymerization starts when the halide atom transfers from the initiator to the catalyst to form a free radical (R•) and a higher oxidation state metal halide CuBr₂ (L) (deactivator). This step is called activation or forward reaction. The deactivation step or backward reaction pushes the reaction to form the dormant species (R–Br).

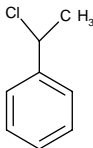
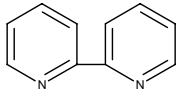
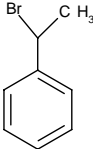
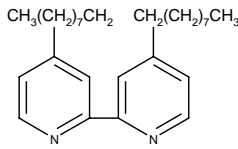
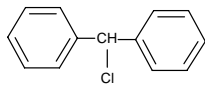
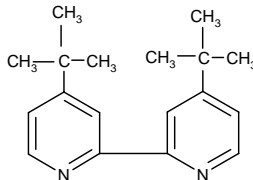
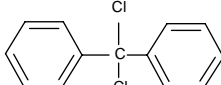


Usually alkyl halides with substituents on the α -carbon such as aryl, carbonyl or allyl groups are used as initiators in ATRP. The carbon halide bond must be relatively weak so that the halogen atom can be easily transferred between the dormant species and the catalyst. Most of

the ATRP initiators use either chlorides or bromides, but some investigations have used iodine as the halogen atom in the initiator.

Compared to conventional free radical polymerization, the new and key component in ATRP is the catalyst. Suitable ligands should complex with a metal halide to form the ATRP catalyst. The metal halide should have at least two oxidation states and should have good affinity toward halogen atoms. Systems using Cu, Ru, Ni, Pd, and Fe transition metals in conjunction with suitable ligands have been used as catalysts. Table 2.2 shows some ATRP initiators, metal halides and ligands [11].

Table 2.2 Some ATRP system components

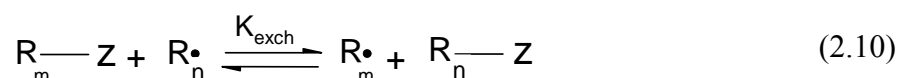
Initiators	Metal halide	Ligand
	CuCl	
	CuBr	
		
		

Nitroxide-mediated radical polymerization (NMRP) is one of the earliest reported methods of CRP. Eq. 2.9 shows the general mechanism of NMRP, where X represents the nitroxide group, R-X is the dormant species, R• is the polymer radical, k_a is the activation rate constant (forward reaction), and k_d is the deactivation rate constant (reverse reaction, according to

typically used CRP terminology). At low temperatures (e.g., 40-60°C), the dormant species is stable and therefore the nitroxide group behaves as an inhibitor [12]. However, at elevated temperatures (e.g., 100-140°C), the dormant chain may undergo homolytic cleavage (dissociation), leading to a polymer radical and nitroxide group [13]. The polymer radical can grow, terminate or couple with the nitroxide group again to form the dormant species. The mechanism and kinetics of NMRP will be discussed in more detail in section 2.2.



Control of radical polymerization with the addition of thiocarbonylthio compounds that serve as reversible addition fragmentation (chain) transfer (RAFT) agents was first reported in the mid 1990's [14]. Contrary to ATRP and NMRP that control chain growth by reversible termination, RAFT polymerization controls chain growth through reversible chain transfer (See Eq. 2.10)



Eq. 2.10 involves the reaction of polymeric radical species ($\text{R}_m\cdot, \text{R}_n\cdot$) that reversibly transfer the capping group (or the chain transfer agent; Z) back and forth to each other. K_{exch} is the equilibrium rate constant. The structures of R_mZ and R_nZ are essentially identical, except that the number of monomer repeat units present (n and m, respectively) may be different. A RAFT polymerization involves a conventional radical initiator (peroxide or AIBN), and a chain transfer agent (Z) which is a compound containing a dithioester, dithiocarbamate, trithiocarbonate or xanthate moiety (See Figure 2.7). The key to the success of RAFT polymerizations lies in the high reactivity of the thiocarbonyl group towards propagating radicals.

It is worth mentioning here that a recent addition to the CRP family has been organotellurium-mediated radical polymerization, or TERP [15]. TERP is able to polymerize monomers such as styrene, acrylates, and methacrylates. Again, as was mentioned before, ATRP, NMRP and

RAFT are the three most promising and popular techniques so far to produce the first commercial materials with controlled structures.

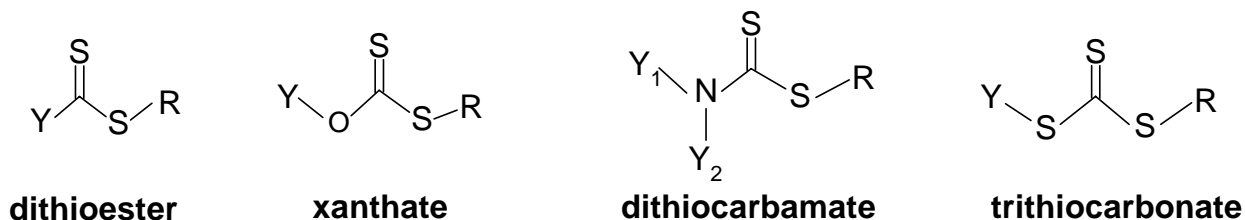


Figure 2.7 General structures for chain transfer agents used in RAFT polymerizations. Y = activating/stabilizing group of thiocarbonyl, R = radical leaving group

2.1.5 Overview of Materials Made by CRP Methods

A brief overview of the types of polymer microstructures that have been produced using CRP methods is given in Figure 2.8.

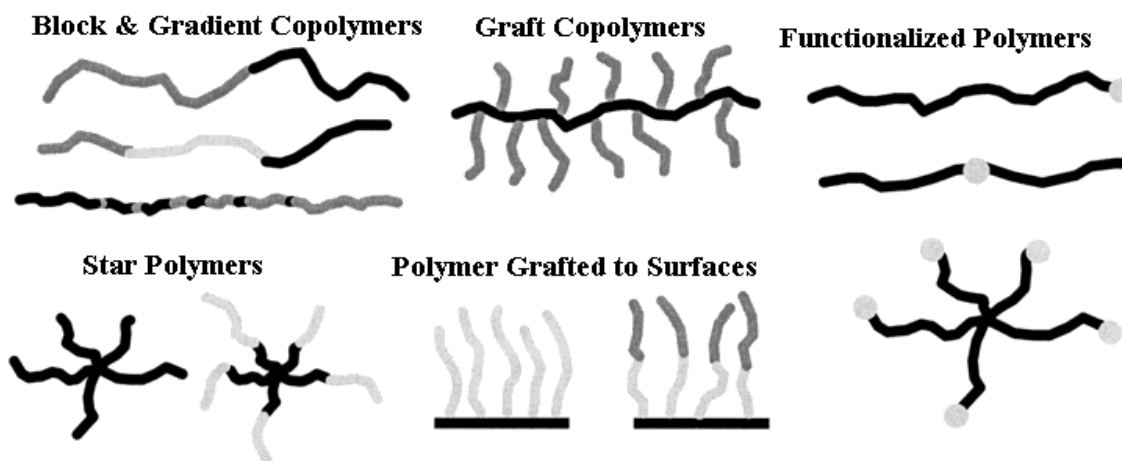


Figure 2.8 Examples of the variety of polymer structures made by CRP techniques ^[4]

These types of structures are the real driving force behind the development and use of CRP methods. Although these general materials can be made through other polymerization mechanisms, ionic polymerizations in particular, the CRP methods provide an avenue to utilizing a large range of vinyl monomers under relatively moderate conditions. Therefore a variety of polymer compositions, functionalities, and architectures can be achieved through CRP.

2.1.6 Material Applications

Materials developed via CRP are gradually finding commercial applications. A few examples are highlighted below.

The first CRP-based products are acrylic block copolymers, commercialized in 2005 through Ciba Specialty Chemicals, which offer superior rheological performance and improved stabilization of pigment dispersions in coating applications [7, 16]. These block copolymers were synthesized through NMRP using n-butylacrylate, dimethylaminoethyl acrylate and styrene as monomers.

RohMax Oil Additives have described commercially feasible and economically acceptable conditions for ATRP preparation of additives based on long chain poly (alkyl methacrylates) that are suitable for use as components of lubricating oils [17].

Dionex used ATRP to nanoengineer the stationary phase of chromatographic columns. This gave rise to a high-resolution, immobilized metal affinity chromatography (IMAC) column capable of peptide and protein enrichment. This was accomplished by grafting a hydrophilic layer from the particle surface, reacting the polymer graft with chelating groups, and then inducing chain collapse by introducing Cu ions for intramolecular coordination crosslinking to form tethered metal-polymer composite nanoparticles. The tethered nanocomposite particles interact with the eluants, causing separation of proteins that differ by only one methyl substituent [18].

Other potential applications include microelectronics, soft lithography, optoelectronics, specialty membranes, sensors and components for microfluidics. Well-defined polymers prepared by CRP are very well suited for biomedical applications such as components of tissue and bone engineering, controlled drug release and drug targeting, antimicrobial surfaces, steering enzyme activity, and many others [19].

2.2 Nitroxide-Mediated Radical Polymerization (NMRP)

2.2.1 Background and Historical Perspective

Nitroxide-mediated radical polymerization (NMRP) is one of the three most popular approaches towards controlled radical polymerization (CRP). The success of this approach can be related to the ability of stable nitroxide free radicals, such as TEMPO, to react with the carbon-centered free radical of the growing polymer chain end in a thermally reversible process (See Figure 2.9). This dramatically lowers the concentration of free radicals in the polymerization system and, coupled with the inability of the nitroxide free radicals to initiate new chain growth, leads to controlled polymerization. These features have been exploited in the preparation of low polydispersity random, block, and graft copolymers as well as star and hyperbranched systems.

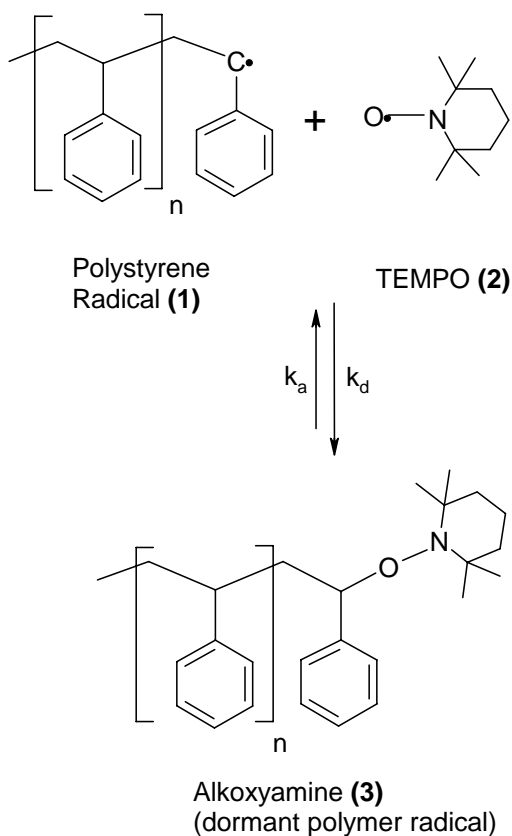


Figure 2.9 Reversible activation, deactivation reaction in NMRP

NMRP has its roots in radical-trapping work of Rizzardo et al., dating back to the early 1980s. In their initial work [12, 20], they demonstrated that at low temperatures (40-60°C), nitroxides such as 2, 2, 6, 6-tetramethylpiperidinyloxy (TEMPO) (**2**) react at near diffusion controlled rates with carbon-centered free radicals (**1**). The resulting alkoxyamine derivatives (**3**) were essentially stable at these temperatures and did not participate in the reaction further, thus acting as radical traps (See Figure 2.9).

The same workers applied a similar concept, albeit at increased temperatures (80-100°C), to the synthesis of low molecular weight oligomers, primarily with acrylates and nitroxides such as TEMPO [21]. The polymerization led to the production of poorly defined materials with uncontrolled molecular weights and high polydispersities. Despite these drawbacks, their work did provide the background information for subsequent studies.

Later in 1993, via a report by the group of Georges at XEROX [13], describing the preparation of low polydispersity polystyrene with controlled structure, the area of nitroxide-mediated radical polymerization really took off. The key feature of this work was the realization that, while nitroxides are polymerization inhibitors at low temperatures, at elevated temperatures they may act as polymerization mediators, not inhibitors.

Georges et al. [13] showed that increasing the temperature to values higher than 100°C and conducting the polymerizations using the stable free radical TEMPO in the presence of Benzoyl Peroxide (BPO) as initiator, can lead to the production of polystyrenes with lower polydispersities (compared to the typical values of ~ 2 for regular free radical polymerization). In addition, molecular weights of the corresponding polystyrenes increase in a linear fashion as a function of monomer conversion.

In these systems, the BPO would initiate polymerization in a normal fashion; however, the polymer radicals would react quickly with TEMPO, forming polymeric alkoxyamines. The C–O bond is weak enough to reversibly dissociate at temperatures greater than 100°C, thus establishing the activation-deactivation equilibrium between dormant and active chains (See Figure 2.10).

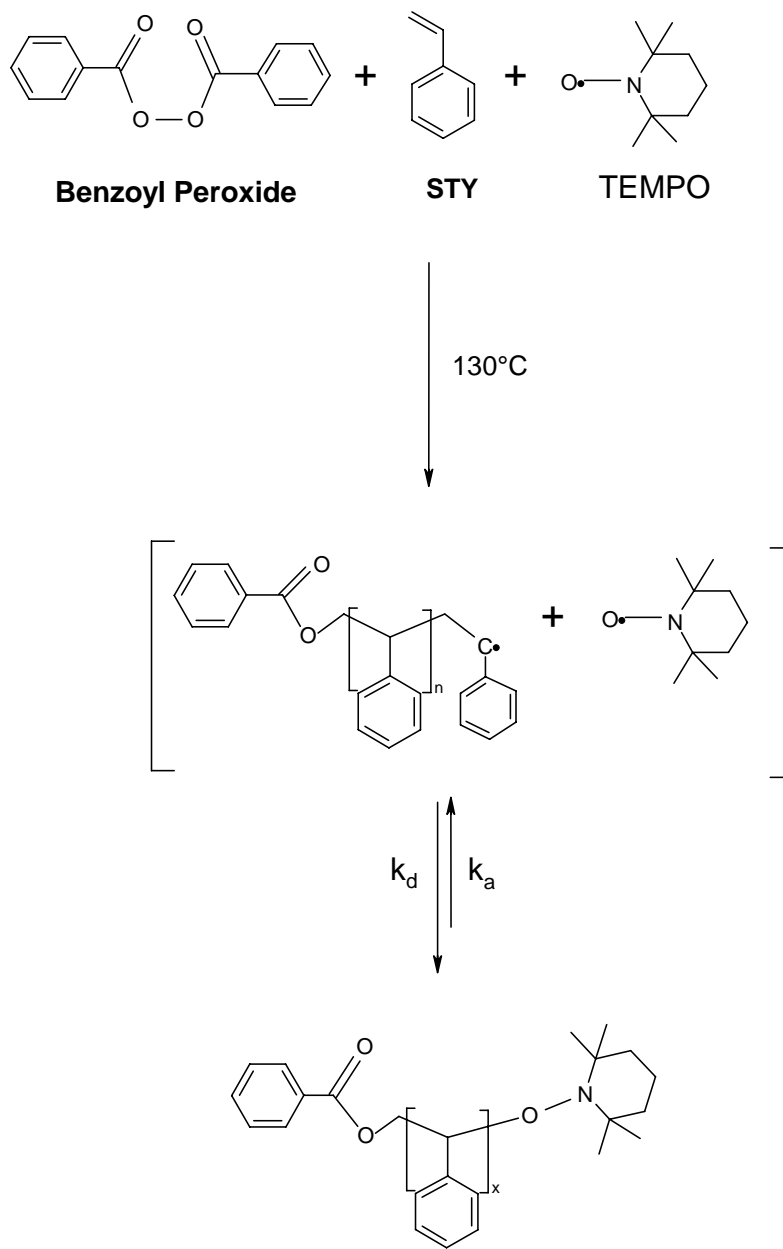


Figure 2.10 Georges' approach to NMRP using bimolecular initiation

Following this observation by Georges et al., a number of other groups embarked on studies of the chemistry, and kinetics of nitroxide-mediated radical polymerization. Table 2.3 cites some of the important contributions.

Table 2.3 Significant contributions to NMRP

Group	Institution	Year*	Main studies	Notes
Georges	XEROX Research Centre, Canada	1993	<ul style="list-style-type: none"> - Kinetics and fundamentals of bimolecular initiation of styrene with BPO and TEMPO (role of excess nitroxide [22], role of thermal initiation [23, 24], mechanism and kinetics [25 - 27], rate enhancement in NMRP [28, 29]) - NMRP in aqueous phase (emulsion, miniemulsion, etc.) [30] 	<ul style="list-style-type: none"> - First group to introduce the concept of NMRP for producing low polydispersity polystyrenes - Bimolecular approach
Matyjaszewski	Carnegie Mellon University, U.S.A	1994	<ul style="list-style-type: none"> - Mechanism, fundamentals and practical aspects [19, 31 - 33] - Synthesis of well defined materials like block and graft copolymers [34, 35] 	<ul style="list-style-type: none"> - Kinetics
Fukuda	Institute for Chemical Research, Kyoto University, Japan	1996	<ul style="list-style-type: none"> - Fundamental kinetic aspects, model simulations for NMRP [36 - 39] - Determination of kinetic rate constants in NMRP by gel permeation chromatography [40 - 42] - Copolymerization of styrene and divinyl-biphenyl [43] 	<ul style="list-style-type: none"> - Mainly using unimolecular initiators as mediators - Kinetics
Fischer	Physical Chemistry Institute, Zurich University, Switzerland	1997	<ul style="list-style-type: none"> - Introducing the concepts of persistent radical effect in NMRP [44, 45] - Defining criteria for livingness and control in NMRP (rate constants required for optimizing the process) [46] - Design and synthesis of β-phosphorus nitroxides and alkoxyamines to be used instead of TEMPO nitroxide [47] - Kinetic investigations on cross-reaction between carbon-centered and nitroxide radicals [48, 49] 	<ul style="list-style-type: none"> - Chemistry & kinetics
Hawker	IBM Almaden Research Centre, U.S.A	1996	<ul style="list-style-type: none"> - Development of variety of TEMPO-based unimolecular initiators to examine the effect of structural variation on the efficiency and usefulness of these derivatives as unimolecular initiators [50] - Examining the effect of acylating agents as rate-accelerating additives [51] - Design of tailor-made nitroxides to improve their performance in NMRP processes [52] - Synthesis of complex macromolecular architectures like star, hyperbranched and dendritic polymers as well as block and graft copolymers [53 - 56] 	<ul style="list-style-type: none"> - Chemistry

* The year that the specific group published their first paper on controlled radical polymerization.

2.2.2 Types of Initiators in Nitroxide-Mediated Radical Polymerization

2.2.2.1 Bimolecular Initiator

In NMRP, two initiating approaches can be used. In the first, TEMPO or another nitroxide radical along with a primary free radical initiator such as BPO or AIBN are used as the initiation system. This approach is called bimolecular initiation, first used by Georges et al. [13] (See Figure 2.10). In this method, initiator (BPO or AIBN) decomposes to primary radicals of high reactivity which initiate the polymerization of monomer. The TEMPO radical then makes a labile bond (C–O) with the radical chain, leading to the formation of alkoxyamines in situ. As mentioned before, the C–O bond is weak enough to reversibly dissociate at temperatures greater than 100°C, thus establishing the activation-deactivation equilibrium between dormant and active chains.

2.2.2.2 Unimolecular Initiator

The second approach uses a single molecule initiator (unimolecular) that, on dissociation, generates two radicals. One of them should be of high reactivity, which will initiate the polymerization, while the second one should be a low reactivity, stable radical. The structure of these initiators is usually based on the alkoxyamine functionality. The C–O bond of the small-molecule alkoxyamine derivative is thermolytically unstable and decomposes on heating to give an initiating radical as well as the stable radical (See Figure 2.11). Following initiation the polymerization would proceed as described previously for the bimolecular case. This approach was first used by Matyjaszewski group [33] and Fukuda et al. [57] almost at the same time.

The advantage of the unimolecular approach is that the structure of the polymers prepared can be controlled to a much greater extent. Since the unimolecular initiator contains the initiating radical and nitroxide radical in the correct (1:1) stoichiometry, the number of initiating sites per polymerization is known. As a result, the molecular weight can be more accurately controlled.

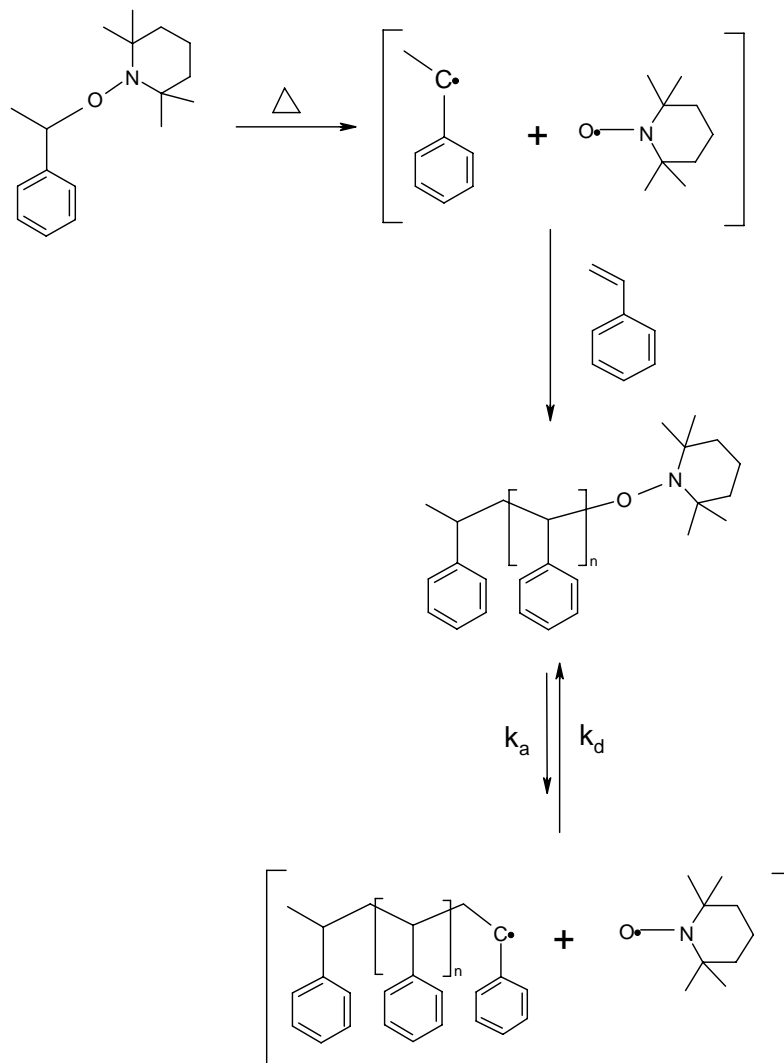


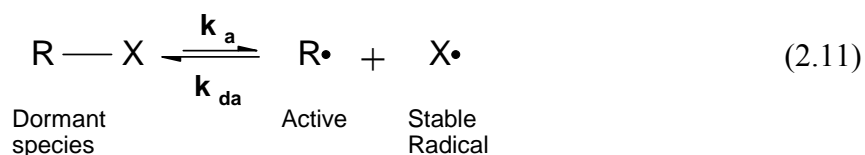
Figure 2.11 Unimolecular initiation approach in NMRP

2.2.3 Kinetics Features

Here, the fundamental kinetic features of nitroxide-mediated radical polymerization (NMRP) will be discussed. The aim is to describe the concentration of reactants and rate of polymerization as a function of time. What is discussed here is a simplified version for basic understanding, whereas more detailed calculations will be presented in Chapter 5 (mathematical modeling).

2.2.3.1 Persistent Radical Effect (PRE)

Here we consider the system including only the initiating adduct R–X and monomer at time $t = 0$ (See Eq. 2.11). When polymerization is started by allowing R – X to dissociate, the same number of R• and X• is produced per unit time, and the concentrations of [R•] and [X•] will increase linearly with time. As [R•] and [X•] increase to a certain level, bimolecular termination between active radicals (R•) and the reaction between R• and X• will become significant. Since the termination of R• results in a decrease of [R•] relative to [X•], [X•] will steadily increase, and therefore the reaction between R• and X• will become more and more important, thus leading back to the formation of R–X. This eventually leads to a balance between the rate of deactivation, $k_{da} [R•][X•]$, and that of activation, $k_d[R–X]$ (quasi-equilibrium will hold).



On the other hand, while the quasi-equilibrium holds, [R•] must be a decreasing function of t , since termination continues to occur. This means that [R•], which increases linearly with t at the onset of polymerization, will at some point start to decrease, thus going through a maximum. This was termed the persistent radical effect (PRE), which is nowadays widely accepted in describing the kinetics of ATRP and NMRP. The model was originally developed by Fischer [44, 45]. Figure 2.12 illustrates the changes in concentration of each species involved in Eq.2.11.

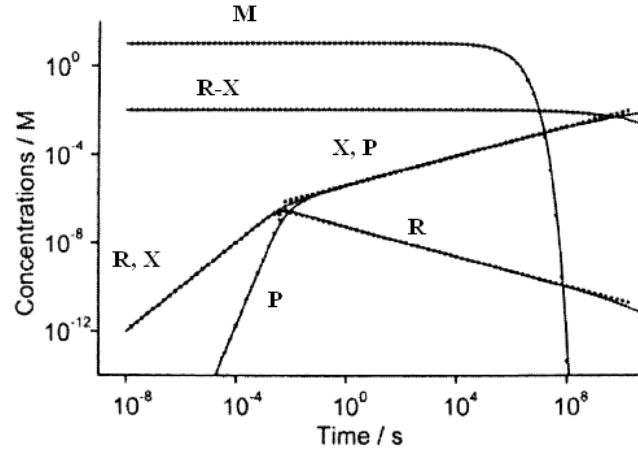


Figure 2.12 Concentration of active radicals (R), stable radicals (X), dormant species (R-X), polymer chains (P) and monomer (M) vs. time for a controlled radical polymerization initiated by homolysis of an initiator (R-X)^[44]

2.2.3.2 Descriptive Equations

In the following, we consider systems where:

- 1) The quasi-equilibrium is reached so fast that the main body of polymerization occurs in the time range of quasi-equilibrium and the pre-equilibrium stage has no significant effect on the polymerization kinetics.
- 2) The cumulative number of dead chains by termination and initiated chains by initiation are sufficiently small compared with the number of dormant chains.
- 3) The initiation rate (R_i) is constant.
- 4) All possible reactions other than those indicated in what follows have been neglected.
- 5) All the rate constants are assumed to be independent of chain length.

The analysis below will follow the developments in [45, 58, 59]. Translating the above statements into equations, we have the following two differential equations:

$$\frac{d[X\cdot]}{dt} = k_a [R - X] - k_d [R\cdot][X\cdot] \quad (2.12)$$

$$\frac{d[R\cdot]}{dt} = k_a [R - X] - k_d [R\cdot][X\cdot] + R_i - k_t [R\cdot]^2 \quad (2.13)$$

Sum of Eqs. 2.12 and 2.13 gives

$$\frac{d[R\bullet]}{dt} = \frac{d[X\bullet]}{dt} + R_i - k_t [R\bullet]^2 \quad (2.14)$$

The quasi-equilibrium ($\frac{d[X\bullet]}{dt} \approx 0$) with negligible fraction of dead chains is represented by Eq. 2.15, where $I_0 = [R-X]_0$.

$$[R\bullet][X\bullet] = K [R - X] = K I_0 \quad (2.15)$$

$$K = \frac{k_a}{k_d} \quad (2.16)$$

Since it usually holds that $[R\bullet] \ll [X\bullet]$, we may neglect $\frac{d[R\bullet]}{dt}$ as compared with $\frac{d[X\bullet]}{dt}$ in Eq. 2.14, which, with Eq. 2.15 gives

$$\frac{d[X\bullet]}{dt} = \frac{k_t K^2 I_0^2 - R_i [X\bullet]^2}{[X\bullet]^2} \quad (2.17)$$

Eq. 2.17 can be solved to provide radical concentrations and subsequently the rate of polymerization. However, only some special cases will be discussed below.

Stationary-state systems (systems with $R_i \gg 0$)

When R_i is sufficiently large, the stationary state ($\frac{d[R\bullet]}{dt} = \frac{d[X\bullet]}{dt} = 0$) is reached at an early stage of polymerization and we obtain

$$R_i = R_t = k_t [R\bullet]^2 \quad (2.18)$$

And so:

$$[R\bullet] = \left(\frac{R_i}{k_t}\right)^{1/2} \quad (2.19)$$

$$[X\bullet] = K I_0 \left(\frac{k_t}{R_i}\right)^{1/2} \quad (2.20)$$

$$R_p = k_p [M] \left(\frac{R_i}{k_t} \right)^{1/2} \quad (2.21)$$

$$\ln \left(\frac{[M]_0}{[M]} \right) = k_p \left(\frac{R_i}{k_t} \right)^{1/2} t \quad (2.22)$$

Power-law systems (systems with $R_i = 0$)

When R_i is zero, Eq. 2.14 becomes

$$\frac{d[X\bullet]}{dt} - \frac{d[R\bullet]}{dt} = k_t [R\bullet]^2 \quad (2.23)$$

Using Eq. 2.15 and substituting for $[R\bullet]$ with a function of $[X\bullet]$ gives

$$([X\bullet]^2 + K I_0) d[X\bullet] = k_t K^2 I_0^2 dt \quad (2.24)$$

This is solved to yield

$$1/3 [X\bullet]^3 + K I_0 [X\bullet] = k_t K^2 I_0^2 t \quad (2.25)$$

From Eq. 2.15, $K I_0 [X\bullet]$ is equal to $[R\bullet][X\bullet]^2$ and that is $\ll [X\bullet]^3$, so we obtain further:

$$[X\bullet] = (3 k_t K^2 I_0^2)^{1/3} t^{1/3} \quad (2.26)$$

$$[R\bullet] = \frac{K I_0}{(3 k_t K^2 I_0^2)^{1/3} t^{1/3}} \quad (2.27)$$

The monomer consumption rate, $-d[M]/dt = k_p [R\bullet][M]$, is integrated using the above equations to finally yield,

$$\ln \left(\frac{[M]_0}{[M]} \right) = (3/2) k_p (K I_0 / 3 k_t)^{1/3} t^{2/3} \quad (2.28)$$

Thus, the monomer consumption index $\ln([M]_0/[M])$ is two-third order in t , in contrast to the first-order dependence of the stationary system (See Eq. 2.22).

2.2.4 Applications and Future Perspective

2.2.4.1 Development of New Nitroxides

Initially, TEMPO was used as the only stable nitroxide in NMRP but the use of TEMPO has several drawbacks. One of the most critical limitations of TEMPO-mediated NMRP is the incompatibility with many monomer families; TEMPO is mainly useful for NMRP of styrene and styrene derivatives. Another limitation of the TEMPO system is the high strength of the C-O bond in the TEMPO polymer adduct. Due to this, the decomposition rate is slow; hence, the time required to complete the polymerization is around 24-72 hrs, 10 to 20 times more than that of regular free radical polymerization. In addition, TEMPO-mediated NMRP needs elevated polymerization temperatures (120- 145 °C).

To overcome these deficiencies it was apparent that changes in the structure of the nitroxide were needed. Unlike the initiating radical, which is involved only at the beginning of the polymerization, the mediating radical is involved in numerous reversible activation and deactivation steps and so changes in its structure would be expected to have a substantial effect on the polymerization.

Initial efforts to develop new nitroxides were centered on TEMPO based derivatives. Keoshkerian et al. [60] were able to polymerize acrylates at 145-155 °C in the presence of 4-oxo-TEMPO (**1**) as the mediating nitroxide. Figure 2.13 shows some of these alternative TEMPO-based nitroxides employed in NMRP. While this was a significant improvement when compared to TEMPO, polydispersities were between 1.4 and 1.67 and the living nature of the polymerization was questionable.

In addition, other nitroxides like ditertiary butyl nitroxide (DTBN) were used as trapping agents, which had no structural resemblance to TEMPO. The optimum temperature range for NMRP mediated by DTBN (See Figure 2.14) is 90-100 °C, which is lower than that of

TEMPO-mediated NMRP [61]. Benoit et al. [62] have introduced a new nitroxide radical, N-tert-butyl-1-deethylphosphono-2,2-dimethylpropyl nitroxide (DEPN; also known as SG-1) (See Figure 2.14). In this nitroxide, an electron-withdrawing dialkyloxy phosphonyl is reported to be more efficient than TEMPO in the NMRP of styrene. DEPN allows faster polymerization than TEMPO mediated polymerization. Moreover, it opens the door to controlled radical polymerization of other monomers like acrylates, acrylamides, and acrylonitriles. Extensive research has been conducted on DEPN by different research groups [63 - 69].

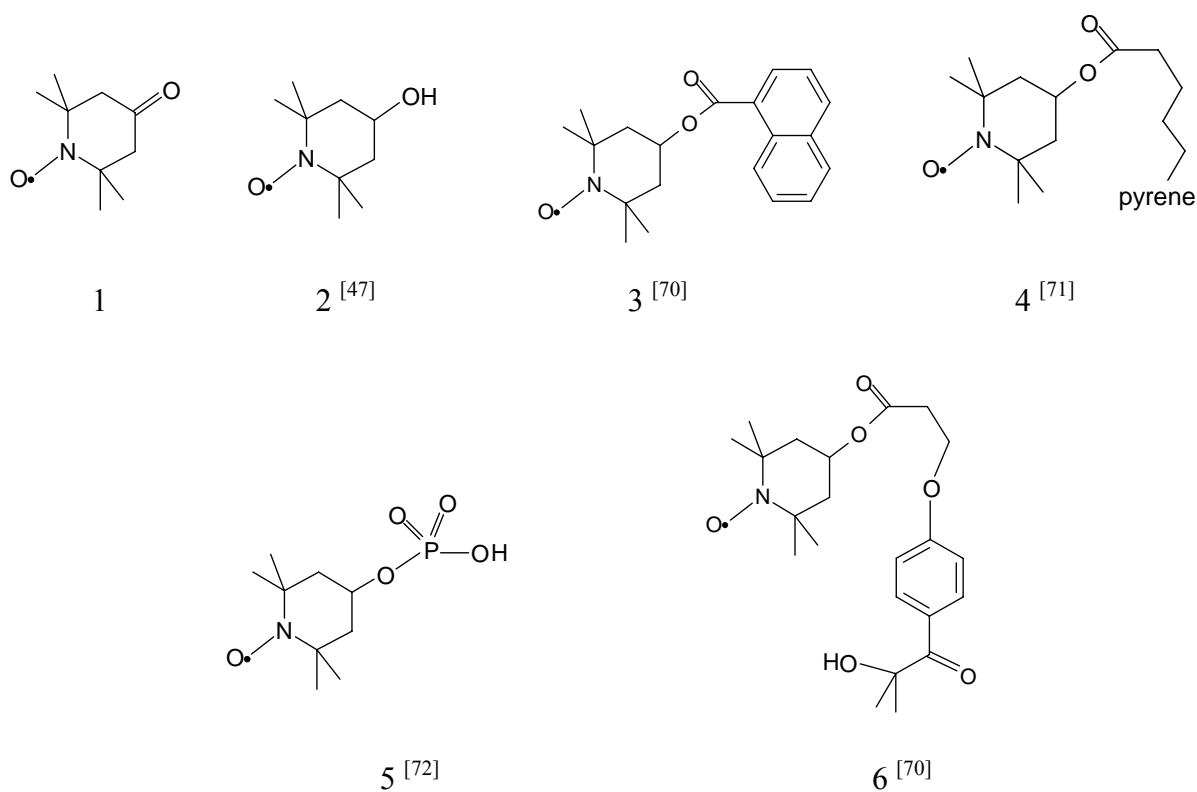


Figure 2.13 Structure of TEMPO-based nitroxides in NMRP

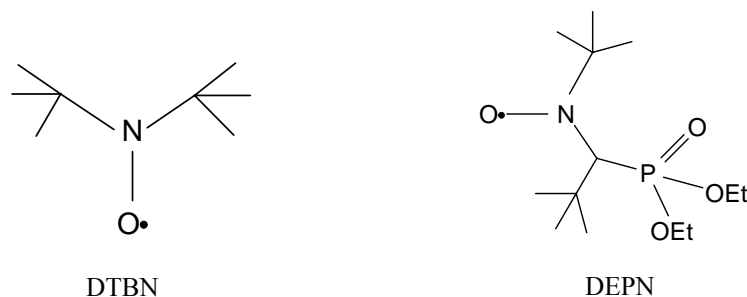


Figure 2.14 Structures of DTBN and DEPN

Design and synthesis of new nitroxides is an ongoing and dynamic research area. A list of nitroxides that have been used as mediators in NMRP can be found in the paper by Hawker et al. [73]. The most recent report on this subject is the paper by Mannan et al. [74] which reports controlled radical polymerization of styrene mediated by a piperidinyl-N-oxyl radical having bulkier substituents (See Figure 2.15) than in TEMPO. This report is a new addition to their previous work on cyclic nitroxides having spiro structures [75].

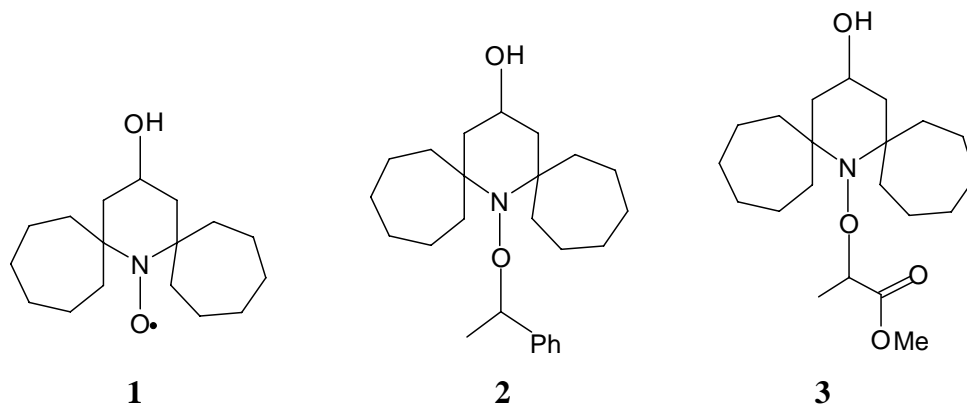


Figure 2.15 Structure of piperidinyl-N-oxyl radical (1) and corresponding alkoxyamines (2, 3)

2.2.4.2 Manufacturing Issues

Controlled radical polymerizations allow the production of well-defined polymeric materials with controlled microstructure (architecture). The future for CRP seems very bright, and it is anticipated that many new products will be introduced to the market within the next several years [76]. Despite the heightened academic interest in the last 10-15 years or so and although the industrial production of materials made by CRP is expanding, it is corresponding to only ~ 10% of all the materials prepared by regular radical polymerization [19]. There are still remaining issues to be resolved to make the production of materials created by CRP comparable to the manufacturing scales in regular radical polymerization. Some of the most important concerns in manufacturing of polymers through NMRP are discussed in Table 2.4 along with some remarks and remedies suggested.

Table 2.4 Manufacturing issues in NMRP

Issues	Remarks
Slow polymerization rates	<ul style="list-style-type: none"> ▪ Adding organic acids and their derivatives ^[28, 29, 51, 77] ▪ Using a combination of two initiators with different half-lives ^[57, 78] ▪ Addition of shots of initiator in a semibatch system ^[79]
Polymerization limited to styrenic monomers	<ul style="list-style-type: none"> ▪ Using nitroxides other than TEMPO or alkoxyamines based on other nitroxides ^[73, 80 - 82]
Low molecular weights	<ul style="list-style-type: none"> ▪ Sometimes production of low molecular weight polymers is desirable ^[83] ▪ If not, the problem can be remedied by working in heterogeneous media or possibly using multifunctional initiators
Inefficient, commercially infeasible mediating agents (nitroxides/ alkoxyamines)	<ul style="list-style-type: none"> ▪ Mediating agents used in research are not suitable for industrial production either because of low efficiency or complicated synthesis steps ▪ Search for new mediating agents necessary
Working in heterogeneous media	<ul style="list-style-type: none"> ▪ It is industrially appealing to conduct nitroxide-mediated polymerizations in heterogeneous media such as emulsion, miniemulsion, dispersion, suspension, etc. ▪ NMRP systems using TEMPO or its derivatives require high temperatures (higher than the boiling point of water), so higher pressure reaction setups are required ▪ Change the mediating nitroxide (use nitroxides that are compatible with water and function at lower temperatures (<100°C))
Narrow polydispersities	<ul style="list-style-type: none"> ▪ Range of desirable polydispersities depends on the application of the polymer produced; narrow polydispersity polymers are desirable for special applications while polymers with broad distributions are easier to process
Cost	<ul style="list-style-type: none"> ▪ There is always a trade-off between cost and value-added product benefits; even if the cost of extra specialty chemicals (nitroxides, other agents) is higher than the regular recipes, if the product benefits (and hence, profits) due to improvements in quality are significant, then the process is acceptable even if it looked very expensive initially

2.3 References

1. Kitayama, T.; Ute, K.; Hatada, K. **1990** "Synthesis of stereoregular polymers and copolymers of methacrylate by living polymerization and their characterization by NMR spectroscopy" *Polymer Journal*, *23*, 5-17.
2. Quirk, R. P.; Kinning, D. J.; Fetters, L. J. "*Comprehensive Polymer Science*", Aggarwal, S. L., ed., Pergamon Press: London, **1989** Vol.7, p 1.
3. Matyjaszewski, K. "Overview: Fundamentals of Controlled/Living Radical Polymerization", In *Controlled Radical Polymerization*; Matyjaszewski, K., ed. American Chemical Society: Washington, DC, **1997**; pp 2-30.
4. Shipp, D. A. **2005** "Living radical polymerization: controlling molecular size and chemical functionality in vinyl polymers" *Polymer Reviews*, *45*, 171-194.
5. Matyjaszewski, K. "General Concepts and History of Living Radical Polymerization", In *Handbook of Radical Polymerization*; Matyjaszewski, K., Davis, T. P., eds. John Wiley and Sons, Inc.: Hoboken, **2002**; pp 361-406.
6. Odian, G. "Radical Chain Polymerization", In *Principles of Polymerization*; John Wiley & Sons, Inc.: Hoboken, New Jersey, **2004**; p 198.
7. Pirrung, F. O. H.; Aushra, C. **2005** "Nitroxide-mediated synthesis of acrylic block copolymers- and their use as coating additives" *Polymer Preprints*, *46*, 316-317.
8. Wang, J. S.; Matyjaszewski, K. **1995** "Controlled living radical polymerization - atom-transfer radical polymerization in the presence of transition-metal complexes" *Journal of the American Chemical Society*, *117*, 5614-5615.
9. Kato, M.; Kamigaito, M.; Sawamoto, M.; Higashimura, T. **1995** "Polymerization of methyl-methacrylate with the carbon-tetrachloride dichlorotris (triphenylphosphine) ruthenium(II) methylaluminum bis(2,6-di-tert-butylphenoxide) initiating system - possibility of living radical polymerization" *Macromolecules*, *28*, 1721-1723.
10. Xia, J. H.; Gaynor, S. G.; Matyjaszewski, K. **1998** "Controlled/"living" radical polymerization. Atom transfer radical polymerization of acrylates at ambient temperature" *Macromolecules*, *31*, 5958-5959.
11. Matyjaszewski, K. "Fundamentals of Atom Transfer Radical Polymerization", In *Handbook of Radical Polymerization*; Matyjaszewski, K., Davis, T. P., eds. John Wiley and Sons, Inc.: Hoboken, **2002**; pp 523-628.
12. Moad, G.; Rizzardo, E.; Solomon, D. H. **1982** "A product study of the nitroxide inhibited thermal polymerization of styrene" *Polymer Bulletin*, *6*, 589-593.
13. Georges, M.; Veregin, R.; Kazmaier, R.; Hamer, G. **1993** "Narrow molecular weight resins by a free- radical polymerization process" *Macromolecules*, *26*, 2987-2988.

14. Chiefari, J.; Chong, Y. K.; Ercole, F.; Krstina, J.; Jeffery, J.; Le, T. P. T.; Mayadunne, R. T. A.; Meijs, G. F.; Moad, C. L.; Moad, G.; Rizzardo, E.; Thang, S. H. **1998** "Living free radical polymerization by reversible addition fragmentation chain transfer : the RAFT process" *Macromolecules*, *31*, 5559-5562.
15. Yamago, S.; Iida, K.; Yoshida, J. **2002** "Organotellurium compounds as novel initiators for controlled/living radical polymerizations. Synthesis of functionalized polystyrenes and end-group modifications" *Journal of the American Chemical Society*, *124*, 2874-2875.
16. Auschra, C.; Eckstein, E.; Muhlebach, A.; Zink, M. O.; Rime, F. **2002** "Design of new pigment dispersants by controlled radical polymerization" *Progress in Organic Coatings*, *45*, 83-93.
17. Woodruff, R. A.; Bollinger, J. M.; Cooper, D. C.; Eisenberg, B.; Mueller, M.; Roos, S.; Scherer, M.; Wang, J. L. **2004** "Preparation of lubricating oil additives by ATRK" *Abstracts of Papers of the American Chemical Society*, *227*, U505.
18. Matyjaszewski, K.; Spanswick, J. **2005** "Controlled/living radical polymerization" *Materials today*, *8*, 26-33.
19. Braunecker, W. A.; Matyjaszewski, K. **2007** "Controlled/living radical polymerization: Features, developments, and perspectives" *Progress in Polymer Science*, *32*, 93-146.
20. Rizzardo, E.; Solomon, D. H. **1979** "New method for investigating the mechanism of initiation of radical polymerization" *Polymer Bulletin*, *1*, 529-534.
21. Solomon, D. H., Rizzardo, E., and Cacioli, P. (**1986**) U.S. Patent. 4,581,429.
22. Veregin, R. P. N.; Odell, P. G.; Michalak, L. M.; Georges, M. K. **1996** "The pivotal role of excess nitroxide radical in living free radical polymerizations with narrow polydispersity" *Macromolecules*, *29*, 2746-2754.
23. Georges, M. K.; Kee, R. A.; Veregin, R. P. N.; Hamer, G. K.; Kazmaier, P. M. **1995** "Nitroxide mediated free-radical polymerization process - autopolymerization" *Journal of Physical Organic Chemistry*, *8*, 301-305.
24. Veregin, R. P. N.; Kazmaier, P. M.; Odell, P. G.; Georges, M. K. **1997** "The role of thermal initiation in nitroxide mediated living free radical polymerizations" *Chemistry Letters*, 467-468.
25. Georges, M. K. **1999** "An overview of the nitroxide-mediated living-radical polymerization process" *Abstracts of Papers of the American Chemical Society*, *217*, U407.
26. Veregin, R. P. N.; Georges, M. K.; Hamer, G. K.; Kazmaier, P. M. **1995** "Mechanism of living free-radical polymerizations with narrow polydispersity - electron-spin-resonance and kinetic-studies" *Macromolecules*, *28*, 4391-4398.

27. Veregin, R. P. N.; Odell, P. G.; Michalak, L. M.; Georges, M. K. **1996** "Molecular weight distributions in nitroxide-mediated living free radical polymerization: Kinetics of the slow equilibria between growing and dormant chains" *Macromolecules*, *29*, 3346-3352.
28. Odell, P. G.; Veregin, R. P. N.; Michalak, L. M.; Brousmiche, D.; Georges, M. K. **1995** "Rate enhancement of living free-radical polymerizations by an organic-acid salt" *Macromolecules*, *28*, 8453-8455.
29. Cunningham, M. F.; Tortosa, K.; Lin, M.; Keoshkerian, B.; Georges, M. K. **2002** "Influence of camphorsulfonic acid in nitroxide-mediated styrene miniemulsion polymerization" *Journal of Polymer Science Part A-Polymer Chemistry*, *40*, 2828-2841.
30. Cunningham, M. F.; Tortosa, K.; Ma, J. W.; McAuley, K. B.; Keoshkerian, B.; Georges, M. K. **2002** "Nitroxide mediated living radical polymerization in miniemulsion" *Macromolecular Symposia*, *182*, 273-282.
31. Mardare, D.; Matyjaszewski, K. **1994** "Thermal polymerization of Styrene in the presence of stable radicals and inhibitors" *Polymer Preprints (Am.Chem.Soc.)*, *35*, 778.
32. Matyjaszewski, K. "Controlled/Living Radical Polymerization: State of the Art in 2002", In *Advances in Controlled/Living Radical Polymerization*; Matyjaszewski, K., ed. American Chemical Society, Washington, DC: **2003**; pp 2-9.
33. Greszta, D.; Matyjaszewski, K. **1996** "Mechanism of controlled/"living" radical polymerization of styrene in the presence of nitroxyl radicals. kinetics and simulations" *Macromolecules*, *29*, 7661-7670.
34. Tang, C. B.; Dufour, B.; Bombalski, L.; Matyjaszewski, K.; Kowalewski, T. **2005** "Well-defined polyacrylonitrile copolymers prepared by various CRP and their applications as nanostructured carbons" *Abstracts of Papers of the American Chemical Society*, *230*, U4216.
35. Tang, C.; Kowalewski, T.; Matyjaszewski, K. **2003** "Preparation of polyacrylonitrile - block- poly (n-butyl acrylate) copolymers using atom transfer radical polymerization and nitroxide mediated polymerization processes" *Macromolecules*, *36*, 1465-1473.
36. Goto, A.; Fukuda, T. **2004** "Kinetics of living radical polymerization" *Progress in Polymer Science*, *29*, 329-385.
37. Goto, A.; Fukuda, T. **1997** "Effects of radical initiator on polymerization rate and polydispersity in nitroxide-controlled free radical polymerization" *Macromolecules*, *30*, 4272-4277.
38. Tsujii, Y.; Fukuda, T.; Miyamoto, T. **1997** "Computer simulation on the kinetics of nitroxide-controlled free radical polymerization" *Abstracts of Papers of the American Chemical Society*, *213*, 305-OLY.

39. Fukuda, T.; Tsujii, Y.; Miyamoto, T. **1997** "Mechanism and kinetics nitroxide-controlled free radical polymerization" *Abstracts of Papers of the American Chemical Society*, *213*, 462-OLY.
40. Fukuda, T. **2004** "Fundamental kinetic aspects of living radical polymerization and the use of gel permeation chromatography to shed light on them" *Journal of Polymer Science Part A-Polymer Chemistry*, *42*, 4743-4755.
41. Goto, A.; Terauchi, T.; Fukuda, T.; Miyamoto, T. **1997** "Gel permeation chromatographic determination of activation rate constants in nitroxide-controlled free radical polymerization .1. Direct analysis by peak resolution" *Macromolecular Rapid Communications*, *18*, 673-681.
42. Fukuda, T.; Goto, A. **1997** "Gel permeation chromatographic determination of activation rate constants in nitroxide-controlled free radical polymerization .2. Analysis of evolution of polydispersities" *Macromolecular Rapid Communications*, *18*, 683-688.
43. Ide, N.; Fukuda, T. **1997** "Nitroxide-controlled free-radical copolymerization of vinyl and divinyl monomers. Evaluation of pendant-vinyl reactivity" *Macromolecules*, *30*, 4268-4271.
44. Fischer, H. **2001** "The persistent radical effect: A principle for selective radical reactions and living radical polymerization" *Chemical Reviews*, *101*, 3581-3610.
45. Fischer H. **1997** "The persistent radical effect in "living" radical polymerization" *Macromolecules*, *30*, 5666-5672.
46. Fischer, H. "Criteria for Livingness and Control in Nitroxide Mediated and Related Radical Polymerizations", In *Advances in Controlled/Living Radical Polymerization*; Matyjaszewski, K., ed. American Chemical Society: Washington, DC, **2003**; pp 10-23.
47. Le Mercier, C.; Acerbis, S. B.; Bertin, D.; Chauvin, F.; Gigmes, D.; Guerret, O.; Lansalot, M.; Marque, S.; Le Moigne, F.; Fischer, H.; Tordo, P. **2002** "Design and use of beta-phosphorus nitroxides and alkoxyamines in controlled/"living" free radical polymerizations" *Macromolecular Symposia*, *182*, 225-247.
48. Sobek, J.; Martschke, R.; Fischer, H. **2001** "Entropy control of the cross-reaction between carbon-centered and nitroxide radicals" *Journal of the American Chemical Society*, *123*, 2849-2857.
49. Fischer, H.; Radom, L. **2002** "Factors controlling the addition of carbon-centered radicals to alkenes" *Macromolecular Symposia*, *182*, 1-14.
50. Hawker, C. J.; Barclay, G. G.; Orellana, A.; Dao, J.; Devonport, W. **1996** "Initiating systems for nitroxide-mediated "living" free radical polymerizations: synthesis and evaluation" *Macromolecules*, *29*, 5245-5254.

51. Malmstrom, E.; Miller, R. D.; Hawker, C. J. **1997** "Development of a new class of rate-accelerating additives for nitroxide-mediated 'living' free radical polymerization" *Tetrahedron*, *53*, 15225-15236.
52. Benoit, D.; Chaplinski, V.; Braslau, R.; Hawker, C. J. **1999** "Development of a universal alkoxyamine for "living" free radical polymerizations" *Journal of the American Chemical Society*, *121*, 3904-3920.
53. Malmstrom, E. E.; Hawker, C. J. **1998** "Macromolecular engineering via 'living' free radical polymerizations" *Macromolecular Chemistry and Physics*, *199*, 923-935.
54. Hawker, C. J.; Benoit, D.; Rivera, F.; Piotti, M.; Rees, I.; Hedrick, J. L.; Zech, C.; Maier, G.; Voit, B.; Braslau, R.; Frechet, J. M. J. **1999** "Versatile route to functionalized block copolymers by nitroxide-mediated "living" free-radical polymerization" *Abstracts of Papers of the American Chemical Society*, *218*, U411-U412.
55. Hawker, C. J.; Mecerreyes, D.; Elce, E.; Dao, J. L.; Hedrick, J. L.; Barakat, I.; Dubois, P.; Jerome, R.; Volksen, W. **1997** ""Living" free radical polymerization of macromonomers: Preparation of well defined graft copolymers" *Macromolecular Chemistry and Physics*, *198*, 155-166.
56. Leduc, M. R.; Hawker, C. J.; Dao, J.; Frechet, J. M. J. **1996** "Dendritic initiators for "living" radical polymerizations: A versatile approach to the synthesis of dendritic-linear block copolymers" *Journal of the American Chemical Society*, *118*, 11111-11118.
57. Fukuda, T.; Terauchi, T.; Goto, A.; Ohno, K.; Tsujii, Y.; Miyamoto, T.; Kobatake, S.; Yamada, B. **1996** "Mechanisms and kinetics of nitroxide-controlled free radical polymerization" *Macromolecules*, *29*, 6393-6398.
58. Fukuda, T.; Goto, A. **2004** "Kinetics of living radical polymerization" *Progress in Polymer Science*, *29*, 329-385.
59. Saldivar-Guerra, E.; Bonilla, J.; Becerril, F.; Zacahua, G.; Albores-Velasco, M.; Alexander-Katz, R.; Flores-Santos, L.; Alexandrova, L. **2006** "On the nitroxide quasi-equilibrium in the alkoxyamine-mediated radical polymerization of styrene" *Macromolecular Theory and Simulations*, *15*, 163-175.
60. Keoshkerian, B.; Georges, M.; Quinlan, M.; Veregin, R.; Goodbrand, B. **1998** "Polyacrylates and polydienes to high conversion by a stable free radical polymerization process: Use of reducing agents" *Macromolecules*, *31*, 7559-7561.
61. Jousset, S.; Hammouch, S. O.; Catala, J. M. **1997** "Kinetic studies of the polymerization of p-tert-butylstyrene and its block copolymerization with styrene through living radical polymerization mediated by a nitroxide compound" *Macromolecules*, *30*, 6685-6687.

62. Benoit, D.; Grimaldi, S.; Robin, S.; Finet, J. P.; Tordo, P.; Gnanou, Y. **2000** "Kinetics and mechanism of controlled free-radical polymerization of styrene and n-butyl acrylate in the presence of an acyclic beta-phosphonylated nitroxide" *Journal of the American Chemical Society*, *122*, 5929-5939.
63. Bertin, D.; Chauvin, F.; Marque, S.; Tordo, P. **2002** "Lack of chain length effect on the rate of homolysis of polystyryl-SG1 alkoxyamines" *Macromolecules*, *35*, 3790-3791.
64. Nicolas, J.; Charleux, B.; Guerret, O.; Magnet, S. **2005** "Use of a novel class of SG1-based water-soluble dialkoxyamine in nitroxide-mediated controlled-free radical emulsion polymerization" *Abstracts of Papers of the American Chemical Society*, *230*, U4226.
65. Nicolas, J.; Charleux, B.; Guerret, O.; Magnet, S. **2004** "Novel SG1-Based water-soluble alkoxyamine for nitroxide-mediated controlled free-radical polymerization of styrene and n-butyl acrylate in miniemulsion" *Macromolecules*, *37*, 4453-4463.
66. Couvreur, L.; Lefay, C.; Belleney, J.; Charleux, B.; Guerret, O.; Magnet, S. **2003** "First nitroxide-mediated controlled free-radical polymerization of acrylic acid" *Macromolecules*, *36*, 8260-8267.
67. Guerret, O.; Couturier, J. L.; Chauvin, F.; El Bouazzy, H.; Bertin, D.; Gigmes, D.; Marque, S.; Fischer, H.; Tordo, P. **2003** "Influence of solvent and polymer chain length on the homolysis of SG1-based alkoxyamines" *Advances in Controlled/Living Radical Polymerization*, *854*, 412-423.
68. Le Mercier, C.; Acerbis, S. B.; Bertin, D.; Chauvin, F.; Gigmes, D.; Guerret, O.; Lansalot, M.; Marque, S.; Le Moigne, F.; Fischer, H.; Tordo, P. **2002** "Design and use of beta-phosphorus nitroxides and alkoxyamines in controlled/"living" free radical polymerizations" *Macromolecular Symposia*, *182*, 225-247.
69. Lacroix-Desmazes, P.; Lutz, J. F.; Boutevin, B. **2000** "N-tert-butyl-1-diethylphosphono-2,2-dimethylpropyl nitroxide as counter radical in the controlled free radical polymerization of styrene: kinetic aspects" *Macromolecular Chemistry and Physics*, *201*, 662-669.
70. Turro, N. J.; Lem, G.; Zavarine, I. S. **2000** "A living free radical exchange reaction for the preparation of photoactive end-labeled monodisperse polymers" *Macromolecules*, *33*, 9782-9785.
71. Rodlert, M.; Harth, E.; Rees, I.; Hawker, C. J. **2000** "End-group fidelity in nitroxide-mediated living free-radical polymerizations" *Journal of Polymer Science Part A-Polymer Chemistry*, *38*, 4749-4763.
72. Matyjaszewski, K.; Gaynor, S. G.; Greszta, D.; Mardare, D.; Shigemoto, T.; Wang, J. S. **1995** "Unimolecular and bimolecular exchange-reactions in controlled radical polymerization" *Macromolecular Symposia*, *95*, 217-231.

73. Hawker, C. J.; Bosman, A. W.; Harth, E. **2001** "New polymer synthesis by nitroxide mediated living radical polymerization" *Chem.Rev.*, *101*, 3661-3688.
74. Mannan, A.; Ichikawa, A.; Miura, Y. **2007** "Living radical polymerization of styrene mediated by a piperidinyl-N-oxyl radical having very bulky substituents" *Polymer*, *48*, 743-749.
75. Miura, Y.; Nakamura, N.; Taniguchi, I. **2001** "Low-temperature "living" radical polymerization of styrene in the presence of nitroxides with spiro structures" *Macromolecules*, *34*, 447-455.
76. Rutsch, W.; Cech, M. A. **2007** "Effects to improve the quality of life: Color, performance and protection from Ciba Specialty Chemicals" *Chimia*, *61*, 33-41.
77. Veregin, R. P. N.; Odell, P. G.; Michalak, L. M.; Georges, M. K. **1996** "Mechanism of rate enhancement using organic acids in nitroxide-mediated living free-radical polymerizations" *Macromolecules*, *29*, 4161-4163.
78. Greszta, D.; Matyjaszewski, K. **1997** "TEMPO-mediated polymerization of styrene: Rate enhancement with dicumyl peroxide" *Journal of Polymer Science Part A-Polymer Chemistry*, *35*, 1857-1861.
79. Diaz-Camacho, F.; Lopez-Morales, S.; Vivaldo-Lima, E.; Saldivar-Guerra, E.; Vera-Graoamp, R.; Alexandrova, L. **2004** "Effect of regime of addition of initiator on TEMPO mediated polymerization of styrene" *Polymer Bulletin*, *52*, 339-347.
80. Benoit, D.; Grimaldi, S.; Finet, J. P.; Tordo, P.; Fontanille, M.; Gnanou, Y. **1997** "Controlled free-radical polymerization in the presence of a novel asymmetric nitroxyl radical" *Abstracts of Papers of the American Chemical Society*, *213*, 465-OLY.
81. Benoit, D.; Harth, E.; Fox, P.; Waymouth, R. M.; Hawker, C. J. **2000** "Accurate structural control and block formation in the living polymerization of 1,3-dienes by nitroxide-mediated procedures" *Macromolecules*, *33*, 363-370.
82. Guillaneuf, Y.; Gimes, D.; Marque, S. R. A.; Astolfi, P.; Greci, L.; Tordo, P.; Bertin, D. **2007** "First effective nitroxide-mediated polymerization of methyl methacrylate" *Macromolecules*, *40*, 3108-3114.
83. Wang, Y.; Naulet, F.; Cunningham, M. F.; Hutchinson, R. A. "Nitroxide-mediated semibatch polymerization for the production of low-molecular weight solvent-borne coating resins", In *Advances in Controlled/Living Radical Polymerization*; Matyjaszewski, K., ed. American Chemical Society: Washington, DC, **2003**; pp 466-480.

CHAPTER 3 – EXPERIMENTAL METHODS

3.1 Reagent Purification

Monomer (styrene, Aldrich Canada Ltd.) was washed three times with a 10 w/v % sodium hydroxide solution, washed three times with distilled water, dried over calcium chloride and distilled under vacuum. Solvents such as ethanol, dichloromethane, and acetone used during the course of the experiment and both BPO and TEMPO were used as received from suppliers (ATOFINA Chemicals, and Aldrich, respectively) without further purification. For more detailed discussions see the ampoule polymerization manual [1].

3.2 Polymer Synthesis

Polymerizations were completed in borosilicate glass ampoules (capacity ~ 4 mL). Reagents were weighed, mixed and pipetted into ampoules. Ampoules were then degassed by several vacuum-freeze-thaw cycles, sealed under vacuum with a gas/oxygen torch and then immersed in a silicone oil bath having a temperature control of ± 0.1 °C. Ampoules were removed at selected time intervals to ensure a well-defined conversion versus time plot. Once removed from the bath, the ampoules were placed in liquid nitrogen to stop the polymerization. Ampoules were then thawed, weighed, and opened. The contents were dissolved in dichloromethane, and poured into a flask containing ethanol to precipitate the polymer. The polymer samples were air-dried to remove the solvent and vacuum-dried for three days at approximately 60°C until a constant weight was reached [2].

3.3 Polymer Characterization

3.3.1 Gravimetry

Conversion levels were determined by gravimetry. Gravimetry involves comparing the weight of isolated polymer to the weight of the monomer initially added in the ampoule as shown below:

$$\text{conversion \%} = \frac{\text{mass of polymer}}{\text{initial mass of monomer in ampoule}} \times 100 \quad (3.1)$$

When that PS-TEMPO (polystyrene capped with TEMPO) was used as initiator, the mass of initiator was subtracted from the amount of polymer produced.

3.3.2 Size Exclusion Chromatography

Size exclusion chromatography (SEC), also referred to as gel permeation chromatography (GPC), is the most popular and convenient method for determining average molecular weights and molecular weight distribution (MWD) of a polymer. As its name implies, SEC works on the principle of size exclusion. A very low concentration of polymer solution is passed through a column of porous particles. The molecules that are large cannot enter the pores of the packing and as such, they elute faster. Smaller molecules that can penetrate or diffuse into the pores are retained in the column and elute at a later time. Thus a sample is fractionated by molecular hydrodynamic volume and the resulting profile describes the molecular weight distribution. A concentration detector (e.g., differential refractometer (RI) or UV detector) is placed downstream of the columns to measure the polymer concentration of each fraction as a function of time. The actual method for determining molecular weight averages and the MWD depends upon the presence of any accompanying detectors. For comprehensive information on SEC refer to "Size Exclusion Chromatography" by Mori and Barth [3].

In this study, two SEC setups were employed in the characterization of polymer samples. Both systems were maintained at 30 °C with tetrahydrofuran as the mobile phase flowing at a rate of 1.0 mL/min. The first set up consisted of a Waters solvent delivery system and autosampler followed by Viscotek's quad detector equipped with a UV detector, low- and right-angle laser light scattering detectors (LALLS/RALLS), differential refractometer (RI) and viscometer in series. One PLgel 10 µm guard column (50×7.5mm, Polymer Laboratories Ltd.) and three HR-5E columns (300 × 7.5 mm, Waters) were used with the detectors. The laser operated at 670 nm and the light-scattering intensity was measured at 7° (LALLS) and 90° (RALLS) [4]. Data analysis for this system was performed using OmniSEC version 3.0 (Viscotek).

In order to check the reproducibility of the molecular weight analysis, independent replicate injections were carried out with a different SEC/GPC setup. The second setup consisted of a Waters size exclusion chromatograph equipped with a multi-angle laser light scattering (MALLS) detector (DAWN DSP, Wyatt Technology Corp.) followed by a refractive index (RI) detector (2410 RI, Waters) in series. This SEC was equipped with one PLgel 10 μm guard column (50 \times 7.5 mm) and three PLgel 10 μm MIXED-B columns (300 \times 7.5 mm) (Polymer Laboratories Ltd.). The DAWN DSP laser operated at 633 nm and the light-scattering intensity was measured at 18 angles between 14 and 152°. Molecular weights were determined using Astra version 4.7 software (Wyatt Technology Corp.).

The polymer was dissolved in THF to obtain concentrations of \sim 0.2 wt% and the injection volume varied between 100 and 200 μL [5]. Prior to injection, polymer solutions were filtered through a 0.45 μm filter to remove any insoluble gels, if present. The second virial coefficient for the light-scattering equation was assumed to be negligible as very low concentrations of polymer were employed. The specific refractive index increment (dn/dc) value of 0.185 mL/g was used in the light scattering analysis for polystyrene (PS).

3.4 References

1. McIsaac, S. L., Dube, M. A., Gao, J., and Penlidis, A. (1993) "Experimental procedures for ampoule polymerization", Internal Report, Department of Chemical Engineering, University of Waterloo, Waterloo, Canada
2. McManus, N. T.; Penlidis, A. 1996 "A kinetic investigation of styrene ethyl acrylate copolymerization" *Journal of Polymer Science Part A-Polymer Chemistry*, 34, 237-248.
3. Mori, S.; Barth, H. G. "Size Exclusion Chromatography", ed., Springer: New York, 1999.
4. Scolah, M. J. (2005) "Experimental and modeling investigation of a novel tetrafunctional initiator in free radical polymerization" PhD Thesis/Dissertation, Department of Chemical Engineering, University of Waterloo, Waterloo, Canada
5. Scolah, M. J., McManus, N. T., and Penlidis, A. (2004) "GPC operating manual", Internal Report, Department of Chemical Engineering, University of Waterloo, Waterloo, Canada

CHAPTER 4 – RESULTS AND DISCUSSION

4.1 Design and Summary of Experiments

In order to maximize the information content and be able to draw valid conclusions from experimental work, it is crucial to have a reasonable experimental design. Thus, it was important to run experiments over a range of operating conditions, which include: the full conversion range, at least two different temperatures, and several [TEMPO]/[BPO] molar ratios.

The details of experiments conducted are summarized in Table 4.1. It had been shown in the literature that in order to have TEMPO act efficiently as a mediator, the polymerization temperature should be sufficiently high, at least 115 °C [1]. Therefore, experiments were carried out at two different temperatures (120, 130 °C).

The molar ratio of TEMPO to BPO affects both the reaction rate and the polydispersity. It has been shown in the literature that typical [TEMPO]/[BPO] ratios are from about 0.5 to 2 [1, 2]. It has also been found that in order to maintain the characteristics of controlled polymerization, the [TEMPO]/[BPO] ratio cannot drop below 0.5. On the other hand, excess amounts of nitroxide in the system will slow down the polymerization rate to impractical values. These observations motivated our studies, to explore the influence of [TEMPO]/[BPO] ratio on polymerization rate and molecular weights and thus, find a region in which we have optimal conditions with respect to productivity (rate) and quality (molecular weights). A series of styrene polymerizations were performed varying the TEMPO to BPO ratio from 0.9 to 1.5 and the results are shown in section 4.3.1. It can be seen in the third column of Table 4.1 that the initial initiator concentration (benzoyl peroxide; BPO) was kept constant for runs 1-4 and 8-10, at 0.036 M (1 wt% with respect to monomer), while TEMPO concentration was changed to give different TEMPO/BPO molar ratios.

To investigate the contribution of thermal self-initiation of styrene in NMRP, runs were performed in the absence of initiator (BPO) at both temperatures (runs 6, 12). As a control,

thermal (self) initiation of styrene in the absence of both nitroxide and initiator was performed at both temperatures (runs 5, 11). The results are discussed in section 4.4.

Finally, an additional run (run # 7) was conducted in the presence of a unimolecular initiator. It was instructive to compare the unimolecular initiation with the corresponding bimolecular initiating systems. The results are presented in section 4.5.

It is important to make sure that the experimental data obtained are reliable and error in each section of the experiment is at a minimum. To do so, individual ampoule replicates were taken out of the oil bath at specific times to check the sampling error. In addition, in order to check the reproducibility of data, completely independent replicates were conducted for runs 2, 7, 9, 10 and 12. Reliability of molecular weight measurements was checked by running GPC replicates at different times. In addition, during GPC analysis, two independent injections were done for every sample. Molecular weight values plotted in subsequent figures are averages from these two injections. Tables A.1 to A.26 in Appendix A cite the raw data for monomer conversion, average molecular weights and polydispersity for the figures used in this chapter.

Table 4.1 Summary of experimental runs

Experiment #	Temperature (°C)	[BPO] ₀ M	[TEMPO] / [BPO]	Remarks
1	120	0.036	0.9	
2		0.036	1.1	+ Replicate
3		0.036	1.2	
4		0.036	1.5	
5		Nil	-	Thermal (self) initiation of styrene
6		Nil	-	Styrene with TEMPO only
7		Nil	-	Styrene with unimolecular initiator + Replicate
8	130	0.036	0.9	
9		0.036	1.1	+ Replicate
10		0.036	1.3	+ Replicate
11		Nil	-	Thermal (self) initiation of styrene
12		Nil	-	Styrene with TEMPO only + Replicate

4.2 Typical Styrene Reaction Profiles in NMRP

Styrene polymerizations in the presence of TEMPO and a conventional initiator (bimolecular NMRP) have been studied for a number of years. Georges et al. [1] initiated these investigations and have since produced many studies examining specific aspects of NMRP (See Table 2.3). However, despite the numerous studies carried out, the existing experimental studies are still limited, conducted over a narrow range of reaction conditions that can not reliably be used as a base for comprehensive kinetic modeling studies.

Figure 4.1 shows conversion vs. time for nitroxide-mediated radical polymerization (NMRP) of styrene at 120°C with TEMPO to BPO molar ratio of 1.1:1 ($R = [\text{TEMPO}] / [\text{BPO}] = 1.1$). The data are quite distinct from those seen for regular free radical polymerization of styrene at these temperatures, the most obvious feature being that the reaction rate is relatively slow. In typical free radical polymerization of styrene, complete conversion is essentially achieved after 5 hrs [3], whereas for the NMRP reaction, due to the presence of TEMPO as the mediator, only about 30% conversion was achieved in that time.

An independent replicate run was conducted to obtain an idea of the reproducibility of our data. It can be seen that data from the two experiments agree very well and the standard error in conversion measurements is $\sim 1.5\%$, showing good reproducibility. For detailed error measurements see Table A.27 in Appendix A.

Figure 4.2 shows a linear relationship between logarithmic monomer concentration and time which is characteristic of a living system (the slope in the first order kinetic plot is the product of rate constant of propagation and the concentration of growing radicals, $[\text{R}\cdot]$; linear kinetic plots indicate a rather constant value of $[\text{R}\cdot]$). It is observed that the living behavior seems to be gradually lost after about 20 hrs (corresponding to about 75% monomer conversion in Figure 4.1). After that time, there is some tailing off in rate as the monomer is depleted. As discussed in subsection 2.1.2, radicals are lost in termination reactions at higher conversions. Since $[\text{R}\cdot]$ drops, the rate of deactivation dominates over propagation and the discrepancy from linearity is observed. This behavior again is quite different from the regular free radical

polymerization in which acceleration in rate at some point in the low or intermediate conversion ranges is observed that is related to diffusional effects in the reaction.

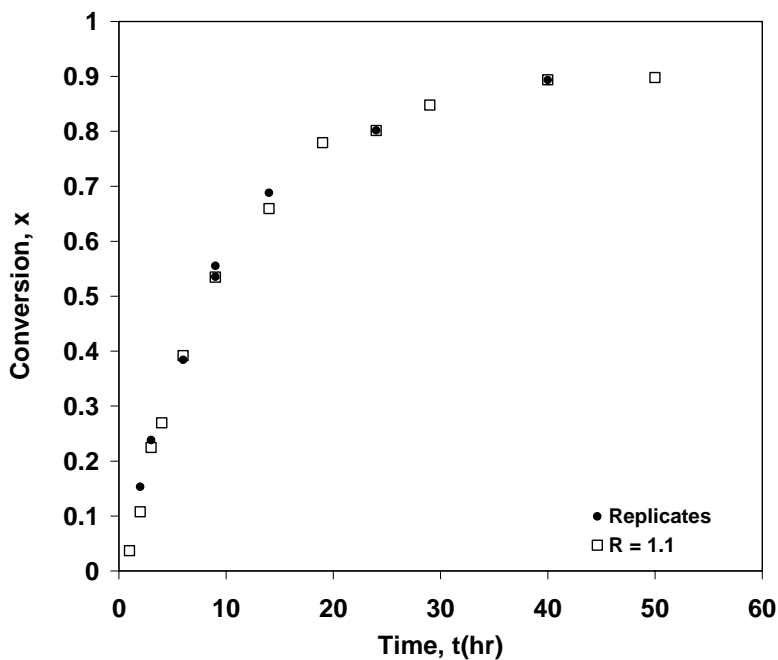


Figure 4.1 Monomer conversion vs. time for NMRP of styrene at 120°C and $R = [\text{TEMPO}]/[\text{BPO}] = 1.1$ (Run #2)

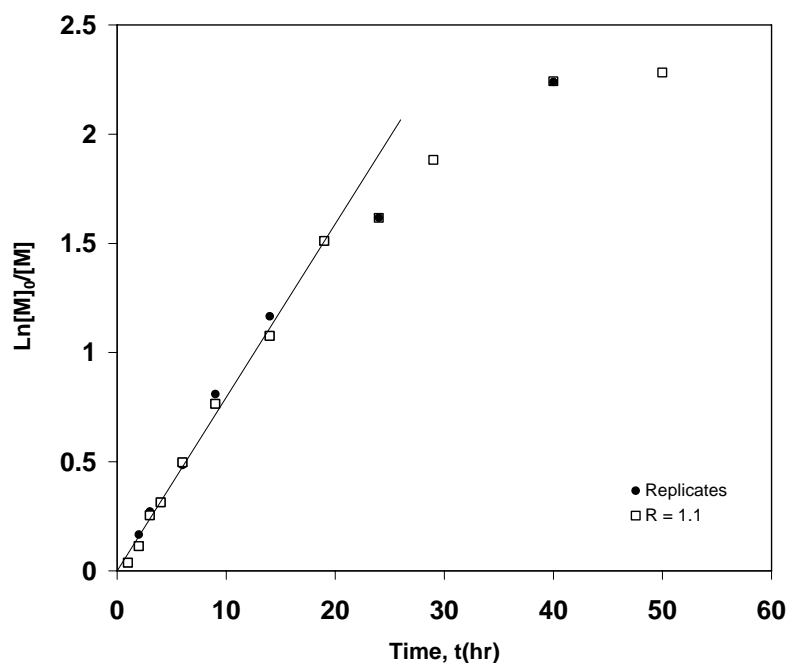


Figure 4.2 First order rate plot for NMRP of styrene at 120°C and $R = [\text{TEMPO}]/[\text{BPO}] = 1.1$

Average molecular weight data, M_n and M_w , are shown in Figure 4.3. A linear relationship with conversion is observed up to about 80% monomer conversion, which serves as another indicator of living/controlled behavior of the polymerization system. This behavior is again quite different from regular radical polymerization, in which the molecular weights of the polymer are independent of conversion. Polydispersities (PDI) vs. conversion are illustrated in Figure 4.3 as well. As can be seen the polydispersity values vary in the range of 1.05 to 1.2, which is well below the typical values for regular free radical polymerization (~ 2 , and above). Run # 2, NMRP of styrene at 120°C with TEMPO to BPO molar ratio of 1.1:1, will act as the base case for TEMPO/BPO ratio comparisons at 120°C in the next section (4.3.1)

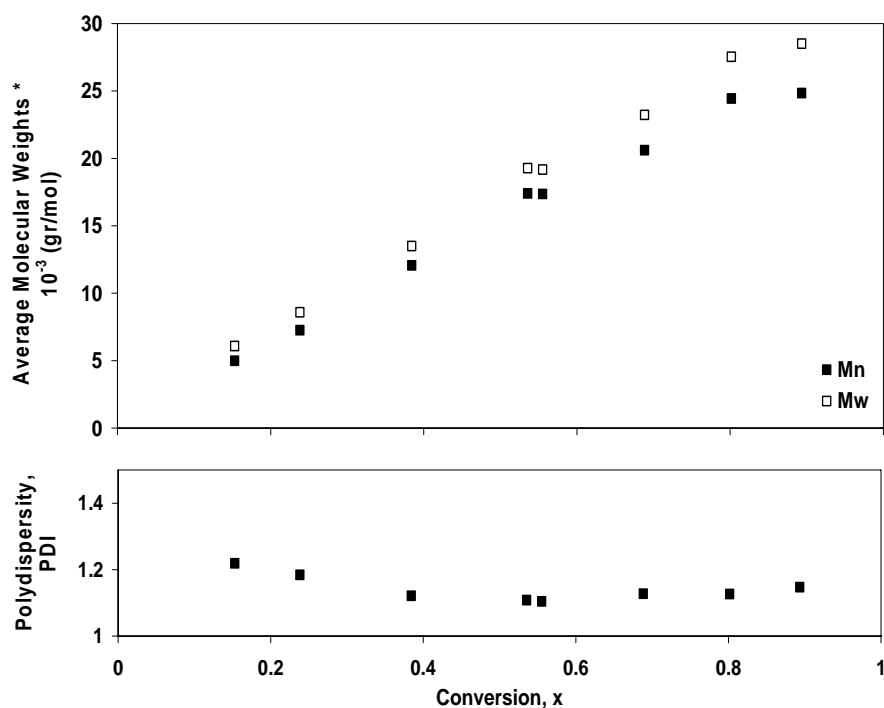


Figure 4.3 Average molecular weights and polydispersity vs. conversion for NMRP of styrene at 120°C and $R = [\text{TEMPO}]/[\text{BPO}] = 1.1$

4.3 Bimolecular NMRP

Figure 4.4 shows the basic steps during the bimolecular nitroxide-mediated radical polymerization of styrene in the presence of TEMPO as the nitroxide radical and benzoyl peroxide (BPO) as the radical initiator (see section 2.2.2.1). The first step is thermal decomposition of BPO into benzoyloxy primary radicals with high reactivity (1), which initiate the polymerization of styrene by attacking the carbon-carbon double bond (2). Radicals with chain length unity will then propagate (3) until they are trapped by TEMPO radicals. The TEMPO radical makes a labile bond (C–O) with the radical chain, leading to the formation of alkoxyamines in situ. As it was mentioned in section 2.2.2.1, the C–O bond is relatively weak at temperatures greater than 100 °C so it reversibly dissociates, establishing the activation-deactivation equilibrium between dormant and active chains (4).

As mentioned in Chapter 2, the core reaction in NMRP is the equilibrium between active and dormant species. $[\text{TEMPO}]/[\text{BPO}]$ ratio and temperature are the factors which influence the equilibrium. $[\text{BPO}]$ dictates the concentration of active radicals early in the reaction while TEMPO influences the concentration of dormant species; so obviously $[\text{TEMPO}]/[\text{BPO}]$ ratio is a leading factor in guiding the equilibrium. Ximenes et al. [4] and Bonilla et al. [5] cite the rate constants, k_a and k_d , as functions of temperature; as a result, temperature is the main factor influencing the equilibrium by affecting the individual rate constants for the equilibrium reaction. Effects of $[\text{TEMPO}]/[\text{BPO}]$ ratio and temperature on molecular weights and polymerization rate are discussed in section 4.3.1 and 4.3.2, respectively.

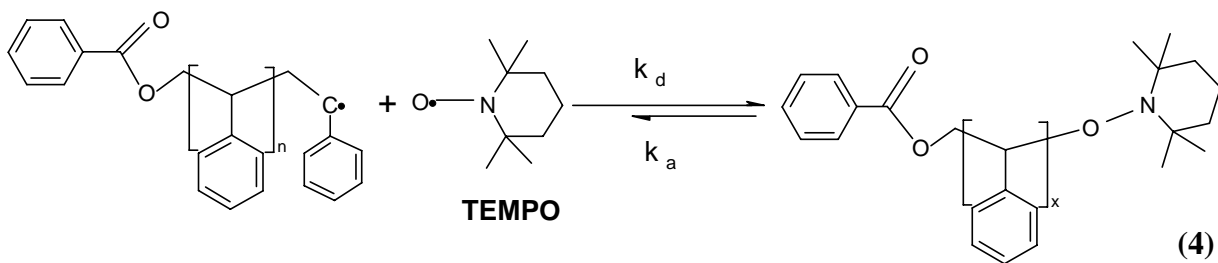
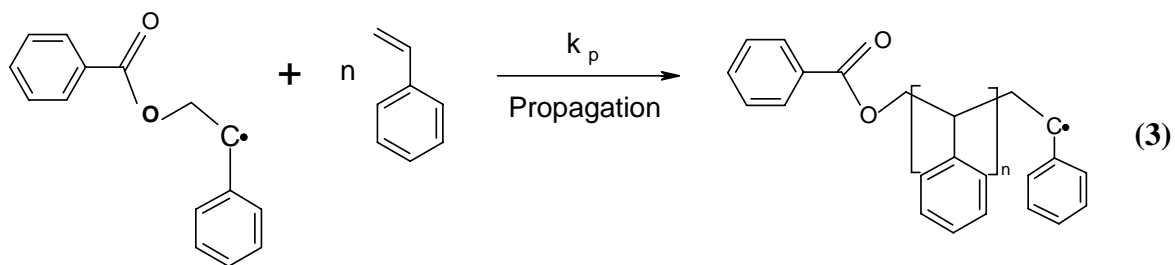
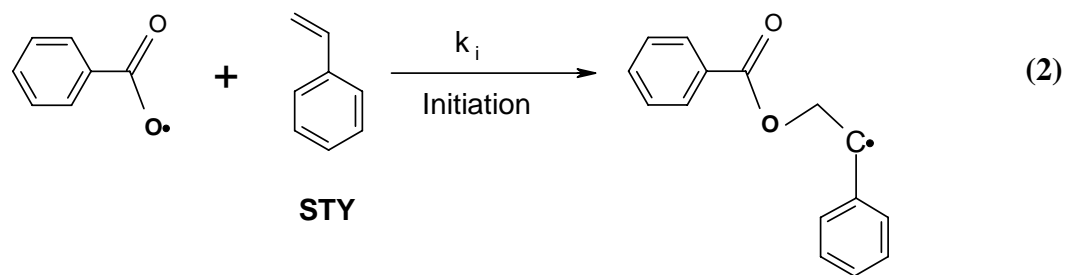
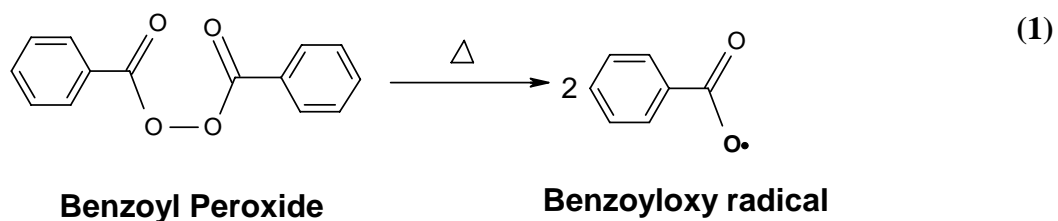


Figure 4.4 Bimolecular NMRP of styrene in the presence of TEMPO and BPO

4.3.1 Effect of [TEMPO]/[BPO] Ratio

Figure 4.5 shows the effect of decreasing the [TEMPO]/[BPO] ratio (R), on rate of polymerization, illustrated as $\ln [M]_0/[M]$ vs. time. As can be seen, decreasing the ratio from 1.1 (our base case) to 0.9, increases the rate of polymerization. Figure 4.6a shows that decreasing the ratio results in higher initial concentration of living radicals. Since the TEMPO concentration is lower at [TEMPO]/[BPO] = 0.9, free radicals cannot all be trapped by TEMPO leading to a decrease in dormant radical concentration in comparison to ratio 1.1 (See Figure 4.6c). Propagation occurs mainly as in the regular radical polymerization for $R = 0.9$, resulting in an increase in dead polymer concentration compared to $R = 1.1$ (See Figure 4.6b). So far, we have established that for $R = 0.9$, relative to $R = 1.1$, the dead polymer concentration (Figure 4.6b) is higher, the dormant radical concentration (Figure 4.6c) is lower, and the living radical concentration (Figure 4.6a) is much higher initially.

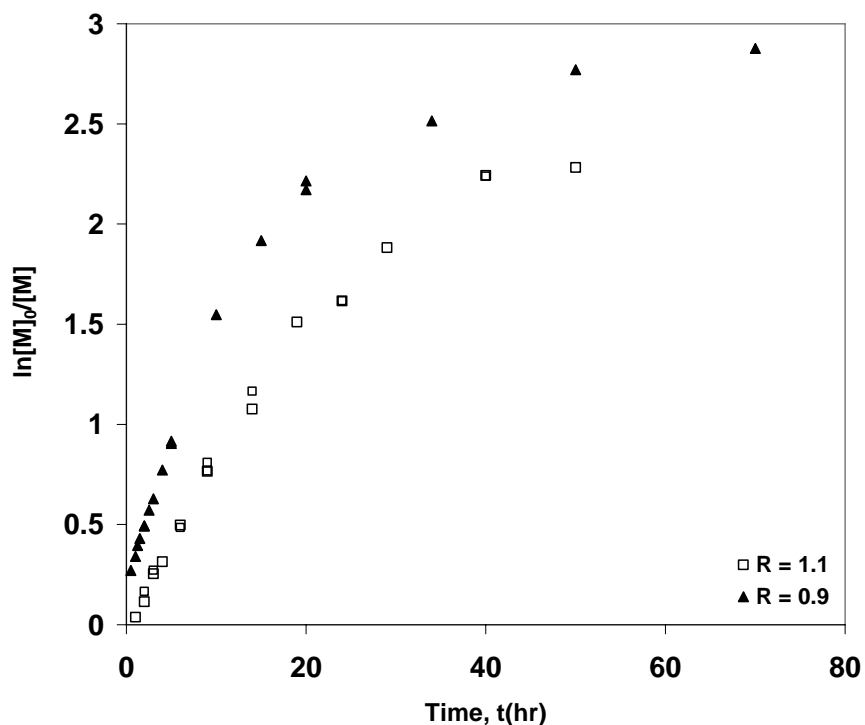
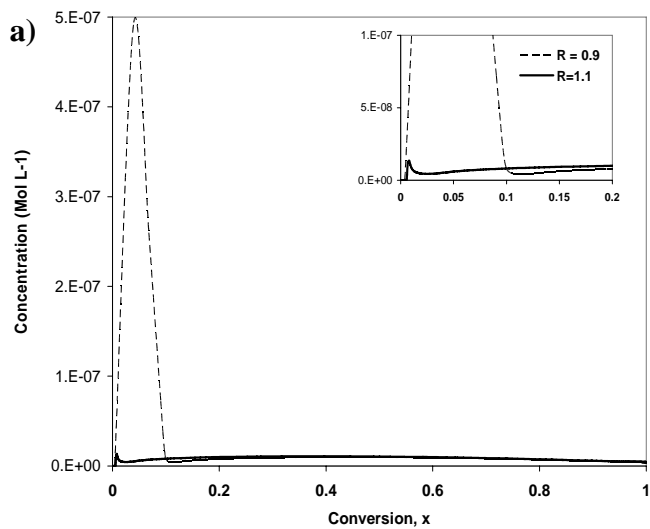


Figure 4.5 Effect of decreasing [TEMPO]/[BPO] ratio (R), on rate of polymerization in NMRP of styrene at 120°C



b)

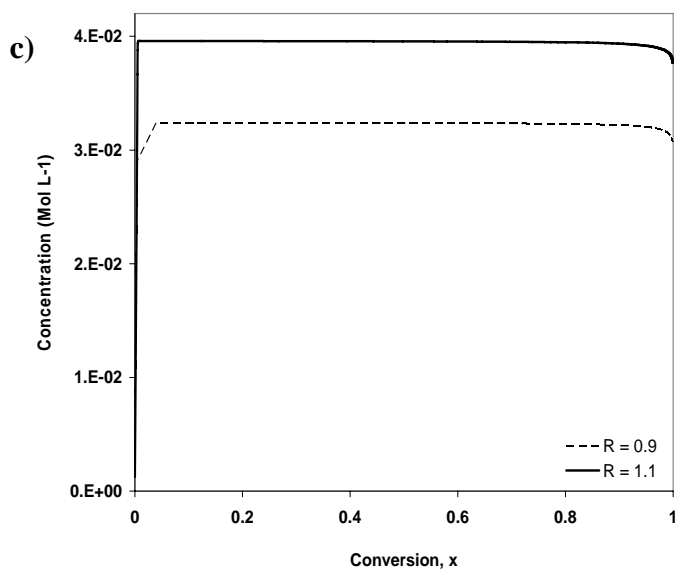
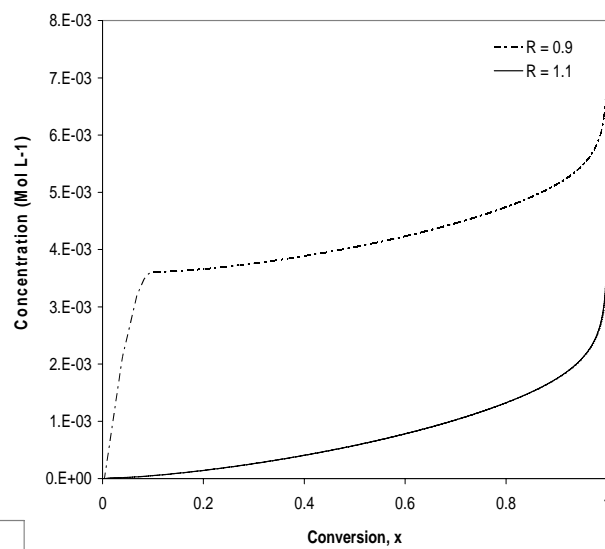


Figure 4.6 Simulated concentrations of: living radicals (a), dead polymer (b), and dormant radicals (c) vs. conversion for $[TEMPO]/[BPO] = 0.9$ and 1.1 at $T = 120^{\circ}C$

Let's now digress a bit and refer to Chapter 5, Eq. 5.26 (the same arguments will hold for Eq. 5.25). It is evident from Eq. 5.26 that if we show that the numerator of the equation is higher for $R = 0.9$, then we would expect that the weight average molecular weight for $R = 0.9$ should be higher (than $R = 1.1$). Careful scrutiny of Eq. 5.26 (along with Figure 4.6) shows that the terms that dominate should be δ_2 and μ_2 . From Eq. 5.21, δ_2 for $R = 0.9$ will be higher (than for $R = 1.1$), since the term $k_a[\delta_2]$ is subtracted, and $[\delta_2]$ is smaller number for $R = 0.9$ (See again Figure 4.6c). In an analogous way, based on Eq. 5.24, μ_2 for $R = 0.9$ will have the tendency to be similar or higher (at least initially, due to larger $[\lambda]$ values; See Figure 4.6a). Hence, the weight average molecular weight (and similarly, the number average molecular weight) will be higher for $R = 0.9$ than $R = 1.1$.

This is exactly what we have observed experimentally: both weight and number average molecular weights are higher at $[\text{TEMPO}]/[\text{BPO}] = 0.9$, as shown in Figures 4.7 and 4.8, respectively. Both number and weight average molecular weights increase linearly at $[\text{TEMPO}]/[\text{BPO}] = 0.9$, showing that polymerization is still controlled at this condition after the initial reaction period. Selective GPC replicates were carried out to check the accuracy of molecular weight measurements at low and high conversions. As can be seen, the results are relatively reproducible. However, it seems that the error in GPC measurements is lower at higher molecular weights. The corresponding conversion vs. time plot is shown in Figure B.1 in Appendix B.

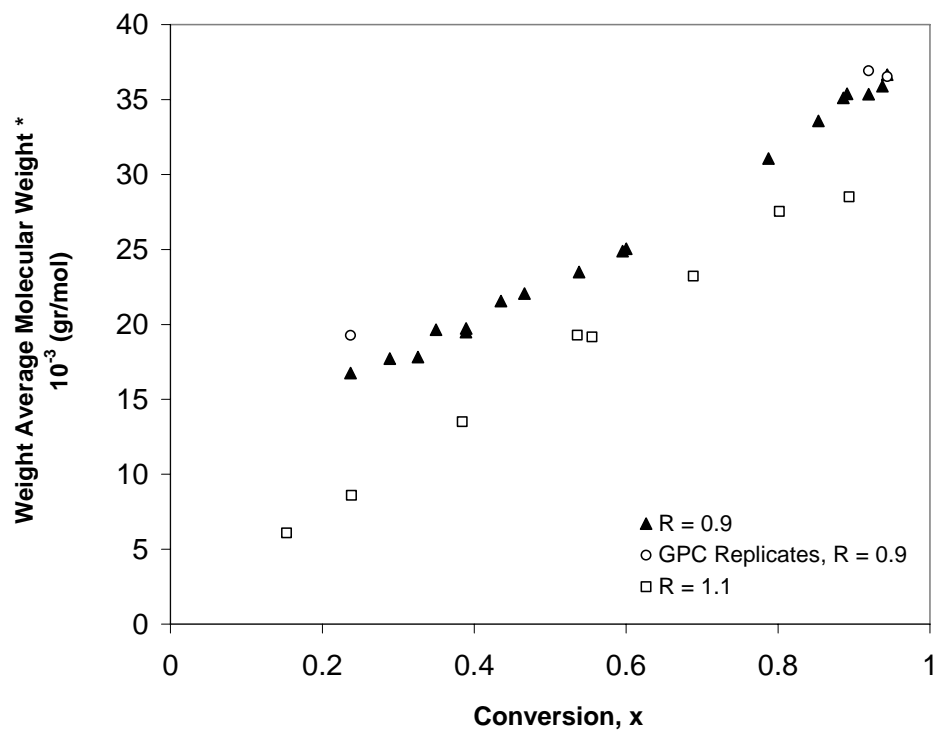


Figure 4.7 Effect of [TEMPO]/[BPO] ratio (R), on weight average molecular weights in NMRP of styrene at 120°C

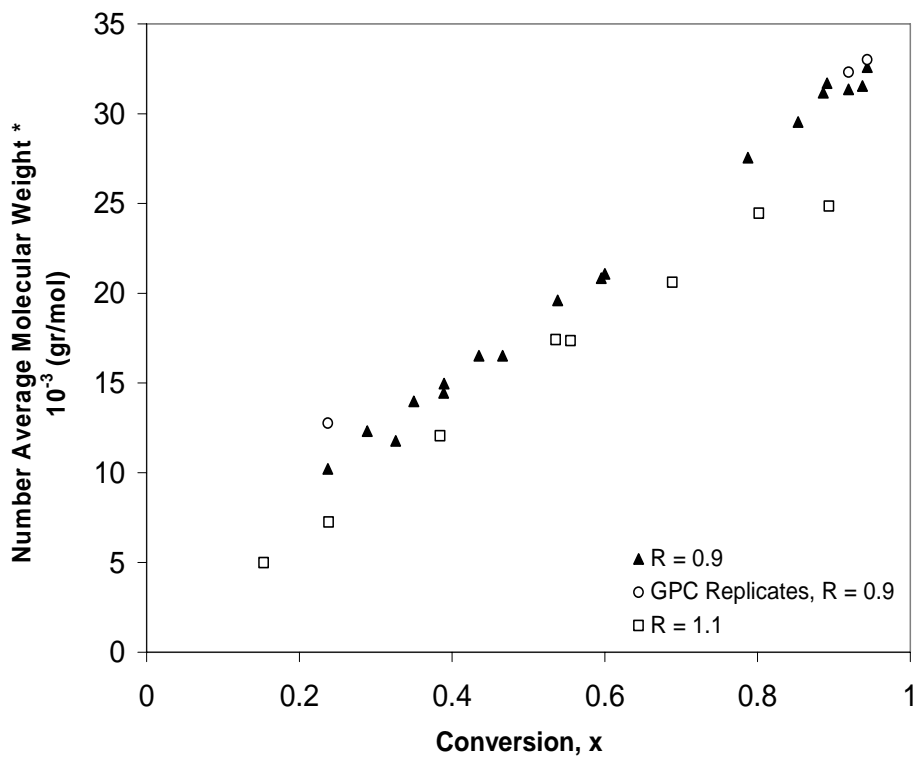


Figure 4.8 Effect of [TEMPO]/[BPO] ratio on number average molecular weights in NMRP of styrene at 120°C

Reducing the [TEMPO]/[BPO] ratio increases the polydispersity at equivalent conversions, for example, from 1.12 at TEMPO/BPO = 1.1 to 1.35 at R = 0.9 at $\approx 40\%$ conversion (see Figure 4.9). Due to the decrease in TEMPO concentration fed to the system and occurrence of “non” controlled polymerization in the initial reaction period, more growing polymer radicals are produced, thus more termination occurs at the same conversion level and a relatively larger fraction of polystyrene (PS) is produced by uncontrolled polymerization (See again Figures 4.6a and 4.6b). However, as conversion increases, polydispersity values become almost identical. For example around 90% conversion, polydispersities are 1.14 and 1.13 for TEMPO/BPO 1.1:1 and 0.9:1, respectively. The reason is that as polymerization proceeds and most polymer molecules are formed by the controlled process (after the initial phase), the fraction of PS produced by uncontrolled process drops and hence over time the cumulative PDI decreases. Since the dormant polymer dominates (See Figure 4.6c), eventually PDI values become almost identical for both values of R.

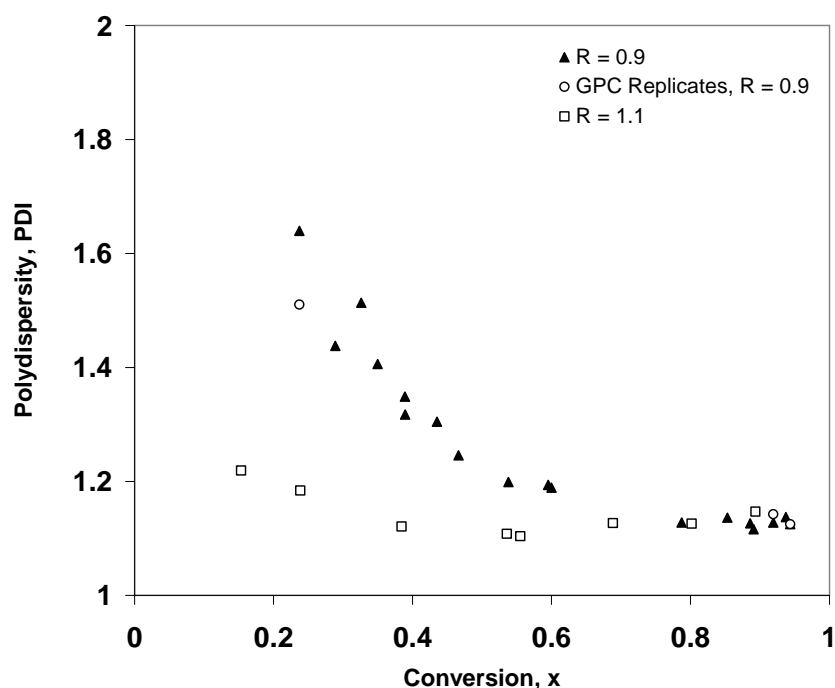


Figure 4.9 Effect of [TEMPO]/[BPO] ratio on polydispersity in NMRP of styrene at 120°C

The individual plots for monomer conversion versus time, average molecular weights and polydispersity versus conversion for NMRP of styrene at 120°C and [TEMPO]/ [BPO] = 0.9 can be found in Figures B.2 to B. 4 in Appendix B.

Figure 4.10 shows the effect of increasing $[\text{TEMPO}]/[\text{BPO}]$ ratio on rate of polymerization, shown as conversion vs. time. Increasing the initial TEMPO concentration decreases the rate of polymerization dramatically. After 10hrs, monomer conversion was around 20% for $[\text{TEMPO}]/[\text{BPO}] = 1.5$ while it was 50% for $[\text{TEMPO}]/[\text{BPO}] = 1.1$.

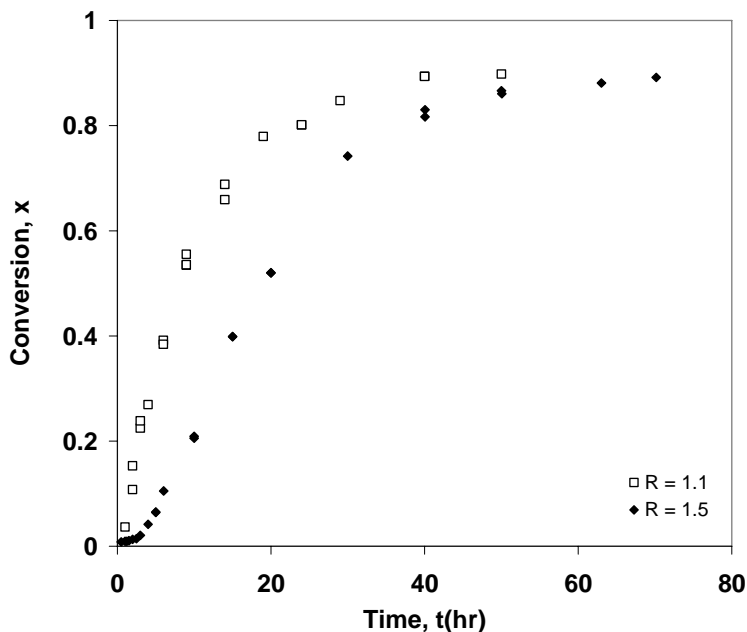


Figure 4.10 Effect of $[\text{TEMPO}]/[\text{BPO}]$ ratio (R), on rate of polymerization in NMRP of styrene at 120°C

In $\text{TEMPO}/\text{BPO} = 1.5$, the concentration of radicals produced by BPO decomposition is lower than the actual concentration of free TEMPO. An excess of free TEMPO remains in the system and it follows that the resulting concentration of living radicals is too small (especially at the beginning) to give significant polymerization rates. Therefore, an induction period arises during which the excess of free TEMPO is consumed by thermally produced radicals. This induction period (about 3hrs as seen in Figure 4.10) can also be confirmed by looking at the simulated results of Figure 4.11. Specifically, one can clearly see from Figure 4.11b that with $R = 1.5$ the living radical concentration profile behaves very differently from that of $R = 1.1$ (with the concentration being almost zero during the initial phase). Eventually, the living radical concentration for $R = 1.5$ starts to build up (See Figure 4.11b), so polymerization proceeds but with a slower rate in comparison to ratio $R = 1.1$ due to the higher concentration of dormant radicals present (See Figure 4.11c). The corresponding first order plot is shown in Figure B.5 in Appendix B.

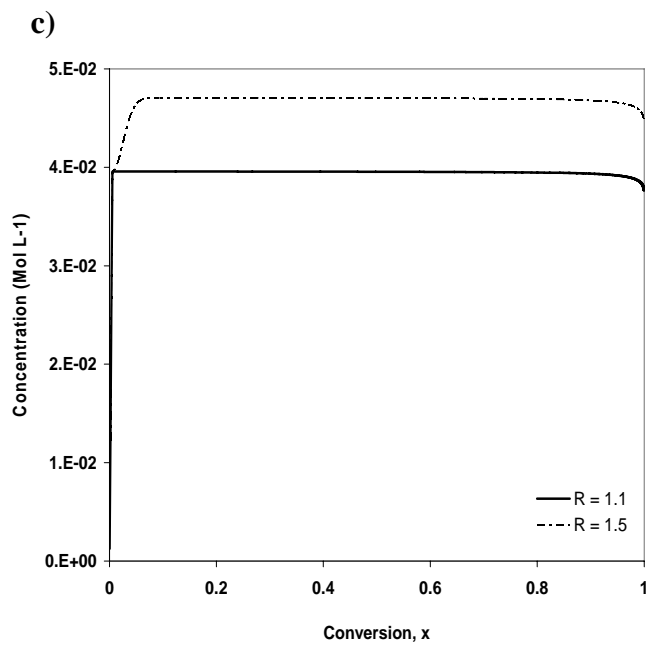
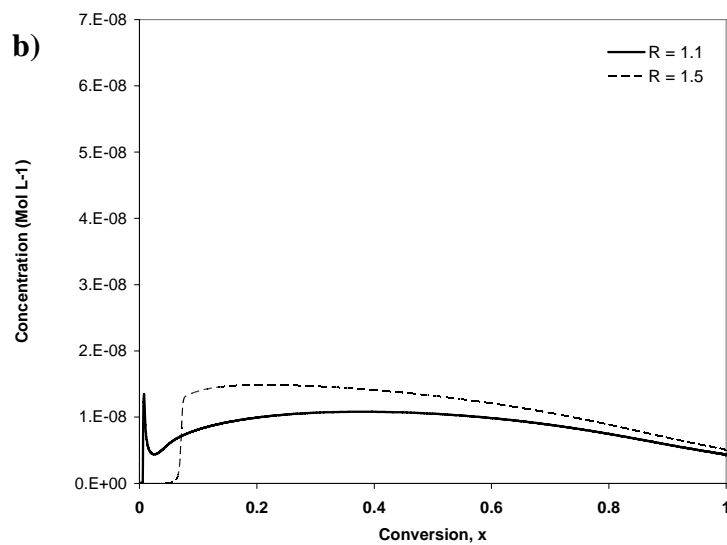
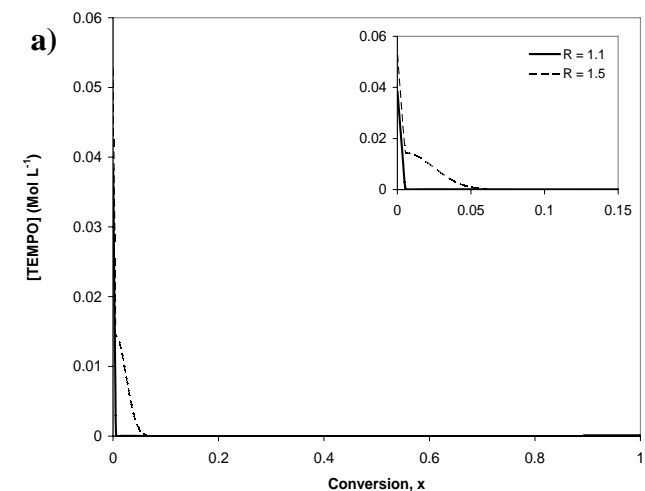


Figure 4.11 Simulated concentrations of: free TEMPO (a), living radicals (b), and dormant radicals (c) vs. conversion for $[\text{TEMPO}]/[\text{BPO}] = 1.1$ and 1.5 at $T = 120^\circ\text{C}$

Figures 4.12 and 4.13 show the corresponding profiles for number and weight average molecular weights, respectively. It is observed that slightly lower average molecular weights (M_w and M_n), are obtained when the $[TEMPO]/[BPO]$ ratio is increased (the explanation is the same as discussed earlier for Figures 4.7 and 4.8 for ratios 0.9 and 1.1). As expected for any CRP process, molecular weights increase linearly with conversion (the linear increase of molecular weights with conversion indicates that the proportion of chains that are self-initiated and terminated is low). Again selective independent GPC replicates for ratio 1.5 show good reproducibility of average molecular weight measurements.

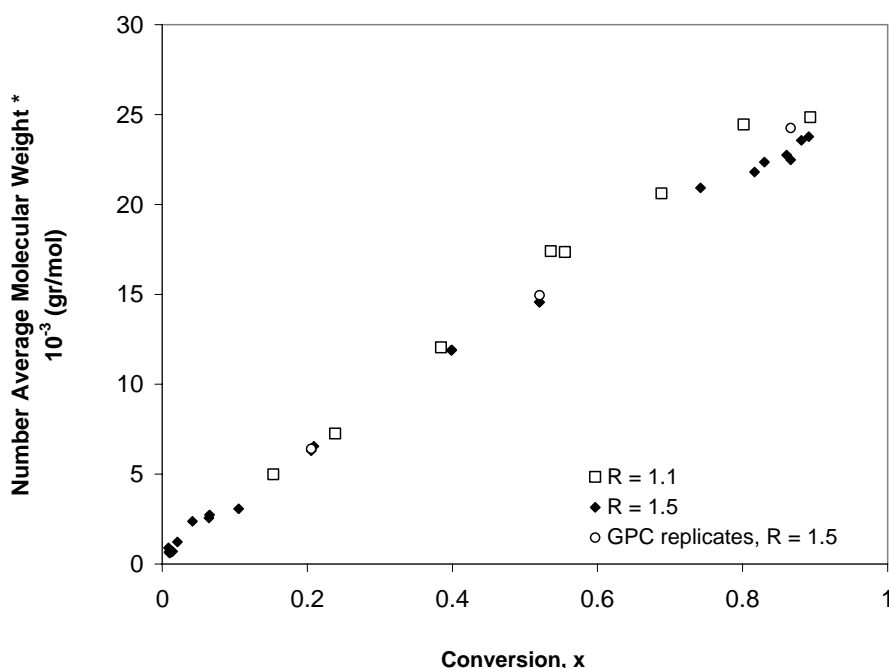


Figure 4.12 Effect of $[TEMPO]/[BPO]$ ratio on number average molecular weights in NMRP of styrene at 120°C

Figure 4.14 shows the polydispersity (PDI) vs. conversion. Frequent sampling for the $[TEMPO]/[BPO]$ ratio of 1.5 was carried out at the beginning of the reaction to capture the initial changes in polydispersity values. Rather large changes in PDI values had been predicted in earlier modeling work [6] but never captured experimentally. This is the first time that such corroborating observations have been made. As can be seen in the insert of Figure 4.14, PDI values do not show much difference for different ratios after 20% conversion and very low values, below 1.2, are obtained. Individual plots for monomer conversion versus time, average

molecular weights and polydispersity versus conversion for NMRP of styrene at 120°C and $[TEMPO]/[BPO] = 1.5$ can be found in Figures B.6 to B.8 in Appendix B.

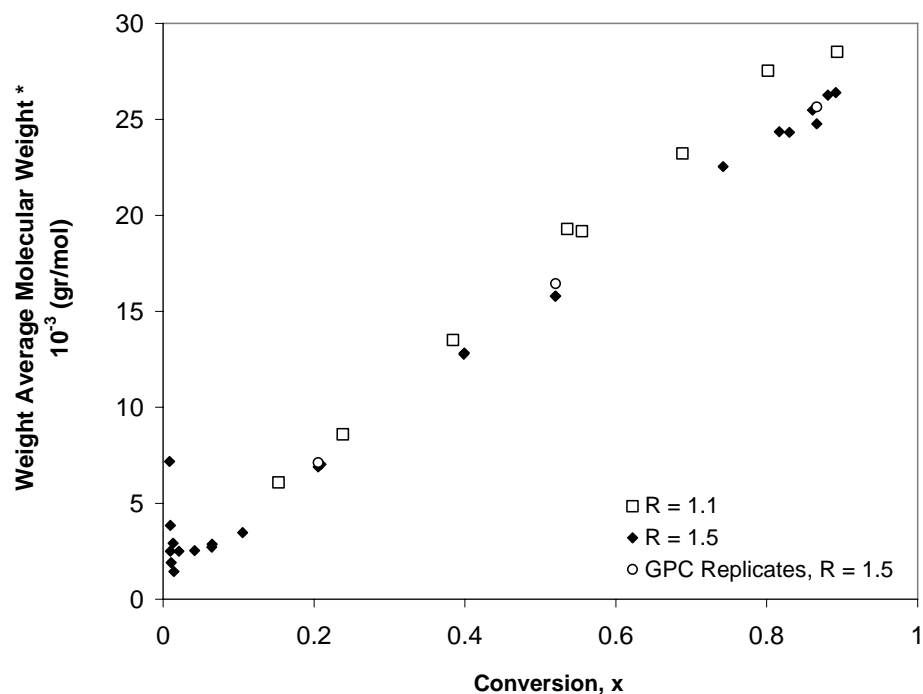


Figure 4.13 Effect of $[TEMPO]/[BPO]$ ratio on weight average molecular weights in NMRP of styrene at 120°C

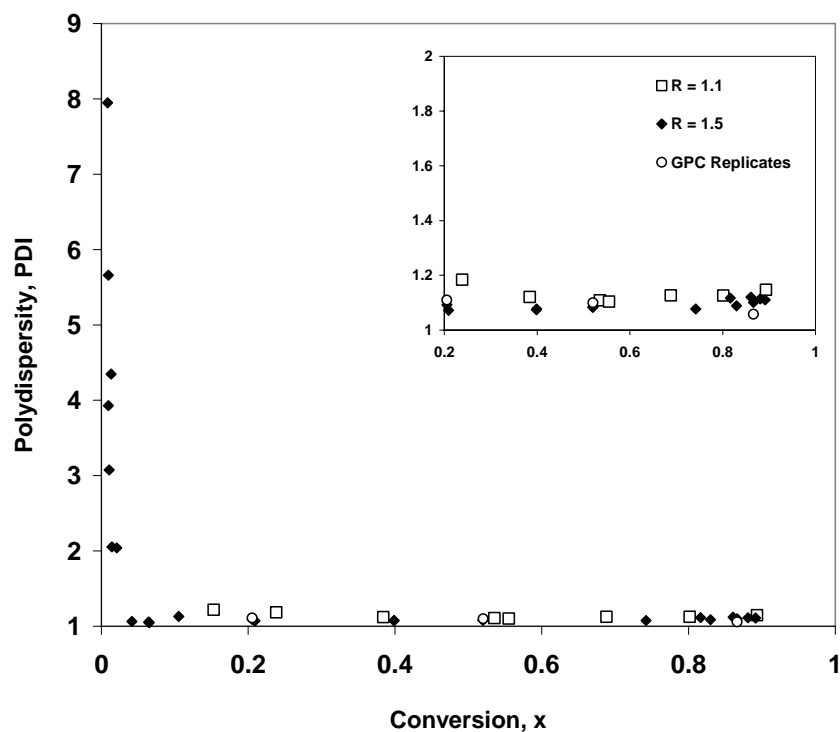


Figure 4.14 Effect of $[TEMPO]/[BPO]$ ratio on polydispersity in NMRP of styrene at 120°C

Figures 4.15 through 4.18 show the full picture of the effect of [TEMPO]/ [BPO] molar ratio on polymerization rate (expressed as conversion versus time), corresponding profiles for number and weight average molecular weights and polydispersity (PDI) vs. conversion at 120°C. As expected, the larger the ratio (the more TEMPO in the recipe), the slower the polymerization proceeds (See Figure 4.15). Polymerization rates are quite similar for TEMPO/BPO = 1.1 and 1.2. Figures 4.16 and 4.17 show number and weight average molecular weights, M_n and M_w . These values, as expected for any CRP process, increase linearly with conversion. It can also be observed that higher values of these averages are obtained as the [TEMPO]/[BPO] ratio decreases. The differences are smaller at low conversion levels but differentiation is clear as conversion level increases. Figure 4.18 shows that the PDI values do not show much difference for various ratios. Very low values, between 1.07 and 1.2, are obtained. The corresponding first order plot can be found in Figure B.9 in Appendix B. Individual plots for monomer conversion versus time, average molecular weights and polydispersity versus conversion for NMRP of styrene at 120°C and [TEMPO]/ [BPO] = 1.2 are also available in Appendix B (Figures B.10 to B.12).

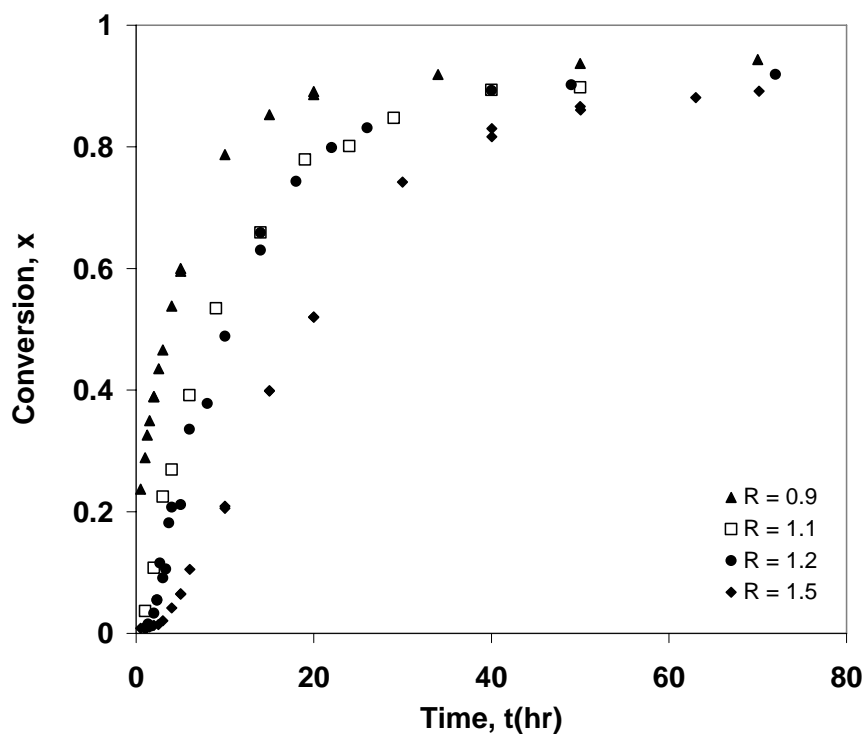


Figure 4.15 Effect of [TEMPO]/ [BPO] ratio on polymerization rate at 120°C

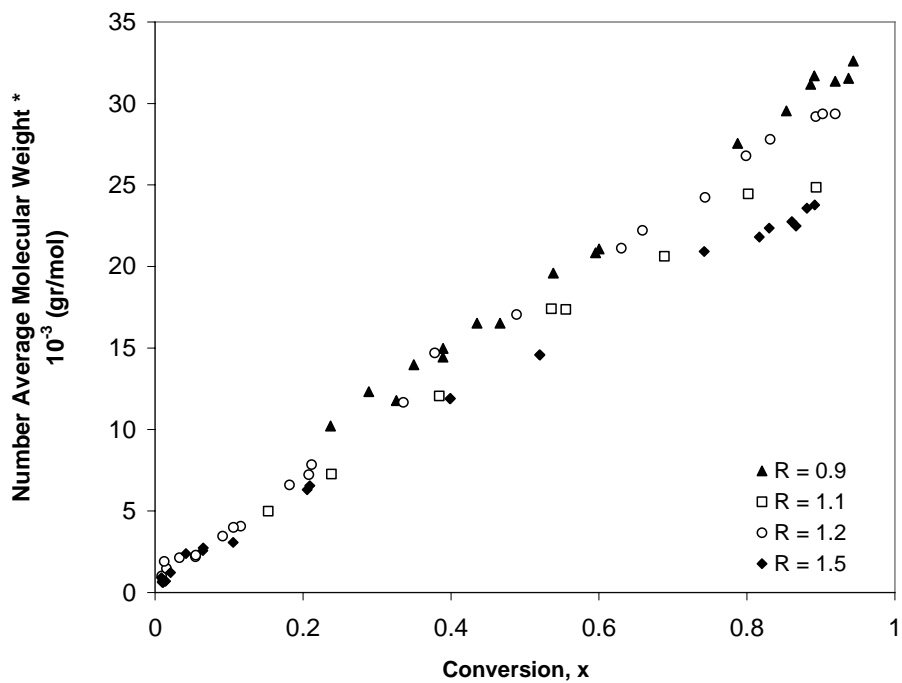


Figure 4.16 Effect of [TEMPO]/ [BPO] ratio on number average molecular weight at 120° C

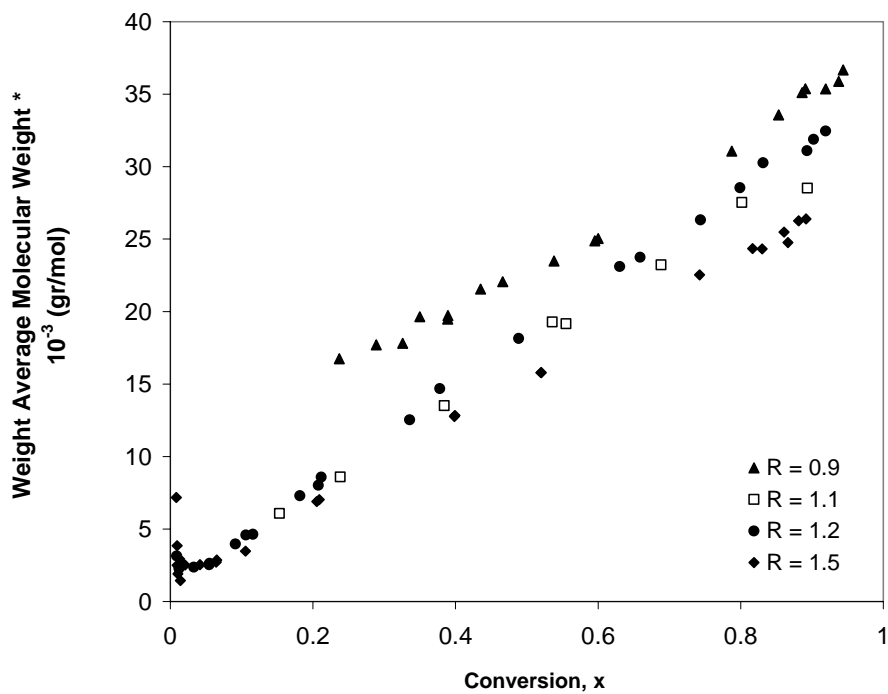


Figure 4.17 Effect of [TEMPO]/ [BPO] ratio on weight average molecular weight at 120° C

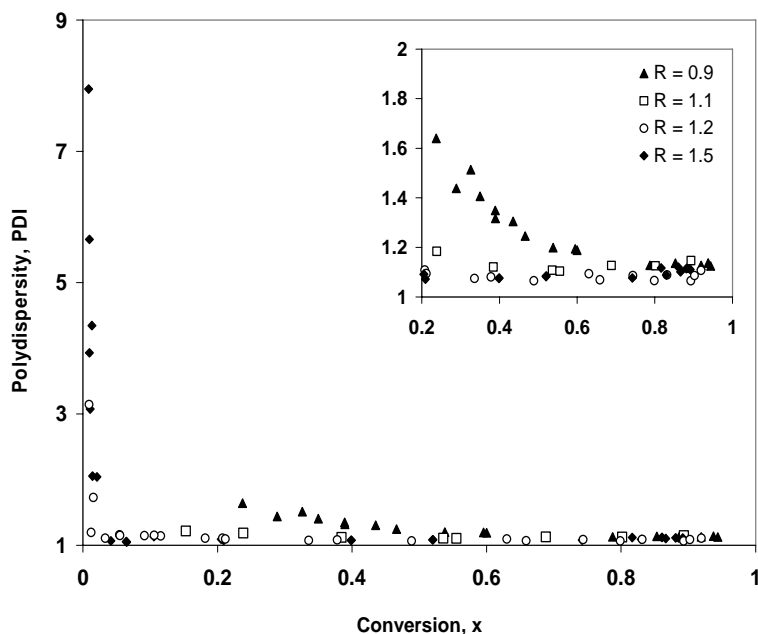


Figure 4.18 Effect of [TEMPO]/ [BPO] ratio on polydispersity, PDI, at 120° C

The experimental data for conversion vs. time, M_n and M_w vs. conversion, and PDI vs. conversion for the NMRP of styrene at 130°C and [TEMPO] / [BPO] = 0.9, 1.1 and 1.3 are shown in Figures 4.19 to 4.22. The general trends are similar to the ones observed at 120°C, accounting of course for the temperature effect. However, the effect of [TEMPO]/[BPO] ratio on polymerization rate and molecular weights at 130°C is not as pronounced as it is at 120°C. We tried to explain the more pronounced effect of R on rate and molecular weights by considering the following group:

$$Q = K (k_p [M]) \frac{[R - X]}{[X \cdot]} \quad (4.1)$$

Nomenclature in Eq. 4.1 is the same as in Section 2.2.3.2. Q in Eq. 4.1 is the expression that describes the rate of polymerization (under certain special conditions to be discussed below) for NMRP.

We plotted Q versus both time and conversion for different values of R at the two different temperatures. We also magnified the differences between curves in the early stages of polymerization. If we had observed that differences between Q-curves corresponding to two values of R were more pronounced over the course of the polymerization at 120 °C rather than

130 °C, then we would be able to explain the experimental observation that the effect of R at 130 °C is not as pronounced as it is at 120 °C. However, the modeling analysis showed either no significant differences or larger differences at 130 °C (opposite to our statement based on our experimental results). At this point, one speculation that we could put forward would be that maybe there was more experimental error at 120 °C, which made the experimental curves at 120 °C look more dispersed than at 130 °C. However, a careful analysis of experimental error (based on all data collected at 120 °C and 130 °C and their replicates, as cited in Appendix A) showed that the errors at the two temperatures were comparable (in fact, if anything, the error was slightly smaller at 120 °C than at 130 °C; for example, for conversion, we established an error of 0.02 at 120 °C vs. 0.03 at 130 °C). A second possible speculation is related to the derivation of Q in Eq. 4.1 above. Eq. 4.1 assumes that $(d[X\bullet]/dt)$ is close to zero (a common assumption to simplify kinetic model equations; see also subsection 2.2.3.2). However, as discussed in detail in Saldivar-Guerra et al. [7], $(d[X\bullet]/dt)$ should never be completely neglected. If neglected during the analysis, considerable error may be introduced and hence large changes may be observed in the predicted course of polymerization. This may explain why the Q-group of Eq. 4.1 was not able to explain the experimentally observed differences.

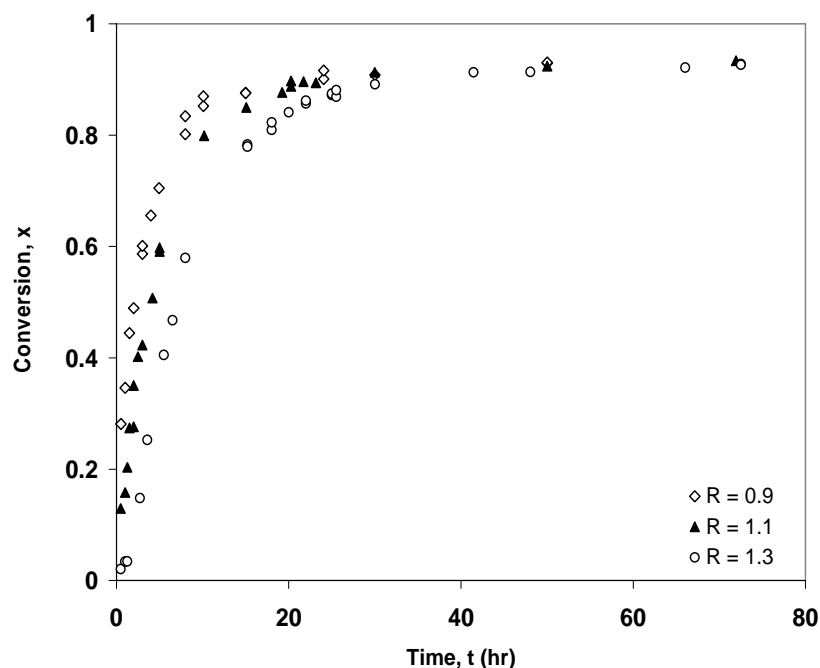


Figure 4.19 Effect of $[TEMPO]/[BPO]$ ratio on polymerization rate at 130°C

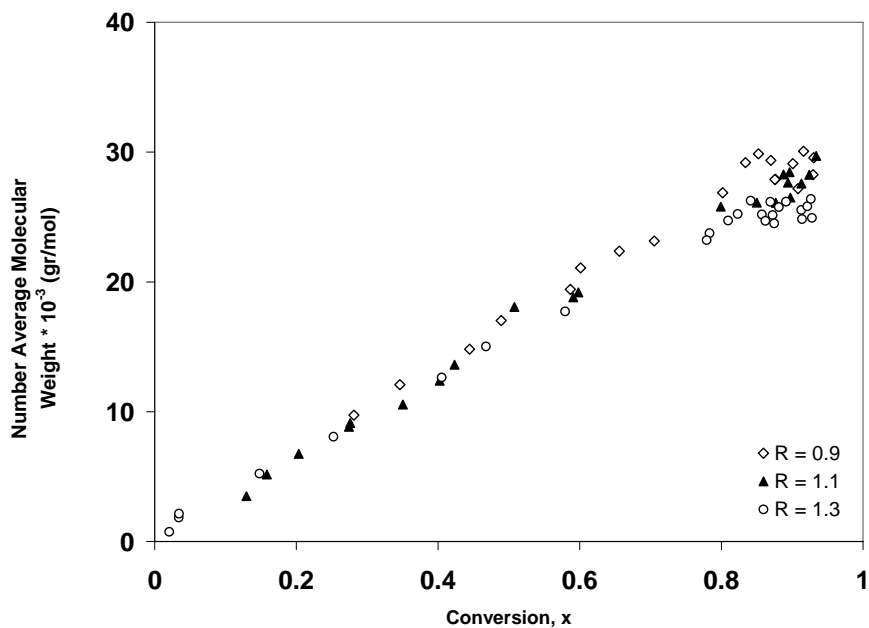


Figure 4.20 Effect of [TEMPO]/ [BPO] ratio on number average molecular weight at 130° C

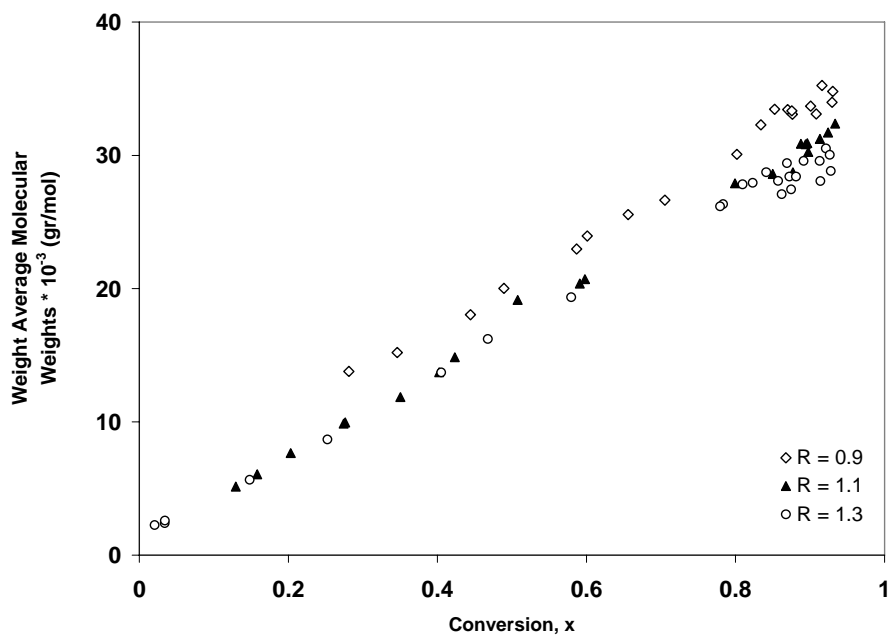


Figure 4.21 Effect of [TEMPO]/ [BPO] ratio on weight average molecular weight at 130° C

The individual plots for monomer conversion versus time, average molecular weights and polydispersity versus conversion for NMRP of styrene at 130°C and [TEMPO]/ [BPO] = 0.9, 1.1 and 1.3 are shown in Figures B.13 to B.19 in Appendix B.

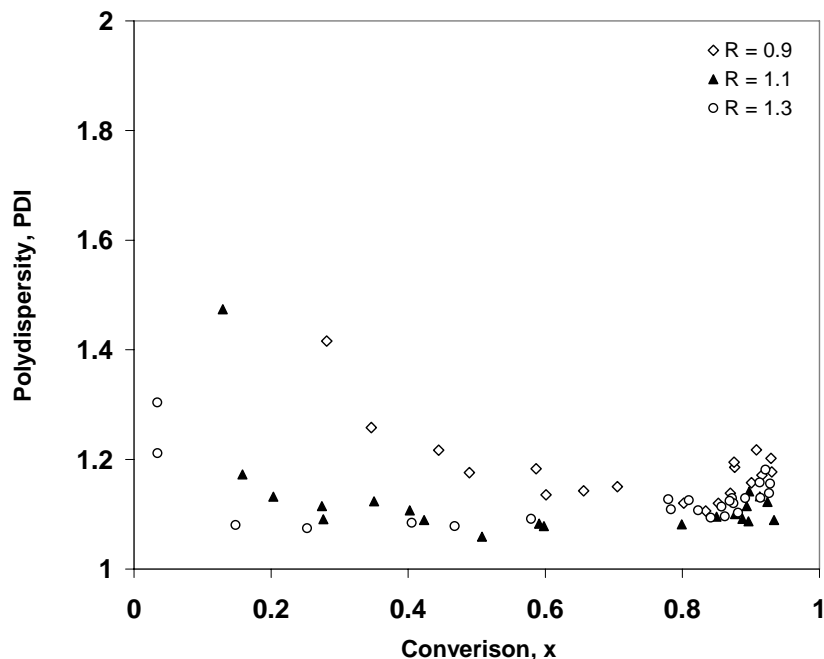


Figure 4.22 Effect of [TEMPO]/ [BPO] ratio on polydispersity, PDI, at 130° C

The results obtained are in agreement with previous studies. Veregin et al. [6, 8] had conducted NMRP of styrene at 125°C, [TEMPO]/[BPO] = 1.1 and 1.3, as part of their kinetic studies. They had captured the linear trend of rate of polymerization with time and also shown that as [TEMPO]/[BPO] increased from 1.1 to 1.3, rate of polymerization decreased (Figure 4.23a). However, their study only captured the first 8hrs of the experiment and low to medium conversions (up to 33% and 50% for [TEMPO]/[BPO] = 1.3 and 1.1, respectively). They had shown that molecular weights increase linearly with conversion and slightly higher values are obtained at [TEMPO]/[BPO] = 1.1 (Figures 4.23c, d). Polydispersity values were higher at [TEMPO]/[BPO] = 1.1 and that is in agreement with our studies that as [TEMPO]/[BPO] ratio increases, lower polydispersities are obtained (Figure 4.23b).

Subsequently, they published a report showing a series of styrene polymerizations performed with varying ratios of [TEMPO]/[BPO], from 1.35 to 0.5 [2]. Results were presented in a table showing number average molecular weights, polydispersity and conversion after 5hrs at 135°C. It was shown that as the ratio was lowered from 1.35 to 0.5, the polydispersity increased, and molecular weights and conversion increased. The results from their paper have been reanalyzed here by plotting polydispersity values as a function of [TEMPO]/[BPO] ratio

(Figure 4.24a). As can be seen, the minimum value is around ratio 1.2, which is in agreement with our studies at 120 and 130°C (See Figure 4.24b, c). The polydispersity versus [TEMPO]/[BPO] ratio plots for different conditions (after 10hrs and 20hrs for styrene polymerization at 120°C, and after 8hrs and 30hrs for styrene polymerization at 130°C) are shown in Figures B.20 and B.21 (Appendix B). The general trends are the same, namely, the optimal operating range to achieve the lowest polydispersity is around [TEMPO]/ [BPO] = 1.1-1.2.

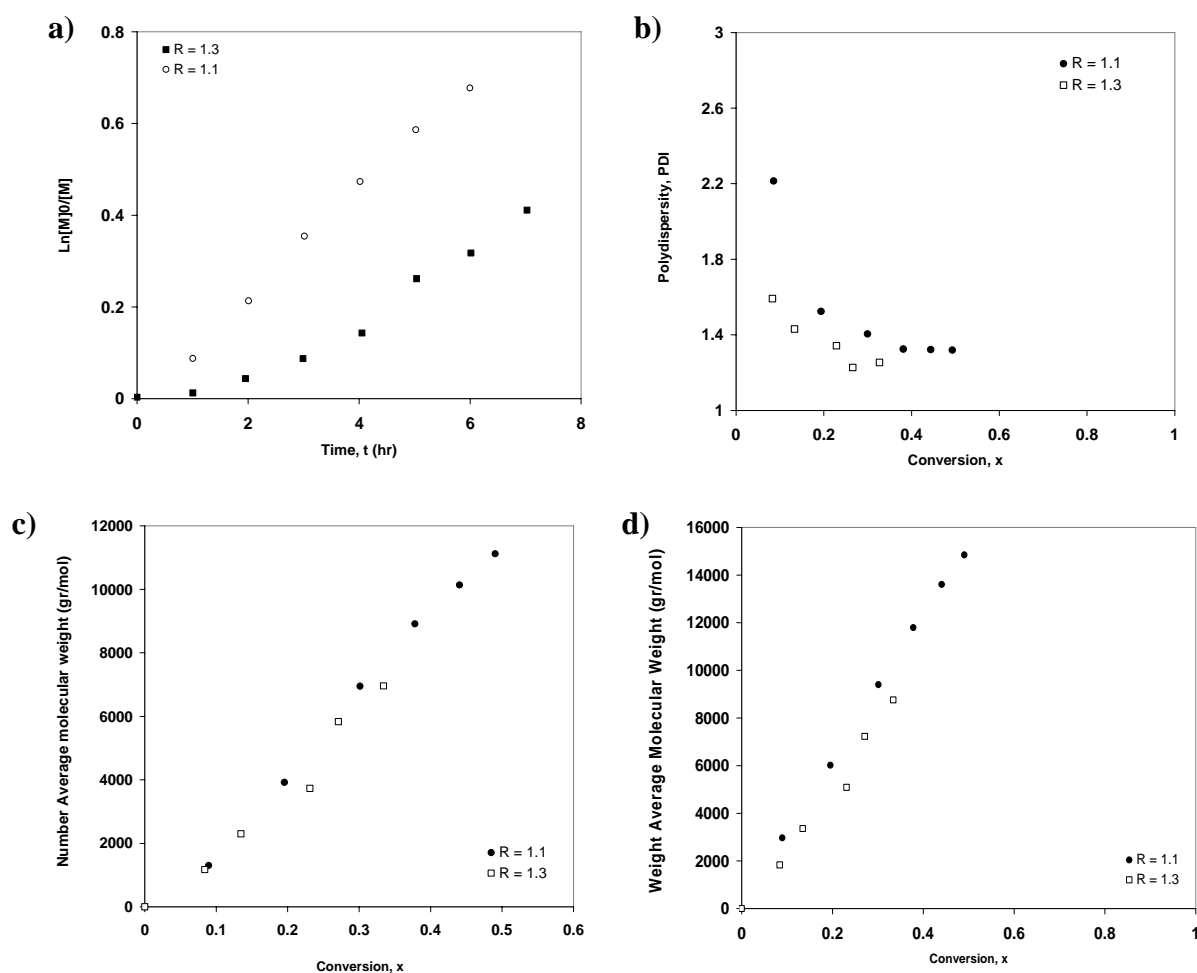


Figure 4.23 Semilog plot of conversion with polymerization time (a), Polydispersity plotted as a function of conversion (b), Polymer molecular weights (M_n and M_w) versus conversion (c, d) for bulk polymerization of styrene with [TEMPO]/[BPO] = 1.1 and 1.3, $T = 125^\circ\text{C}$ [6, 8]

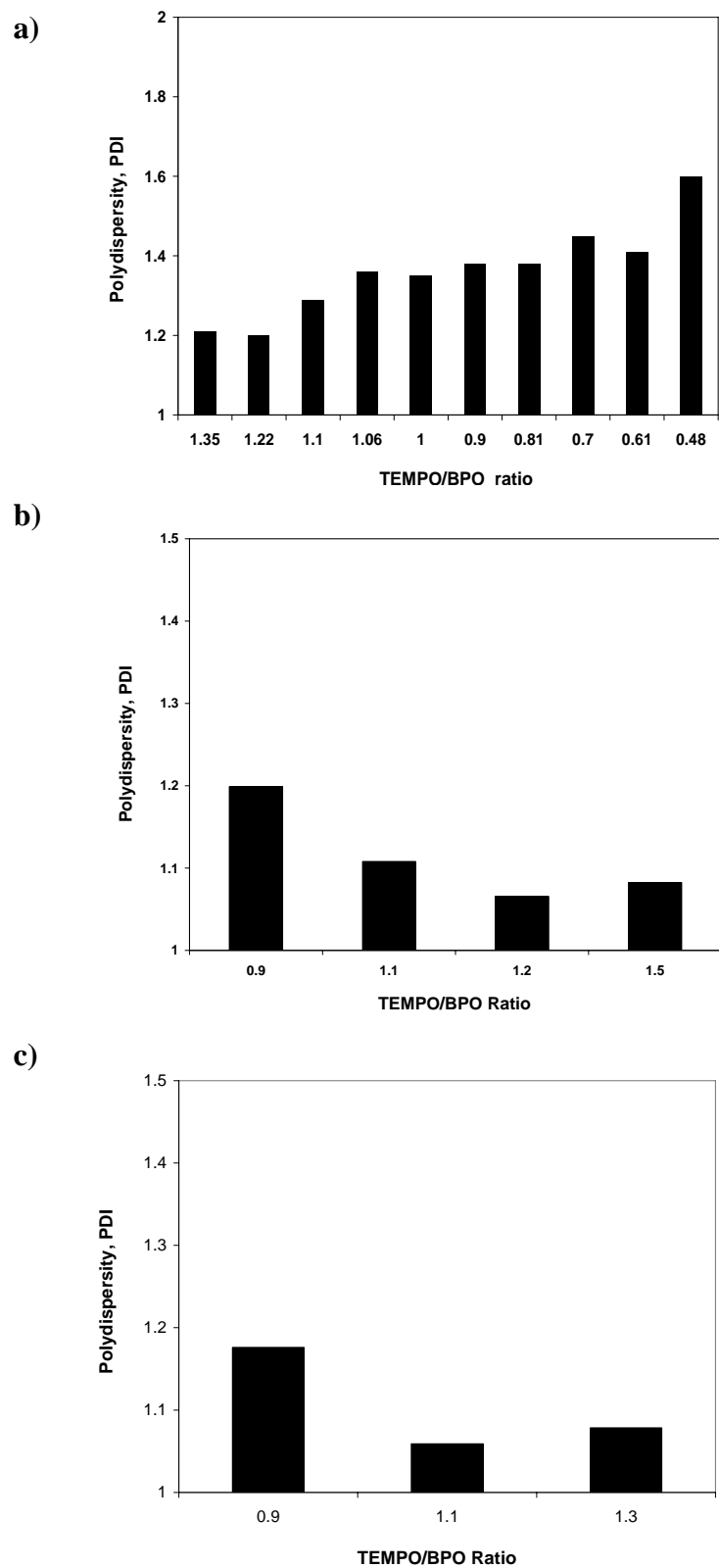


Figure 4.24 Polydispersity as a function of the [TEMPO]/[BPO] ratio for NMRP of styrene: a) after 5 hrs at 135°C ^[2], b) at 50% conversion at 120°C, c) at 50% conversion at 130°C

Butte et al. [9] have presented the effect of [TEMPO]/[AIBN] ratio on rate of polymerization, for NMRP of styrene at 125°C and [TEMPO]/[AIBN] = 1.1, 1.3, and 1.5, as part of their kinetic studies on “living” free radical polymerization. Although they have used a different initiator (2,2'-Azobisisobutyronitrile; AIBN) from our study, the trends observed are similar. As the TEMPO/AIBN ratio increases from 1.1 to 1.5, polymerization rate decreases. They have also captured the induction period for ratio 1.5, which is around 1 hr at their conditions.

Effect of nitroxide/ initiator ratio is an important factor in NMRP systems. Several other groups have also investigated the effect of this variable on polymerization rate and molecular weights in different systems. Wang et al. [10] have conducted a series of styrene polymerizations in a semi batch reactor with various nitroxide to initiator ratios, using Luperox 7M75 as initiator and 4-hydroxy-TEMPO as nitroxide. They illustrated that better control of the molecular weight distribution can be achieved by increasing the amount of nitroxide used. This benefit unfortunately comes at the expense of a significantly reduced rate.

Styrene polymerization experiments were also carried out by Cuatrecasas-Diaz et al. [11] in bulk at 100 and 120°C with BPO or AIBN as initiators and diphenyl-azabutane type nitroxides as mediators. Different nitroxide/ initiator ratios (1.5, 1.65, 1.7, 1.75, and 1.8) were evaluated at 100°C and the results showed that variation in ratio produces a large difference in the kinetic plots and controlled behavior of the system. The corresponding molecular weights and polydispersity plots illustrated that the process with nitroxide/ initiator ratio 1.75 leads to the optimum results, having a M_n vs. conversion curve closest to the controlled polymerization and polydispersity values around 1.4.

Effect of nitroxide/ initiator ratio has also been investigated in NMRP of monomers other than styrene [12 - 14]. According to the kinetics of NMRP, the success of systems controlled by nitroxides depends on the activation and deactivation rate constants (k_a , k_d) and on the concentrations of active, dormant and nitroxide radicals which are influenced by the nitroxide and propagating radical structures, and nitroxide/ initiator ratio, respectively.

4.3.2 Effect of Temperature

Figure 4.25 shows the effect of temperature on polymerization rate as indicated by conversion vs. time, for $[\text{TEMPO}]/[\text{BPO}] = 0.9$ and 1.1 . As expected, polymerization proceeds faster at 130°C than at 120°C . The effect of temperature is more pronounced at $[\text{TEMPO}]/[\text{BPO}] = 1.1$ (Figure 4.25b).

Veregin et al. have illustrated the effect of temperature on rate of polymerization in NMRP of styrene at $[\text{TEMPO}]/[\text{BPO}] = 1.1$ [8]. In Figure 4.26 data from this group are plotted with the experimental data from our lab. The curves are in good agreement with each other; as temperature increases from 115 to 135°C , the polymerization rate increases. It can be seen here that the experimental data from Veregin et al. is only capturing the first 8hrs of the experiment while our data (Figure 4.25) covers the whole conversion range (up to 72 hrs).

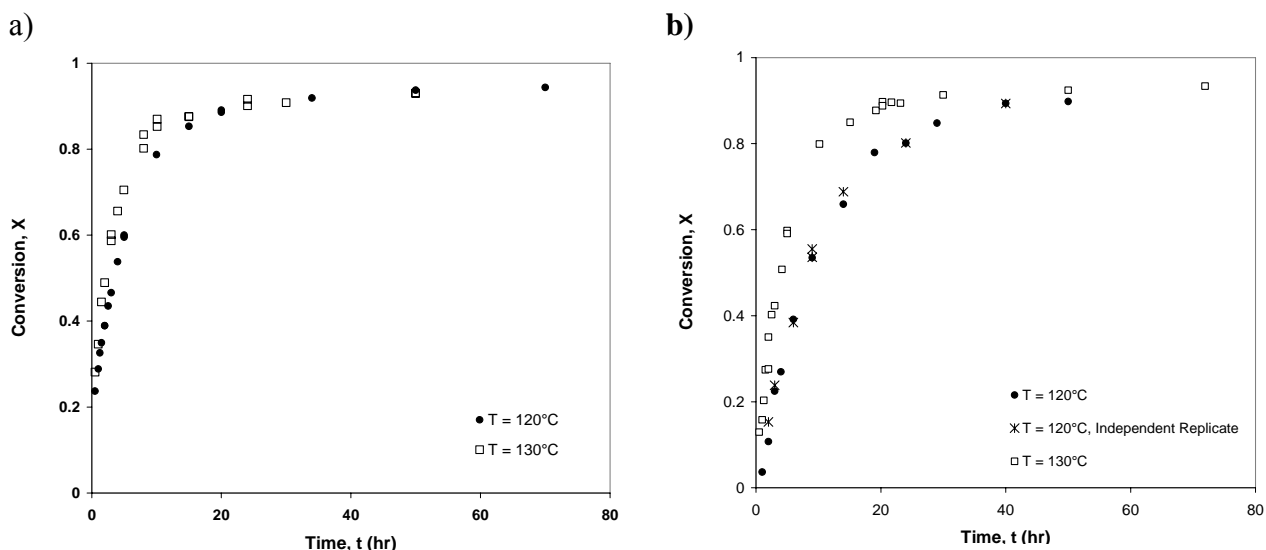


Figure 4.25 Effect of temperature on rate of polymerization at a) $[\text{TEMPO}]/[\text{BPO}] = 0.9$ b) $[\text{TEMPO}]/[\text{BPO}] = 1.1$

Figure 4.27 shows profiles for number and weight average molecular weights at $[\text{TEMPO}]/[\text{BPO}] = 0.9$. A slight reduction in the values of M_n and M_w , with respect to the profile obtained at 120°C , is observed at 130°C . In conventional free radical polymerization molecular weight decreases due to the increased rate of bimolecular termination when

temperature increases, which dominates over the increase of propagation rate. In any CRP process, the effect

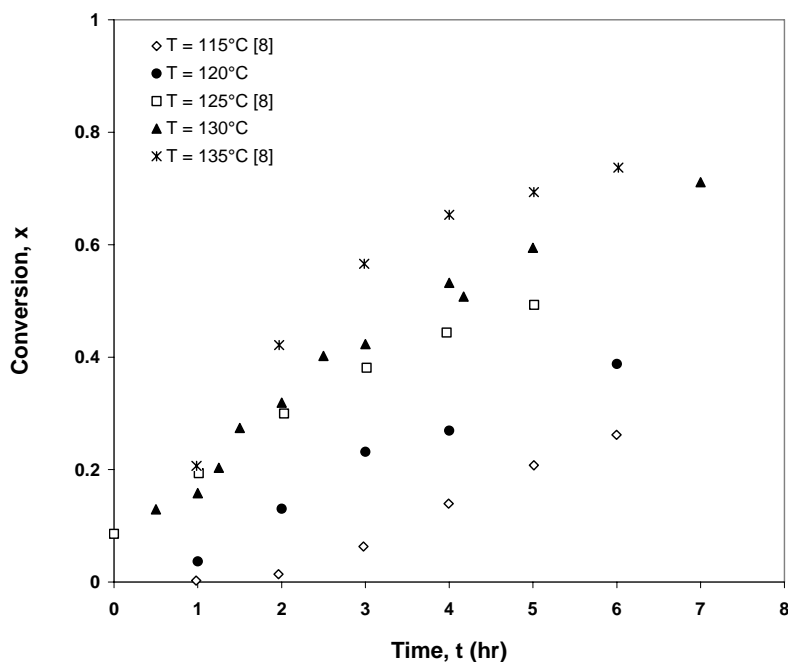


Figure 4.26 Effect of temperature on rate of polymerization at $[\text{TEMPO}]/[\text{BPO}] = 1.1$ [8]

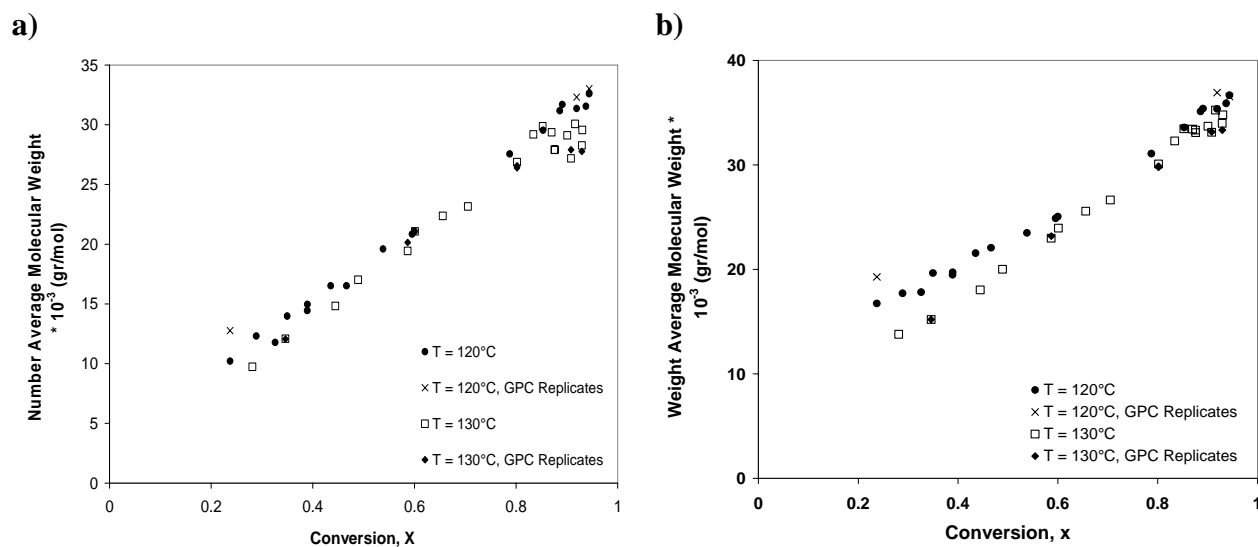


Figure 4.27 Effect of temperature on a) number average molecular weight and b) weight average molecular weight at $[\text{TEMPO}]/[\text{BPO}] = 0.9$

of bimolecular termination is suppressed to a great extent; so increasing temperature promotes the controlled growth of the polymer chains, with the increase in termination step not being

significant. That is the reason why there is not a significant change in molecular weight vs. conversion curve when temperature increases from 120°C to 130°C. Figure 4.28 shows the corresponding plots for $[\text{TEMPO}]/[\text{BPO}] = 1.1$. The general trends are reasonable and similar to the ones observed at $[\text{TEMPO}]/[\text{BPO}] = 0.9$. However, the effect of temperature is more prominent at $[\text{TEMPO}]/[\text{BPO}] = 0.9$.

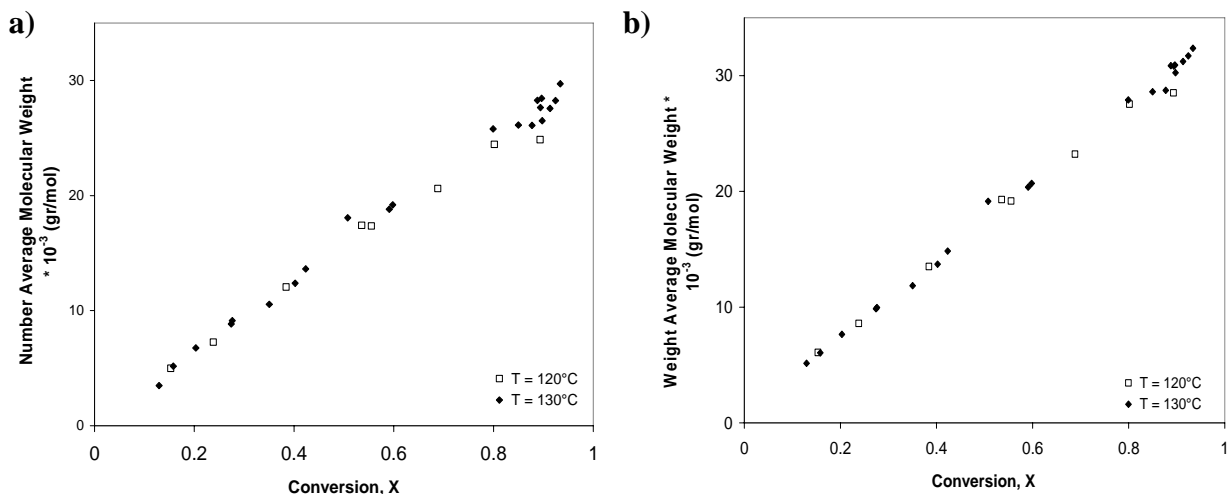


Figure 4.28 Effect of temperature on a) number average molecular weight and b) weight average molecular weight at $[\text{TEMPO}]/[\text{BPO}] = 1.1$

This can be explained based on the polymerization degree (run length; see also Wang et al. [10]). As shown in Eq. 4.2, Run Length per Activation Cycle (RLPAC) is calculated as the ratio of propagation rate over deactivation rate (nomenclature in Eq. 4.2 is the same as described in section 2.2.3.2).

$$\text{Run Length Per Activation Cycle (RLPAC)} = \frac{R_p}{R_d} = \frac{k_p [M][R\cdot]}{k_d [X\cdot][R\cdot]} = \frac{k_p [M]}{k_d [X\cdot]} \quad (4.2)$$

Figure 4.29, illustrates RLPAC at $R = 0.9$ for two different temperatures. Comparing this figure with its counterpart at $R = 1.1$ (Figure 4.30) shows that the effect of temperature on RLPAC is more pronounced at $R = 0.9$. According to Wang et al. [10], RLPAC represents the mean polymerization degree increase of a chain for each activation/deactivation cycle. So higher RLPAC results in higher molecular weights (given the fact that the number of cycles is

almost the same for both cases). This could be the explanation for a more pronounced temperature effect at $R = 0.9$ (contrast again Figures 4.27 and 4.28).

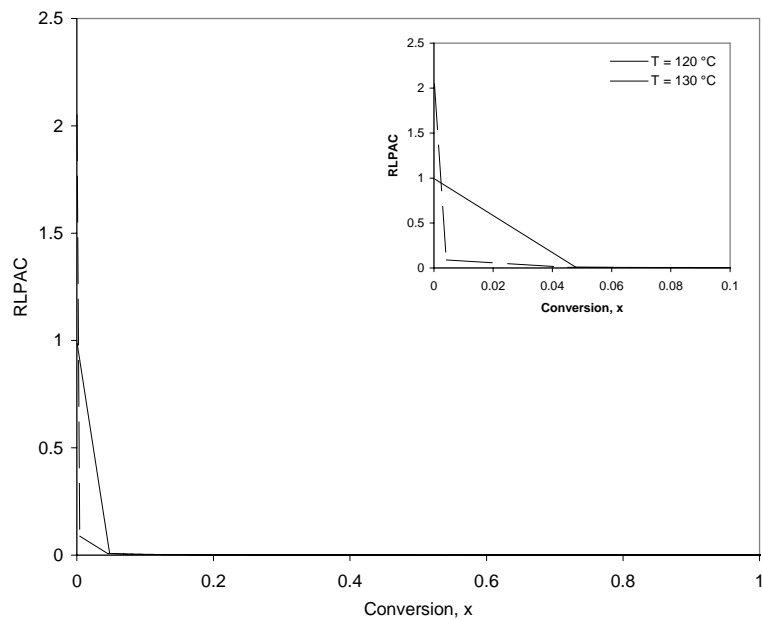


Figure 4.29 Effect of temperature on RLPAC at $[\text{TEMPO}]/[\text{BPO}] = 0.9$

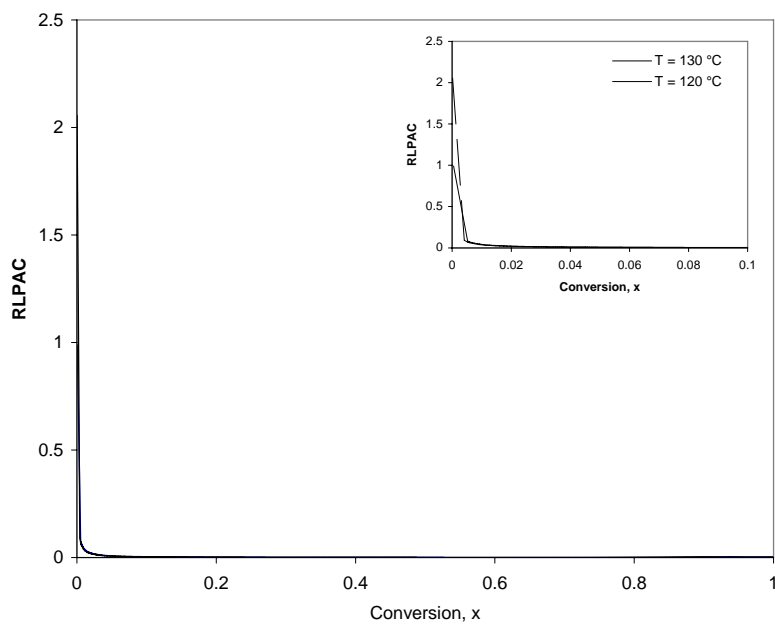


Figure 4.30 Effect of temperature on RLPAC at $[\text{TEMPO}]/[\text{BPO}] = 1.1$

Figure 4.31 shows the effects of temperature on polydispersity for $[\text{TEMPO}]/[\text{BPO}] = 0.9$ and 1.1. Although slightly higher polydispersity values are obtained at lower temperature (120°), in general the effect of temperature is not prominent on polydispersity values.

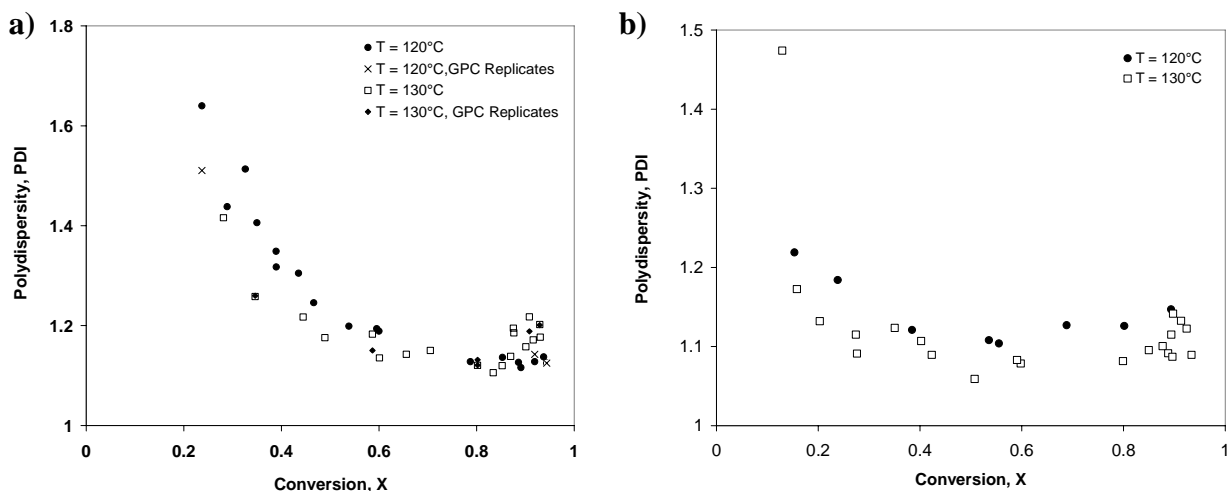


Figure 4.31 Effect of temperature on polydispersity at a) $[\text{TEMPO}]/[\text{BPO}] = 0.9$ and b) $[\text{TEMPO}]/[\text{BPO}] = 1.1$

Veregin et al. have conducted experiments for $[\text{TEMPO}]/[\text{BPO}] = 1.1$ at 115 , 125 and 135°C [6]. In Figure 4.32 the polydispersity data from this group is plotted vs. conversion in the same plot with the experimental data from our lab. It can be seen that the experimental data obtained from Veregin et al. show higher polydispersity values in comparison to our experimental data. The reason could be related to the different polymerization and/or measurement methods used. It has been shown that using different polymerization methods can affect polymerization rate, molecular weights and polydispersity experimental data [15]. Veregin et al. had used a round three necked flask under argon or nitrogen blanket, and had withdrawn samples with a pipette [16] while in our lab polymerization had been carried out in ampoules (See Chapter 3; polymer synthesis). Studies have shown that faster polymerization rates, lower molecular weights and more scattered polydispersity values are obtained using Schlenk techniques for polymerization (which is very similar to the method used by Georges et al.) in comparison to ampoule polymerization [15].

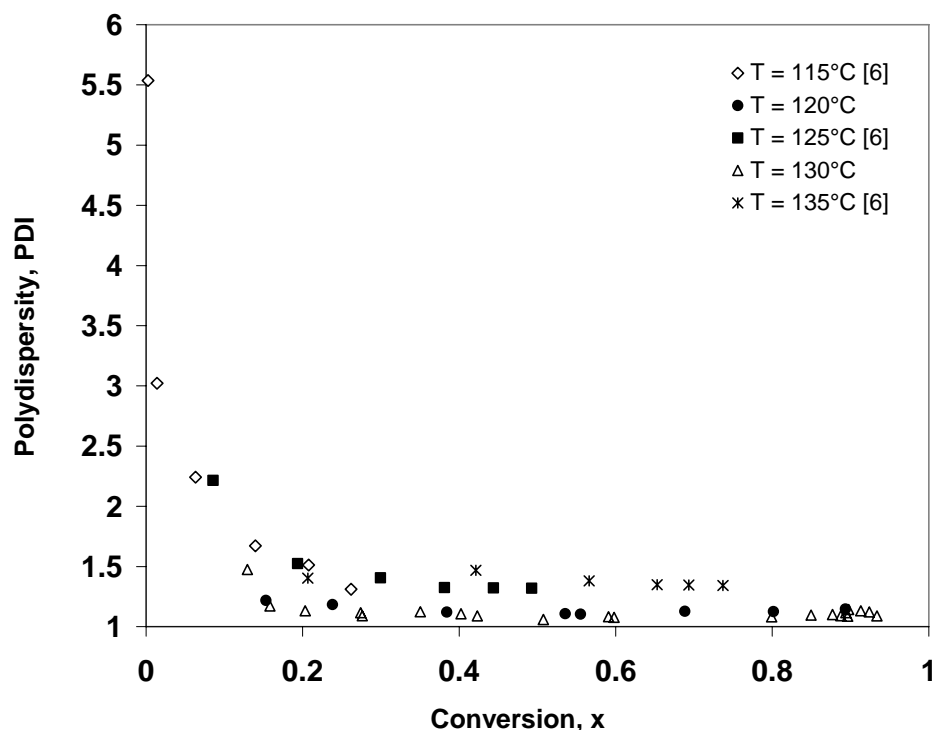


Figure 4.32 Effect of temperature on polydispersity at $[\text{TEMPO}]/[\text{BPO}] = 1.1$ [6]

Becer et al. [14] have used automated parallel synthesizers to optimize the polymerization temperature and nitroxide concentration in homopolymerization of styrene and tert-butyl acrylate. Their objective has been to improve the control over the polymerization while reasonable polymerization rates were retained. They have used a (SG-1)-based alkoxyamine initiator (MAMA) at 90, 100, 110, 115, 120, 125, and 130 °C. Higher polymerization rates were achieved for styrene with the elevated reaction temperatures. The semilogarithmic first order kinetic plots for polymerization of styrene at different temperatures illustrated linear first order behavior for all polymerization temperatures. The number average molecular weights were generally close to each other at temperatures between 110-125 °C while these values were lower for the polymerizations at 90 and 100°C. Although increasing the reaction temperature will increase the rate of polymerization, however this increase should be provided without loss of control over the polymerization. They showed that in the case of polymerization of styrene with MMA at 130°C, the molecular weights were not increasing in a controlled fashion and polydispersity values higher than 1.4 were obtained. They indicated that the loss of control is most likely due to a combination of increase in termination reactions and self initiation of styrene.

Sciannamea et al. [17] have investigated the effect of temperature in polymerization of styrene in the presence of C-phenyl-N-tert-butyl nitron (PBN) and 2,2-azobis(isobutyronitrile) (AIBN). The polymerizations had been carried out at 90, 100, 110 and 120 °C with PBN/AIBN = 2. The semilogarithmic first order kinetic plots at different temperatures illustrated linear first order behavior except at 90°C in which the monomer consumption is not ideally linear along the polymerization time. In their experiments effect of temperature on number average molecular weights is not pronounced; the same linear evolution of molecular weight with conversion is observed whatever the temperature (of course within experimental error).

Effect of temperature on NMRP of monomers other than styrene has also been investigated by different groups. For instance, Ding et al. have examined the influence of temperature on the NMRP of 3-vinylpyridine (3VP) using TEMPO as mediating nitroxide and BPO as initiator at 110, 125 and 138 °C [12]. They have shown that a decrease in temperature induces a decrease in the slope of the plot of $\ln([M]_0/[M])$ versus time. Plots of M_n versus conversion are straight lines, therefore it can be inferred that the polymerization of 3VP is controlled.

4.4 Contribution of Thermal Self-Initiation of Styrene

Since nitroxide-mediated radical polymerization (NMRP) of styrene is typically conducted at temperatures higher than 100°C, the contribution of thermal self-initiation to the outcome of the polymerization process is of considerable interest.

Georges et al. [16] had reported experimental work showing that thermal self-initiation of styrene is suppressed in the presence of nitroxide radicals and benzoic acid (BA; a byproduct of the reaction between TEMPO and the BPO initiator). They demonstrated that in the presence of BA, thermal self-initiation should not be a concern for the NMRP of styrene if the reaction is completed in less than about 15hrs. Subsequently, the same group conducted ¹H NMR analysis of low molecular weight resins initiated by BPO in the presence of TEMPO, and the results showed a one to one ratio between benzoyloxy-initiating fragments on one end and nitroxide fragments on the other [18]. The outcome implied that the majority of chains were initiated by the initiator species and are not produced as a result of thermal self-initiation.

By contrast, other researchers reported that the thermal initiation plays a key role in maintaining a reasonable polymerization rate in NMRP systems. Fukuda et al. [19] have conducted bulk polymerization of styrene at 125°C in the presence of a PS-TEMPO adduct and predicted that the polymerization rate of the NMRP system is independent of the adduct concentration, and equal to the polymerization rate of the adduct-free system, i.e., the rate of thermal self-initiation of styrene. Almost at the same time, Fischer [20], Greszta et al. [21], and Devonport et al. [22] confirmed that the propagation rate of styrene is independent of the concentration of PS-TEMPO adduct and it rather closely follows the rates observed in pure thermal self-polymerization of styrene.

It is apparent from above that the role of thermal initiation in NMRP systems has been a rather controversial issue. To clarify this matter, thermal self-initiation of styrene has been carried out at our operating temperatures (See section 4.4.1) and the results have been compared to NMRP of styrene in the presence of TEMPO (See section 4.4.2) and also to NMRP of styrene with both unimolecular and bimolecular initiators (See section 4.5.2).

4.4.1 Polymerization of Styrene

The thermal self-initiation of styrene has been studied extensively and is generally accepted to occur according to the Mayo mechanism [23] outlined in Figure 4.33. As proposed by Mayo, the thermal initiation of styrene involves a reversible reaction between two styrene molecules to form a Diels-Alder adduct (D), followed by reaction of D with a styrene molecule to form two benzylic radicals, M_1^\bullet and M_2^\bullet , that can add monomer to initiate polymerization. k_1 ($\text{L}\cdot\text{mol}^{-1}\cdot\text{s}^{-1}$) is the rate coefficient for dimerization; k_{-1} (s^{-1}) is the rate coefficient for dimer decomposition, and k_i ($\text{L}\cdot\text{mol}^{-1}\cdot\text{s}^{-1}$) is the thermal initiation rate coefficient. Hui et al. [24] have shown that the rate of polymerization in thermal self-initiation of styrene is proportional to the third power of monomer concentration.

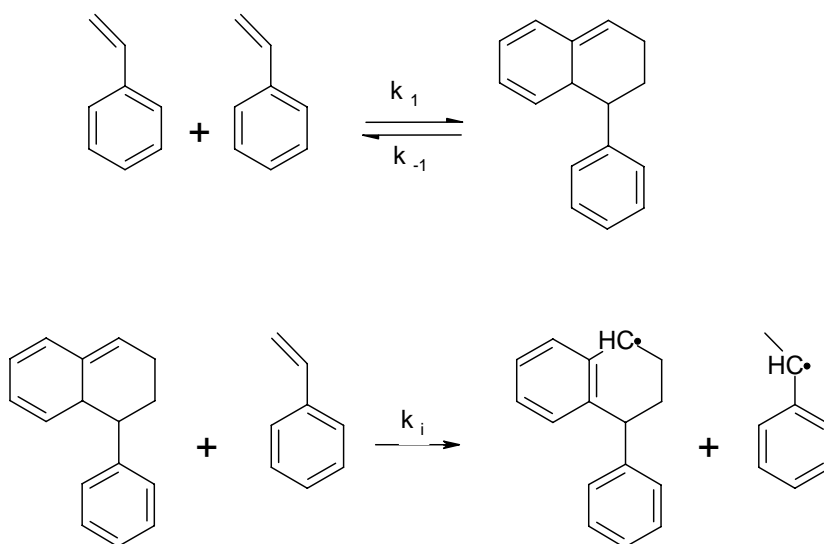


Figure 4.33 Thermal self-initiation of styrene

Since styrene self-initiation plays an important role in NMRP of styrene it was worthwhile to have a good example of the course of reaction at our operating conditions. Styrene polymerizations were conducted at 120 and 130°C (runs # 5 and 11, respectively) without added initiator (BPO) or nitroxide mediating agent (TEMPO). Figure 4.34 shows conversion versus time plots. As can be seen conversion reaches $\approx 40\%$ after 3 hrs at 130°C while it takes 4.5 hrs at 120°C. These results are consistent with the literature. Gao et al. [25] cite experimental data that show that monomer conversion for styrene thermal self-initiation

reaches 40% conversion after 5 hrs at 120°C; also, conversion reaches 94% after 30 hrs while our conversion reached 92% in the experiment at 120°C.

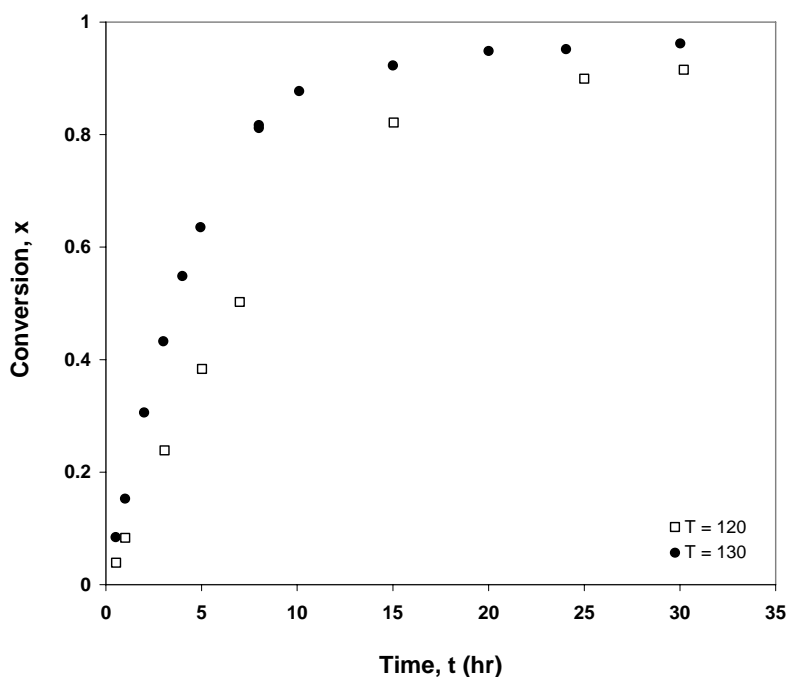


Figure 4.34 Monomer conversion vs. time for thermal self-initiation of styrene at T = 120 and 130°C

It can be seen in Figure 4.35 that molecular weights and polydispersities stay relatively constant with conversion, as observed in previous studies [24, 25]. Number average molecular weights are in the range of $\approx 200,000$ - $300,000$ at 130°C while these values are higher at 120°C. Weight average molecular weights are in the order of 400,000 at 130°C while these values reach up to 500,000 at 120°C. Polydispersity values for both temperatures are between 1.6 - 1.8 at low to medium conversions while these values are around 2.2 at near 100% conversion.

In related literature, Georges et al. have compared thermally self-initiated styrene polymerization, styrene polymerization in the presence of BPO, and styrene polymerization with BPO and TEMPO at 135°C [2]. They showed that the presence of even a small amount of nitroxide (TEMPO/BPO = 0.5) had a significant moderating effect over the rate of polymerization and magnitude of molecular weights of the purely thermal polymerization of

styrene. Further comparisons between styrene self-initiation and styrene NMRP are discussed in the following subsection.

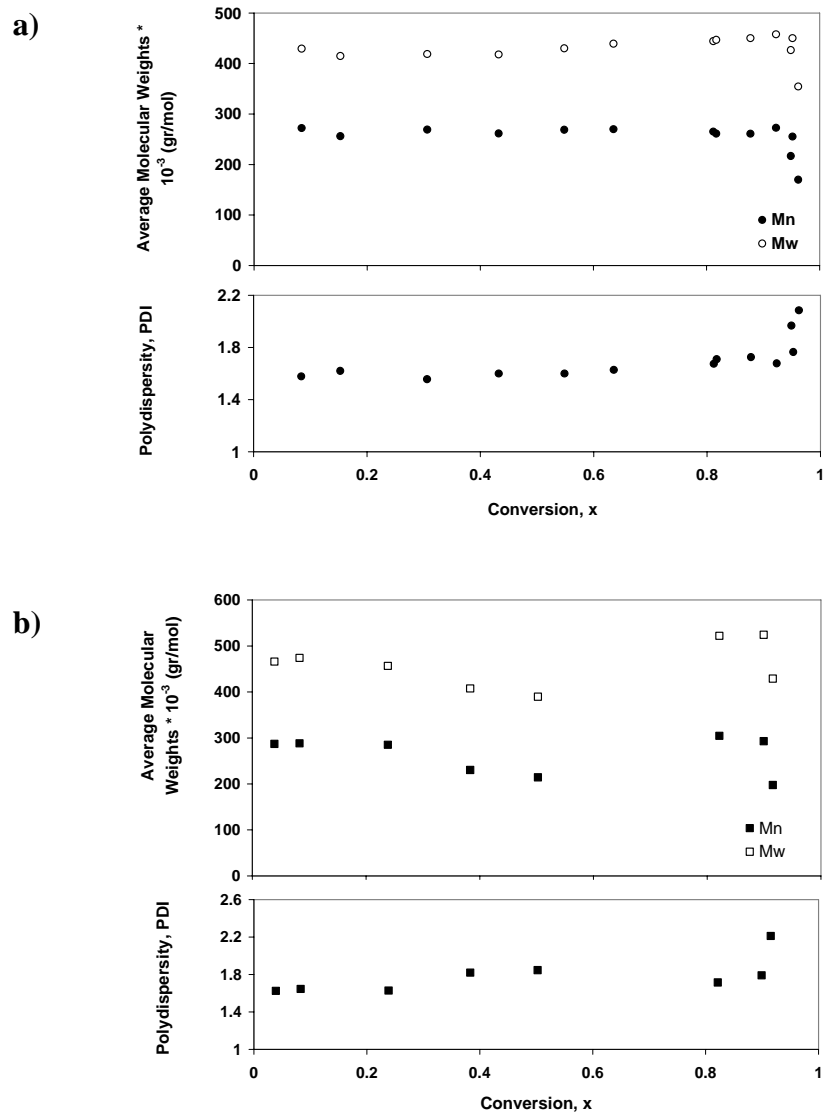


Figure 4.35 Average molecular weights and polydispersity vs. conversion for thermal self-initiation of styrene at a) T = 130°C, b) T = 120°C

4.4.2 Polymerization of Styrene with TEMPO

As discussed in the previous section, styrene-based monomers at elevated temperatures exhibit thermal self-initiation. Significant formation of thermally initiated radicals is undesirable and is one main source for deviations from ideal controlled polymerization when bimolecular or unimolecular initiating systems are employed in NMRP. However, the presence of thermal self-initiation is important because it continuously generates radicals to compensate for the loss of radicals due to termination reactions, and thereby helps maintain a reasonable reaction rate. In addition, radicals produced through styrene self-initiation could be captured by added nitroxides to give “in situ” unimolecular initiators. So the question arises: would it be possible to conduct “controlled” free radical polymerization in the absence of added initiating systems, relying only on added nitroxide radicals to mediate the polymerization?

Preliminary work in thermal self-initiation of styrene in the presence of TEMPO has been reported almost simultaneously by Georges et al. [16] and Matyjaszewski et al. [26, 27]. Different results were obtained, with one group reporting polydispersities of 2 – 2.5 [16] , while under similar conditions the other group obtained polymers with polydispersities in the range of 1.2 – 1.3 [26, 27]. Subsequently, Devonport et al. [22] revisited the thermal initiation of styrene in the presence of TEMPO at 125°C. They showed that low polydispersities and controlled molecular weights can be achieved under these conditions, although the degree of control was not as great as for unimolecular or bimolecular initiating systems.

In 1999, Boutevin et al. [28] conducted a detailed kinetic study on thermal polymerization of styrene with TEMPO at 120°C. They confirmed that controlled molecular weights and low polydispersities were obtained; however, they demonstrated that at the end of polymerization, the concentration of macromolecular chains (here, “macromolecular chains” includes the dormant and living radicals) is higher than the free TEMPO concentration and as a main consequence not all macromolecular chains are controlled by nitroxide radicals, and hence polymerization is not controlled. They also showed that the rate of radical formation is proportional to the initial TEMPO concentration.

Pan et al. [29] have studied thermal self-initiation of styrene in the presence of TEMPO in miniemulsion and compared it to the corresponding bulk systems. The length of the induction period was found to increase linearly with increasing TEMPO concentration. Nearly identical relationships between the length of the induction periods and the initial TEMPO concentrations were found for the miniemulsion and corresponding bulk systems. Faster initial polymerization rates after the induction period were found in bulk polymerizations than in the subsequent miniemulsion polymerizations. This difference was explained to result from different thermal initiation efficiencies in different media.

More recently, Saldivar-Guerra et al. [30] conducted thermal polymerization of styrene with TEMPO at 120-125°C and moderate TEMPO concentrations (0.02-0.08M). They discussed the reaction mechanism in detail in thermal NMRP of styrene in the presence of different concentrations of TEMPO. Their mathematical simulations show that from the induction period to the polymerization regime, there is an abrupt change in the dominant mechanism for generating radicals, mainly due to the sudden decrease in the nitroxide radicals and the relative magnitude of the relevant kinetic rate constants.

In this work, thermal self-initiation of styrene was conducted in the presence of TEMPO at 120 and 130°C (Table 4.1, runs #6, 12). Typical trends for polymerization rate, molecular weights and polydispersity are shown. The results are further compared with regular thermal polymerization of styrene and bimolecular NMRP at the same conditions. Finally, the effect of temperature on polymerization rate, induction period, molecular weights and polydispersity is discussed.

Figure 4.36 shows the kinetic scheme for thermal polymerization of styrene with TEMPO suggested by Saldivar-Guerra et al. [30]. As discussed in the previous subsection, the spontaneous generation of radicals from styrene involves an initial Diels-Alder reaction between two molecules of styrene. This gives the Mayo adduct (**1**), which undergoes a homolysis reaction with another molecule of styrene to give radicals (**2**, **3**). Under normal thermal polymerization conditions, **2** and **3** would initiate uncontrolled polymerization, leading to high molecular weight and high polydispersity polystyrene as shown in previous studies and also in Figure 4.35. In the presence of nitroxides however, the opportunity exists to control this

thermal polymerization by either reaction of **2** and **3** with TEMPO to give the alkoxyamines **4** and **5** or direct reaction between Mayo adduct (**1**) and TEMPO to form initiating radical (**2**) and hydroxylamine (**6**). The initiating radical (**2**) is further trapped by TEMPO to yield **4**.

Another reaction that can produce radicals and consume TEMPO is addition of either hydroxylamine (**6**) or TEMPO to styrene to give radical product **7**, which can further react with another TEMPO radical to yield a bis-TEMPO adduct, **8**. However, Devonport et al. [22] and Saldivar-Guerra et al. [30] have shown that under typical polymerization conditions, the concentration of TEMPO is low and therefore the formation of **8** would be expected to be less favored, thus **4** and **5** are considered as major products in styrene thermal self-initiation in the presence of TEMPO. Of course, other reactions like propagation, reversible capping of growing radicals by TEMPO, and irreversible termination can also be present in these systems (See Figure 4.36)

In Figure 4.37, case **a** shows conversion vs. time for thermal self-initiation of styrene in the presence of TEMPO at 130°C. The initial TEMPO concentration was chosen to be 0.0396M, the same as the concentration levels used earlier in the base case run of TEMPO/BPO = 1.1, in order to establish a good comparative basis (comparisons will be presented later in this subsection). Independent replicates were carried out to check for reproducibility; as can be seen there is good agreement between individual replicates (see triangular points vs. circles of case a). The reaction rate is significantly low (after 64hrs the monomer conversion was 85%). This behavior is dramatically different from that observed for thermal polymerization of styrene (see curve **b** of Figure 4.37). As can be seen, adding TEMPO to the system decreases the polymerization rate dramatically; the rate of styrene thermal polymerization is five times faster in the absence of TEMPO nitroxide. As discussed earlier (see comments on Figure 4.36), the polymerization mechanism for thermal NMRP is no longer controlled by the thermal radical generation but is dominated instead by the nitroxide equilibrium and that can be the reason for the dramatic difference observed in Figure 4.37 between cases **a** and **b**.

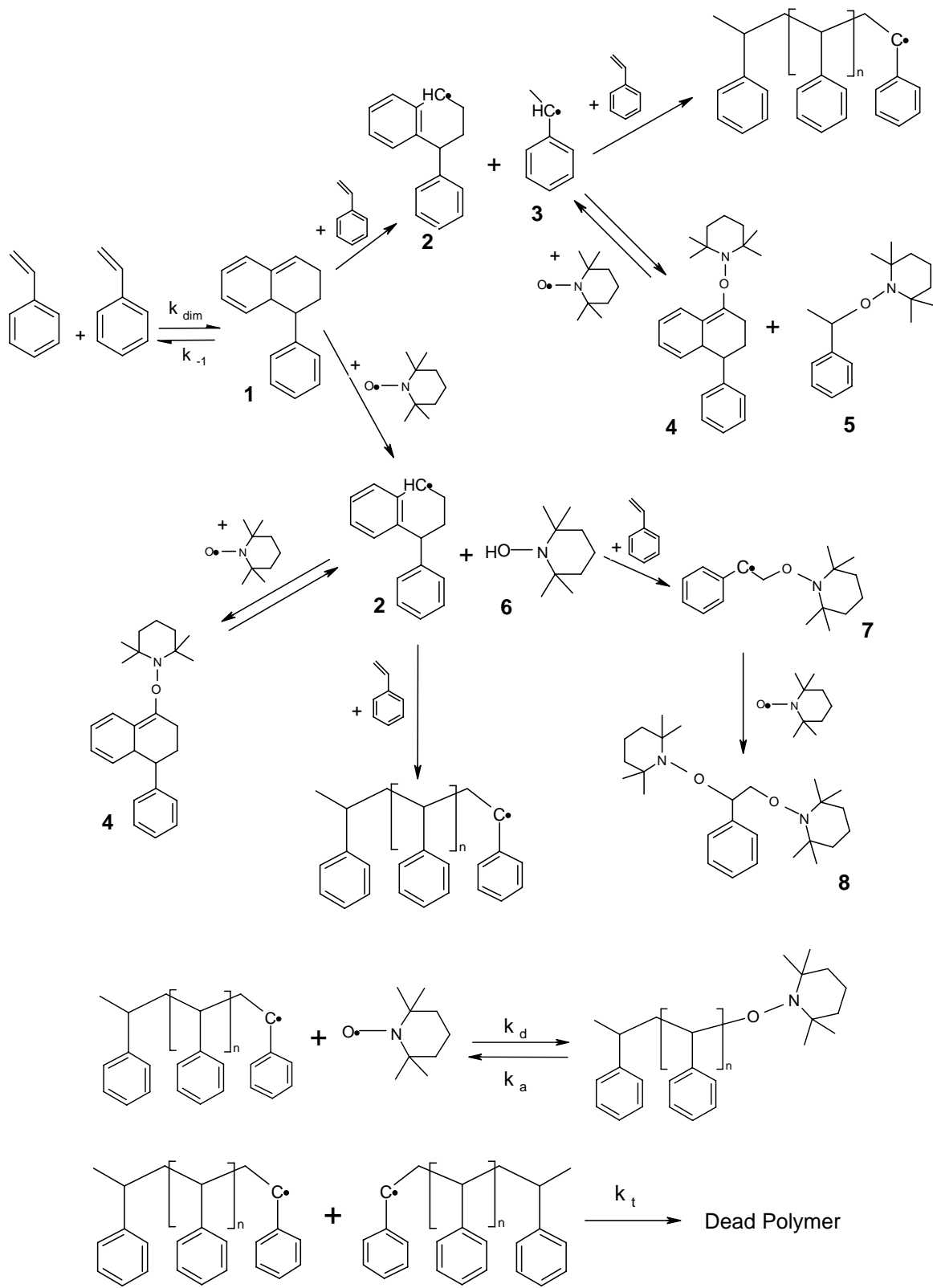


Figure 4.36 Main kinetic scheme for thermal polymerization of styrene with TEMPO^[30]

There is an apparent induction period observed for thermal NMRP (See Figure 4.37, case a), which lasts around 3.5 hrs at these conditions. As also observed by other researchers [22, 27 - 30], styrene/ TEMPO polymerization mixtures show a definite incubation period, during which polymer formation could not be detected. The reason for this observed behavior is that the radicals generated spontaneously by thermal self-initiation of styrene are trapped by TEMPO in the initial stages of the reaction to give “in situ” generated unimolecular initiators. In the presence of excess TEMPO, these initiators do not lead to significant amounts of polymerization and an induction period is observed. However, when the excess TEMPO is consumed, and a sufficiently large concentration of radicals is formed, polymerization can proceed further (but at a significantly lower rate overall).

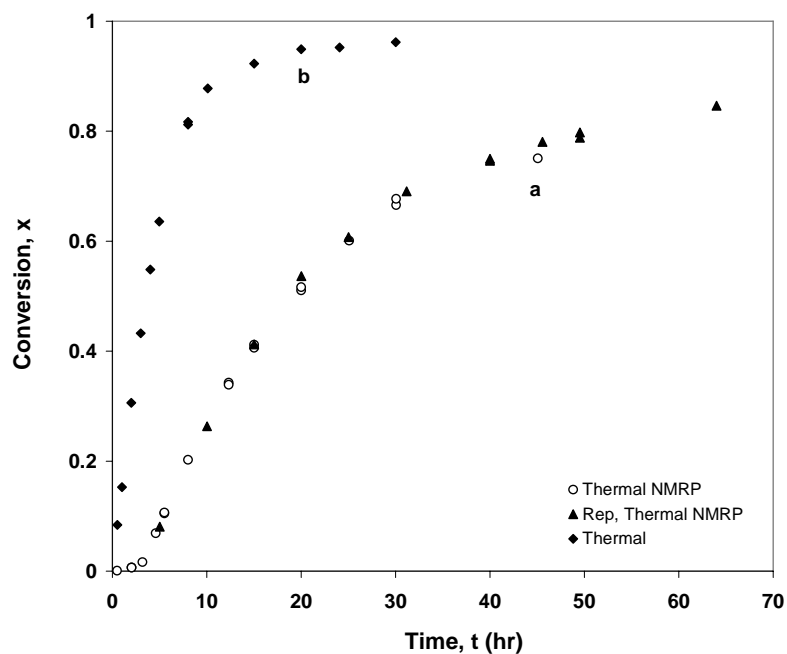


Figure 4.37 Monomer conversion vs. time for: a) thermal polymerization of styrene in the presence of TEMPO with $[\text{TEMPO}]_0 = 0.0396 \text{ M}$ b) thermal styrene, at 130°C

It has been shown experimentally by Matyjaszewski et al. [26] and Devonport et al. [22] that the length of this incubation time depends on the amount of TEMPO present in the polymerization mixture, with increasing amounts of TEMPO leading to longer incubation times. The simulation work by Saldivar-Guerra et al. [30] confirms these results. Saldivar-Guerra et al. [30] showed that this induction period, t_{ind} , is proportional to initial TEMPO concentration $[\text{N}\cdot]_0$, as shown below:

$$t_{\text{ind}} = [\text{N}\cdot]_0 / (2k_{\text{dim}} [\text{M}]_0^2) \quad (4.3)$$

k_{dim} is the kinetic rate constant for dimerization which is $2.51 \times 10^4 \exp[-93,500/(RT)] \text{ L}\cdot\text{mol}^{-1}\cdot\text{s}^{-1}$ (R is the universal gas constant in $\text{J mol}^{-1} \text{ K}^{-1}$; T is temperature in K) [30]. The value of t_{ind} calculated from Eq 4.3 is around 4 hrs at 130°C , which is close to the induction period observed experimentally ($t \approx 3.5$ hrs).

Figure B.22 in Appendix B illustrates the corresponding conversion versus time plot for thermal NMRP at 120°C and $[\text{TEMPO}]_0 = 0.0396 \text{ M}$. In order to check once more the precision of our experimental data, the experimental data from Saldival-Guerra et al. [30] with different initial TEMPO concentrations (but at the same temperature) are plotted in Figure B.22 and as can be seen there is good agreement between the two laboratories.

Figure 4.38 shows the average molecular weights and polydispersity vs. conversion for thermal self-initiation of styrene in the presence of TEMPO at 130°C . It can be seen that both weight and number average molecular weights increase in a linear fashion until 20-30% conversion but deviate from linearity after that stage, with number average molecular weights reaching a plateau at higher conversions. Comparing this figure with Figure 4.35 (average molecular weights for thermal styrene), one can see the effect of TEMPO on molecular weights. As can be seen, adding TEMPO in the system decreases the molecular weights dramatically. In addition, molecular weights behave in a controlled manner (up to 20-30% conversion) in the presence of TEMPO.

Various groups in the literature like Matyjaszewski et al. [26] and Devonport et al. [22] had previously shown that number average molecular weights increase in an almost linear fashion with conversion through the whole conversion range. On the contrary, Boutevin et al. [28] had shown that the M_n dependence versus conversion is not linear for conversions higher than 40-50%. Our observations disagree with those of the former groups and are closer to those of the latter.

Figure 4.38 also shows polydispersity values for thermal NMRP that are lower than 1.4. Again, by comparing with Figure 4.35a (polydispersity for regular thermal polymerization) it can be

concluded that preparation of polymers with relatively low polydispersities is possible with styrene thermal polymerization in the presence of TEMPO. However, polydispersities are not as low as the ones observed in bimolecular NMRP (See Figure 4.41c) and an increase of this factor with conversion can be noticed.

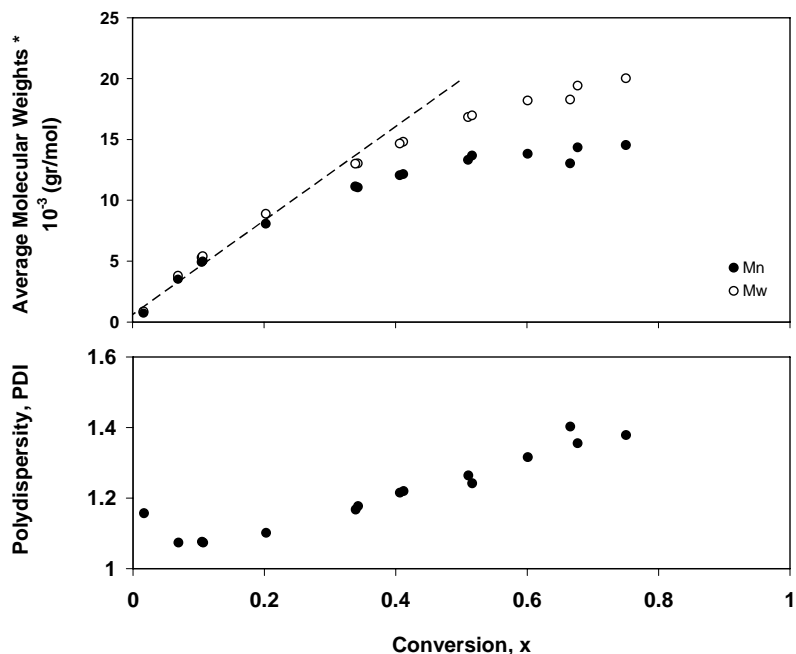


Figure 4.38 Average molecular weights and polydispersity vs. conversion for thermal polymerization of styrene in the presence of TEMPO at 130°C and $[\text{TEMPO}]_0 = 0.0396 \text{ M}$

As explained previously in Chapter 2, the ideal controlled radical polymerization with a linear relationship between the average molecular weights and conversion, and low polydispersity values, is achievable only under a fast initiation step. In purely thermal NMRP however, the initiation of chains is slow, with more chains being formed near the start of reaction because the concentration of monomer is higher at the start of reaction. According to Zhu [31], at a low initiation rate, radicals born earlier experience much longer periods of chain growing than the later-born radicals and thus have higher molecular weights. In particular, those radicals born at the final stage of polymerization form short-chain oligomers that dramatically increase the polydispersity. This statement can be confirmed by Figure 4.39, which illustrates size exclusion chromatographs for regular thermal polymerization and thermal NMRP at 50% conversion. As can be observed, there is a pronounced tailing at lower molecular weights for thermal NMRP (case **b**). This low molecular weight tail is believed to be due to polymer

chains formed by continued thermally initiated polymerization throughout the complete reaction period, as well as minor amounts of termination products [16, 22]. In general, Figure 4.39 shows that there is certainly a significant reduction in polydispersity for thermal polymerization with TEMPO, compared to regular thermal styrene polymerization (case a).

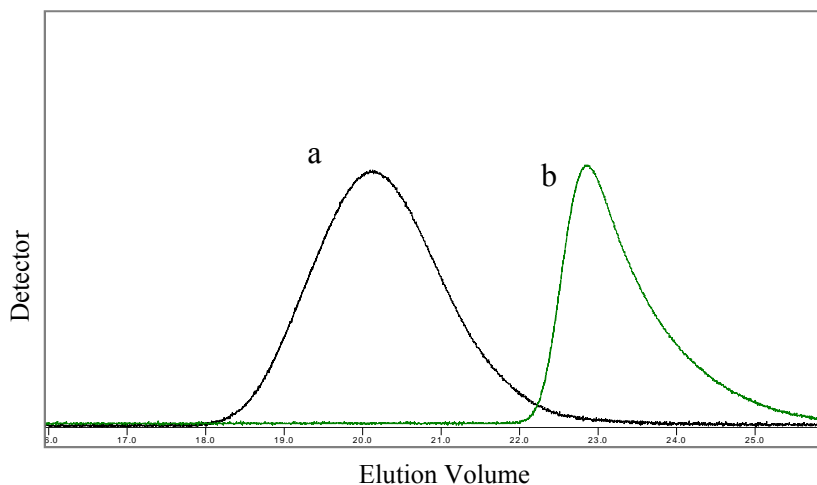


Figure 4.39 Comparison of SEC Chromatograms for a) Styrene thermal polymerization b) Styrene thermal polymerization in the presence of TEMPO, at 50% conversion and 130°C

Increase of polydispersity values with conversion for thermal NMRP has also been reported in the literature [27, 28]. According to Matyjaszewski et al. [27], this result could be due to the competition between degeneration transfer and bimolecular termination reaction as shown in Figure 4.40. Li et al. [32] and Ding et al. [12] have linked the increase of polydispersity with conversion to side reactions and particularly to the irreversible decomposition of the terminal C-TEMPO bond, which inevitably occur through the polymerization, reducing the efficiency of TEMPO and thus broadening the molecular weight distribution.

Figure B.23 in Appendix B has two plots that show the corresponding average molecular weights and polydispersity vs. conversion for thermal self-initiation of styrene in the presence of TEMPO at 120°C. The general trends are the same as the ones at 130°C (See Figure 4.38). Molecular weights increase linearly with conversion only up to 30%. Polydispersity values increase with conversion and values lower than 1.4 are obtained. A comparison between rates of polymerization for thermal NMRP and regular thermal polymerization of styrene at a different temperature (120°C) are shown in Figure B.24. The results are the same as in Figure 4.37; rate of polymerization is dramatically decreased in the presence of TEMPO. Figure B.25

in Appendix B shows the size exclusion chromatographs for regular thermal polymerization and thermal NMRP at 50% conversion at 120°C. As in 130°C, there is certainly a significant reduction in polydispersity for thermal polymerization with TEMPO. The presence of a pronounced tailing at lower molecular weights for thermal NMRP is also observed at 120°C.

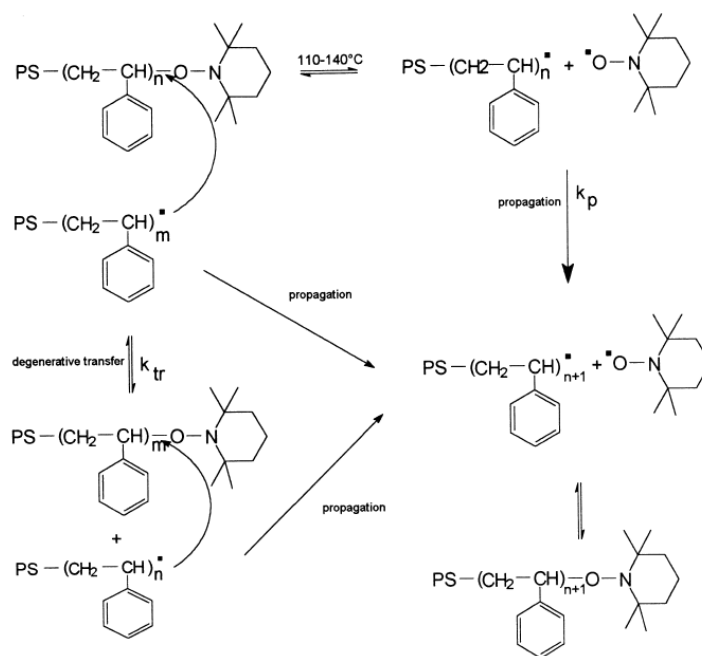


Figure 4.40 Degenerative transfer process for bulk polymerization of styrene in presence of TEMPO ^[27]

Figure 4.41 compares the polymerization rates, molecular weights and polydispersities for thermal NMRP in the absence of initiator with NMRP of styrene with $[\text{TEMPO}]/[\text{BPO}] = 1.1$. As can be seen, the rate of polymerization is dramatically slower in the absence of initiator. Number average molecular weights are comparable up to 40% conversion, whereas after that point there is a plateau for thermal NMRP while molecular weights increase linearly for NMRP with BPO. Figure 4.41c compares polydispersity values; as can be seen, polydispersity values decrease with conversion for NMRP with BPO, approaching values around 1.2, while PDI values increase with conversion for thermal NMRP. As explained before, this is due to the slower rate of polymerization in thermal NMRP. Our results are not in agreement with Devonport et al. [22], who stated that the rate of polymerization in nitroxide-mediated thermal polymerization of styrene will eventually be the same as the rate for normal nitroxide-mediated polymerizations after the incubation period, and controlled molecular weights and low

polydispersities can be prepared in the absence of initiator by only the thermal polymerization of styrene in the presence of TEMPO.

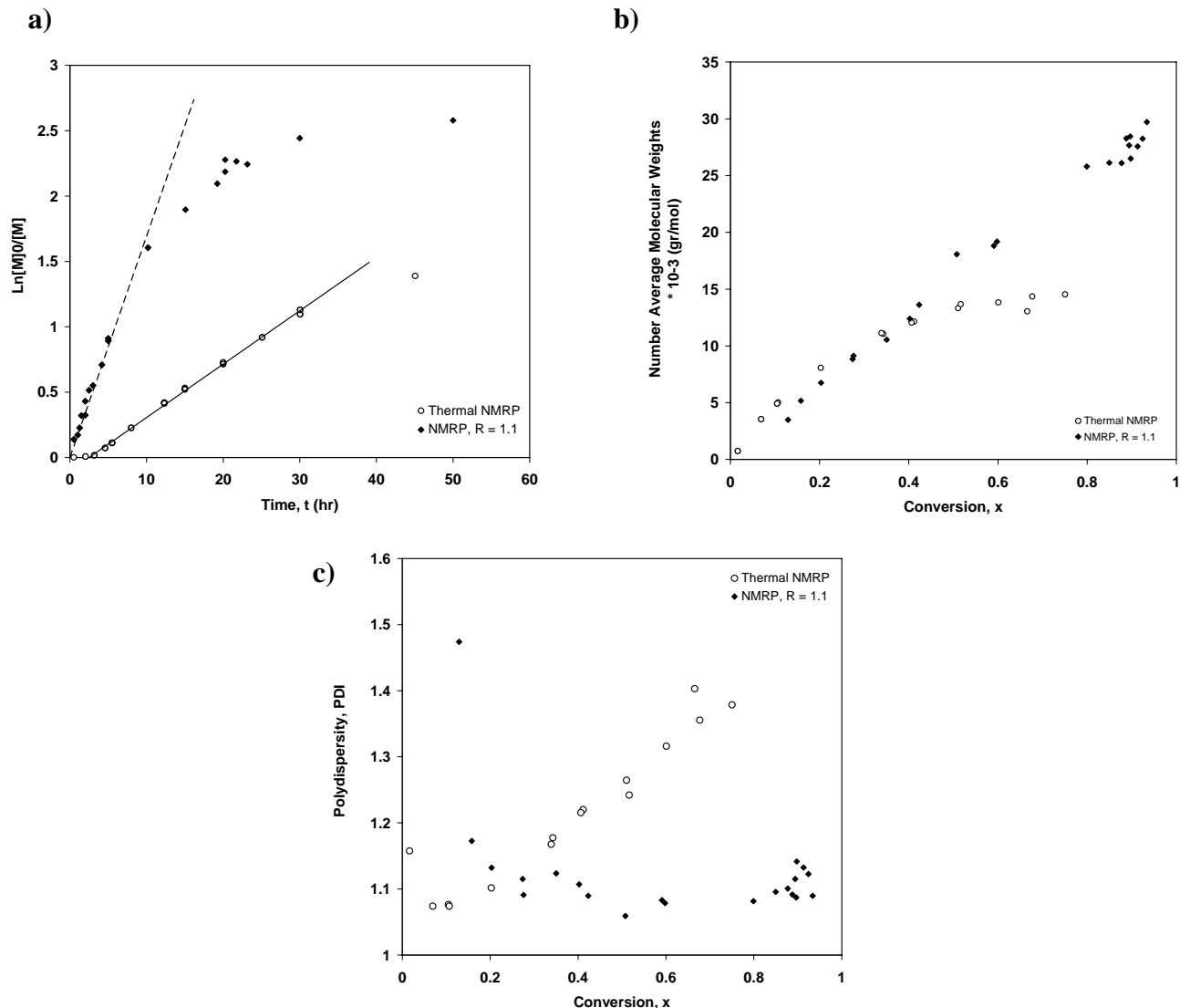


Figure 4.41 Comparison between thermal NMRP and NMRP with $[\text{TEMPO}]/[\text{BPO}] = 1.1$ at 130°C and $[\text{TEMPO}]_0 = 0.0396 \text{ M}$

Comparisons between thermal NMRP in the absence of initiator (BPO) with NMRP of styrene with $[\text{TEMPO}]/[\text{BPO}] = 1.1$ at a different temperature (120°C) can be found in Figures B.26 and B.27 in Appendix B. The general trends are the same as 130°C ; namely, rate of polymerization is slower in thermal NMRP in comparison to bimolecular NMRP with $R = 1.1$, molecular weights are comparable but not at higher conversions and the trends for polydispersity values are identical to the ones at 130°C .

Figure 4.42 compares the corresponding SEC chromatograms. As can be seen, NMRP of styrene in the presence of BPO has a narrower distribution compared to thermal NMRP polymerization which is again related to the slower initiation rate for thermal polymerization as discussed in detail before.

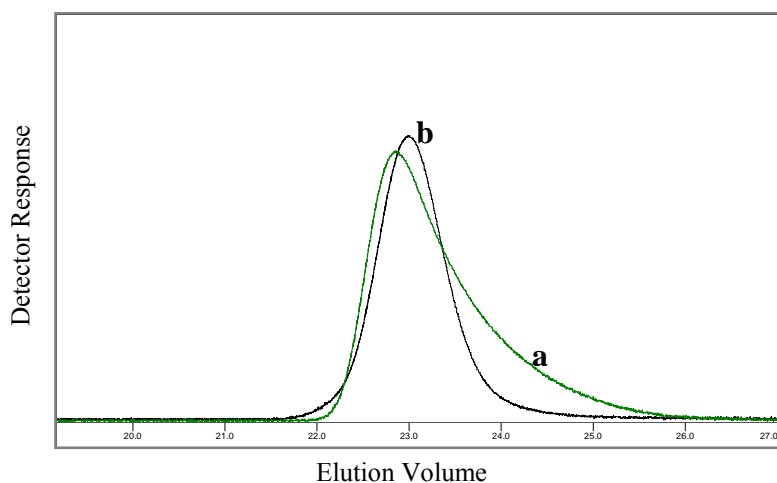


Figure 4.42 Comparison of SEC Chromatograms for a) thermal NMRP b) NMRP with BPO, at 50% conversion and 130°C

Figure 4.43 illustrates the effect of polymerization temperature on rate, molecular weights and polydispersity. At higher temperature, 130°C, an increase in polymerization rate was observed, as clearly seen from Figure 4.43 a and b (one may argue that there are also signs of a certain curvature in the kinetic plot, Figure 4.43 b, around 30hrs (corresponding to ~ 65% conversion), which might indicate variations in the number of growing radicals). It is worth noticing that the induction period decreases at higher temperature. According to Eq. 4.3, the length of the induction period is inversely proportional to the kinetic rate constant for dimerization (k_{dim}) and k_{dim} increases with temperature. As a result the induction period decreases as temperature increases.

The effect of temperature on molecular weights and polydispersity is not pronounced and the data from both runs seem like replicates. The molecular weights deviate from linearity quite early in the reaction (around 20% conversion). This is contrary to what is reported by Matyjaszewski et al. [26] and Devonport et al. [22] for the temperature range 110-140°C. However, given that their collected samples were fewer than ours and, in addition, their

[TEMPO]₀ = 0.1 M was much higher than ours, it is difficult to speculate further as to what might have caused the difference.

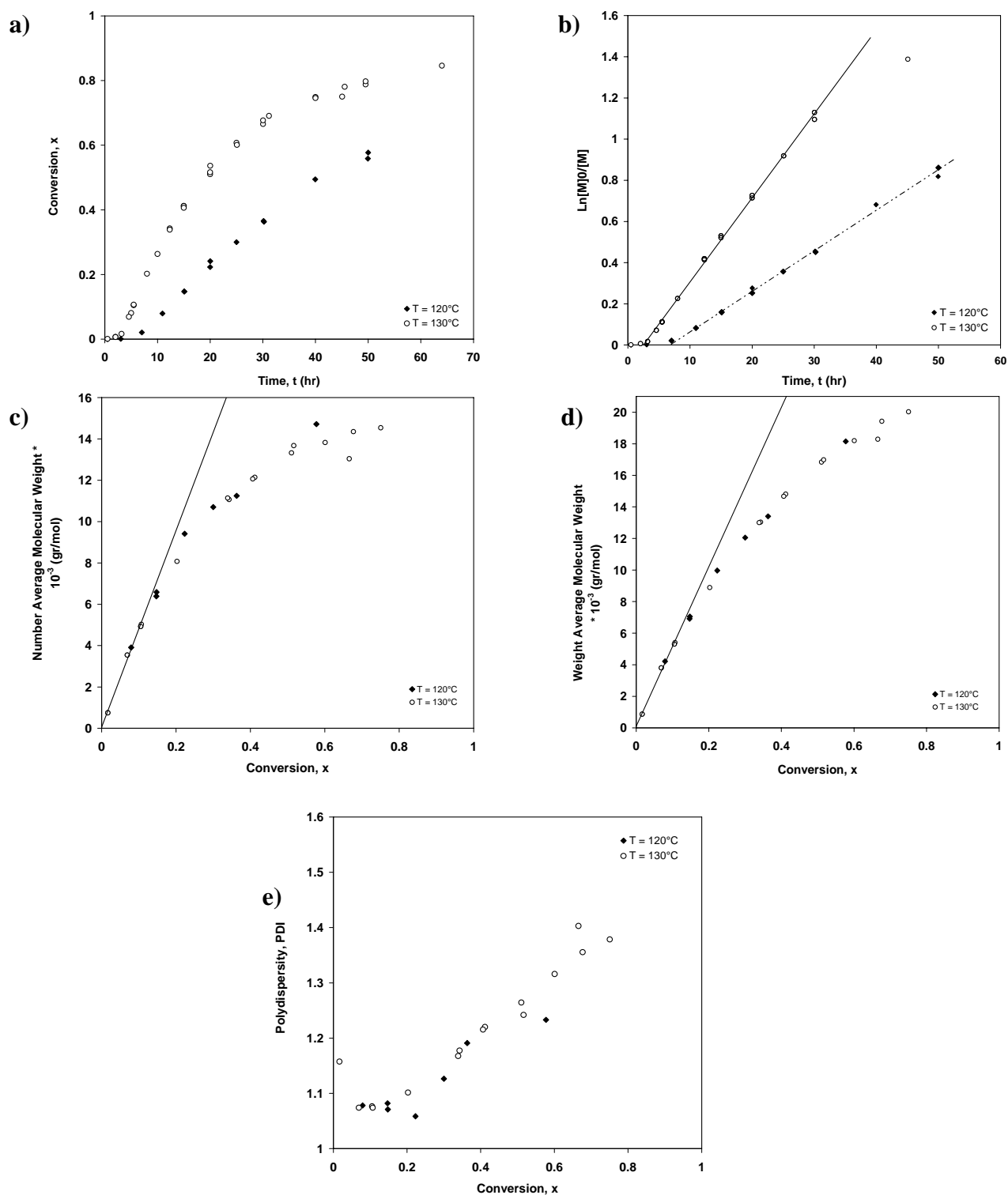


Figure 4.43 Effect of temperature on nitroxide-mediated thermal polymerization of styrene, [TEMPO]₀ = 0.0396 M

Finally, it should be pointed out that although the thermal polymerization of styrene can be controlled to some extent in the presence of TEMPO to provide narrower polydispersity polymer, the results are never as controlled as those that are obtained by a BPO initiated NMRP. As discussed before, this is due to the nature of the thermal initiation phenomenon itself. Thermal initiation relies on the presence of monomer and thus it is a continuous process during the entire course of polymerization as long as residual monomer molecules exist in the system. This is equivalent to a slow initiation rate in the presence of a chemical initiator. Polymer chains are born at different times. The early-born chains are long, whereas the late-born chains are short and that causes a broad molecular weight distribution and subsequently deviation from controlled polymerization.

4.5 Unimolecular NMRP

As discussed in section 2.2.2, NMRP systems can be initiated in two different ways. Conventional radical initiators like BPO or AIBN can be used in the presence of persistent radicals (like TEMPO), as discussed earlier. Alternatively, dormant species can be prepared in advance and used as initiators (unimolecular initiators). The structure of these species is based on the alkoxyamine functionality generated at the chain end during NMRP. The thermally unstable C-O bond decomposes upon heating to give the initiating species. A variety of different unimolecular initiators can be employed in NMRP which may be synthesized through different procedures.

There are different opinions about which initiating system is superior. Some researchers believe that the unimolecular approach is simpler because many of the complex reactions related to initiator decomposition and side reactions between initiator and nitroxide are avoided. In addition these initiating systems can provide perfect balance between nitroxide and polymeric chains leading to greater control and elimination of any induction periods. Other researchers, on the other hand, argue that although the unimolecular approach offers greater control, bimolecular systems are most likely to be used by industry because of the simple one-step production procedure.

Although there are many studies on bimolecular and unimolecular modes separately, there are few works [10, 21, 33] that have compared the two approaches at the same operating conditions. We decided to conduct an experiment (run# 7) with the unimolecular initiator produced based on a procedure suggested by Fukuda et al. [19] and compare it to the corresponding bimolecular system with the same level of nitroxide to get an insight on the advantages and disadvantages of each system (See section 4.5.1).

Preparation of Polystyrene (PS)-TEMPO Adduct: A mixture of freshly distilled styrene, BPO (6.1×10^{-2} M), and TEMPO (7.3×10^{-2} M) were charged in ampoules, degassed with several freeze-thaw cycles and sealed off under vacuum. To ensure complete decomposition of BPO, the mixture was preheated for 3.5 hrs at 95 °C, where no appreciable polymerization proceeded. Then the system was heated at 125 °C for 4 hrs and the polymer was recovered as a

precipitate from a large excess of ethanol, purified by reprecipitation with a methylene chloride (Solvent)/ethanol (non solvent) system, filtered and thoroughly dried (conversion: 16.4%). By GPC analysis, this polymer was found to have a M_n of 3,650 and a polydispersity of 1.075. This polymer has a TEMPO molecule capping the active chain end and will be termed as PS-TEMPO adduct. The subsequent polymerization was carried out in the same way as described in Chapter 3, using the PS-TEMPO adduct as the unimolecular initiator without any extra addition of TEMPO.

Figure 4.44 shows the SEC chromatographs of the PS-TEMPO adduct (**a**) and the corresponding polystyrenes obtained after heating a mixture of adduct and styrene at 120 °C for 3 hrs (**b**), 8 hrs (**c**) and 60 hrs (**d**). As can be seen, the polydispersity remains low while the molecular weights increase as indicated by reduction in average elution time.

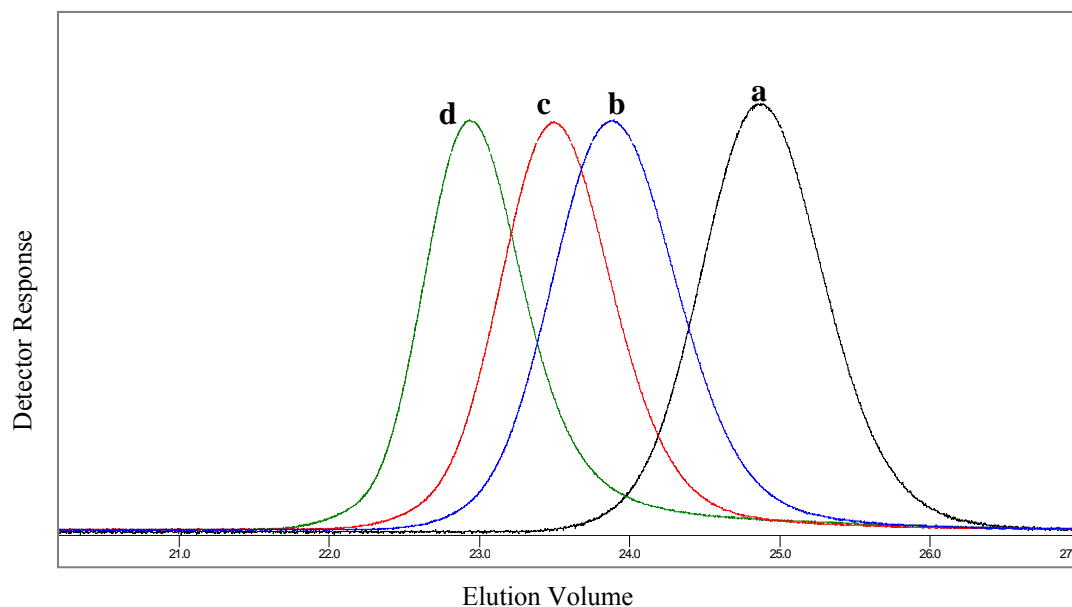


Figure 4.44 SEC Chromatographs for the polymerization of styrene at 120 °C in the presence of PS-TEMPO adduct: a) the precursor adduct; b) the product after 3hrs c) 8hrs d) 60hrs

Several researchers [19 - 22] have reported that the rate of polymerization of styrene in NMRP is independent of the initiation approach and is equal to the rate of the thermal self-initiation of styrene. To examine this issue, rates of polymerization for the bimolecular and unimolecular cases are compared to the thermal self-initiation of styrene (See section 4.5.2).

4.5.1 Comparison with Bimolecular Mode

Figure 4.45 compares conversion vs. time plots for styrene polymerization with the unimolecular initiator and the corresponding bimolecular initiating system with $\text{TEMPO}/\text{BPO} = 1.1$ and $[\text{BPO}]_0 = 0.036\text{M}$ at $120\text{ }^\circ\text{C}$. As can be seen, initially both systems display similar polymerization rates. However, at higher conversions, $> 65\%$, the polymerization with the bimolecular system is noticeably faster than with the unimolecular system. In order to check the possibility of experimental error effects at higher conversions, independent replicates for the unimolecular case were carried out. As can be seen the deviation in rates is not due to experimental error.

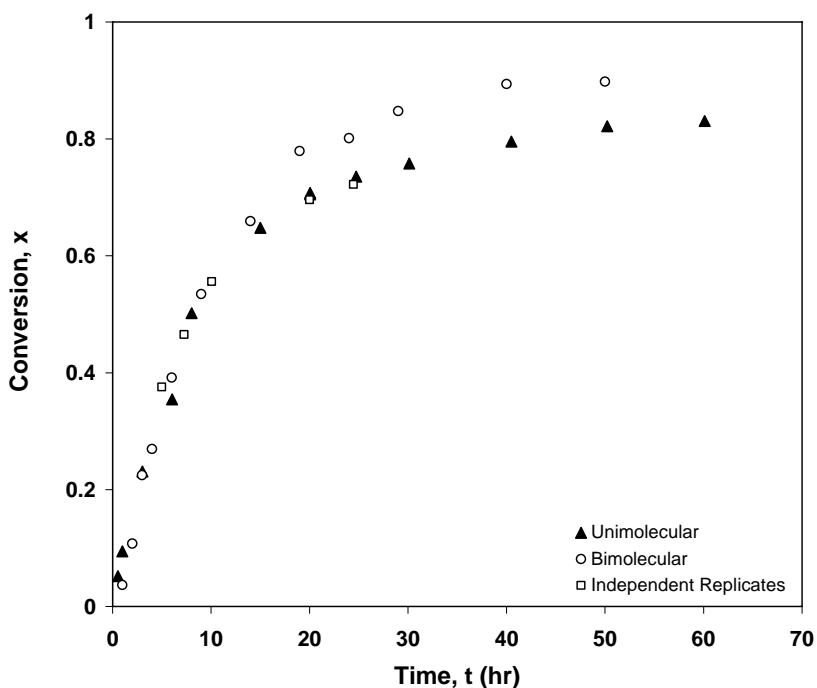


Figure 4.45 Comparison of conversion vs. time plots for the polymerization of styrene at $120\text{ }^\circ\text{C}$ using the unimolecular initiator (\blacktriangle) and a bimolecular system $[\text{TEMPO}]/[\text{BPO}] = 1.1$ (\circ)

A couple of points of speculation to explain this discrepancy in rate of polymerization in Figure 4.45 at $x > 65\%$: a) free monomer concentration is lower in unimolecular case compared to bimolecular. The reason is that in the unimolecular case a portion of the initial mixture volume is occupied by the unimolecular initiator so the amount of monomer present is less (considering the same volume as in the bimolecular case), b) the unimolecular case has a higher level of “free/active” TEMPO, (hence, a slower overall rate) compared to bimolecular

initiator since some of the TEMPO is lost due to side reactions between BPO and TEMPO in the bimolecular case (as will be discussed further in subsection 4.6.1).

The corresponding number and weight average molecular weights increase in an approximately linear fashion with conversion for both initiating systems (See Figure 4.46). However, the molecular weights for bimolecular initiator are higher. A plausible explanation for this deviation may be a loss of TEMPO in the bimolecular approach because of participation in “promoted dissociation” of BPO, proposed by Moad et al. [34] and further clarified by Georges et al. [35] and Cunningham et al. [10, 36]. Georges et al. [35] suggested that as much as 50% of TEMPO may be lost in a reaction system consisting of TEMPO, BPO and styrene, at 70 °C. That loss of TEMPO was reported to be less important at higher temperatures (Georges et al. [35] concluded that the promoted dissociation of BPO is important at temperatures lower than 80 °C). However, during the preparation and handling of the ampoules in bimolecular initiation, the reaction stock solutions are maintained at ambient temperatures for significant periods, and that may account for a significant loss in TEMPO concentration and hence, overall, a lower initiator efficiency. A lower TEMPO level causes the bimolecular system to act more like regular radical polymerization and produce higher molecular weights than observed for the unimolecular approach. More detailed discussion including the side reactions between TEMPO and BPO will be presented in the next section.

Modeling work by our group [37] and Cunningham et al. [10] has been carried out to take into account the “promoted dissociation” effect. Running the simulations with a reduced effective concentration of TEMPO significantly increased the average molecular weights for given monomer conversion levels. The best agreement was obtained when a loss in TEMPO of 30 - 40% was assumed.

Figure 4.47 illustrates that low polydispersities (1.1-1.2) are maintained throughout the polymerization for both systems. However, as can be seen, the polydispersities obtained from the bimolecular approach are higher (and more so initially) than the ones for the unimolecular system at the same conversion levels.

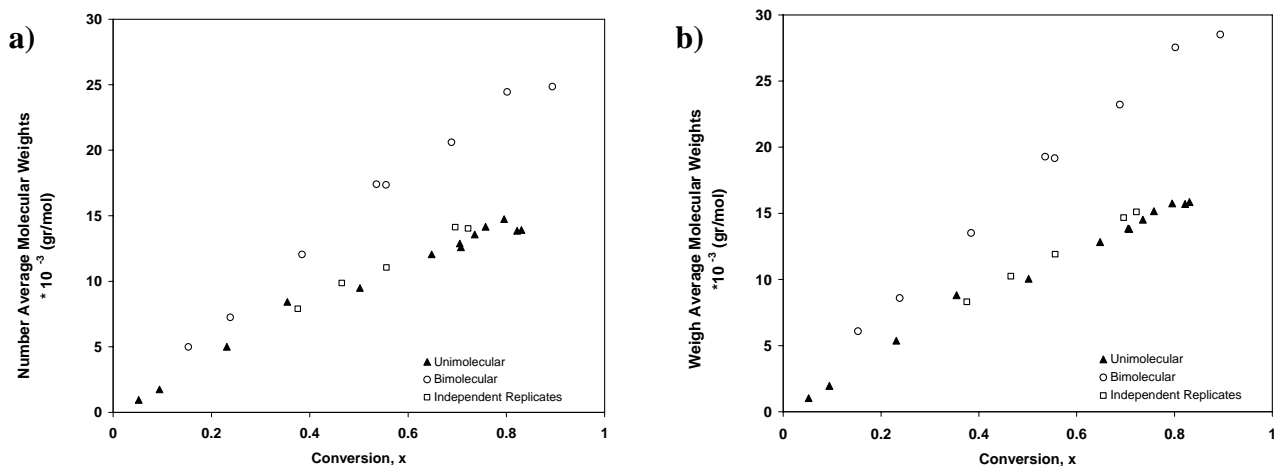


Figure 4.46 Comparison of the number average molecular weights (a) and weight average molecular weights (b) for unimolecular and bimolecular initiators

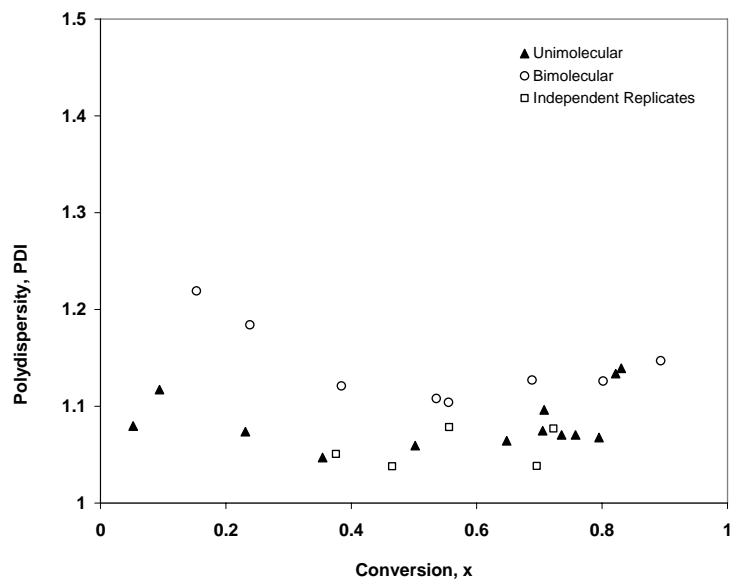


Figure 4.47 Comparison of polydispersity vs. conversion for bimolecular and unimolecular initiating systems

From these results, it can be concluded that unimolecular initiators allow the preparation of macromolecules with greater control over molecular weights and polydispersity than the corresponding bimolecular systems. This general behavior can be rationalized by an examination of the initial steps in both processes. For the bimolecular system, the initial step is decomposition of the benzoyl peroxide followed by reaction of the radicals with styrene monomer and subsequent trapping of these species with TEMPO. As discussed above, these series of reactions are complicated by a variety of side reactions which may eventually lead to

lower initiator efficiency and loss of TEMPO. This results in slightly higher polydispersities and a lower degree of control over molecular weights. In contrast, this inefficient initiating step does not occur with the unimolecular initiators since the TEMPO adducts are preformed. Therefore the polymerizations occur effectively with a higher TEMPO level and lower amounts of undesirable side products, giving rise to more accurate control over molecular weights and lower polydispersities.

Although at first glance unimolecular initiation seems like the best approach to produce controlled polystyrenes, it may not be so. The unimolecular approach is complicated because of a lack of efficient synthetic procedures for initiator (adduct) preparation, procedures which often result in low yields and a wide range of byproducts. Our attempts to produce different batches of PS-TEMPO initiator from the same concentrations of BPO and TEMPO have resulted in products with very different molecular weights. This is a good indication that more detailed studies on producing unimolecular initiators are required to find the optimum synthetic procedures to produce adducts with low molecular weights and good yields for practical applications.

4.5.2 Comparison with Thermal Self-initiation of Styrene

Figure 4.48 compares the polymerization rates for both unimolecular and bimolecular styrene NMRP with styrene self-initiation at 120 °C. As can be seen, polymerization rates are identical at the first 10-15 hrs but after that they deviate from each other and thermal self-initiation exhibits the highest rate. This would confirm literature observations (see [19 - 22]) in that in the early stages (up to 65% conversion) the rates of unimolecular, bimolecular and styrene self-initiation are the same. However, our experimental data show that these rates are not the same over the whole conversion range (as claimed previously in the literature). The reason here might be that the data reported in the literature cover only the first 10 to 15 hrs of the plots while our experimental data has been collected for up to 60 hrs.

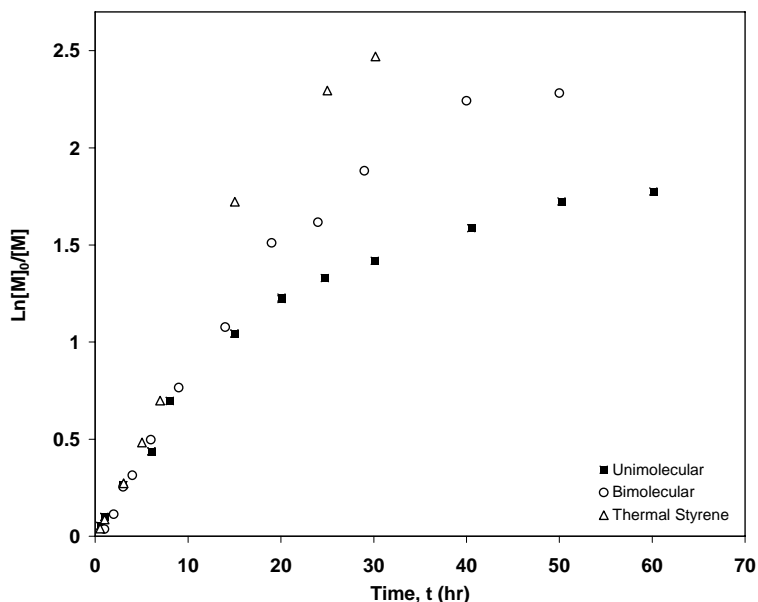


Figure 4.48 First order kinetic plots for unimolecular NMRP (■), bimolecular NMRP (○) and thermal self-self initiation of styrene (Δ)

4.6 Other Aspects

4.6.1 Side Reactions

From the discussion up to this point, it is clear that nitroxide-mediated radical polymerization (NMRP) has attracted an enormous amount of attention, creating high expectations that these polymerizations will provide many new structurally controlled materials for future high performance applications. But in order to use these polymerizations wisely it is necessary to understand the detailed mechanism of each step in the polymerization in order to define the capabilities and limitations of the process. Therefore it is important to be aware of side reactions taking place in these systems.

As discussed in chapter 2, the core reaction in NMRP is the reversible activation/ deactivation reaction, causing a large fraction of the polymer chains to exist in the dormant state, suppressing radical termination rate and giving the system its controlled characteristics. However, there are some side reactions occurring in these systems that affect the overall livingness of NMRP processes. For instance, one of the reactions is, despite its low probability, termination which leads to formation of dead polymer and accumulation of released stable radicals. Another reaction in NMRP of styrene is the thermal initiation of monomer following the Mayo process as discussed in section 4.4. These reactions are responsible for broadening of the molecular weight distribution.

In addition, as reported by different groups [32, 38 - 40], decomposition of the dormant species (alkoxyamine) is another side reaction occurring in NMRP (See Figure 4.49). The decomposition of alkoxyamine happens through the abstraction of the β -proton of the polymer radical by the nitroxyl, producing terminally unsaturated polymer and hydroxylamine which can further act as a transfer agent.

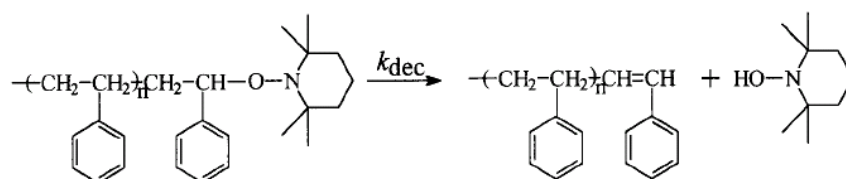


Figure 4.49 Decomposition of dormant species (alkoxyamine) in NMRP of styrene ^[39]

Another side reaction that takes place is the reaction between TEMPO and BPO or “promoted dissociation” of BPO, proposed by Moad et al. [34] and further clarified by Georges et al. [35] and Cunningham et al. [36]. As discussed by Georges et al. [35], formation of the benzoyloxy radical can occur either by the thermal or promoted dissociation of BPO. They showed that at temperatures below 80 °C the promoted dissociation is the dominant reaction while at higher temperatures the thermal dissociation mechanism plays a larger role. The promoted dissociation begins with a one-electron transfer from TEMPO to BPO to give an oxoammonium cation, a carboxylate anion and a benzoyloxy radical. As can be seen in Figure 4.50, the oxoammonium and carboxylate ions react to give a short lived intermediate which reacts further with BPO to give a five membered nitrene.

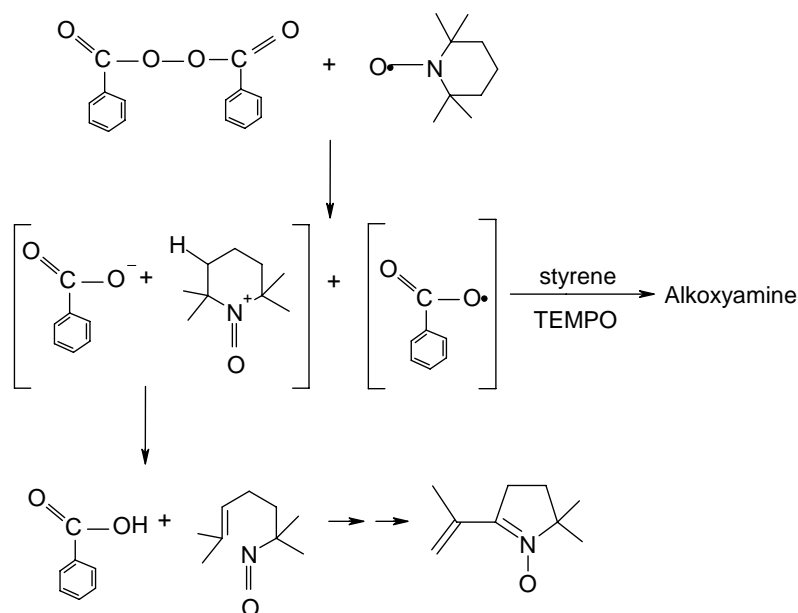


Figure 4.50 Promoted dissociation of benzoyl peroxide by TEMPO in the presence of styrene ^[35]

The side reaction between BPO and TEMPO affects both TEMPO concentration and BPO efficiency factor, since it consumes quantities of both. Georges et al. [35] suggested that as much as 50% of TEMPO may be lost in these reactions at 70 °C. Although our experiments were carried out at higher temperatures (120, 130 °C), during the preparation and handling of the ampoules, the reaction stock solutions were maintained at room temperature for significant periods, and that would allow the occurrence of these side reactions.

Cunningham et al. [36] have shown that they can obtain better agreement between their mathematical model and experimental data if they reduce the TEMPO concentration to 40% of its experimental value and change initiator efficiency from 0.5 to 0.28.

4.6.2 Significance of Gel Effect

Diffusion effects are important in regular free radical polymerization systems and they lead to a pronounced acceleration in the rate of polymerization. Diffusion controlled effects are due to a significant reduction of termination and propagation rate coefficients and initiator efficiency, resulting from increased viscosity of the reaction medium. Since concentration of radicals is established by balancing rates of initiation and termination, a relative drop in the latter rate increases the concentration of radicals and accelerates the propagation (and hence the overall polymerization) rate. Since polymerization is highly exothermic, temperature may increase, further enhancing overall rate and that may result in a polymerization runaway.

The degree of diffusion-controlled effects (DC effects) is questionable and rather controversial in nitroxide-mediated radical polymerizations. Several groups have assumed that DC effects are significant and speculated that it is because of DC effects that the living character of the system is lost at higher conversions, where the system exhibits regular radical polymerization features (the nonlinearity in plots of average molecular weights vs. conversion and increase in polydispersity values). Other groups have considered these effects to be negligible due to the lower molecular weight ranges and low radical concentrations typical of NMRP.

Saban et al. [41] have suggested that since initiation and termination are controlled, nitroxide-mediated polymerizations should not exhibit a gel effect. They have shown that even when the polymerization is performed at relatively high reaction rates, by adding camphorsulfonic acid (CSA), no gel effect is evident. Subsequently, these results have been confirmed by Greszta et al. [21]. Recently, Cunningham et al. [36] have performed simulations both without considering DC effects and also using a simple empirical equation, with the termination rate coefficient (k_t) dependent on the weight fraction of polymer in the reaction system. Their simulations showed that including the gel effect for styrene leads to a slight overestimation of the reaction rate, and an underestimation of the number average molecular weight, M_n . Based

on these results they concluded that there was no large improvement in model predictions by using a gel effect correlation.

Other groups, like Butte et al. [9] and Zhang et al. [42], have proposed that if the polymer chains are long and polymer mass in the reactor is sufficiently high, the gel effect can affect polymerization behavior and they have considered an empirical correlation for k_t in their model if the number average chain length of the polymer is above 150. Roa-Luna et al. [43] have considered diffusion-controlled effects in their model not only for termination rate constant (k_t) but also for propagation, activation and deactivation rate constants. However, they concluded that although the inclusion of overall DC-effects into the kinetic model improved the performance of the model by slightly reducing the deviations obtained from experimental data of polymerization rate and molecular weight in NMRP of styrene, it did not seem to justify adding an extra four (free-volume) parameters in the model.

As can be understood from above, the effect of diffusion-controlled reactions on NMRP processes is still not clear and it has not been studied and understood as systematically as in standard free radical polymerization. In most of the cases, researchers have developed a mathematical model and have included diffusion limitations mainly for the termination rate constant (k_t) whenever there has been a mismatch between experimental data and model predictions.

In order to clarify the issue, it was decided to look at a “worst case scenario”, creating conditions where radicals are exposed to higher viscosities from the outset of reaction, in order to “mimic” DC effects. Size exclusion chromatography (SEC) polystyrene standards or preformed nitroxyl-capped polystyrenes (prepolymer) were added to a typical recipe for the bimolecular NMRP of styrene and the effect of their presence on polymerization rate and molecular weights was investigated. The study was carried out with varying concentrations of prepolymer (5% - 45%) of molecular weights ranging from 5,000 – 1,000,000 and at two temperatures (120 °C – 130 °C) [37].

Results were compared with modeling simulations using the Predici® commercial software, considering DC effects and the presence of prepolymer (either as inert “solvent” or as

monomolecular controller of high molecular weight). All the kinetic rate constants used in the calculations presented in this study can be found later in Chapter 5 (Mathematical modeling), along with more details on the mathematical model.

Figure 4.51 shows a typical result for profiles of conversion vs. time and number average molecular weight. As can be seen, profiles of styrene NMRP at the presence of prepolymers with molecular weights ranging from 188,000 to 1,210,000 practically overlap with the plot of NMRP of styrene without any prepolymer (within experimental error).

Figure 4.52 shows the modeling simulations considering DC effects and no DC effects. As can be seen there is no big difference between the two profiles and the simulated profile without DC effects in fact is closer to the experimental data.

Overall, based on the investigations so far, DC effects seem to be insignificant. It is likely that the low importance of DC effects in NMRP is related to the relatively short molecules (as compared to the chain lengths typical of regular radical polymerization), as well as to the typical operating temperatures being well above the T_g of resulting polymer. This result may have significant benefits for industrial scale bulk polymerization of styrene where not only would the concern of runaway reactions be minimized but also less expensive reactors of simpler design could be used.

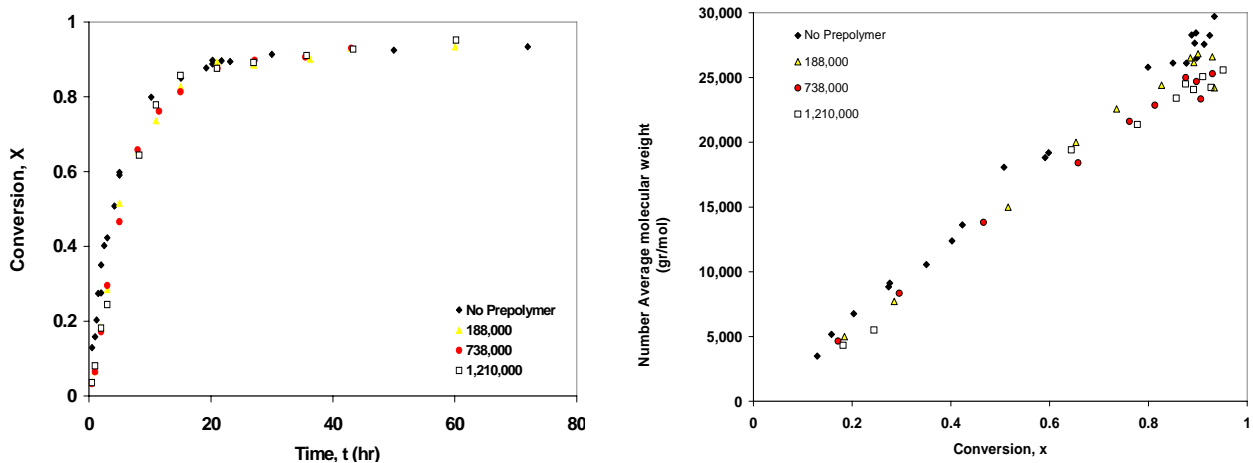


Figure 4.51 Effect of addition of prepolymer (5%) on rate of polymerization and number average molecular weights in NMRP of styrene at 130 °C, TEMPO/BPO = 1.1 and $[BPO]_0 = 0.036$ M

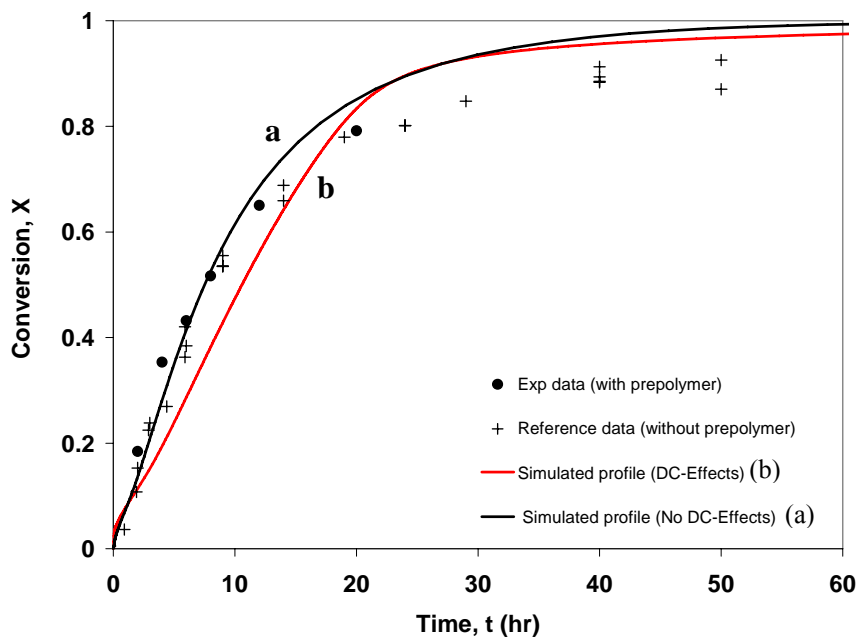


Figure 4.52 Comparison of experimental data and model predictions of conversion versus time for NMRP of styrene at 120 °C, TEMPO/BPO = 1.1 and $[BPO]_0 = 0.0192$ M, 45% prepolymer with $M_n = 17,400$

4.7 References

1. Georges, M.; Veregin, R.; Kazmaier, R.; Hamer, G. **1993** "Narrow molecular weight resins by a free- radical polymerization process" *Macromolecules*, *26*, 2987-2988.
2. MacLeod, P. J.; Veregin, R. P. N.; Odell, P. G.; Georges, M. K. **1997** "Stable free radical polymerization of styrene: Controlling the process with low levels of nitroxide" *Macromolecules*, *30*, 2207-2208.
3. Tuinman, E.; McManus, N. T.; Roa-Luna, M.; Vivaldo-Lima, E.; Lona, L. M. F.; Penlidis, A. **2006** "Controlled free-radical copolymerization kinetics of styrene and divinylbenzene by bimolecular NMRP using TEMPO and dibenzoyl peroxide" *Journal of Macromolecular Science Part A: Pure and Applied Chemistry*, *43*, 1-17.
4. Belincanta-Ximenes, J.; Mesa, P. V. R.; Lona, L. M. F.; Vivaldo-Lima, E.; McManus, N. T.; Penlidis, A. **2007** "Simulation of styrene polymerization by monomolecular and bimolecular nitroxide-mediated radical processes over a range of reaction conditions" *Macromolecular Theory and Simulations*, *16*, 194-208.
5. Bonilla, J.; Saldivar, E.; Flores-Tlacuabuac, A.; Vivaldo-Lima, E.; Pfaendner, R.; Tiscareno-Lechuga, F. **2002** "Detailed modeling, simulation, and parameter estimation of nitroxide mediated living free radical polymerization of styrene" *Polymer Reaction Engineering Journal*, *10*, 227-263.
6. Veregin, R. P. N.; Odell, P. G.; Michalak, L. M.; Georges, M. K. **1996** "Molecular weight distributions in nitroxide-mediated living free radical polymerization: Kinetics of the slow equilibria between growing and dormant chains" *Macromolecules*, *29*, 3346-3352.
7. Saldivar-Guerra, E.; Bonilla, J.; Becerril, F.; Zacahua, G.; Albores-Velasco, M.; Alexander-Katz, R.; Flores-Santos, L.; Alexandrova, L. **2006** "On the nitroxide quasi-equilibrium in the alkoxyamine-mediated radical polymerization of styrene" *Macromolecular Theory and Simulations*, *15*, 163-175.
8. Veregin, R. P. N.; Odell, P. G.; Michalak, L. M.; Georges, M. K. **1996** "The pivotal role of excess nitroxide radical in living free radical polymerizations with narrow polydispersity" *Macromolecules*, *29*, 2746-2754.
9. Butte, A.; Storti, G.; Morbidelli, M. **1999** "Kinetics of "living" free radical polymerization" *Chemical Engineering Science*, *54*, 3225-3231.
10. Wang, Y.; Hutchinson, R. A.; Cunningham, M. F. **2005** "A semi-batch process for nitroxide mediated radical polymerization" *Macromolecular Materials and Engineering*, *290*, 230-241.
11. Cuatepotzo-Diaz, R.; Albores-Velasco, M.; Saldivar-Guerra, E.; Jimenez, F. B. **2004** "Nitroxide mediated polymerization using diphenyl azabutane N-oxides. A study of

- electronic effects and of the [nitroxide]/[initiator] ratio on the polymerization control" *Polymer*, *45*, 815-824.
12. Ding, X. Z.; Fischer, A.; Brembilla, A.; Lochon, P. **2000** "Behavior of 3-vinylpyridine in nitroxide-mediated radical polymerization: The influence of nitroxide concentration, solvent, and temperature" *Journal of Polymer Science Part A-Polymer Chemistry*, *38*, 3067-3073.
 13. Pradel, J. L.; Boutevin, B.; Ameduri, B. **2000** "Controlled radical polymerization of 1,3-butadiene. II. Initiation by hydrogen peroxide and reversible termination by TEMPO" *Journal of Polymer Science Part A-Polymer Chemistry*, *38*, 3293-3302.
 14. Becer, C. R.; Paulus, R. M.; Hoogenboom, R.; Schubert, U. S. **2006** "Optimization of the nitroxide-mediated radical polymerization conditions for styrene and tert-butyl acrylate in an automated parallel synthesizer" *Journal of Polymer Science Part A-Polymer Chemistry*, *44*, 6202-6213.
 15. Roa-Luna, M.; Nabifar, A.; Diaz-Barber, M. P.; McManus, N. T.; Vivaldo-Lima, E.; Lona, L. M. F.; Penlidis, A. **2007** "Another perspective on the nitroxide mediated radical polymerization (NMRP) of styrene using 2,2,6,6-tetramethyl-1-piperidinyloxy (TEMPO) and dibenzoyl peroxide (BPO)" *Journal of Macromolecular Science Part A: Pure and Applied Chemistry*, *44*, 337-349.
 16. Georges, M. K.; Kee, R. A.; Veregin, R. P. N.; Hamer, G. K.; Kazmaier, P. M. **1995** "Nitroxide mediated free-radical polymerization process - autopolymerization" *Journal of Physical Organic Chemistry*, *8*, 301-305.
 17. Sciannamea, V.; Catala, J. M.; Jerome, R.; Detrembleur, C. **2007** "Controlled radical polymerization of styrene mediated by the C-phenyl-N-tert-butyl nitron/AIBN pair: Kinetics and electron spin resonance analysis" *Journal of Polymer Science Part A-Polymer Chemistry*, *45*, 1219-1235.
 18. Georges, M. K.; Odell, P. G.; Veregin, R. P. N.; Keoshkerian, B. **1997** "The nitroxide-mediated stable free radical polymerization process - Mechanistic considerations" *Abstracts of Papers of the American Chemical Society*, *213*, 461-OLY.
 19. Fukuda, T.; Terauchi, T.; Goto, A.; Ohno, K.; Tsujii, Y.; Miyamoto, T.; Kobatake, S.; Yamada, B. **1996** "Mechanisms and kinetics of nitroxide-controlled free radical polymerization" *Macromolecules*, *29*, 6393-6398.
 20. Fischer H. **1997** "The persistent radical effect in "living" radical polymerization" *Macromolecules*, *30*, 5666-5672.
 21. Greszta, D.; Matyjaszewski K. **1996** "Mechanism of controlled/"living" radical polymerization of styrene in the presence of nitroxyl radicals. kinetics and simulations" *Macromolecules*, *29*, 7661-7670.

22. Devonport, W.; Michalak, L.; Malmstrom, E.; Mate, M.; Kurdi, B.; Hawker, C. J.; Barclay, G. G.; Sinta, R. **1997** ""Living" free-radical polymerizations in the absence of initiators: controlled autopolymerization" *Macromolecules*, *30*, 1929-1934.
23. Mayo, F. R. **1968** "Dimerization of styrene" *Journal of the American Chemical Society*, *90*, 1289.
24. Hui, A. W.; Hamielec, A. E. **1972** "Thermal polymerization of styrene at high conversions and temperatures - an experimental study" *Journal of Applied Polymer Science*, *16*, 749-769.
25. Gao, J.; Penlidis, A. **1998** "A comprehensive simulator database package for reviewing free-radical copolymerizations" *Journal of Macromolecular Science-Reviews in Macromolecular Chemistry and Physics*, *C38*, 651-780.
26. Mardare, D.; Matyjaszewski, K. **1994** "Thermal polymerization of Styrene in the presence of stable radicals and inhibitors" *Polymer Preprints (Am.Chem.Soc.)*, *35*, 778.
27. Gaynor, S.; Greszta, D.; Mardare, D.; Teodorescu, M.; Matyjaszewski, K. **1994** "Controlled radical polymerization" *Journal of Macromolecular Science-Pure and Applied Chemistry*, *A31*, 1561-1578.
28. Boutevin, B.; Bertin, D. **1999** "Controlled free radical polymerization of styrene in the presence of nitroxide radicals - I. Thermal initiation" *European Polymer Journal*, *35*, 815-825.
29. Pan, G. F.; Sudol, E. D.; Dimonie, V. L.; El Aasser, M. S. **2004** "Thermal self-initiation of styrene in the presence of TEMPO radicals: Bulk and miniemulsion" *Journal of Polymer Science Part A-Polymer Chemistry*, *42*, 4921-4932.
30. Saldivar-Guerra, E.; Bonilla, J.; Zacahua, G.; Albores-Velasco, M. **2006** "Incubation period in the 2,2,4,4-tetramethyl-1-piperidinyloxy-mediated thermal autopolymerization of styrene: Kinetics and simulations" *Journal of Polymer Science Part A-Polymer Chemistry*, *44*, 6962-6979.
31. Zhu, S. P. **1999** "Modeling stable free-radical polymerization" *Journal of Polymer Science Part B-Polymer Physics*, *37*, 2692-2704.
32. Li, I.; Howell, B. A.; Matyjaszewski, K.; Shigemoto, T.; Smith, P. B.; Priddy, D. B. **1995** "Kinetics of decomposition of 2,2,6,6-tetramethyl-1-(1-phenylethoxy)piperidine and its implications on nitroxyl-mediated styrene polymerization" *Macromolecules*, *28*, 6692-6693.
33. Hawker, C. J.; Barclay, G. G.; Orellana, A.; Dao, J.; Devonport, W. **1996** "Initiating systems for nitroxide-mediated "living" free radical polymerizations: synthesis and evaluation" *Macromolecules*, *29*, 5245-5254.

34. Moad, G.; Rizzardo, E.; Solomon, D. H. **1981** "The reaction of acyl peroxides with 2,2,6,6-tetramethylpiperidinyl-1-oxy" *Tetrahedron Letters*, *22*, 1165-1168.
35. Georges, M. K.; Hamer, G.; Szkurhan, A. R.; Kazemedah, A.; Li, J. **2002** "Stable free radical polymerization process - Initiation mechanisms with benzoyl peroxide and various nitroxides" *Abstracts of Papers of the American Chemical Society*, *224*, U464.
36. Fu, Y.; Cunningham, M. F.; Hutchinson, R. A. **2007** "Modeling of nitroxide-mediated semibatch radical polymerization" *Macromolecular Reaction Engineering*, *1*, 243-252.
37. Roa-Luna, M.; Nabifar, A.; McManus, N. T.; Vivaldo-Lima, E.; Lona, L. M. F.; Penlidis, A. **2007** "Effect of the addition of inert or TEMPO-capped prepolymer on polymerization rate and molecular weight development in the nitroxide-mediated radical polymerization of styrene" *Submitted to Journal of Applied Polymer Science (Aug 2007), Manuscript length 37 pages*.
38. Ohno, K.; Tsujii, Y.; Fukuda, T. **1997** "Mechanism and kinetics of nitroxide-controlled free radical polymerization. Thermal decomposition of 2,2,6,6-tetramethyl-1-polystyroxypiperidines" *Macromolecules*, *30*, 2503-2506.
39. He, J. P.; Li, L.; Yang, Y. L. **2000** "Effect of hydrogen transfer reaction on kinetics of nitroxide-mediated free-radical polymerization" *Macromolecules*, *33*, 2286-2289.
40. Souaille, M.; Fischer, H. **2001** "Living free radical polymerizations mediated by the reversible combination of transient propagating and persistent nitroxide radicals. The role of hydroxylamine and alkene formation" *Macromolecules*, *34*, 2830-2838.
41. Saban, M. D.; Georges, M. K.; Veregin, R. P. N.; Hamer, G. K.; Kazmaier, P. M. **1995** "Nitroxide-mediated free-radical polymerization of styrene - absence of the gel effect" *Macromolecules*, *28*, 7032-7034.
42. Zhang, M.; Ray, W. H. **2002** "Modeling of "living" free-radical polymerization processes. I. batch, semibatch, and continuous tank reactors" *Journal of Applied Polymer Science*, *86*, 1630-1662.
43. Roa-Luna, M.; Diaz-Barber, M. P.; Vivaldo-Lima, E.; Lona, L. M. F.; McManus, N. T.; Penlidis, A. **2007** "Assessing the importance of diffusion-controlled effects on polymerization rate and molecular weight development in nitroxide-mediated radical polymerization of styrene" *Journal of Macromolecular Science, Part A: Pure and Applied Chemistry*, *44*, 193-203.

CHAPTER 5 – MATHEMATICAL MODELING

This chapter focuses on the mathematical modeling of nitroxide-mediated radical polymerization of styrene. Table 5.1 lists some of the pioneering and important papers on this subject. In our work, a detailed kinetic mechanism for the NMRP of styrene is considered and the corresponding mathematical model, based on the method of moments, is derived. The result is a system of ordinary differential equations (ODE's), which was tested against experimental data. The model includes several side reactions which have been found to be relevant for the detailed explanation of molecular weight development (MWD) features of the polymer formed. Parameter sensitivity analysis is carried out to obtain a better understanding of the controlling reactions. By simple manipulation of the ODE's initial conditions and tuning of the model by turning on/off the appropriate kinetic steps, via their corresponding kinetic rate constants, the model presented here is capable of representing bimolecular and unimolecular NMRP techniques.

Table 5.1 Pioneering papers on modeling of NMRP

Authors	Year of Publication	Method of Solution and Comments
Johnson et al. ^[1]	1990	Numerical solution of all balance equations
Greszta et al. ^[2]	1996	Predici
Zhu ^[3]	1999	Method of moments
Butte et al. ^[4]	1999	Method of moments and an empirical expression for diffusion-controlled termination
Fukuda et al. ^[5]	2000	Simplified model including thermal initiation and steady state hypothesis
He et al. ^[6]	2000	Monte Carlo simulation
Faliks et al. ^[7]	2001	Minimizing reaction time by maintaining constant PDI using optimal control technique
Bonilla et al. ^[8]	2002	Method of moments; detailed mechanism of reaction
Zhang et al. ^[9]	2002	Method of moments
Tobita ^[10]	2006	Monte Carlo simulation
Saldivar- Guerra ^[11]	2006	An analysis of the applicability and limitations of quasi-steady state (QSS) and quasi steady equilibrium (QSE); Sensitivity analysis

5.1 Reaction Scheme and General Considerations

A kinetic model based on a detailed reaction mechanism for the nitroxide-mediated radical polymerization (NMRP) of styrene is presented. The reaction mechanism used as the basis for the derivation of the model is the one proposed by Bonilla et al. [8] and is summarized in Table 5.2. The mechanism includes the following reactions: chemical initiation, reversible nitroxyl ether decomposition (for the monomolecular process), monomer dimerization, thermal self-initiation, propagation, reversible monomeric and polymeric alkoxyamine formation (production of dormant species), alkoxyamine decomposition, rate enhancement, transfer to monomer and dimer, as well as conventional termination.

As discussed in subsection 4.6.2, diffusion-controlled (DC) effects do not influence the NMRP systems in any significant fashion, so they are not considered in the model and all rate constants are assumed to be independent of chain length. Table 5.3 cites the kinetic rate constants used which are presented as Arrhenius functions of activation energies and temperature [12] (Reference [12] also shows an extensive parametric sensitivity analysis).

The physical properties of the monomer (styrene, sty), polymer and initiator (BPO) used in the calculations are listed in Table 5.4. The model development and results obtained in the remainder of this chapter rely heavily on the work of Vivaldo-Lima et al. [8] and their simulation efforts [8, 12, 13].

Table 5.2 General mechanism for NMRP kinetics ^[8]

Description	Step
Chemical initiation	$I \xrightarrow{k_d} 2R_{in}^\bullet$
Nitroxyl ether decomposition	$NO_E \xrightleftharpoons[k_{d2}]{k_{d2}} R_{in}^\bullet + NO_x^\bullet$
Mayo dimerization	$M + M \xrightarrow{k_{dim}} D$
Thermal initiation	$M + D \xrightarrow{k_{ia}} D^\bullet + M^\bullet$
First propagation (primary radicals)	$R_{in}^\bullet + M \xrightarrow{k_p} R_1^\bullet$
First propagation (monomeric radicals)	$M^\bullet + M \xrightarrow{k_p} R_1^\bullet$
First propagation (dimeric radicals)	$D^\bullet + M \xrightarrow{k_p} R_1^\bullet$
Propagation	$R_r^\bullet + M \xrightarrow{k_p} R_{r+1}^\bullet$
Dormant living exchange (monomeric alkoxyamine)	$M^\bullet + NO_x^\bullet \xrightleftharpoons[k_{da}]{k_a} MNO_x$
Dormant living exchange (polymeric alkoxyamine)	$R_r^\bullet + NO_x^\bullet \xrightleftharpoons[k_{da}]{k_a} R_rNO_x$
Alkoxyamine decomposition	$MNO_x \xrightarrow{k_{decomp}} M + HNO_x$
Rate enhancement reaction	$D + NO_x^\bullet \xrightarrow{k_{h3}} D^\bullet + HNO_x$
Termination by combination	$R_r^\bullet + R_s^\bullet \xrightarrow{k_{tc}} P_{r+s}$
Termination by disproportionation	$R_r^\bullet + R_s^\bullet \xrightarrow{k_{td}} P_r + P_s$
Transfer to monomer	$R_r^\bullet + M \xrightarrow{k_{fM}} P_r + M^\bullet$
Transfer to dimer	$R_r^\bullet + D \xrightarrow{k_{fD}} P_r + D^\bullet$

Table 5.3 Kinetic rate constants for the monomolecular and bimolecular NMRP processes (T [K] and R [cal mol⁻¹ K⁻¹])^[12]

Variable	Unit	Bimolecular	Monomolecular
k _d (BPO)	s ⁻¹	$1.7 \times 10^{15} \exp\left(-\frac{30000}{RT}\right)$	-
f ₀		0.54-0.55 ^{a)}	-
k _{dim}	L mol ⁻¹ s ⁻¹	$188.97 \exp\left(-\frac{16185.1}{RT}\right)$	$188.97 \exp\left(-\frac{16185.1}{RT}\right)$
k _{ia}	L mol ⁻¹ s ⁻¹	$6.359 \times 10^{12} \exp\left(-\frac{36598.55}{RT}\right)$	$6.359 \times 10^{12} \exp\left(-\frac{36598.55}{RT}\right)$
k _{p0}	L mol ⁻¹ s ⁻¹	$4.266 \times 10^7 \exp\left(-\frac{7769.17}{RT}\right)$	$4.266 \times 10^7 \exp\left(-\frac{7769.17}{RT}\right)$
k _{t0}	L mol ⁻¹ s ⁻¹	$2.002 \times 10^{10} \exp\left(-\frac{3081.84}{RT}\right)$	$2.002 \times 10^{10} \exp\left(-\frac{3081.84}{RT}\right)$
k _{td} /k _{t0}		0.0	0.0
k _{fM}	L mol ⁻¹ s ⁻¹	$9.376 \times 10^6 \exp\left(-\frac{13372}{RT}\right)$	$9.376 \times 10^6 \exp\left(-\frac{13372}{RT}\right)$
k _{fD}	L mol ⁻¹ s ⁻¹	50	50
k _{a2}	s ⁻¹	0.0	$2.0 \times 10^{13} \exp\left(-\frac{29683}{RT}\right)$
k _{d2}	L mol ⁻¹ s ⁻¹	0.0	$5.03 \times 10^9 \exp\left(-\frac{3722}{RT}\right)$
k _{da}	L mol ⁻¹ s ⁻¹	$5.03 \times 10^9 \exp\left(-\frac{3722}{RT}\right)$	$5.03 \times 10^9 \exp\left(-\frac{3722}{RT}\right)$
k _a	s ⁻¹	$2.0 \times 10^{13} \exp\left(-\frac{29683}{RT}\right)$	$2.0 \times 10^{13} \exp\left(-\frac{29683}{RT}\right)$
k _{decomp}	s ⁻¹	$5.7 \times 10^{14} \exp\left(-\frac{36639.6}{RT}\right)$	$5.7 \times 10^{14} \exp\left(-\frac{36639.6}{RT}\right)$
k _{h3}	L mol ⁻¹ s ⁻¹	0.001	0.001

^{a)} Initiator efficiency (f) range depending on the reaction temperature.

Table 5.4 Physical properties

Property	Unit	Value
ρ_M	kg L^{-1}	$0.9193 - 0.000665(T - 273.15)$
ρ_P	kg L^{-1}	$0.9926 - 0.000265(T - 273.15)$
MW_M	g mol^{-1}	104.12
MW_{init}	g mol^{-1}	242.23
T_{gM}	K	185.0
T_{gP}	K	378.0

5.2 Overall Mass (Molar) Balances and Moment Equations

Based on the reaction mechanism shown in Table 5.2, the mass balance equations are given by Equation 5.1 to 5.12 for a batch reactor.

$$\frac{d[I]}{dt} = -k_d [I] \quad (5.1)$$

$$\begin{aligned} \frac{d[M]}{dt} = & -2k_{\text{dim}} [M]^2 - k_{\text{ia}} [M][D] - k_p [M] ([D^\bullet] + [M^\bullet] + [R_{\text{in}}^\bullet]) \\ & - k_p [M][R^\bullet] - k_{\text{fM}} [M][R^\bullet] + k_{\text{decomp}} [MNO_x] \end{aligned} \quad (5.2)$$

$$\frac{d[NO_E]}{dt} = -k_{a2} [NO_E] + k_{d2} [NO_x^\bullet] [R_{\text{in}}^\bullet] \quad (5.3)$$

$$\frac{d[M^\bullet]}{dt} = +k_{\text{ia}} [M][D] - k_p [M][M^\bullet] - k_{\text{da}} [NO_x^\bullet] [M^\bullet] + k_a [MNO_x] + k_{\text{fM}} [M][R^\bullet] \quad (5.4)$$

$$\frac{d[R_{\text{in}}^\bullet]}{dt} = +2fk_d [I] - k_p [M][R_{\text{in}}^\bullet] + k_{a2} [NO_E] - k_{d2} [NO_x^\bullet] [R_{\text{in}}^\bullet] \quad (5.5)$$

$$\frac{d[D^\bullet]}{dt} = +k_{ia}[M][D] - k_p[M][D^\bullet] + k_{h3}[NO_x^\bullet][D] + k_{fD}[D][R^\bullet] \quad (5.6)$$

$$\begin{aligned} \frac{d[NO_x^\bullet]}{dt} = & -k_{h3}[D][NO_x^\bullet] - k_{da}[NO_x^\bullet][R^\bullet] + k_a[R_1NO_x] \\ & - k_{da}[NO_x^\bullet][M^\bullet] + k_a[MNO_x] - k_{d2}[NO_x^\bullet][R_{in}^\bullet] + k_{a2}[NO_E] \end{aligned} \quad (5.7)$$

$$\frac{d[HNO_x]}{dt} = +k_{h3}[NO_x^\bullet][D] + k_{decomp}[MNO_x] \quad (5.8)$$

$$\frac{d[MNO_x]}{dt} = +k_{da}[NO_x^\bullet][M^\bullet] - k_a[MNO_x] - k_{decomp}[MNO_x] \quad (5.9)$$

$$\frac{d[RNO_x]}{dt} = +k_{da}[NO_x^\bullet][R^\bullet] - k_a[RNO_x] \quad (5.10)$$

$$\begin{aligned} \frac{d[R^\bullet]}{dt} = & +k_p[M]([M^\bullet] + [D^\bullet] + [R_{in}^\bullet]) - (k_{tc} + k_{td})([R^\bullet])^2 \\ & - k_{da}[NO_x^\bullet][R^\bullet] + k_a[R_1NO_x] - k_{fM}[R^\bullet][M] - k_{fD}[R^\bullet][D] \end{aligned} \quad (5.11)$$

$$\frac{d[P]}{dt} = +k_{fM}[R^\bullet][M] + k_{fD}[R^\bullet][D] + k_t[R^\bullet]^2 \quad (5.12)$$

The rates of initiator decomposition and monomer and nitroxyl ether consumption are given in Eqs. 5.1 to 5.3. Eqs. 5.4 to 5.7 are the corresponding rate equations for monomeric, primary, dimeric, and stable nitroxyl radicals, respectively. The mass balances for hydroxylamine species, monomeric and polymeric alkoxyamines (dormant species) are given by Eqs. 5.8 to 5.10. Eqs. 5.11 and 5.12 present the mass balances for polymeric radicals and dead polymer species, respectively.

In order to follow the molecular weight development, in terms of number and weight averages, the method of moments is used. There are three polymer populations in this system: “living”

polymer radicals, dead polymer molecules, and dormant species. The moments for “living” radical, dormant and dead species are defined in Eqs. 5.13 to 5.15.

$$\lambda_i = \sum_r r^i R_r \quad (5.13)$$

$$\delta_i = \sum_r r^i R_r ON_x \quad (5.14)$$

$$\mu_i = \sum_r r^i P_r \quad (5.15)$$

Once the mass balance equations for polymer molecules of the three types and for all lengths are derived, based on the reaction mechanism of Table 5.2, the application of the method of moments produces Eqs. 5.16 to 5.18 for moments zero, one and two, respectively, of living polymer radicals; Eqs. 5.19 to 5.21 for the respective moments of dormant polymer, and Eqs. 5.22 to 5.24 for the moments of the dead polymer.

$$\begin{aligned} \frac{d(\lambda_0)}{dt} = & +k_p [M] ([M^\bullet] + [D^\bullet] + [R_{in}^\bullet]) - k_t [\lambda_0]^2 \\ & - k_{fM} [\lambda_0] [M] - k_{fD} [D] [\lambda_0] - k_{da} [NO_x^\bullet] [\lambda_0] + k_a [\delta_0] \end{aligned} \quad (5.16)$$

$$\begin{aligned} \frac{d(\lambda_1)}{dt} = & +k_p [M] ([M^\bullet] + [D^\bullet] + [R_{in}^\bullet]) + k_p [M] [\lambda_0] \\ & - k_t [\lambda_0] [\lambda_1] - k_{fM} [\lambda_1] [M] - k_{fD} [D] [\lambda_1] - k_{da} [NO_x^\bullet] [\lambda_1] + k_a [\delta_1] \end{aligned} \quad (5.17)$$

$$\begin{aligned} \frac{d(\lambda_2)}{dt} = & - k_{da} [NO_x^\bullet] [\lambda_2] + k_a [\delta_2] - k_t [\lambda_0] [\lambda_2] \\ & + k_p [M] ([M^\bullet] + [D^\bullet] + [R_{in}^\bullet] + [\lambda_0] + 2[\lambda_1]) - k_{fM} [\lambda_2] [M] - k_{fD} [D] [\lambda_2] \end{aligned} \quad (5.18)$$

$$\frac{d(\delta_0)}{dt} = +k_{da} [NO_x^\bullet] [\lambda_0] - k_a [\delta_0] \quad (5.19)$$

$$\frac{d(\delta_1)}{dt} = +k_{da} [NO_x^\bullet] [\lambda_1] - k_a [\delta_1] \quad (5.20)$$

$$\frac{d(\delta_2)}{dt} = +k_{da} [\text{NO}_x \bullet] [\lambda_2] - k_a [\delta_2] \quad (5.21)$$

$$\frac{d(\mu_0)}{dt} = +\frac{1}{2}k_{tc} [\lambda_0]^2 + k_{td} [\lambda_0]^2 + k_{fM} [\lambda_0][M] + k_{fD} [\lambda_0][D] \quad (5.22)$$

$$\frac{d(\mu_1)}{dt} = +k_{tc} [\lambda_0][\lambda_1] + k_{td} [\lambda_0][\lambda_1] + k_{fM} [\lambda_1][M] + k_{fD} [\lambda_1][D] \quad (5.23)$$

$$\frac{d(\mu_2)}{dt} = +k_{tc} ([\lambda_0][\lambda_2] + [\lambda_1]^2) + k_{td} [\lambda_0][\lambda_2] + k_{fM} [\lambda_2][M] + k_{fD} [\lambda_2][D] \quad (5.24)$$

Finally calculation of the number and weight average molecular weights, based on the moments of the polymer populations, is carried out using Eqs. 5.25 and 5.26.

$$\text{Mn} = \text{MW}_M \left(\frac{\mu_1 + \lambda_1 + \delta_1}{\mu_0 + \lambda_0 + \delta_0} \right) \quad (5.25)$$

$$\text{MW} = \text{MW}_M \left(\frac{\mu_2 + \lambda_2 + \delta_2}{\mu_1 + \lambda_1 + \delta_1} \right) \quad (5.26)$$

In order to avoid numerical problems due to the possible stiffness of the system of differential equations, the 21 ordinary differential equations that describe the kinetic behavior and the molecular weight development were transformed into dimensionless differential equations [8].

5.3 Comparison of Simulated Profiles and Experimental Data

Figure 5.1 shows a comparison of experimental data and model predictions for conversion versus time at 120 °C and [TEMPO]/[BPO] = 1.1. As can be seen, the agreement between model predictions obtained and experimental data is very good up to 50% monomer conversion, but the model overestimates the polymerization rate at high conversions, and the maximum conversion achieved at the polymerization conditions. The model predicts 90% conversion at about 20 hrs, and total conversion at about 50 hrs, whereas the experimental data reach 90% monomer conversion at around 40hr, and the conversion does not go beyond 93%.

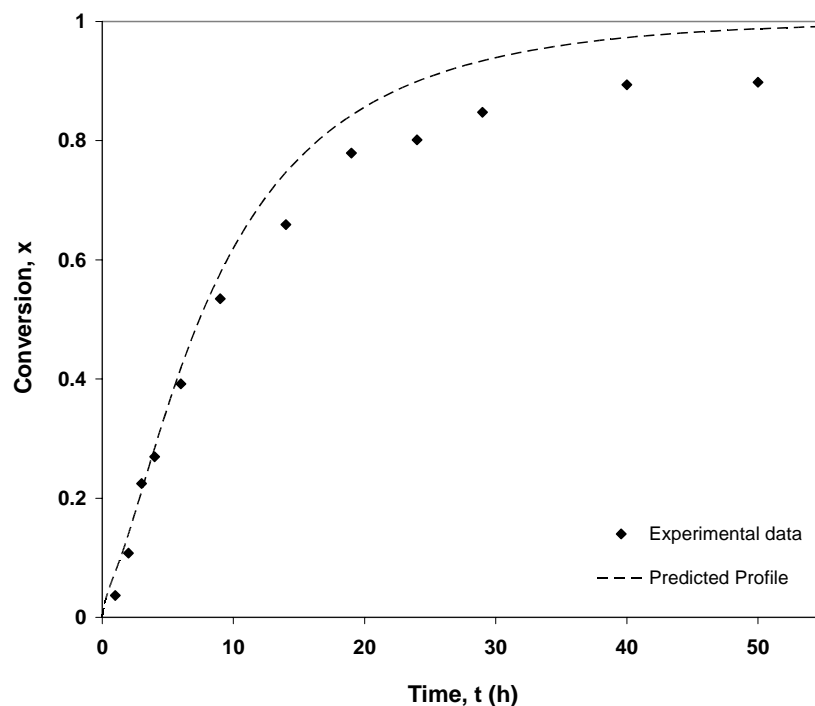


Figure 5.1 Comparison of experimental data and model predictions of conversion vs. time, at 120 °C and $[\text{TEMPO}]/[\text{BPO}] = 1.1$

Figure 5.2 shows the corresponding plot of number average molecular weight versus conversion. The model predictions capture the linear trend in average molecular weight but underestimate the experimental data. It was first speculated that this may be caused by the transfer to monomer reaction in the reaction mechanism being considered in the mathematical model, or possibly by inaccurate estimates of some of the kinetic rate constants involved in the reaction mechanism [13]. More recently, we have come to the conclusion that possible side reactions, such as the “promoted dissociation” of BPO, which decrease the effective concentration of TEMPO, could also be responsible for these discrepancies [14]. (See also sections 4.5.1 and 4.6.1)

The model predicted profile of PDI vs. conversion shown in Figure 5.3 agrees well with the experimental data, which lie on the average PDI most of the time. The calculated profile predicts high PDIs (higher than 5) at the beginning of the polymerization, decreasing to lower than 2 at about 10% monomer conversion, and remaining fairly constant around 1.1 and 1.2, showing a very slight increase at very high conversions.

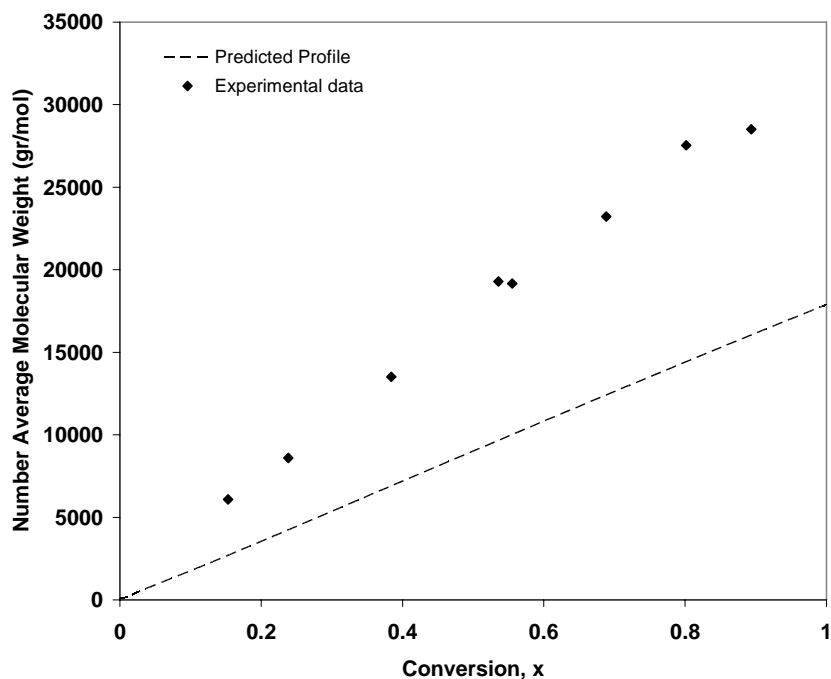


Figure 5.2 Comparison of experimental data and model predictions of number average molecular weight vs. conversion, at 120 °C and [TEMPO]/[BPO] = 1.1

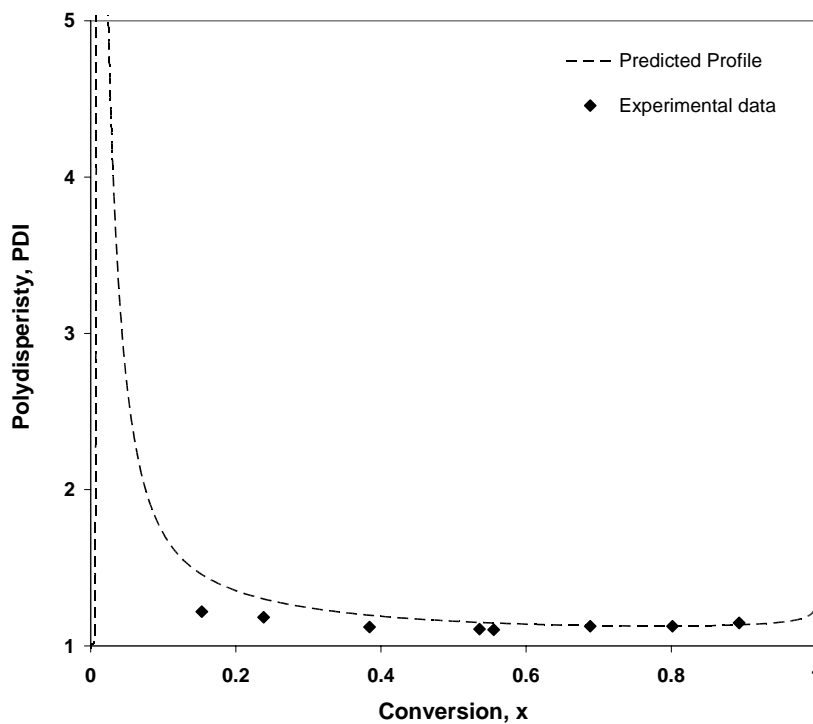


Figure 5.3 Comparison of experimental data and model predictions of polydispersity vs. conversion, at 120 °C and [TEMPO]/[BPO] = 1.1

The model is capable of simulating the intermediate species like nitroxyl radicals, dead, dormant and living species. This is extremely useful, as it offers additional insight in the polymerization behavior, and can be used in formulating viable explanations for the behavior of many variables. It is observed in Figure 5.4a that there is a significant amount of nitroxyl radicals at the very beginning of the polymerization, which are immediately consumed by the free radicals released by the initiator, to generate dormant species (Figure 5.4b). At the beginning of the polymerization, the concentration of living radicals increases at a rate proportional to the consumption of nitroxyl radicals. As can be seen in Figure 5.4a, once the equilibrium has been established, the concentration of nitroxyl radicals is stabilized, but it is later increased again (at conversions higher than 0.8) due to the long-term effect of bimolecular radical termination that leads to increasing dead polymer formation. This is accompanied by a slight decrease of living radicals (which is converted to dead polymer) and release of nitroxyl radicals that increase their concentration towards the end of the reaction (See Figures 5.4a and 5.4b at conversion levels higher than 0.8). It is also interesting to see in Figure 5.4b that the concentration of dead polymer grows very quickly at the beginning of the reaction, due to the rapid increase in the concentration of living radicals. The rapid growth of living radicals and dead polymer stops shortly after the beginning of the reaction and the concentrations of both species enter a region of much slower, but still closely correlated, rate of change (See the two curves after 45% conversion).

Experimental data and simulated profiles at $[\text{TEMPO}]/[\text{BPO}]$ ratios of 0.9, 1.1, 1.2 and 1.5 are shown in Figure 5.5. As expected, the larger the ratio (the more TEMPO fed to the recipe), the slower the polymerization will proceed. Both the experimental data and predicted profiles show that trend. However, the effect is much more pronounced in the experimental data than the predictions of the model. The model predicts a crossover of curves, with the limiting conversion reaching higher values as the $[\text{TEMPO}]/[\text{BPO}]$ ratio is increased. That crossover of curves is not captured with the experimental data, but that may be explained by the fact that the experimental error seems to be higher than the sensitivity needed in the high conversion region to observe that effect. Model predictions also capture the induction time for $[\text{TEMPO}]/[\text{BPO}] = 1.5$ which lasts about 2.5 h at those conditions.

Figure 5.6 shows the corresponding profiles to Figure 5.5 for number average molecular weight development. It is observed that higher values of the number average molecular weight, M_n , are obtained when the $[\text{TEMPO}]/[\text{BPO}]$ ratio is decreased, namely, when the polymerization rate is increased. The model captures nicely this behavior, but all the profiles lie lower than the experimental data, as noted previously (Figure 5.2).

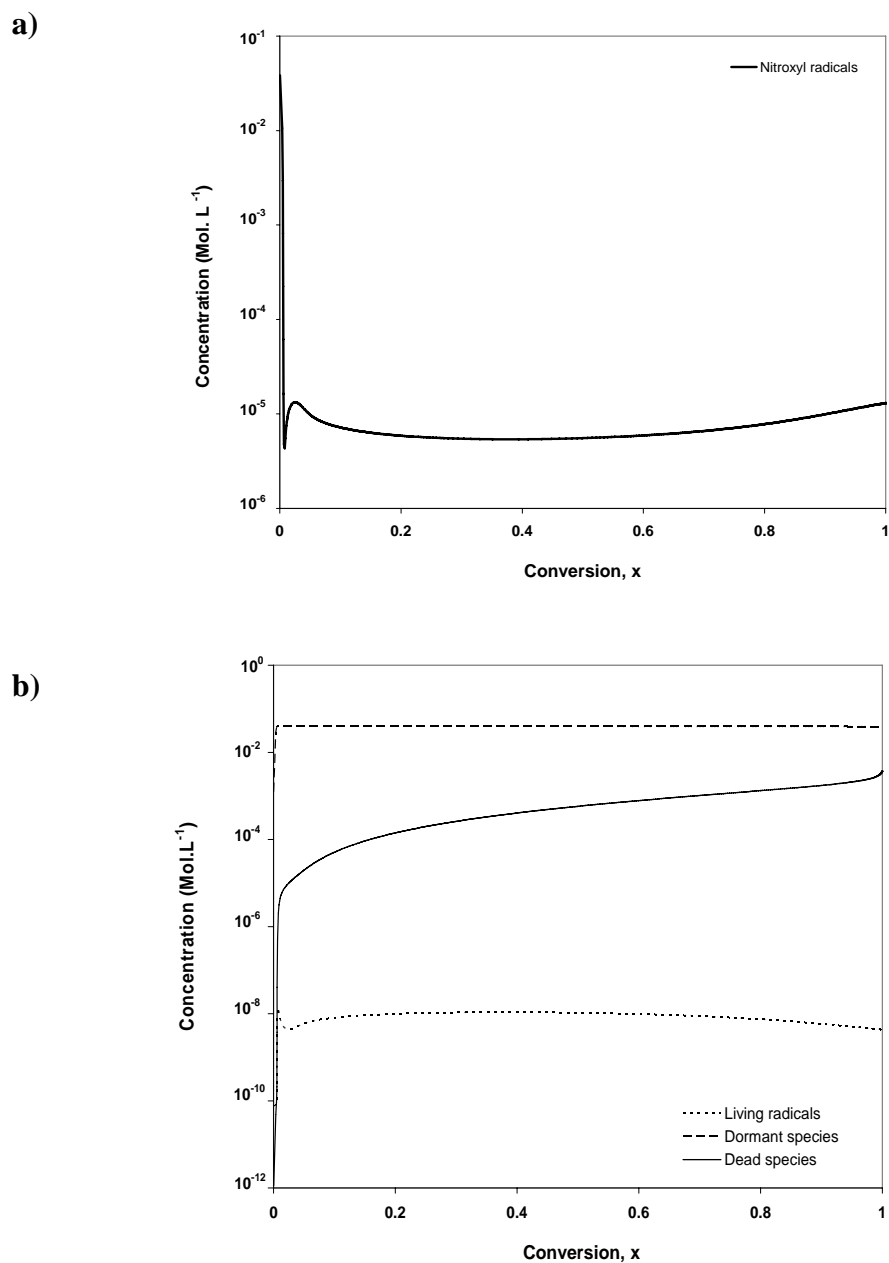


Figure 5.4 a) Simulated concentration of nitroxyl radicals vs. conversion, b) Simulated concentrations of dead, dormant and living radicals vs. conversion, for NMRP of styrene at 120 and $[\text{TEMPO}]/[\text{BPO}] = 1.1$

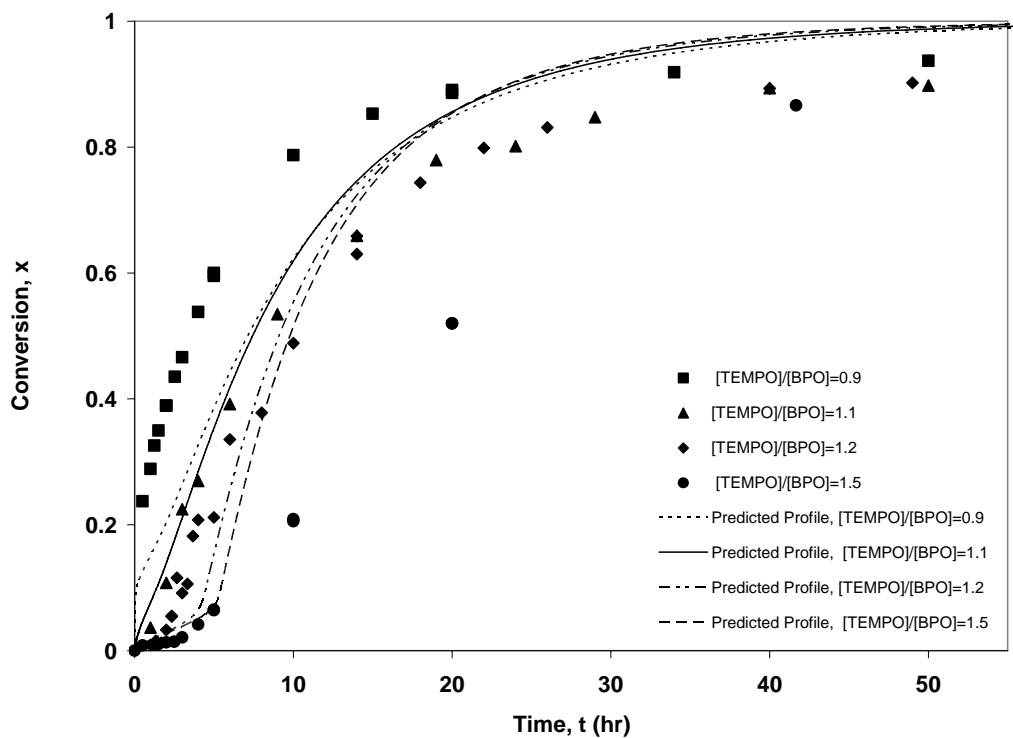


Figure 5.5 Effect of $[\text{TEMPO}]/[\text{BPO}]$ ratio on polymerization rate at $120\text{ }^{\circ}\text{C}$; comparison of experimental data and model predictions

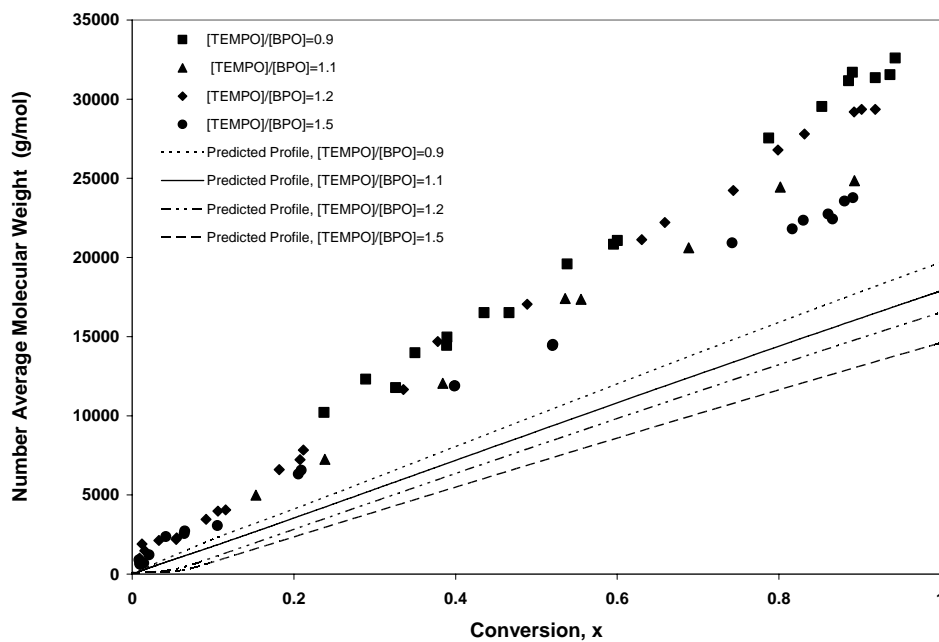


Figure 5.6 Effect of $[\text{TEMPO}]/[\text{BPO}]$ ratio on number average molecular weight at $120\text{ }^{\circ}\text{C}$; comparison of experimental data and model predictions

Figure 5.7 shows a comparison of model simulations against experimental data of PDI vs. conversion at 120 °C and the same [TEMPO]/[BPO] ratios analyzed in Figures 5.5 and 5.6 for polymerization rate and Mn development, respectively. The predicted profiles at [TEMPO]/[BPO] = 0.9 and 1.1 show that very high PDIs are predicted at very low conversions, with higher PDIs from the reaction where [TEMPO]/[BPO] = 0.9. The predicted profiles at [TEMPO]/[BPO] = 1.2 and 1.5 show that the maximum on PDI is significantly reduced, but shifted towards higher conversion values, as the ratio increases, although the profile at [TEMPO]/[BPO] = 1.5 shows slightly higher PDIs than the profile at [TEMPO]/[BPO] = 1.2. Many samples were taken during the very low conversion range in the experiments at [TEMPO]/[BPO] = 1.5. It is interesting to see that the new experimental data of frequently measured PDI's in the early stages of reaction did show very high values of PDI, which in a sense confirmed early model predictions by [8, 15, 16] and also our model predictions herein. However, although the model results arguably capture experimental trends in PDI, the qualitative agreement is not always good at all ratios. For instance, those measured PDIs at [TEMPO]/[BPO] = 1.5 in the early stages of the polymerization, do not agree with the predicted profile at that ratio, which showed a maximum PDI of 1.93 at 11% monomer conversion, whereas the experimental maximum of PDI = 7.95 was obtained at 0.8% (less than one percent) monomer conversion. The corresponding conversion, molecular weights and polydispersity profiles for the other temperature (130 °C) can be found in Figures B.28 to B.30 in Appendix B. The general trends are the same as the ones observed at 120°C.

Figure 5.8 shows the simulated profiles for nitroxyl radicals, living species, dormant species, and dead species versus conversion for different [TEMPO]/[BPO] ratios at 120°C. As can be seen in Figure 5.8a there is more free TEMPO present in the system for higher [TEMPO]/[BPO] ratios at the beginning of the reaction but as the reaction proceeds and the equilibrium is established the level of free TEMPO is almost the same for all the ratios.

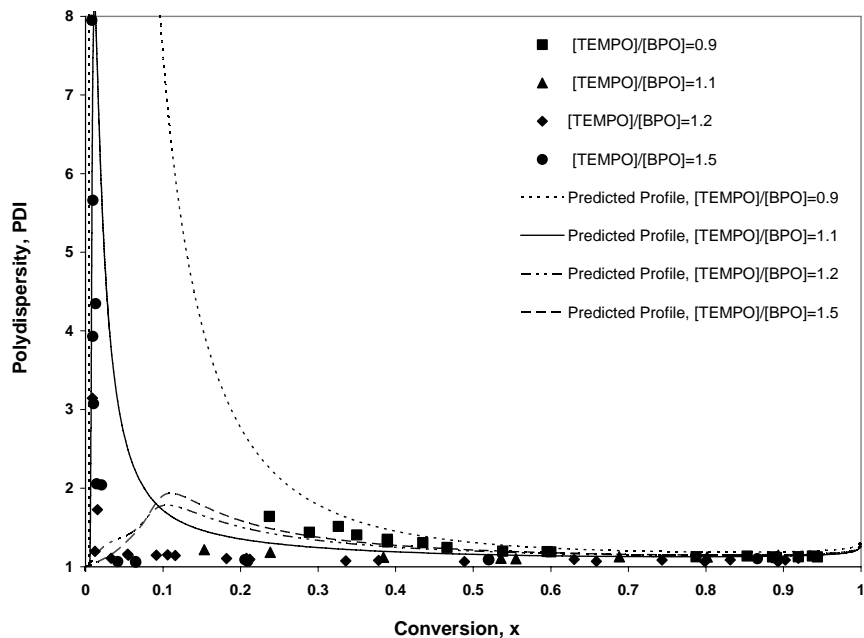


Figure 5.7 Effect of [TEMPO]/[BPO] ratio on polydispersity at 120 °C; comparison of experimental data and model predictions

Figure 5.8b shows the corresponding living radical concentrations. As expected the highest concentration belongs to ratio 0.9 at the beginning of the reaction. Since there is less TEMPO present, the system acts like a less controlled polymerization and there is a high concentration of free radicals present in the systems which results in more bimolecular termination and an increase in the concentration of dead polymer molecules, as can be seen in Figure 5.8d. However, as the reaction proceeds and the equilibrium is established, the highest living radical concentration belongs to ratio 1.5. The reason for this behavior can be explained by Eqs. 5.27 and 5.28. The value of the kinetic rate constant (K) should be the same for all the ratios. As expected, an increase in the initial concentration of nitroxyl radicals increases the concentration of dormant species (Figure 5.8c); the concentration of free TEMPO radicals are almost the same for all the ratios (Figure 5.8a) so according to Eq. 5.28 concentration of living radicals should increase for higher ratios to keep K constant.



$$\text{K} = [\text{R} - \text{TEMPO}] / [\text{TEMPO}] \cdot [\text{R}\cdot] \quad (5.28)$$

Figure 5.8d shows the dead polymer concentration for all ratios. As can be seen, the highest concentration belongs to ratio 0.9 since there is less TEMPO present in the system, fewer radicals are capped by TEMPO and more termination occurs. The dead polymer concentrations for ratios 1.1, 1.2 and 1.5 are almost zero at the beginning of the reaction but as the reactions proceed and the concentrations of radicals increase (See Figure 5.8b), termination reactions become significant and dead polymer concentrations start to increase (gradually) for ratios 1.1, 1.2 and 1.5 as well (of course these concentrations are still lower than the dead polymer concentration for ratio 0.9). The highest profile belongs to ratio 1.5 since the concentration of living radicals for this case is higher as shown in Figure 5.8b.

The predictions obtained with the model of NMRP of styrene overestimate the polymerization rate at high conversions, and although they usually provide satisfactory predictions of polydispersity vs. time, they underestimate the average molecular weights. Although predictions from the mathematical model are not in good quantitative agreement with experimental data, overall they capture the general polymerization trends. This, combined with the fact that with the model one has access to profiles and thus behavior of many important “intermediate” species (variables), which otherwise are not readily apparent (For instance, see the discussion around Figure 5.8), make the model a very versatile and flexible tool that contributes tremendously in further process understanding and comprehension of important nonlinear interactions (inter-relationships, 2- and 3- factor effects) between the main polymerization variables.

Comparisons suggest that some of the kinetic rate constants reported in the literature are inaccurate and they are not reliable enough for predictive purposes. In addition, the discrepancies between the mathematical model and experimental data can be related to some possible side reactions not included in the model that affect the concentration of different species in the reaction. It seems that our understanding of the underlying mechanism and possible side reactions occurring in these systems is still incomplete, despite the extensive literature studies and claims on the subject.

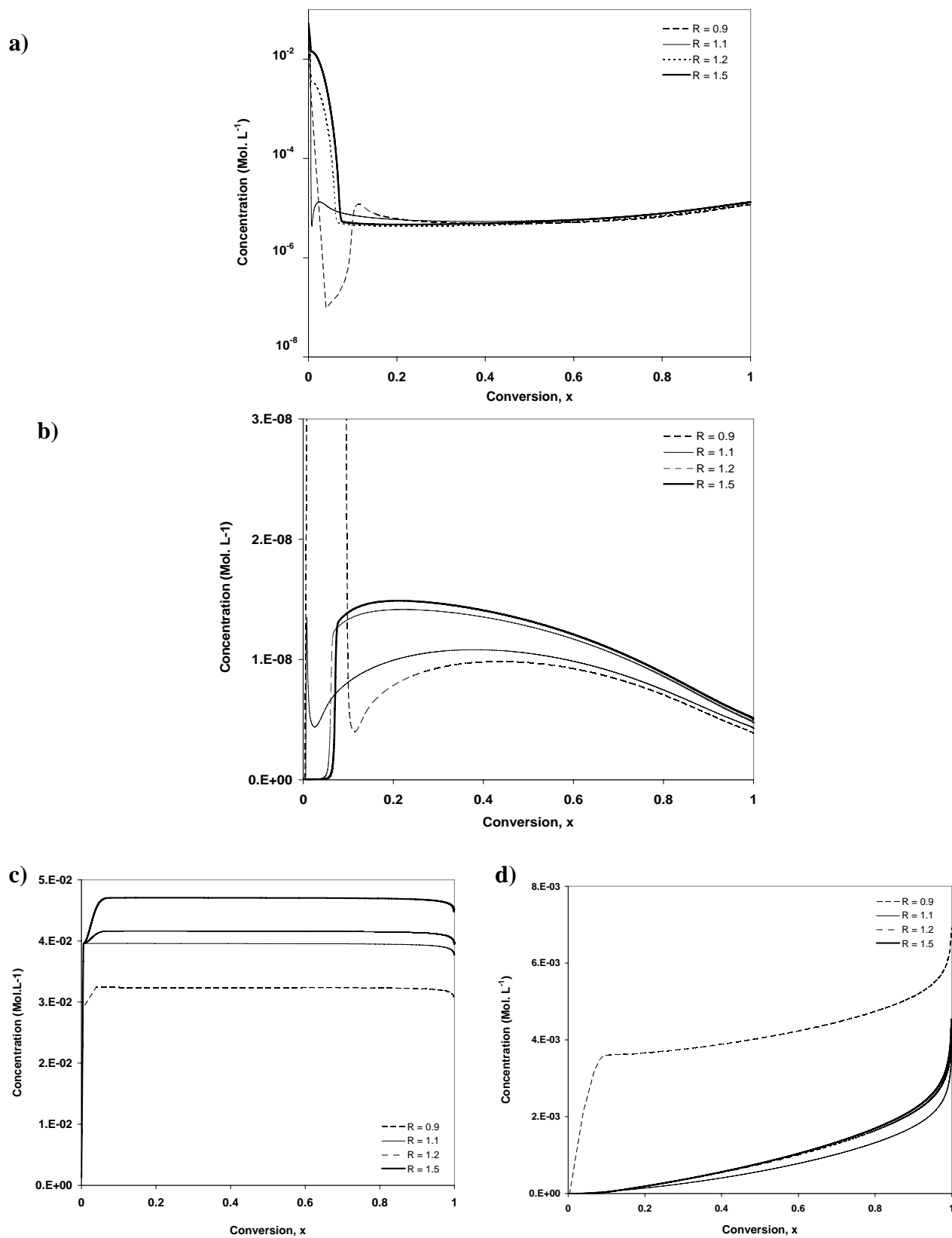


Figure 5.8 Effect of $[\text{TEMPO}]/[\text{BPO}]$ on simulated profiles of a) Nitroxyl radical, b) Living species, c) Dormant Species, and d) Dead species for NMRP of styrene at 120°C

5.4 References

1. Johnson, C. H. J.; Moad, G.; Solomon, D. H.; Spurling, T. H.; Vearing, D. J. **1990** "The application of supercomputers in modeling chemical-reaction kinetics - kinetic simulation of quasi-living radical polymerization" *Australian Journal of Chemistry*, *43*, 1215-1230.
2. Greszta, D.; Matyjaszewski K. **1996** "Mechanism of controlled/"living" radical polymerization of styrene in the presence of nitroxyl radicals. kinetics and simulations" *Macromolecules*, *29*, 7661-7670.
3. Zhu, S. P. **1999** "Modeling stable free-radical polymerization" *Journal of Polymer Science Part B-Polymer Physics*, *37*, 2692-2704.
4. Butte, A.; Storti, G.; Morbidelli, M. **1999** "Kinetics of "living" free radical polymerization" *Chemical Engineering Science*, *54*, 3225-3231.
5. Fukuda, T.; Goto, A.; Ohno, K. **2000** "Mechanisms and kinetics of living radical polymerizations" *Macromolecular Rapid Communications*, *21*, 151-165.
6. He, J. P.; Li, L.; Yang, Y. L. **2000** "Effect of hydrogen transfer reaction on kinetics of nitroxide-mediated free-radical polymerization" *Macromolecules*, *33*, 2286-2289.
7. Faliks, A.; Yetter, R. A.; Floudas, C. A.; Wei, Y.; Rabitz, H. **2001** "Optimization of living polymerization through distributed control of a nitroxide radical" *Polymer*, *42*, 2061-2065.
8. Bonilla, J.; Saldivar, E.; Flores-Tlacuabuac, A.; Vivaldo-Lima, E.; Pfaendner, R.; Tiscareno-Lechuga, F. **2002** "Detailed modeling, simulation, and parameter estimation of nitroxide mediated living free radical polymerization of styrene" *Polymer Reaction Engineering Journal*, *10*, 227-263.
9. Zhang, M.; Ray, W. H. **2002** "Modeling of "living" free-radical polymerization processes. I. batch, semibatch, and continuous tank reactors" *Journal of Applied Polymer Science*, *86*, 1630-1662.
10. Tobita, H. **2006** "Molecular weight distribution of living radical polymers - 2. Monte Carlo simulation" *Macromolecular Theory and Simulations*, *15*, 23-31.
11. Saldivar-Guerra, E.; Bonilla, J.; Becerril, F.; Zacahua, G.; Albores-Velasco, M.; Alexander-Katz, R.; Flores-Santos, L.; Alexandrova, L. **2006** "On the nitroxide quasi-equilibrium in the alkoxyamine-mediated radical polymerization of styrene" *Macromolecular Theory and Simulations*, *15*, 163-175.
12. Belincanta-Ximenes, J.; Mesa, P. V. R.; Lona, L. M. F.; Vivaldo-Lima, E.; McManus, N. T.; Penlidis, A. **2007** "Simulation of styrene polymerization by monomolecular and bimolecular nitroxide-mediated radical processes over a range of reaction conditions" *Macromolecular Theory and Simulations*, *16*, 194-208.

13. Roa-Luna, M.; Nabifar, A.; Diaz-Barber, M. P.; McManus, N. T.; Vivaldo-Lima, E.; Lona, L. M. F.; Penlidis, A. **2007** "Another perspective on the nitroxide mediated radical polymerization (NMRP) of styrene using 2,2,6,6-tetramethyl-1-piperidinyloxy (TEMPO) and dibenzoyl peroxide (BPO)" *Journal of Macromolecular Science Part A: Pure and Applied Chemistry*, *44*, 337-349.
14. Roa-Luna, M.; Nabifar, A.; McManus, N. T.; Vivaldo-Lima, E.; Lona, L. M. F.; Penlidis, A. **2007** "Effect of the addition of inert or TEMPO-capped prepolymer on polymerization rate and molecular weight development in the nitroxide-mediated radical polymerization of styrene" *Submitted to Journal of Applied Polymer Science (Aug 2007)*, *Manuscript length 37 pages*.
15. Veregin, R. P. N.; Odell, P. G.; Michalak, L. M.; Georges, M. K. **1996** "Molecular weight distributions in nitroxide-mediated living free radical polymerization: Kinetics of the slow equilibria between growing and dormant chains" *Macromolecules*, *29*, 3346-3352.
16. Goto, A.; Fukuda, T. **1997** "Effects of radical initiator on polymerization rate and polydispersity in nitroxide-controlled free radical polymerization" *Macromolecules*, *30*, 4272-4277.

CHAPTER 6 – CONCLUSIONS AND RECOMMENDATIONS

6.1 Concluding Remarks

Nitroxide-mediated radical polymerization (NMRP) of styrene using 2,2,6,6-tetramethyl-1-piperidinyloxy (TEMPO) as controller was investigated over a range of operating conditions, namely, different temperatures, different controller to initiator molar ratios, and different initiating systems. The experimental work showed that increasing temperature increases the rate of polymerization while slightly decreasing molecular weight averages. It was also observed that increasing the ratio of controller to initiator decreases both the rate of polymerization and molecular weights. Our observations have confirmed that thermal self-initiation of styrene plays an important role in NMRP of styrene by maintaining the polymerization rate by constant production of radicals. However, it has been shown that thermal self-initiation alone is not enough to produce narrow polydispersity materials in NMRP and presence of another initiating source is necessary to obtain a controlled polymerization. Comparisons between unimolecular and bimolecular initiating systems showed that although unimolecular initiators allow the preparation of macromolecules with greater control over molecular weights and polydispersity than the corresponding bimolecular systems, they may not be a practical approach because of a lack of efficient synthetic procedures for preparation. This is the first time that experimental data for NMRP of styrene at various operating conditions were collected over the full conversion range, and different initiating systems were contrasted at comparable conditions including polymerization rates, molecular weights and polydispersities. In addition, this is also the first time that polydispersity data were collected systematically even at the early stages of conversion, thus giving a full picture and at the same time confirming (unsubstantiated so far) mathematical model predictions.

One can look at Figures 6.1 and 6.2 as an attempt to give a “bird’s eye-view” of our experimental observations, complementary to Figures 4.24 and B.20/B.21. These summary snapshots (shown in Figure 6.1 and 6.2 for 120°C) can give a useful overview of the process data if one is interested in, say, an optimization problem. One can easily establish from the

above mentioned summary figures a “corridor of operation” for the process in question, in addition to a summary of the sensitivity of the process (process outputs and hence properties) to specific important factors (inputs). For instance, if polydispersity (PDI) were the sole variable in an optimization performance index, and one were interested in minimizing PDI, then a figure such as Figure 4.24 would suggest choosing a range for R values between 1.1-1.2. Figures 6.1 and 6.2 would allow one to consider additional variables in a multi-objective optimization framework (Figure 6.1 shows different measurements corresponding to a polymerization duration of 10hrs; Figure 6.2 shows measured properties corresponding to 50% conversion). For instance, if one would like to minimize time to reach 50% conversion at 120°C, at the same time keeping PDI at low values and, say, achieving an average molecular weight target of not more than 20,000, then Figure 6.2 would guide one to pick a value of $R \sim 1$. In this way, one can easily appreciate opposite trends and make practical compromises.

The simulations obtained from the kinetic model were subsequently compared against the experimental data. The evaluations suggest that the disagreement observed can be explained in terms of the potential inaccuracy of some of the kinetic rate constants in the model, or possible side reactions that take place in the experiment but are not taken into account in the kinetic model. In addition, the experimental investigations confirmed (using a “worst case scenario” approach) that diffusion-controlled effects are insignificant in nitroxide-mediated radical polymerization of styrene and these results were corroborated by the corresponding modeling work. It is worth mentioning that this has been the first time that the absence of diffusion-controlled effects has been supported by experimental work.

Although a considerable amount of experimental work has already been conducted on the kinetics of nitroxide-mediated polymerizations (and an extensive body of literature exists), there is still a lot that can be done to improve the understanding of the polymerization system and bring it closer to industrial production.

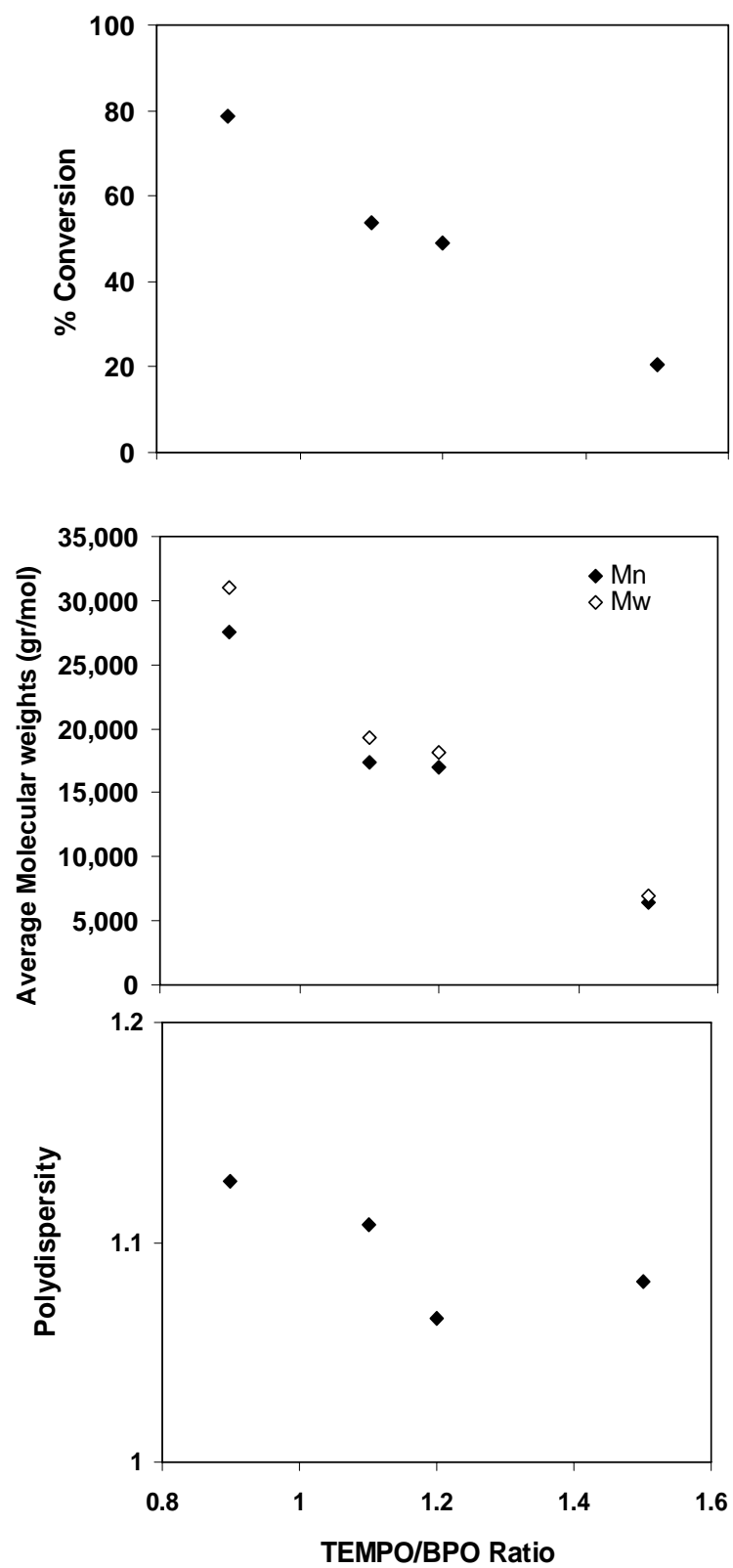


Figure 6.1 %conversion, molecular weights and polydispersity versus TEMPO/BPO ratio after 10 hrs; T = 120°C

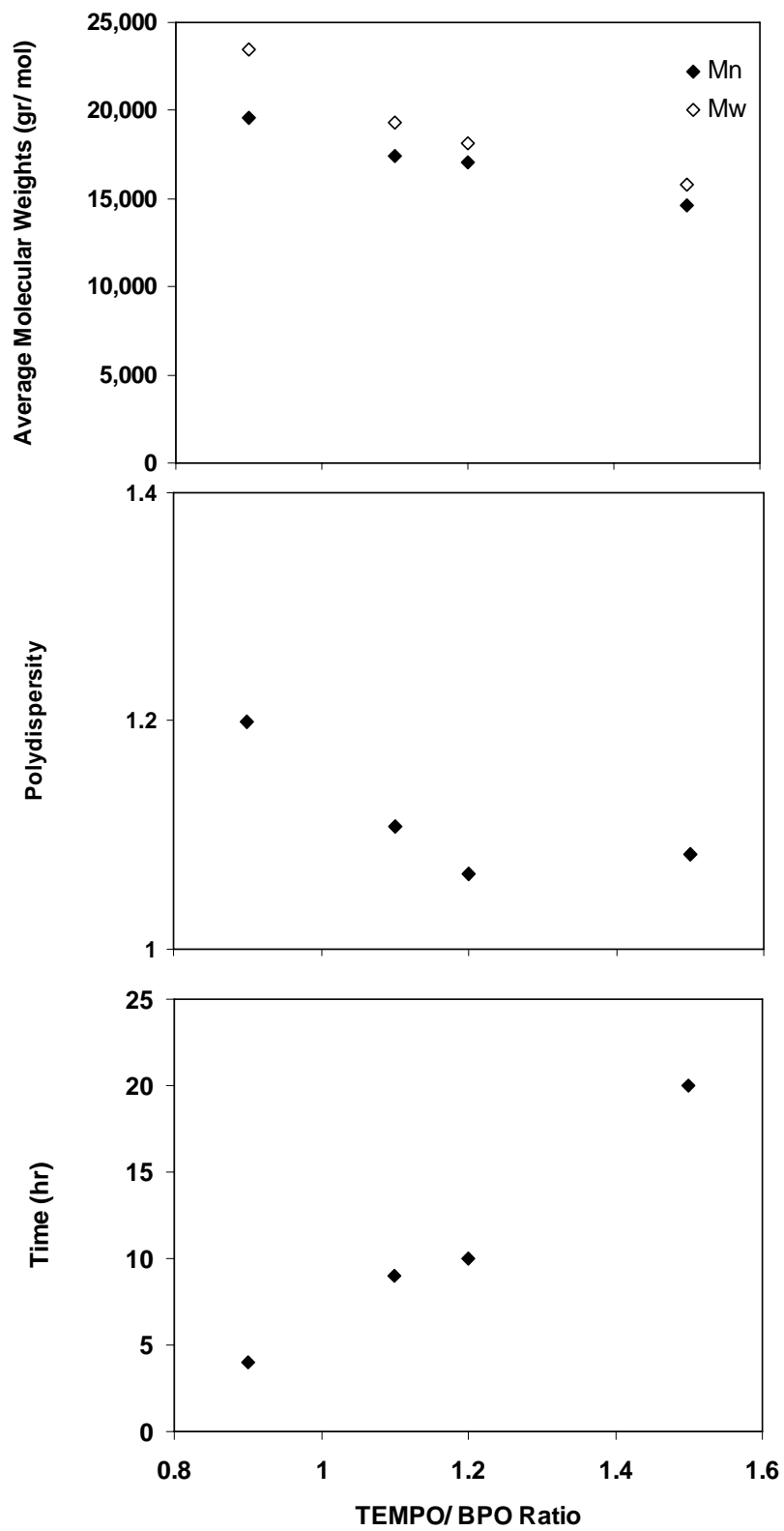


Figure 6.2 Molecular weights, polydispersity and time versus TEMPO/BPO ratio at 50% conversion; T = 120°C

6.2 Recommendations for Future Work

- **Different Initiators**

The main drawback of nitroxide-mediated radical polymerization is that the polymerization rate is slow [1]. Several attempts have been made to find ways to increase the rate without any significant increase in polydispersity; namely, adding organic acids [2 - 4], using a combination of two initiators with different half-lives [5, 6], and different regimes of addition of initiator in a semi-batch reactor [7]. Another interesting approach would be using a multifunctional initiator. Previous work carried out in our group [8, 9] showed that using a tetrafunctional initiator (JWEB50) in the free radical polymerization of styrene increases the rate of polymerization when compared to the monofunctional counterpart while maintaining the molecular weight averages. Selective experiments could be done to investigate the performance of JWEB50, as a tetrafunctional initiator, in NMRP of styrene. It will be interesting to investigate whether a tetrafunctional initiator could increase the rate of polymerization and form any branching while maintaining low polydispersity. In order to be able to compare the tetra vs. monofunctional initiator, a monofunctional initiator with the same decomposing characteristics, like tert-butylperoxy-2-ethylhexyl carbonate (TBEC), should be used. Therefore, it is necessary to carry out NMRP of styrene in the presence of TBEC at the same operating conditions in order to have a sound comparative basis with JWEB50.

- **Different Controllers**

As discussed in Chapter 2, due to the relatively high strength of the C-O bond in the TEMPO polymer adduct, TEMPO-mediated NMRP needs long reaction times and high polymerization temperatures. To overcome this deficiency, changes in the structure of the nitroxide are agreeable. In our lab we have access to a recently developed nitroxide by CIBA Chemicals, a PP-based nitroxide (NOR) with the trade name Irgatec CR76 [10]. Selective runs could be planned to examine the effect of this new nitroxide in NMRP of styrene and compare it to TEMPO-mediated NMRP and see if the new nitroxide can offer any improvements.

- **NMRP at Elevated Temperatures**

Nitroxide-mediated polymerization is normally conducted in the temperature range of 110 - 140 °C. It is worth trying NMRP at elevated temperature (150 - 220°C) to see if the controlled nature of polymerization is maintained at higher temperatures or not. It is worth adding that it is industrially appealing to conduct NMRP at higher temperatures since elevated temperatures promise faster polymerization rates and easier heat transfer with the cooling system.

- **Potential of Crosslinking in CRP**

Crosslinked polymers (polymer networks) are very important in medicine, biotechnology, agriculture, and other areas. The synthesis, characterization and modeling of polymer networks by controlled radical polymerization processes are research areas where few reports are available in the literature [11]. It is an interesting area of research to examine the NMRP polymerization of styrene (sty, well studied under controlled polymerization conditions) with a common crosslinker, divinyl benzene (DVB) (largely unstudied) at elevated temperatures (higher than 100 °C). The crosslinked copolymer of sty-DVB is used for chromatographic applications and as a precursor for ion-exchange resins. It is also a system studied under regular radical polymerization conditions, hence an excellent system for fundamental comparisons between NMRP and regular crosslinking (network) polymerizations.

- **Bayesian Design of Experiments in CRP**

Bayesian design is a relatively new experimental design methodology which has many advantages over other conventional designs. This approach incorporates the prior knowledge about the process into the design to predict the “best” set of experiments in a sequential fashion. Bayesian design allows for the use of a nonlinear (fully mechanistic) model and has the flexibility to change the levels of the factors with relative ease. The Bayesian experimental design technique can be exploited in nitroxide-mediate polymerization of styrene to determine the relative importance of different operating factors and also to detect the “best” operating condition. In addition, this approach can further shed light on the most uncertain parts of our process understanding, and hence identify the least reliable (less well known) parameter values

(e.g., uncertain values of kinetic rate constants), thus guiding further sensitivity analysis studies focusing on key uncertain parameters (for representative cases, see [12 - 14])

6.3 References

1. Dias, R. S.; Gonçalves, M. C.; Lona, L. M. F.; Vivaldo-Lima, E.; McManus, N. T.; Penlidis, A. **2007** "Nitroxide-mediated radical polymerization of styrene using mono- and di-functional initiators" *Chemical Engineering Science*, *62*, 5240-5244.
2. Baumann, M.; Schmidt-Naake, G. **2001** "Acetic anhydride - Accelerating agent for nitroxide-controlled free-radical copolymerization of styrene and acrylonitrile" *Macromolecular Chemistry and Physics*, *202*, 2727-2731.
3. Malmstrom, E.; Miller, R. D.; Hawker, C. J. **1997** "Development of a new class of rate-accelerating additives for nitroxide-mediated 'living' free radical polymerization" *Tetrahedron*, *53*, 15225-15236.
4. Odell, P. G.; Veregin, R. P. N.; Michalak, L. M.; Brousmiche, D.; Georges, M. K. **1995** "Rate Enhancement of Living Free-Radical Polymerizations by An Organic-Acid Salt" *Macromolecules*, *28*, 8453-8455.
5. Fukuda, T.; Terauchi, T.; Goto, A.; Ohno, K.; Tsujii, Y.; Miyamoto, T.; Kobatake, S.; Yamada, B. **1996** "Mechanisms and kinetics of nitroxide-controlled free radical polymerization" *Macromolecules*, *29*, 6393-6398.
6. Greszta, D.; Matyjaszewski, K. **1997** "TEMPO-mediated polymerization of styrene: Rate enhancement with dicumyl peroxide" *Journal of Polymer Science Part A-Polymer Chemistry*, *35*, 1857-1861.
7. Diaz-Camacho, F.; Lopez-Morales, S.; Vivaldo-Lima, E.; Saldivar-Guerra, E.; Vera-Graza, R.; Alexandrova, L. **2004** "Effect of Regime of Addition of Initiator on TEMPOMediated Polymerization of Styrene" *Polymer Bulletin*, *52*, 339-347.
8. Fityani-Trimmi, S.; Dhib, R.; Penlidis, A. **2003** "Free radical polymerization of styrene with a new tetrafunctional peroxide initiator" *Macromolecular Chemistry and Physics*, *204*, 436-442.
9. Scolah, M. J.; Dhib, R.; Penlidis, A. **2005** "Use of a novel tetrafunctional initiator in the free radical homo- and copolymerization of styrene, methyl methacrylate and alpha-methyl styrene" *Journal of Macromolecular Science-Pure and Applied Chemistry*, *A42*, 403-426.
10. Psareas, A., McManus, N. T., Tzoganakis, C., and Penlidis, A. **(2007)** "Nitroxide-mediated controlled degradation of polypropylene" *ANTEC 2007*, May 6-10, 2007, Cincinnati, OH, USA

11. Tuinman, E.; McManus, N. T.; Roa-Luna, M.; Vivaldo-Lima, E.; Lona, L. M. F.; Penlidis, A. **2006** "Controlled free-radical copolymerization kinetics of styrene and divinylbenzene by bimolecular NMRP using TEMPO and dibenzoyl peroxide" *Journal of Macromolecular Science Part A: Pure and Applied Chemistry*, *43*, 1-17.
12. Dube, M. A.; Penlidis, A.; Reilly, P. M. **1996** "A systematic approach to the study of multicomponent polymerization kinetics: The butyl acrylate/methyl methacrylate vinyl acetate example .4. Optimal Bayesian design of emulsion terpolymerization experiments in a pilot plant reactor" *Journal of Polymer Science Part A-Polymer Chemistry*, *34*, 811-831.
13. Vivaldo-Lima, E.; Penlidis, A.; Wood, P. E.; Hamielec, A. E. **2006** "Determination of the relative importance of process factors on particle size distribution in suspension polymerization using a Bayesian experimental design technique" *Journal of Applied Polymer Science*, *102*, 5577-5586.
14. Polic, A. L.; Lona, L. M. F.; Duever, T. A.; Penlidis, A. **2004** "A protocol for the estimation of parameters in process models: Case studies with polymerization scenarios" *Macromolecular Theory and Simulations*, *13*, 115-132.

APPENDIX A – TABLES OF RAW DATA

Table A.1 Raw Data for Experiment #1

Time (hr)	Conversion	$\ln[M]_0/[M]$	Mn - (Daltons)	Mn*10-3	Mw - (Daltons)	Mw*10-3	Mw / Mn (PDI)
0.5	0.237	0.27	10,213	10.21	16,747	16.75	1.64
1	0.289	0.34	12,318	12.32	17,713	17.71	1.44
1.25	0.326	0.39	11,775	11.78	17,817	17.82	1.51
1.5	0.350	0.43	13,976	13.98	19,648	19.65	1.41
2	0.389	0.49	14,973	14.97	19,731	19.73	1.32
2	0.389	0.49	14,446	14.45	19,488	19.49	1.35
2.53	0.435	0.57	16,517	16.52	21,556	21.56	1.31
3	0.466	0.63	16,517	16.52	22,064	22.06	1.25
4	0.538	0.77	19,597	19.60	23,493	23.49	1.20
5	0.595	0.90	20,842	20.84	24,888	24.89	1.19
5	0.600	0.92	21,075	21.08	25,052	25.05	1.19
10	0.787	1.55	27,551	27.55	31,074	31.07	1.13
15	0.853	1.92	29,541	29.54	33,571	33.57	1.14
20	0.891	2.22	31,696	31.70	35,383	35.38	1.12
20	0.886	2.17	31,168	31.17	35,112	35.11	1.13
34	0.919	2.52	31,360	31.36	35,364	35.36	1.13
50	0.937	2.77	31,547	31.55	35,887	35.89	1.14
70	0.944	2.88	32,598	32.60	36,669	36.67	1.13

Table A.2 GPC replicates for Experiment #1

Time (hr)	Conversion	Mn - (Daltons)	Mn*10-3	Mw - (Daltons)	Mw*10-3	Mw / Mn (PDI)
0.5	0.237	12,766	13	19,273	19	1.51
34	0.919	32,315	32	36,924	37	1.14
70	0.944	33,010	33	36,530	37	1.125

Table A.3 Raw Data for Experiment #2

Time (hr)	Conversion	$\ln[M]_0/[M]$	Mn - (Daltons)	Mn*10-3	Mw - (Daltons)	Mw*10-3	Mw / Mn (PDI)
2	0.153	0.166	4,990	4.99	6,084	6.08	1.219
3	0.238	0.272	7,256	7.26	8,595	8.60	1.184
6	0.384	0.485	12,056	12.06	13,509	13.51	1.121
9	0.536	0.767	17,412	17.41	19,286	19.29	1.108
14	0.688	1.166	20,613	20.61	23,223	23.22	1.127
24	0.802	1.618	24,450	24.45	27,537	27.54	1.126
40	0.893	2.239	24,857	24.86	28,516	28.52	1.147
9	0.555	0.810	17,358	17.36	19,166	19.17	1.104

Table A.4 Replicate Run for Experiment #2

Time (hr)	Conversion	$\ln[M]_0/[M]$
1	0.037	0.037
2	0.108	0.114
3	0.225	0.255
4	0.269	0.314
6	0.392	0.497
9	0.535	0.765
14	0.659	1.077
19	0.779	1.511
24	0.801	1.617
29	0.848	1.882
40	0.894	2.242
50	0.898	2.282

Table A.5 Raw data for Experiment # 3

Time (hr)	Conversion	$\ln[M]_0/[M]$	Mn - (Daltons)	Mn*10-3	Mw - (Daltons)	Mw*10-3	Mw / Mn (PDI)
1.00	0.0091	0.009	1,016	1.02	3,139	3.14	3.143
1.33	0.0154	0.016	1,480	1.48	2,556	2.56	1.727
1.67	0.0122	0.012	1,906	1.91	2,272	2.27	1.195
2.00	0.0330	0.034	2,134	2.13	2,363	2.36	1.108
2.33	0.0544	0.056	2,192	2.19	2,543	2.54	1.160
2.33	0.0551	0.057	2,291	2.29	2,630	2.63	1.148
2.67	0.1157	0.123	4,060	4.06	4,636	4.64	1.142
3.00	0.0913	0.096	3,460	3.46	3,967	3.97	1.147
3.33	0.1059	0.112	3,986	3.99	4,591	4.59	1.152
3.67	0.1818	0.201	6,598	6.60	7,300	7.30	1.107
4.00	0.2077	0.233	7,230	7.23	8,013	8.01	1.109
5.00	0.2117	0.238	7,842	7.84	8,583	8.58	1.095
6.00	0.3356	0.409	11,661	11.66	12,533	12.53	1.075
8.00	0.3780	0.475	14,691	14.69	14,691	14.69	1.081
10.00	0.4886	0.671	17,046	17.05	18,156	18.16	1.066
14.00	0.6301	0.995	21,125	21.12	23,105	23.11	1.094
14.00	0.6588	1.075	22,212	22.21	23,755	23.75	1.070
18.00	0.7435	1.361	24,236	24.24	26,326	26.33	1.086
22.00	0.7988	1.603	26,789	26.79	28,553	28.55	1.066
26.00	0.8314	1.780	27,800	27.80	30,274	30.27	1.089
40.00	0.8930	2.235	29,193	29.19	31,104	31.10	1.066
49.00	0.9023	2.326	29,355	29.35	31,884	31.88	1.086
72.00	0.9192	2.516	29,358	29.36	32,458	32.46	1.108

Table A.6 GPC replicates for Experiment #3

Time (hr)	Conversion	Mn - (Daltons)	Mn*10-3	Mw - (Daltons)	Mw*10-3	Mw / Mn (PDI)
3.67	0.1818	6,771	6.77	7,637	7.64	1.128
22.00	0.7988	27,955	27.95	30,001	30.00	1.073
72.00	0.9192	31580	31.58	33480	33.48	1.06

Table A.7 Raw data for Experiment # 4

Time (hr)	Conversion	$\ln[M]_0/[M]$	Mn - (Daltons)	Mn*10-3	Mw - (Daltons)	Mw*10-3	Mw / Mn (PDI)
0.5	0.008	0.008	903	0.90	7,180	7.18	7.95
1	0.010	0.010	683	0.68	3,845	3.84	5.66
1.25	0.009	0.010	638	0.64	2,505	2.51	3.93
1.5	0.011	0.011	621	0.62	1,909	1.91	3.07
2	0.013	0.013	681	0.68	2,922	2.92	4.35
2.5	0.014	0.014	701	0.70	1,439	1.44	2.05
3	0.021	0.021	1,228	1.23	2,506	2.51	2.04
4	0.042	0.043	2,380	2.38	2,536	2.54	1.07
5	0.064	0.067	2,567	2.57	2,712	2.71	1.06
5	0.065	0.067	2,731	2.73	2,865	2.87	1.05
10	0.209	0.235	6,551	6.55	7,024	7.02	1.07
10	0.205	0.230	6,309	6.31	6,891	6.89	1.09
20	0.520	0.734	14,583	14.58	15,786	15.79	1.08
20	0.520	0.734	14,564	14.56	15,800	15.80	1.09
50	0.866	2.012	22,480	22.48	24,767	24.77	1.10

Table A.8 GPC replicates for Experiment #4

Time (hr)	Conversion	Mn - (Daltons)	Mn*10-3	Mw - (Daltons)	Mw*10-3	Mw / Mn (PDI)
10	0.205	6,415	6.41	7,118	7.12	1.11
20	0.520	14,949	14.95	16,445	16.44	1.10
50	0.866	24,250	24.25	25,650	25.65	1.06

Table A.9 Raw data for complementary run for Experiment # 4

Time (hr)	Conversion	$\ln[M]_0/[M]$	Mn - (Daltons)	Mn*10-3	Mw - (Daltons)	Mw*10-3	Mw / Mn (PDI)
6.03	0.105	0.111	3,071	3.07	3,472	3.47	1.131
15	0.399	0.509	11,908	11.91	12,826	12.83	1.077
15	0.398	0.508	11,883	11.88	12,769	12.77	1.075
30	0.742	1.355	20,926	20.93	22,536	22.54	1.077
40.05	0.830	1.772	22,355	22.35	24,327	24.33	1.089
40.05	0.817	1.696	21,806	21.81	24,356	24.36	1.117
50.05	0.861	1.971	22,748	22.75	25,487	25.49	1.121
63.03	0.881	2.129	23,569	23.57	26,264	26.26	1.114
70.15	0.891	2.221	23,775	23.78	26,398	26.40	1.111

Table A.10 Raw data for Experiment # 5

Time (hr)	Conversion	$\ln[M]_0/[M]$	Mn - (Daltons)	Mn*10-3	Mw - (Daltons)	Mw*10-3	Mw / Mn (PDI)
0.5333333	0.039	0.04	286,851	287	465,880	466	1.62
1.0166667	0.083	0.09	288,336	288	473,958	474	1.64
3.0666667	0.239	0.27	284,934	285	456,397	456	1.63
5.0333333	0.383	0.48	230,296	230	407,497	407	1.82
7	0.503	0.70	214,231	214	389,499	389	1.84
25	0.899	2.30	292,809	293	524,209	524	1.79
15.05	0.821	1.72	304,528	305	522,056	522	1.71
30.2	0.915	2.47	197,689	198	428,858	429	2.21

Table A.11 Raw data for Experiment # 6

Time (hr)	Conversion	ln[M]₀/[M]	Mn - (Daltons)	Mn*10-3	Mw - (Daltons)	Mw*10-3	Mw / Mn (PDI)
0.52	0.000	0.000	-	-	-	-	-
3.03	0.001	0.001	-	-	-	-	-
7.03	0.021	0.021	-	-	-	-	-
10.95	0.079	0.083	3,907	3.91	4,212	4.21	1.078
15.08	0.147	0.159	6,387	6.39	6,912	6.91	1.082
15.08	0.148	0.160	6,587	6.59	7,053	7.05	1.071
20.00	0.223	0.252	9,414	9.41	9,968	9.97	1.059
25.00	0.300	0.357	10,702	10.70	12,051	12.05	1.127
30.22	0.363	0.451	11,249	11.25	13,401	13.40	1.191
50.00	0.577	0.861	14,719	14.72	18,149	18.15	1.233

Table A.12 GPC replicates for Experiment #6

Time (hr)	Conversion	Mn - (Daltons)	Mn*10-3	Mw - (Daltons)	Mw*10-3	Mw / Mn (PDI)
10.95	0.0794	3,987	3.99	4,280	4.28	1.069
25.00	0.3001	11,090	11.09	12,180	12.18	1.109
30.22	0.363	10,427	10.43	13,383	13.38	1.186
50.00	0.5774	14,146	14.15	18,081	18.08	1.268

Table A.13 Replicate Run for Experiment #6

Time (hr)	Conversion	ln[M]₀/[M]
20.02	0.241	0.276
30.15	0.366	0.456
39.96	0.494	0.682
49.95	0.559	0.818

Table A.14 Raw data for Experiment # 7

Time (hr)	Conversion	$\ln[M]_0/[M]$	Mn - (Daltons)	Mn*10-3	Mw - (Daltons)	Mw*10-3	Mw / Mn (PDI)
0.55	0.052	0.054	955	0.96	1,031	1.03	1.08
1.00	0.094	0.099	1,751	1.75	1,956	1.96	1.12
3.03	0.231	0.263	5,000	5.00	5,368	5.37	1.07
6.05	0.354	0.438	8,423	8.42	8,818	8.82	1.05
8.03	0.502	0.697	9,486	9.49	10,048	10.05	1.06
24.73	0.735	1.329	13,567	13.57	14,522	14.52	1.07
15.00	0.648	1.044	12,053	12.05	12,828	12.83	1.06
20.07	0.705	1.221	12,884	12.88	13,847	13.85	1.07
20.07	0.707	1.229	12,598	12.60	13,809	13.81	1.10
40.50	0.795	1.586	14,747	14.75	15,743	15.74	1.07
30.12	0.758	1.418	14,161	14.16	15,157	15.16	1.07
60.12	0.831	1.775	13,913	13.91	15,850	15.85	1.14
50.22	0.822	1.724	13,854	13.85	15,706	15.71	1.13

Table A.15 Replicate Run for Experiment #7

Time (hr)	Conversion	$\ln[M]_0/[M]$	Mn - (Daltons)	Mn*10-3	Mw - (Daltons)	Mw*10-3	Mw / Mn (PDI)
5	0.376	0.471	7,910	7.91	8,310	8.31	1.05
7.27	0.465	0.626	9,869	9.87	10,243	10.24	1.04
10.07	0.556	0.812	11,048	11.05	11,914	11.91	1.08
24.45	0.722	1.281	14,030	14.03	15,110	15.11	1.08
20	0.696	1.190	14,131	14.13	14,673	14.67	1.04

Table A.16 Raw data for Experiment #8

Time (hr)	Conversion	$\ln[M]_0/[M]$	Mn - (Daltons)	Mn*10-3	Mw - (Daltons)	Mw*10-3	Mw / Mn (PDI)
0.52	0.281	0.33	9,734	9.73	13,785	13.78	1.42
1	0.346	0.42	12,083	12.08	15,198	15.20	1.26
1.5	0.444	0.59	14,821	14.82	18,037	18.04	1.22
2	0.489	0.67	17,021	17.02	20,014	20.01	1.18
3	0.587	0.88	19,429	19.43	22,972	22.97	1.18
3	0.601	0.92	21,077	21.08	23,939	23.94	1.14
4	0.656	1.07	22,369	22.37	25,560	25.56	1.14
4.95	0.705	1.22	23,159	23.16	26,637	26.64	1.15
8	0.802	1.62	26,872	26.87	30,078	30.08	1.12
8	0.834	1.80	29,191	29.19	32,279	32.28	1.11
10.1	0.852	1.91	29,870	29.87	33,450	33.45	1.12
10.1	0.870	2.04	29,366	29.37	33,425	33.43	1.14
24.05	0.901	2.31	29,110	29.11	33,689	33.69	1.16
24.05	0.916	2.48	30,070	30.07	35,236	35.24	1.17
15	0.876	2.09	27,908	27.91	33,082	33.08	1.19
15	0.876	2.08	27,894	27.89	33,333	33.33	1.20
30.02	0.908	2.39	27,185	27.18	33,108	33.11	1.22
50	0.929	2.65	28,263	28.26	33,972	33.97	1.20
50	0.930	2.67	29,565	29.56	34,791	34.79	1.18

Table A.17 GPC replicates for Experiment #8

Time (hr)	Conversion	Mn - (Daltons)	Mn*10-3	Mw - (Daltons)	Mw*10-3	Mw / Mn (PDI)
1	0.346	12,064	12.06	15,202	15.20	1.260
3	0.587	20,141	20.14	23,175	23.18	1.151
8	0.802	26,395	26.39	29,872	29.87	1.132
8	0.802	26,564	26.56	29,772	29.77	1.121
30.02	0.908	27,906	27.91	33,165	33.17	1.189
50	0.929	27,767	27.77	33,327	33.33	1.201

Table A.18 Raw data for Experiment #9

Time (hr)	Conversion	$\ln[M]_0/[M]$	Mn - (Daltons)	Mn*10-3	Mw - (Daltons)	Mw*10-3	Mw / Mn (PDI)
0.50	0.129	0.14	3,492	3.49	5,146	5.15	1.47
1.00	0.158	0.17	5,168	5.17	6,058	6.06	1.17
1.25	0.203	0.23	6,759	6.76	7,651	7.65	1.13
1.50	0.274	0.32	8,845	8.84	9,861	9.86	1.12
2.00	0.350	0.43	10,552	10.55	11,856	11.86	1.12
2.00	0.276	0.32	9,129	9.13	9,960	9.96	1.09
2.50	0.402	0.51	12,389	12.39	13,711	13.71	1.11
3.00	0.423	0.55	13,623	13.62	14,846	14.85	1.09
4.17	0.508	0.71	18,071	18.07	19,138	19.14	1.06
5.00	0.598	0.91	19,194	19.19	20,698	20.70	1.08
5.00	0.591	0.89	18,816	18.82	20,372	20.37	1.08
10.18	0.799	1.61	25,798	25.80	27,902	27.90	1.08
15.08	0.850	1.90	26,120	26.12	28,604	28.60	1.10
19.23	0.877	2.10	26,105	26.11	28,733	28.73	1.10
20.27	0.897	2.28	26,503	26.50	30,256	30.26	1.14
20.27	0.888	2.19	28,284	28.28	30,868	30.87	1.09
21.72	0.896	2.27	28,447	28.45	30,921	30.92	1.09
23.15	0.894	2.24	27,656	27.66	30,827	30.83	1.12
29.98	0.913	2.44	27,573	27.57	31,231	31.23	1.13
50.00	0.924	2.58	28,251	28.25	31,709	31.71	1.12
71.93	0.934	2.72	29,715	29.72	32,374	32.37	1.09

Table A.19 Replicate Run for Experiment #9

Time (hr)	Conversion	$\ln[M]_0/[M]$	Mn - (Daltons)	Mn*10-3	Mw - (Daltons)	Mw*10-3	Mw / Mn (PDI)
2	0.331	0.40	8,293	8.29	10,669	10.67	1.29
4	0.532	0.76	12,765	12.77	16,765	16.77	1.31
7	0.711	1.24	17,158	17.16	22,038	22.04	1.28
10	0.778	1.51	19,016	19.02	23,989	23.99	1.26
13	0.823	1.73	22,359	22.36	25,149	25.15	1.13
16	0.857	1.95	21,950	21.95	26,255	26.26	1.20
22	0.880	2.12	21,058	21.06	26,519	26.52	1.26
28	0.900	2.31	22,917	22.92	26,485	26.49	1.16
34	0.909	2.40	23,120	23.12	26,863	26.86	1.16
40	0.912	2.43	23,050	23.05	27,356	27.36	1.19
50	0.917	2.49	25,255	25.26	28,010	28.01	1.11

Table A.20 Raw data for Experiment #10

Time (hr)	Conversion	$\ln[M]_0/[M]$	Mn - (Daltons)	Mn*10-3	Mw - (Daltons)	Mw*10-3	Mw / Mn (PDI)
1	0.027	0.028	1,147	1.15	2,105	2.11	1.84
2	0.084	0.088	3,404	3.40	3,768	3.77	1.11
3	0.162	0.177	6,440	6.44	6,955	6.96	1.08
4	0.246	0.282	9,016	9.02	9,844	9.84	1.09
5	0.323	0.390	12,650	12.65	13,473	13.47	1.07
5(rep)	0.335	0.407	12,120	12.12	13,120	13.12	1.08
6	0.432	0.566	15,528	15.53	16,489	16.49	1.06
7	0.490	0.673	18,040	18.04	19,164	19.16	1.06
8	0.566	0.834	19,269	19.27	20,992	20.99	1.09
8(rep)	0.543	0.782	19,345	19.35	20,990	20.99	1.09
9	0.622	0.972	21,106	21.11	22,990	22.99	1.09

Table A.21 GPC replicates for Experiment #10

Time (hr)	Conversion	Mn - (Daltons)	Mn*10-3	Mw - (Daltons)	Mw*10-3	Mw / Mn (PDI)
4	0.24606	8939	8.94	9948	9.95	1.113
8	0.56561	19850	19.85	20820	20.82	1.0895
9	0.62151	22950	22.95	24150	24.15	1.089

Table A.22 Replicate Run for Experiment #10

Time (hr)	Conversion	$\ln[M]_0/[M]$	Mn - (Daltons)	Mn*10-3	Mw - (Daltons)	Mw*10-3	Mw / Mn (PDI)
0.5	0.021	0.02	748	0.75	2,254	2.25	3.01
1	0.034	0.03	1,839	1.84	2,398	2.40	1.30
1.25	0.034	0.03	2,134	2.13	2,585	2.59	1.21
2.72	0.148	0.16	5,227	5.23	5,646	5.65	1.08
3.58	0.252	0.29	8,070	8.07	8,675	8.67	1.07
5.5	0.405	0.52	12,638	12.64	13,702	13.70	1.08
6.5	0.468	0.63	15,032	15.03	16,210	16.21	1.08
8	0.579	0.87	17,723	17.72	19,348	19.35	1.09
15.2	0.783	1.53	23,749	23.75	26,336	26.34	1.11
15.2	0.779	1.51	23,218	23.22	26,173	26.17	1.13
18.03	0.810	1.66	24,728	24.73	27,825	27.82	1.13
18.03	0.823	1.73	25,243	25.24	27,941	27.94	1.11
20	0.841	1.84	26,258	26.26	28,730	28.73	1.09
22	0.857	1.95	25,200	25.20	28,085	28.08	1.11
22	0.862	1.98	24,711	24.71	27,080	27.08	1.10
25	0.872	2.06	25,150	25.15	28,406	28.41	1.13
25	0.875	2.08	24,503	24.50	27,438	27.44	1.12
25.52	0.869	2.03	26,163	26.16	29,408	29.41	1.12
25.52	0.881	2.13	25,762	25.76	28,409	28.41	1.10
30	0.891	2.22	26,185	26.19	29,573	29.57	1.13
41.47	0.913	2.44	25,548	25.55	29,581	29.58	1.16
48.05	0.914	2.45	24844.5	24.84	28073.5	28.07	1.13
66.03	0.921	2.54	25820	25.82	30511.5	30.51	1.1815
72.5	0.928	2.63	24937.5	24.94	28818.5	28.82	1.156
72.5	0.926	2.61	26386	26.39	30032	30.03	1.1385

Table A.23 Raw data for Experiment #11

Time (hr)	Conversion	$\ln[M]_0/[M]$	Mn - (Daltons)	Mn*10-3	Mw - (Daltons)	Mw*10-3	Mw / Mn (PDI)
0.52	0.0842	0.09	272,253	272	429,501	430	1.58
1	0.1528	0.17	256,074	256	414,973	415	1.62
2	0.3060	0.37	269,070	269	418,732	419	1.56
3	0.4326	0.57	261,392	261	418,071	418	1.60
4	0.5485	0.80	268,870	269	430,085	430	1.60
4.95	0.6356	1.01	269,974	270	439,320	439	1.63
8	0.8119	1.67	265,242	265	444,381	444	1.68
8	0.8170	1.70	261,322	261	446,825	447	1.71
10.1	0.8776	2.10	261,030	261	450,401	450	1.73
24.05	0.9520	3.04	255,473	255	450,312	450	1.77
15	0.9228	2.56	272,768	273	457,930	458	1.68
30.02	0.9620	3.27	170,026	170	354,440	354	2.09
20	0.9488	2.97	216,777	217	426,575	427	1.97

Table A.24 Raw data for Experiment #12

Time (hr)	Conversion	ln[M]0/[M]	Mn - (Daltons)	Mn*10-3	Mw - (Daltons)	Mw*10-3	Mw / Mn (PDI)
0.50	0.001	0.001	-	-	-	-	-
2.03	0.007	0.007	-	-	-	-	-
2.03	0.007	0.007	-	-	-	-	-
3.18	0.017	0.017	751	0.75	869	0.87	1.16
4.58	0.069	0.072	3,543	3.54	3,805	3.81	1.07
5.50	0.105	0.111	4,927	4.93	5,302	5.30	1.08
5.50	0.107	0.113	5,030	5.03	5,401	5.40	1.07
8.00	0.203	0.226	8,074	8.07	8,889	8.89	1.10
12.32	0.343	0.420	11,071	11.07	13,037	13.04	1.18
12.32	0.339	0.414	11,140	11.14	13,003	13.00	1.17
15.00	0.412	0.531	12,145	12.14	14,811	14.81	1.22
15.00	0.406	0.521	12,065	12.06	14,667	14.67	1.22
20.00	0.510	0.714	13,326	13.33	16,842	16.84	1.26
20.00	0.516	0.727	13,676	13.68	16,987	16.99	1.24
25.08	0.601	0.919	13,827	13.83	18,195	18.19	1.32
30.05	0.666	1.095	13,042	13.04	18,287	18.29	1.40
30.05	0.677	1.130	14,352	14.35	19,427	19.43	1.36
45.07	0.750	1.388	14,538	14.54	20,027	20.03	1.38

Table A.25 GPC replicates for Experiment #12

Time (hr)	Conversion	Mn - (Daltons)	Mn*10-3	Mw - (Daltons)	Mw*10-3	Mw / Mn (PDI)
5.5	0.107	5,027	5.03	5,390	5.39	1.07
15	0.412	13,475	13.48	16,886	16.89	1.26
20	0.510	13,694	13.69	15,429	15.43	1.14
25.083333	0.601	13,422	13.42	19,474	19.47	1.45
30.05	0.666	13,965	13.96	18,865	18.87	1.35
45.066667	0.750	14,283	14.28	18,925	18.93	1.33

Table A.26 Replicate Run for Experiment #12

Time (hr)	Conversion	ln[M]0/[M]	Mn - (Daltons)	Mn*10-3	Mw - (Daltons)	Mw*10-3	Mw / Mn (PDI)
5.00	0.081	0.085	3,971	3.97	4,284	4.28	1.08
10.02	0.264	0.306	8,760	8.76	10,364	10.36	1.18
15.00	0.412	0.531	12,538	12.54	14,841	14.84	1.18
20.02	0.537	0.769	13,738	13.74	17,138	17.14	1.25
25.00	0.608	0.936	15,031	15.03	18,423	18.42	1.23
31.17	0.691	1.174	14,182	14.18	19,434	19.43	1.37
40.00	0.749	1.384	14,992	14.99	20,446	20.45	1.36
40.00	0.746	1.371	12,055	12.06	19,171	19.17	1.59
45.55	0.781	1.517	13,476	13.48	19,921	19.92	1.48
49.52	0.788	1.551	13,549	13.55	20,010	20.01	1.48
49.52	0.798	1.599	14,105	14.11	20,243	20.24	1.44
64.00	0.846	1.873	14,290	14.29	20,705	20.71	1.45

Table A.27 Typical Standard Error in Conversion Measurements *

Time (hr)	2		3		6		9		14		24		40	
Conversion	0.1531	0.1076	0.2383	0.2247	0.3842	0.3917	0.5356	0.5369	0.6883	0.6593	0.8010	0.8014	0.8935	0.8938
Variance	1.035E-03		9.287E-05		2.782E-05		8.192E-07		4.210E-04		7.722E-08		5.035E-08	
Pooled Variance	2.254E-04													
Standard Error	1.501E-02													

* Based on run # 2 (See Table A.3 and A.4)

APPENDIX B – COMPLEMENTARY FIGURES

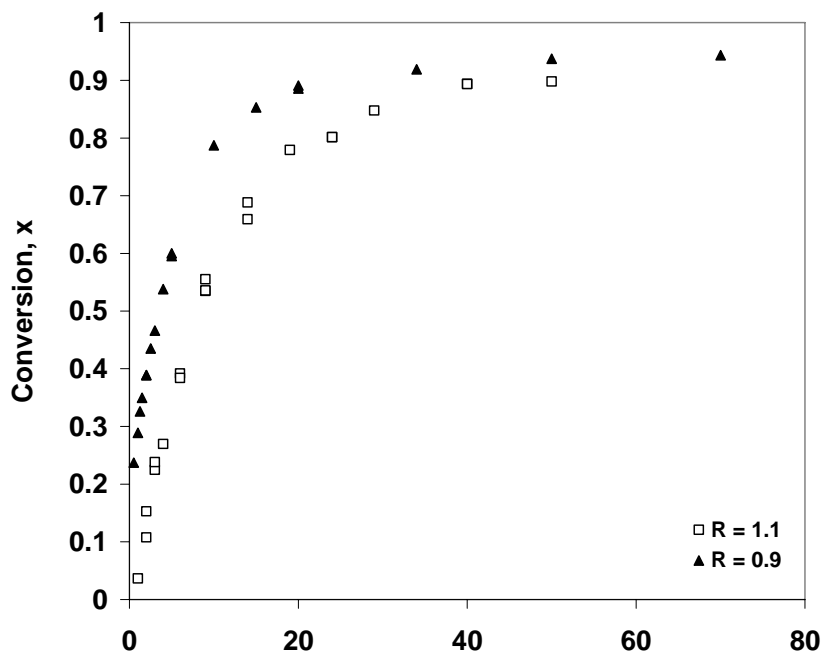


Figure B.1 Effect of decreasing TEMPO/BPO ratio on first order plot in NMRP of styrene at 120°C

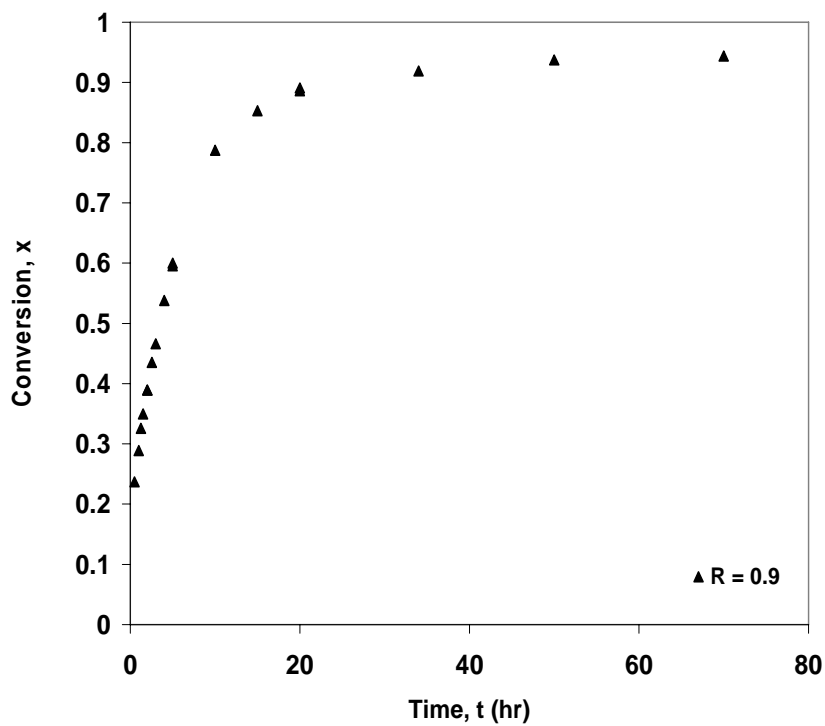


Figure B.2 Monomer conversion vs. time for NMRP of styrene at 120°C and [TEMPO]/[BPO] = 0.9 (Run #1)

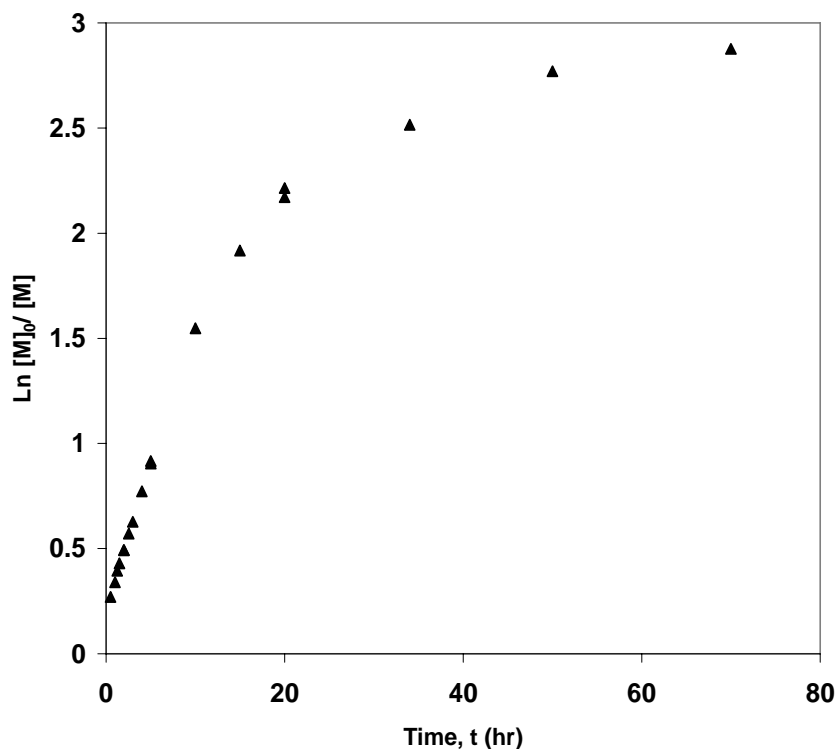


Figure B.3 First order rate plot for NMRP of styrene at 120°C and [TEMPO]/[BPO] = 0.9

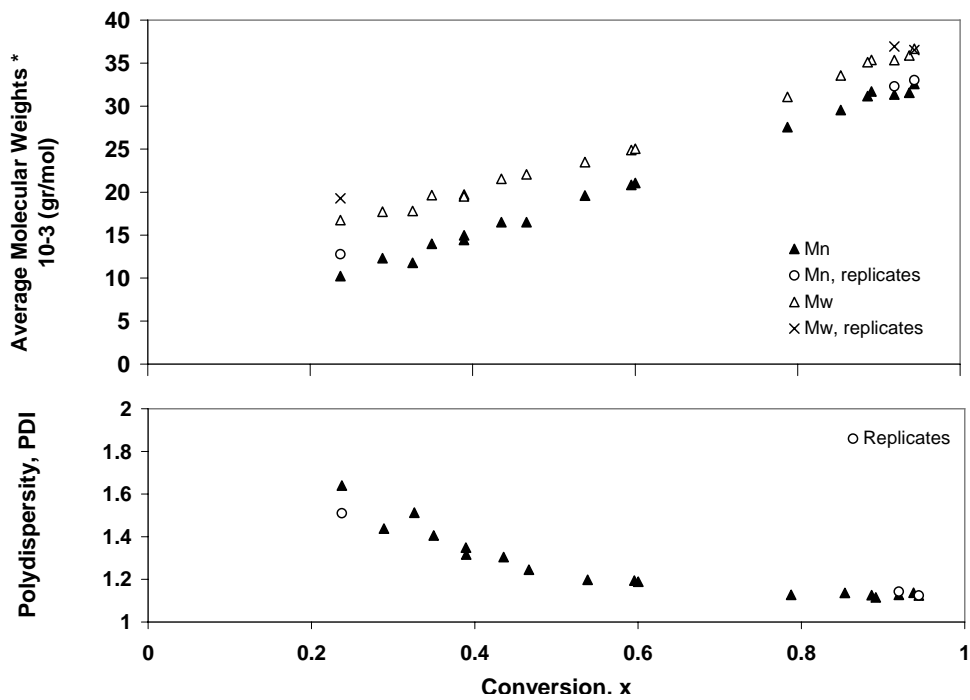


Figure B.4 Average molecular weights and polydispersity vs. conversion for NMRP of styrene at 120°C and [TEMPO]/[BPO] = 0.9

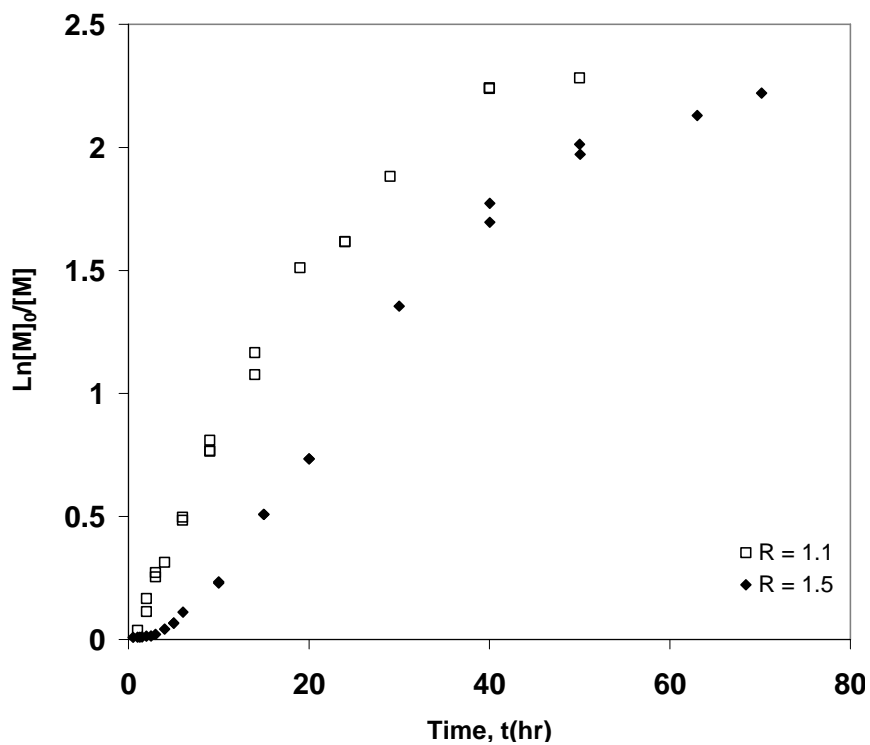


Figure B.5 Effect of increasing TEMPO/BPO ratio on first order plot in NMRP of styrene at 120°C.

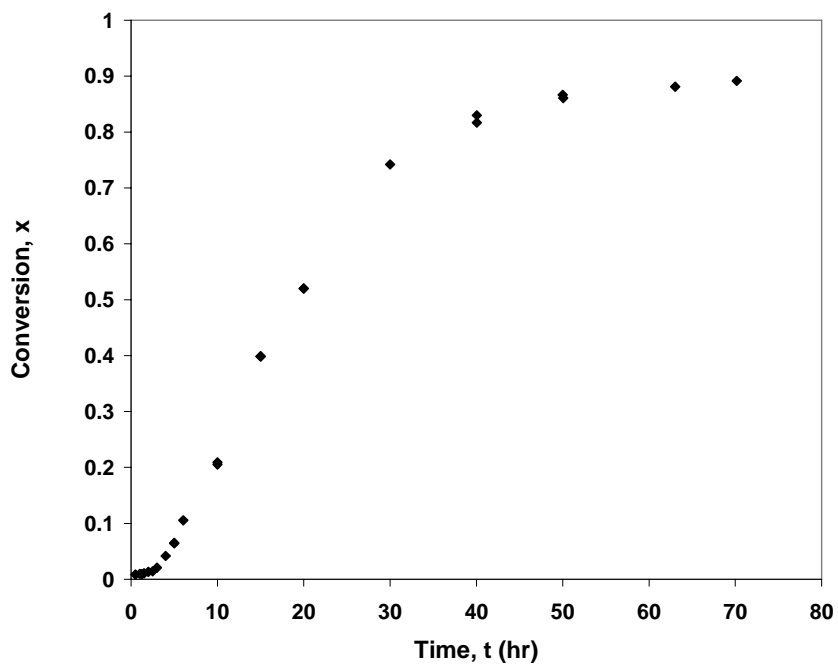


Figure B.6 Monomer conversion vs. time for NMRP of styrene at 120°C and [TEMPO]/[BPO] = 1.5 (Run #4)

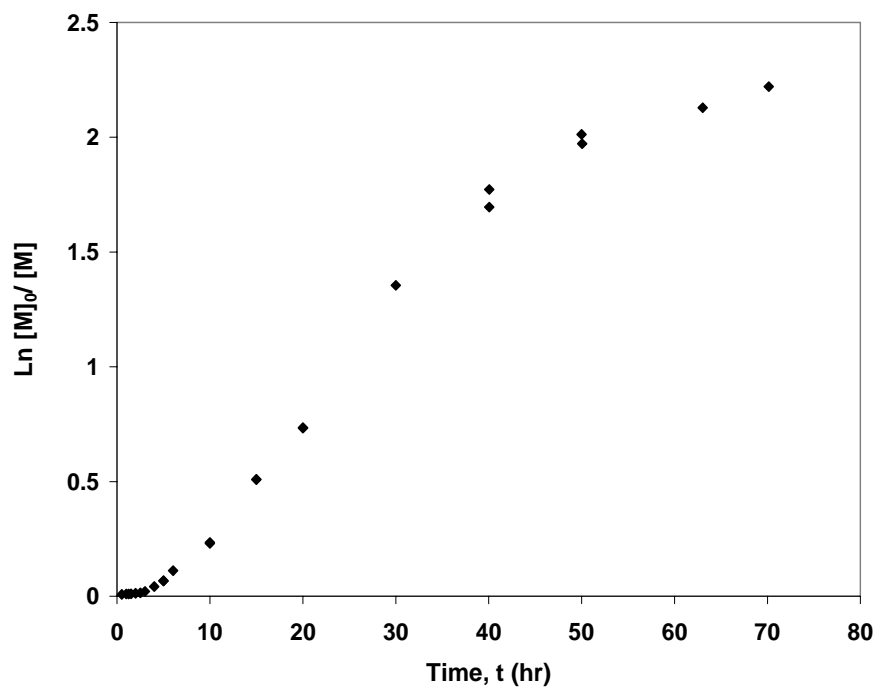


Figure B.7 First order rate plot for NMRP of styrene at 120°C and $[\text{TEMPO}]/[\text{BPO}] = 1.5$

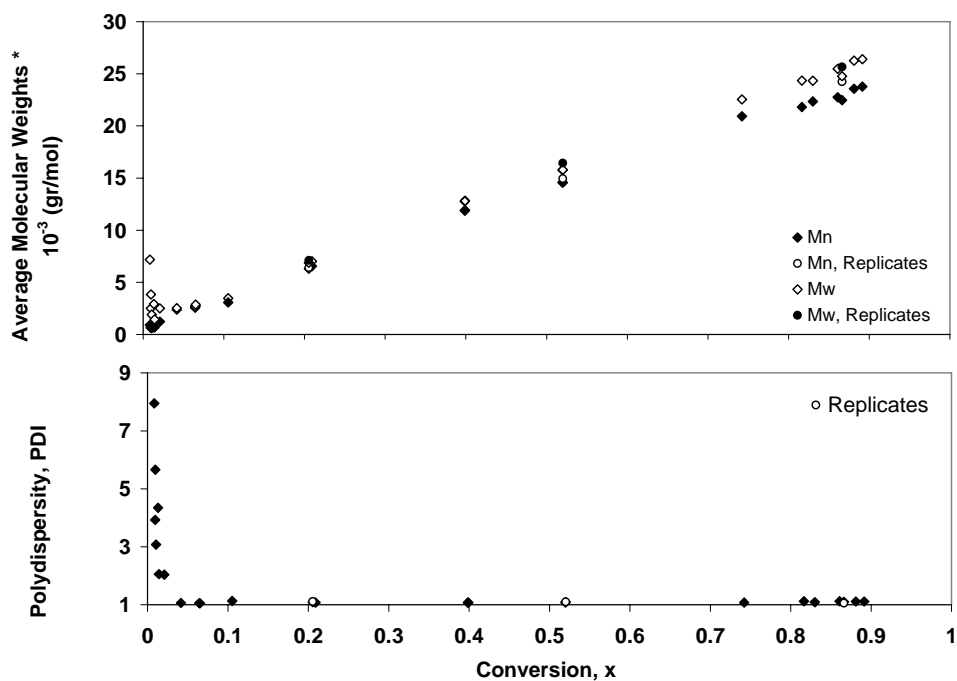


Figure B.8 Average molecular weights and polydispersity vs. conversion for NMRP of styrene at 120°C and $[\text{TEMPO}]/[\text{BPO}] = 1.5$

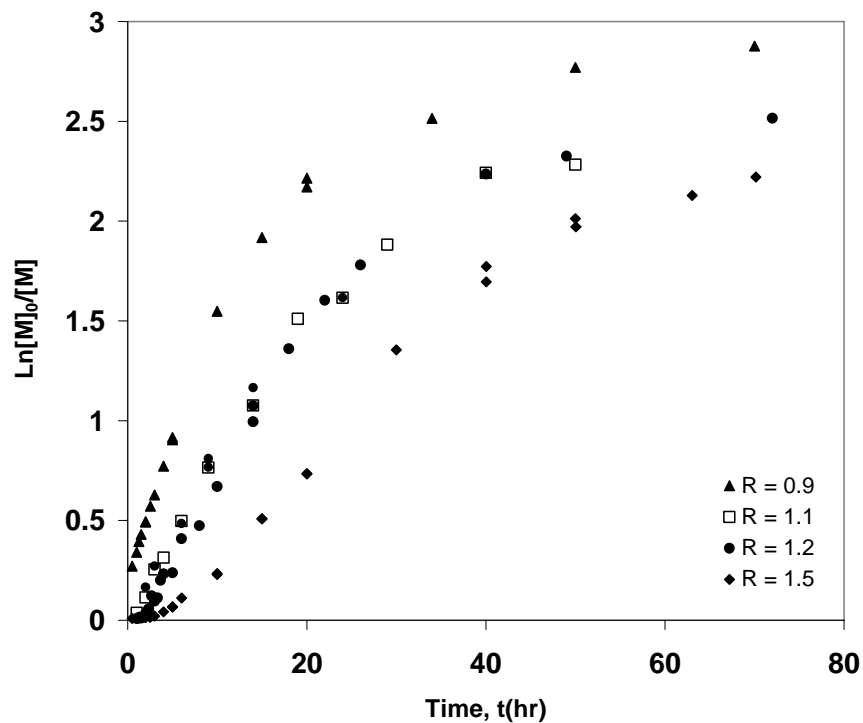


Figure B.9 Effect of [TEMPO]/[BPO] ratio on first order plot in NMRP of styrene at 120°C

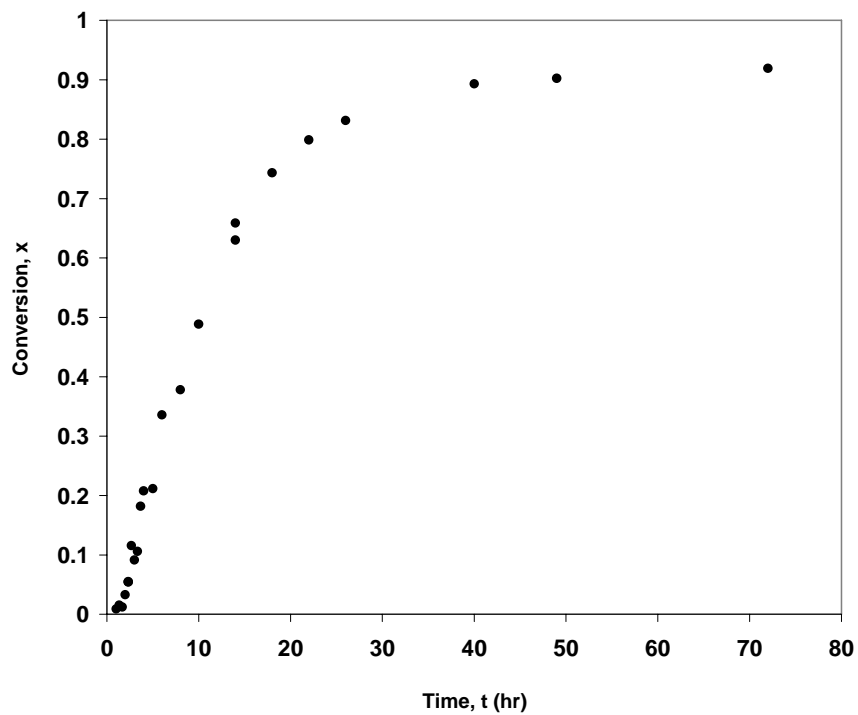


Figure B.10 Monomer conversion vs. time for NMRP of styrene at 120°C and [TEMPO]/[BPO] = 1.2 (Run #3)

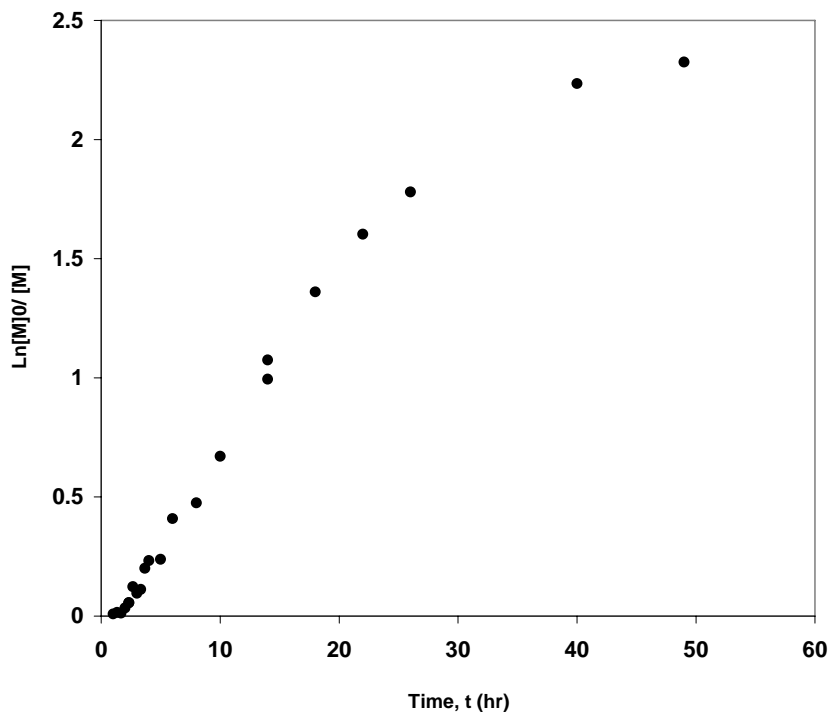


Figure B.11 First order rate plot for NMRP of styrene at 120°C and [TEMPO]/[BPO] = 1.2

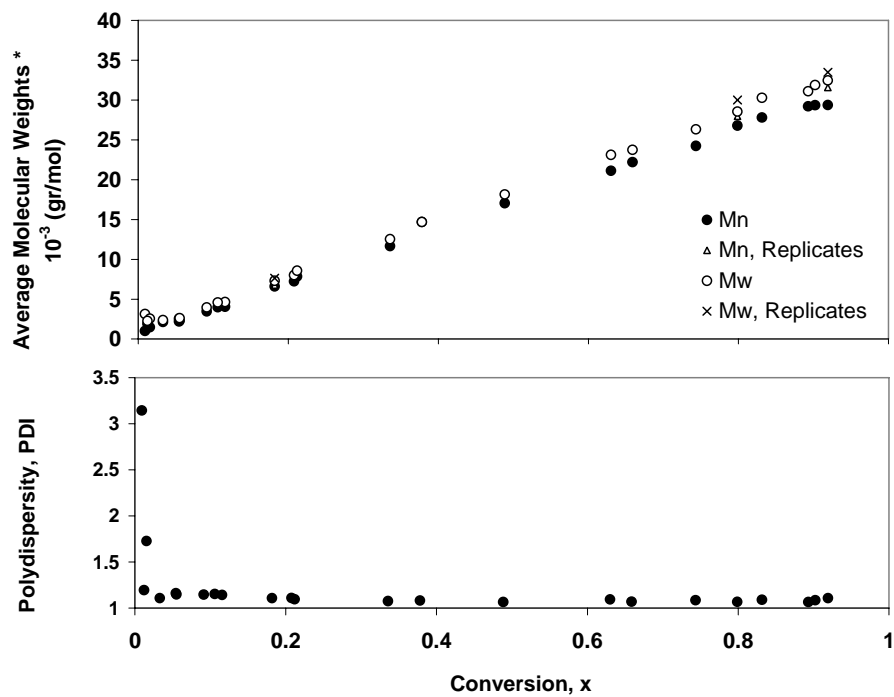


Figure B.12 Average molecular weights and polydispersity vs. conversion for NMRP of styrene at 120°C and [TEMPO]/[BPO] = 1.2

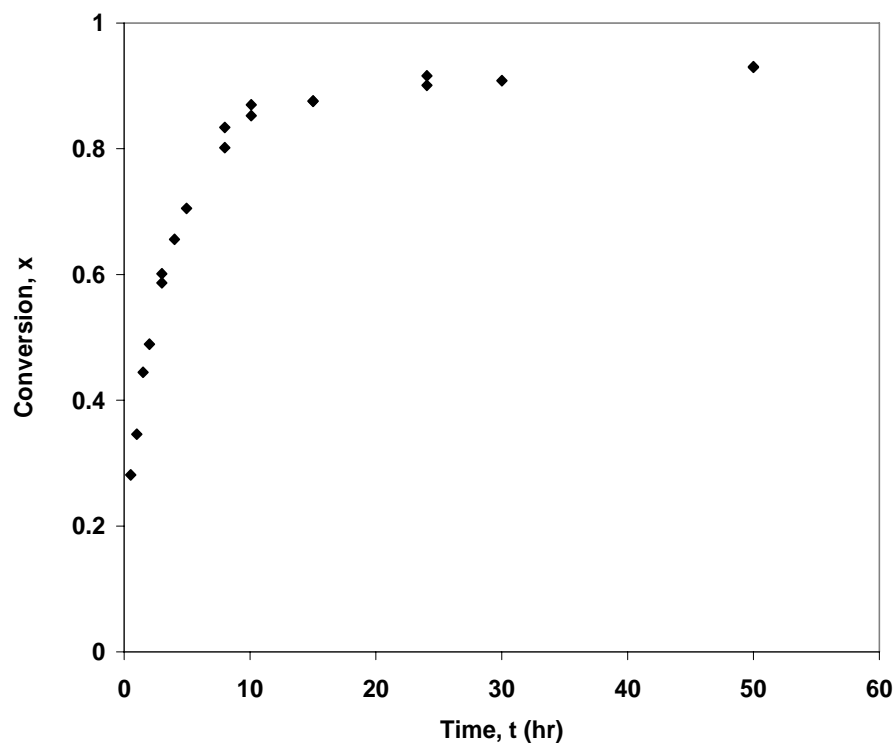


Figure B.13 Monomer conversion vs. time for NMRP of styrene at 130°C and [TEMPO]/[BPO] = 0.9 (Run #8)

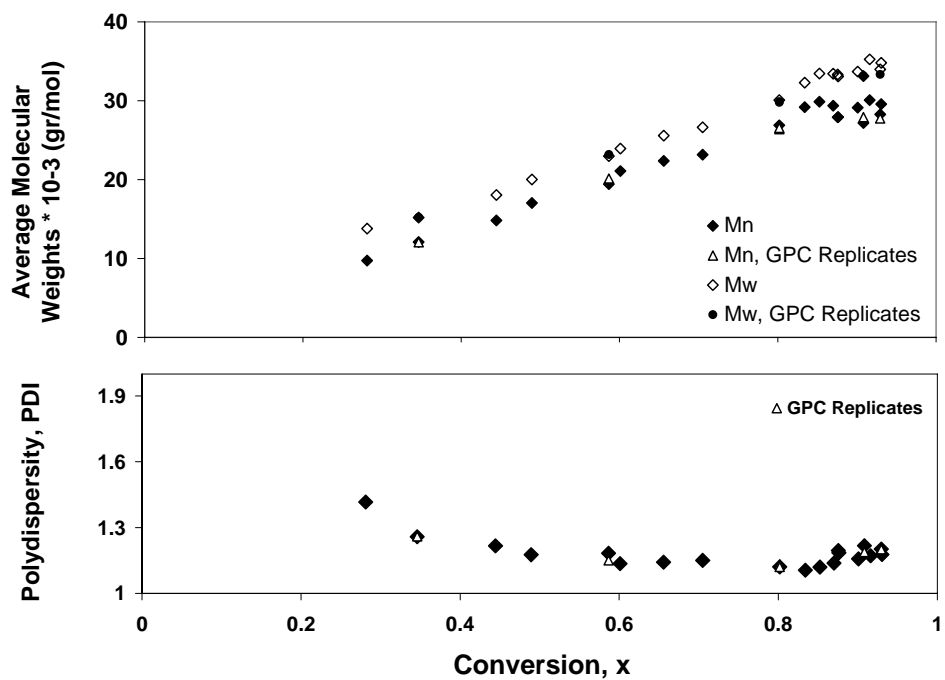


Figure B.14 Average molecular weights and polydispersity vs. conversion for NMRP of styrene at 130°C and [TEMPO]/[BPO] = 0.9

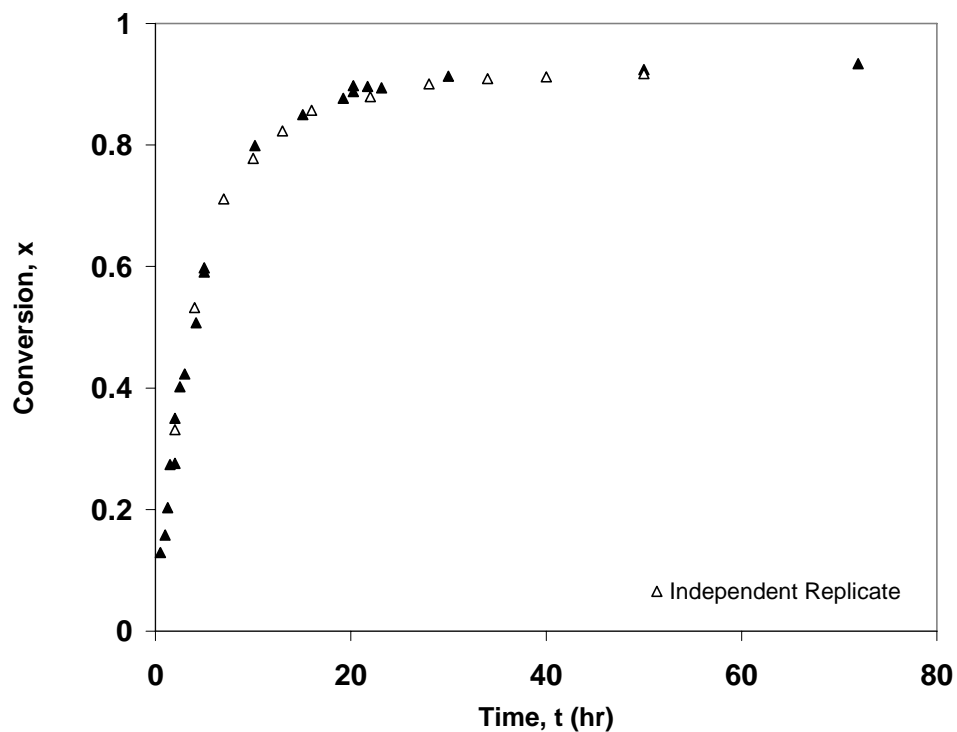


Figure B.15 Monomer conversion vs. time for NMRP of styrene at 130°C and $[\text{TEMPO}]/[\text{BPO}] = 1.1$ (Run #9)

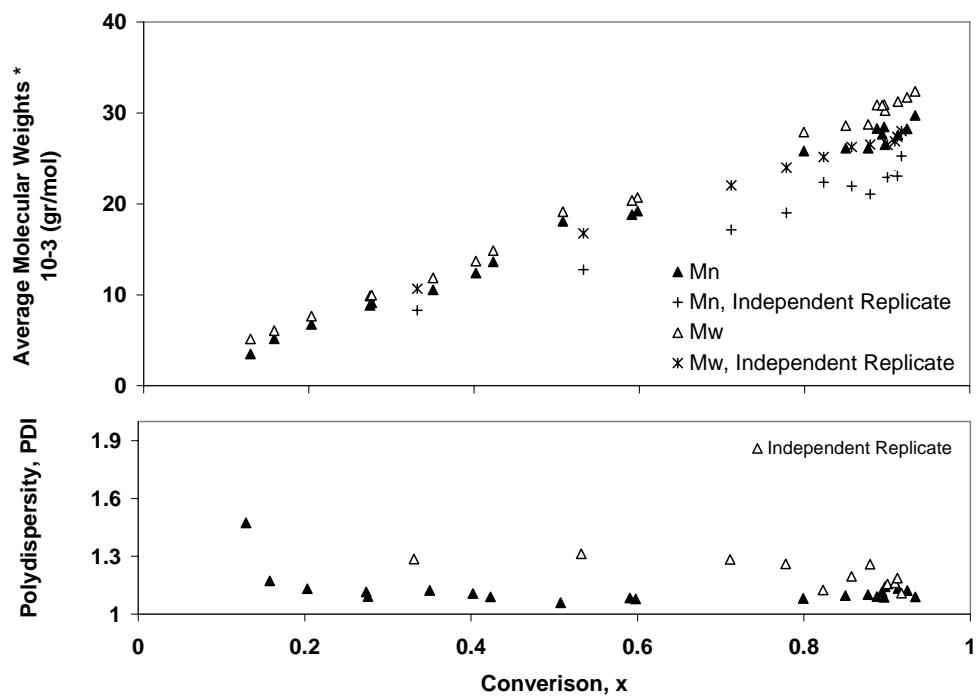


Figure B.16 Average molecular weights and polydispersity vs. conversion for NMRP of styrene at 130°C and $[\text{TEMPO}]/[\text{BPO}] = 1.1$

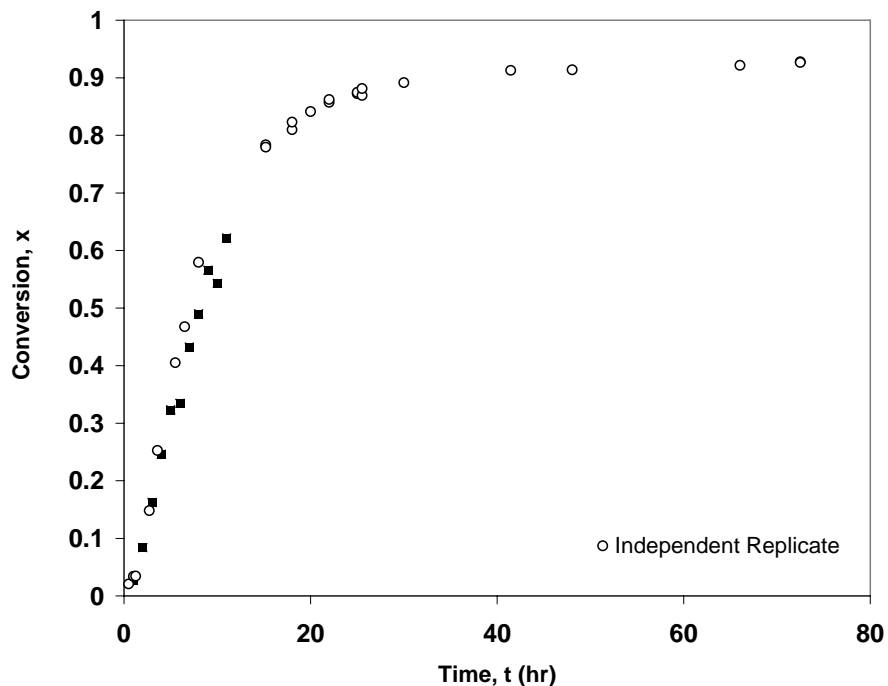


Figure B.17 Monomer conversion vs. time for NMRP of styrene at 130°C and $[TEMPO]/[BPO] = 1.3$ (Run #10)

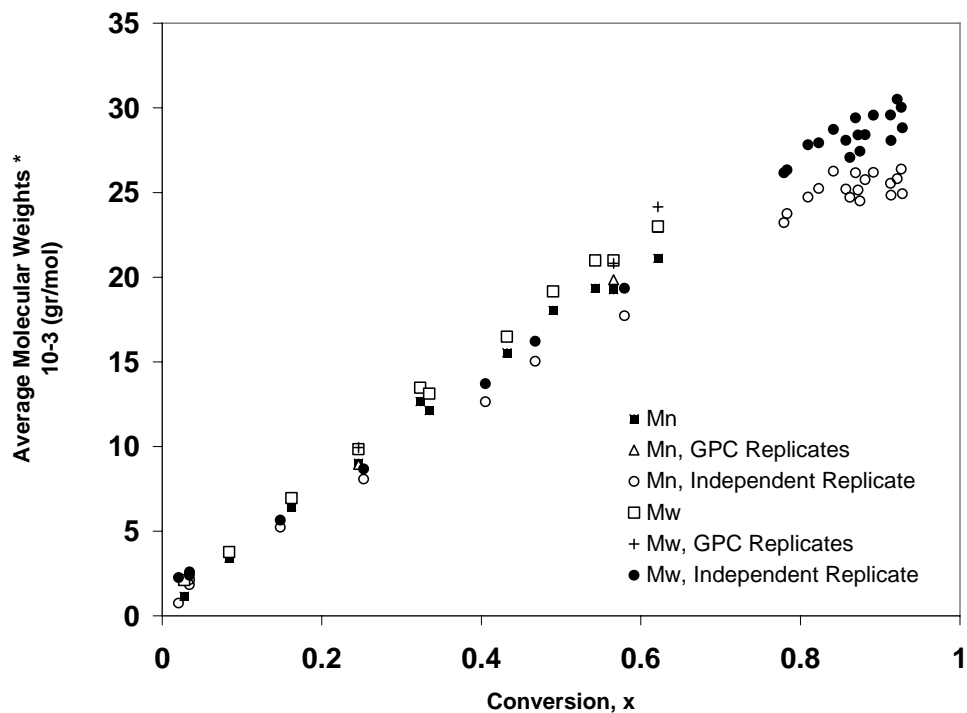


Figure B.18 Average molecular weights vs. conversion for NMRP of styrene at 130°C and $[TEMPO]/[BPO] = 1.3$

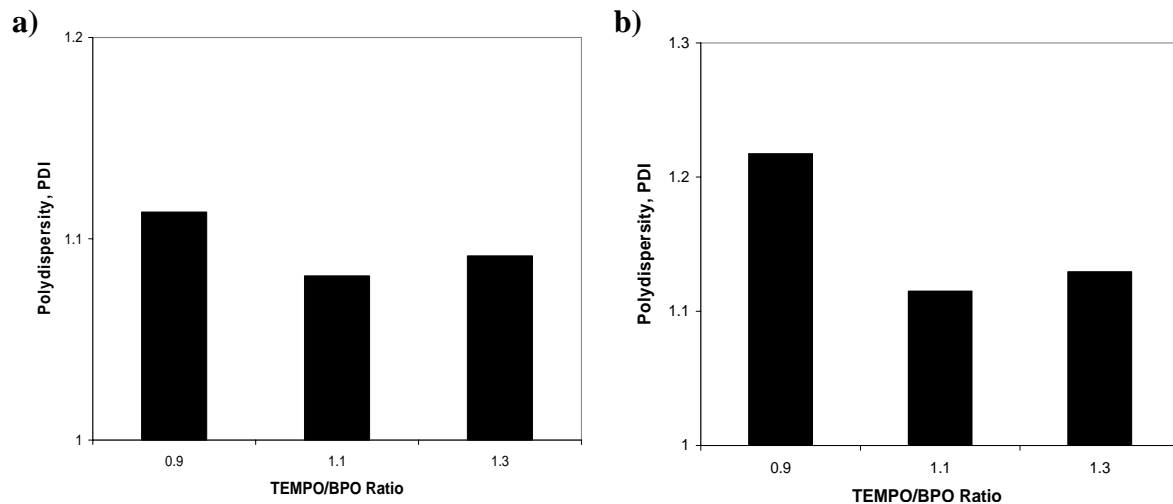


Figure B.21 Polydispersity as a function of the TEMPO/BPO ratio for NMRP of styrene a) after 8 hrs, b) after 30hrs at 130°C

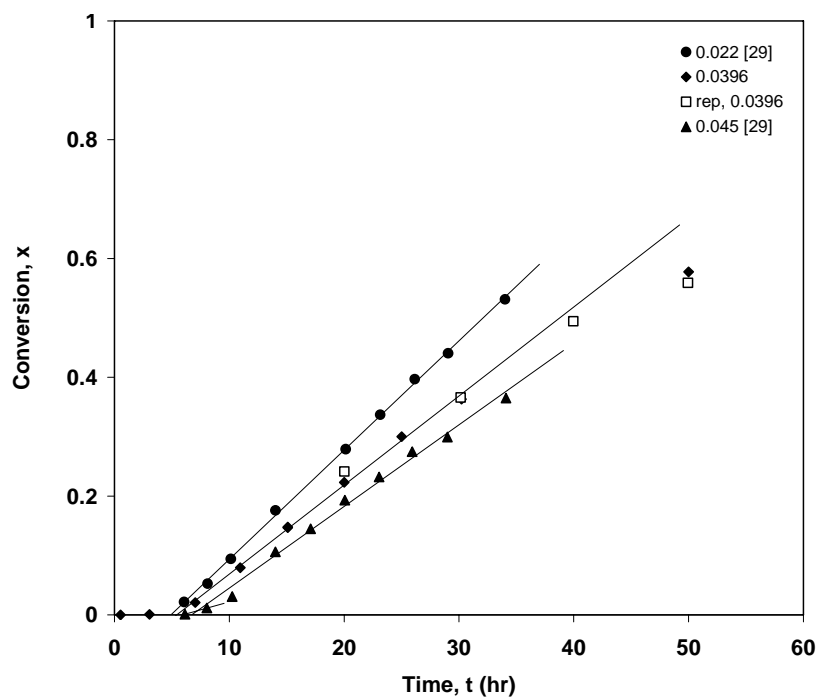


Figure B.22 Monomer conversion vs. time for thermal polymerization of styrene in the presence of TEMPO at 120°C and $[\text{TEMPO}]_0 = 0.0396$ M (compared to experimental work from Saldivar-Guerra et al. [30])

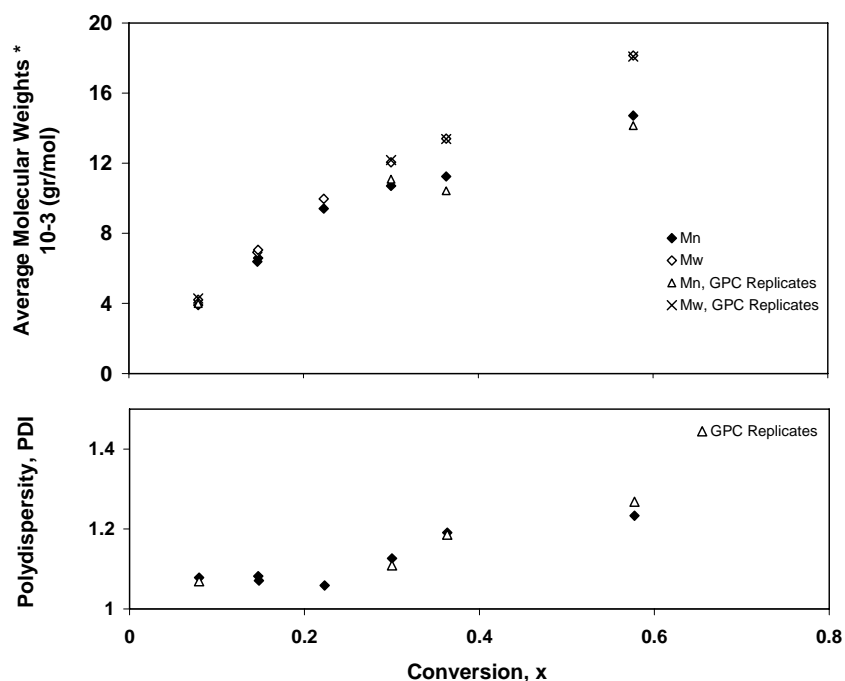


Figure B.23 Average molecular weights and polydispersity vs. conversion for thermal polymerization of styrene in the presence of TEMPO at 120°C and $[\text{TEMPO}]_0 = 0.0396 \text{ M}$

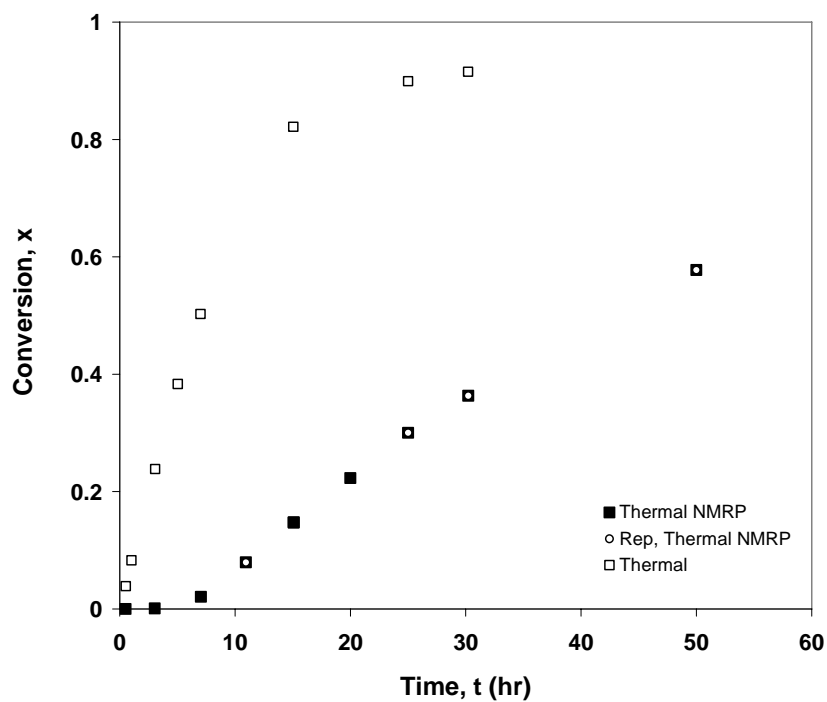


Figure B.24 Monomer conversion vs. time for: a) thermal polymerization of styrene in the presence of TEMPO with $[\text{TEMPO}]_0 = 0.0396 \text{ M}$ b) thermal styrene, at 120°C

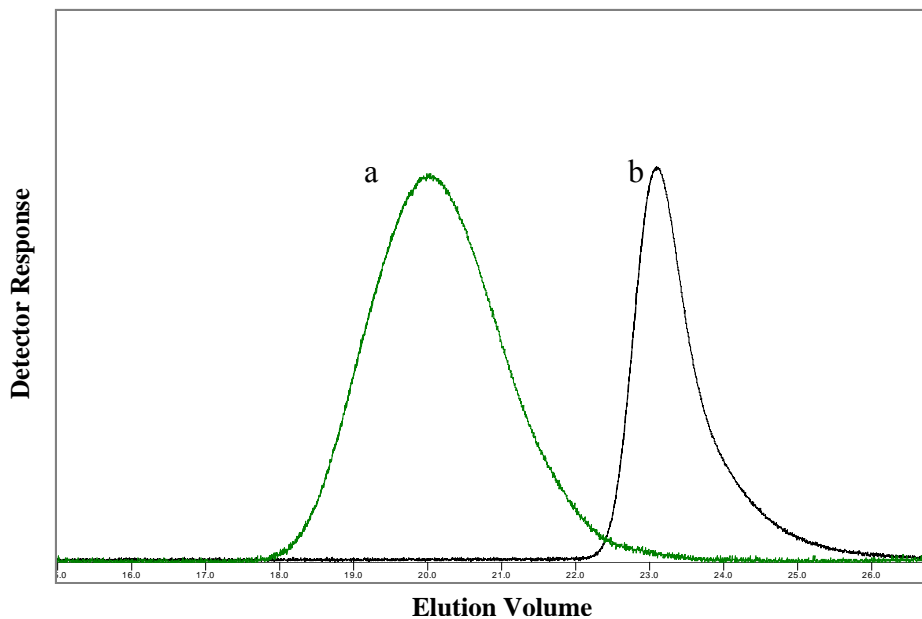


Figure B.25 Comparison of SEC Chromatograms for a) Styrene thermal polymerization b) Styrene thermal polymerization in the presence of TEMPO, at 35% conversion and 120°C

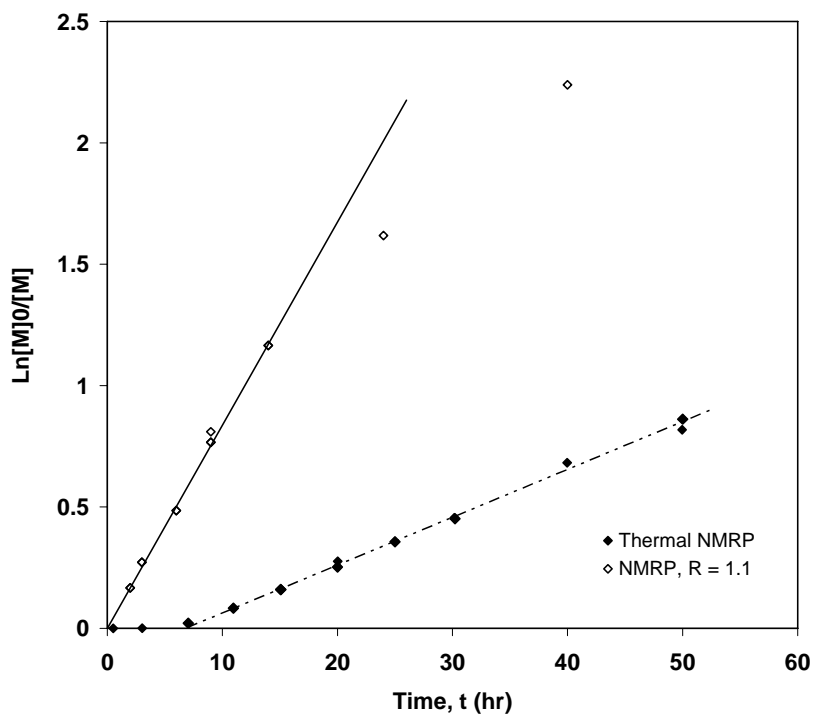


Figure B.26 Rate of polymerization presented as first order plot; comparison between thermal NMRP and NMRP with $[\text{TEMPO}]/[\text{BPO}] = 1.1$ at 120°C and $[\text{TEMPO}]_0 = 0.0396 \text{ M}$

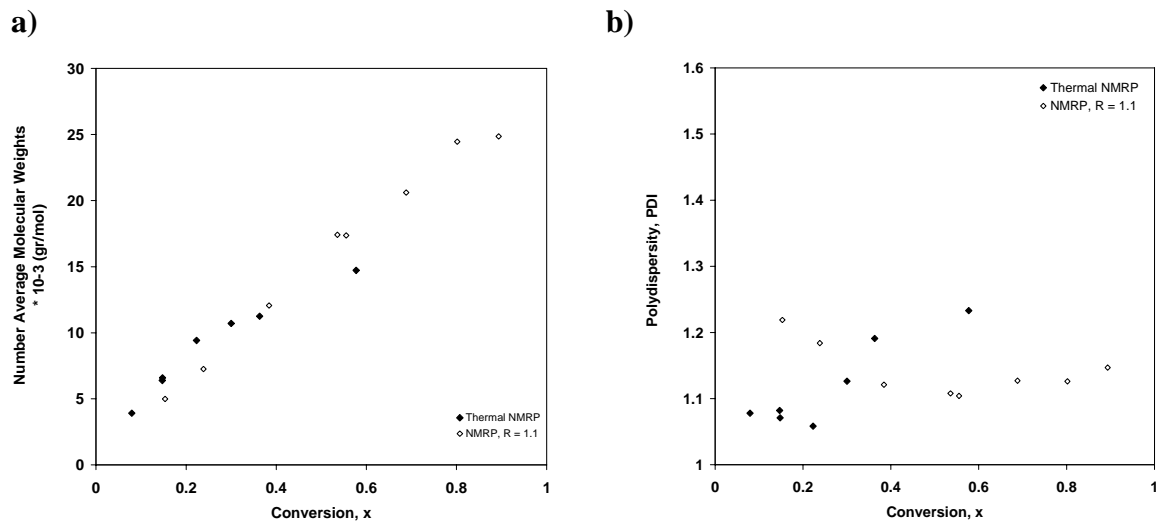


Figure B.27 Number average molecular weights (a) and polydispersities (b) vs. conversion; Comparison between thermal NMRP and NMRP with $[\text{TEMPO}]/[\text{BPO}] = 1.1$ at 120°C and $[\text{TEMPO}]_0 = 0.0396 \text{ M}$

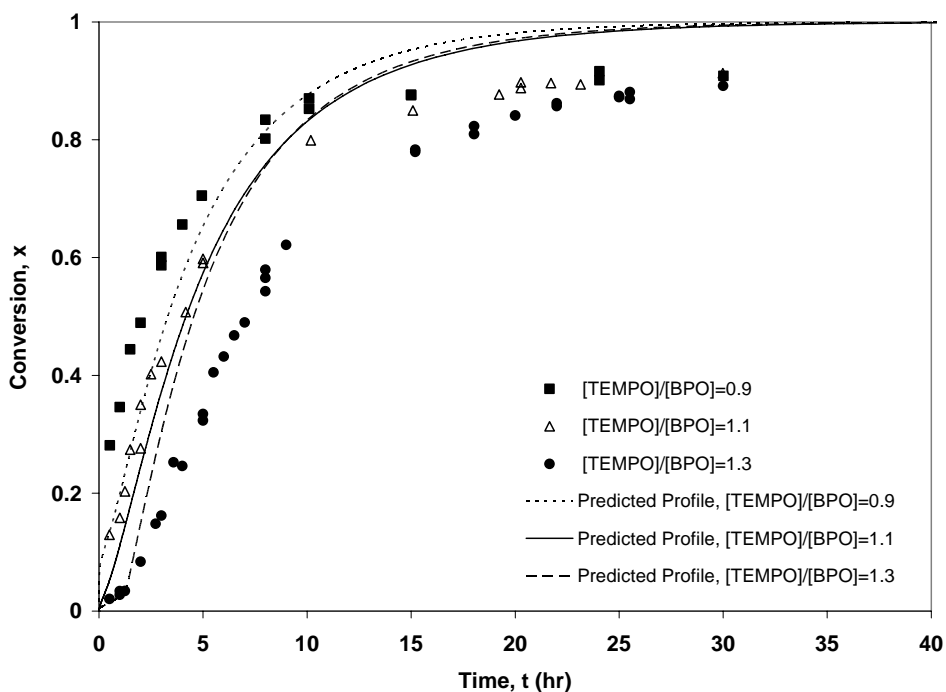


Figure B.28 Effect of $[\text{TEMPO}]/[\text{BPO}]$ ratio on polymerization rate at 130°C ; comparison of experimental data and model predictions

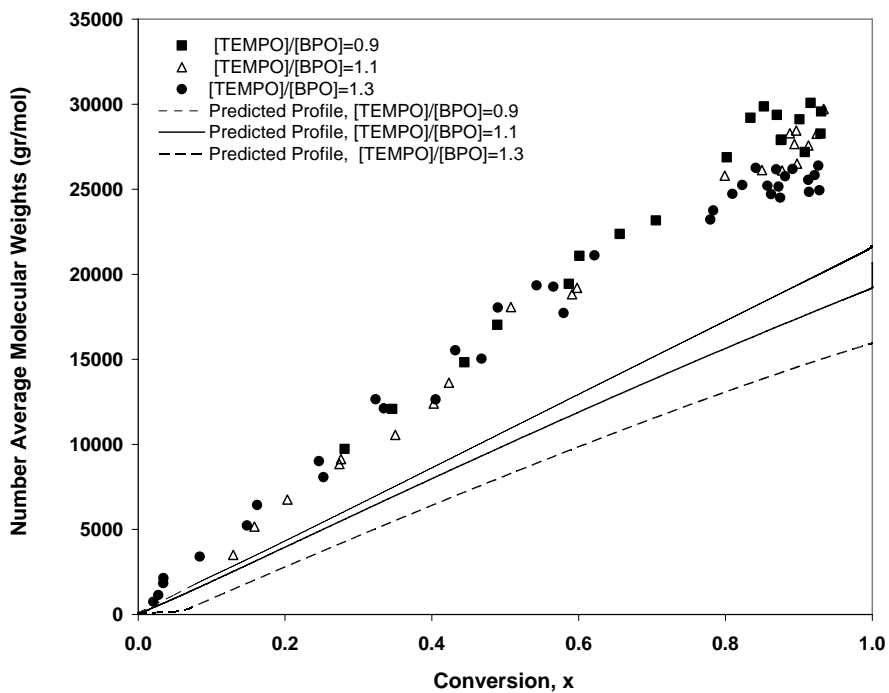


Figure B.29 Effect of $[\text{TEMPO}]/[\text{BPO}]$ ratio on number average molecular weight at 130 °C; comparison of experimental data and model predictions

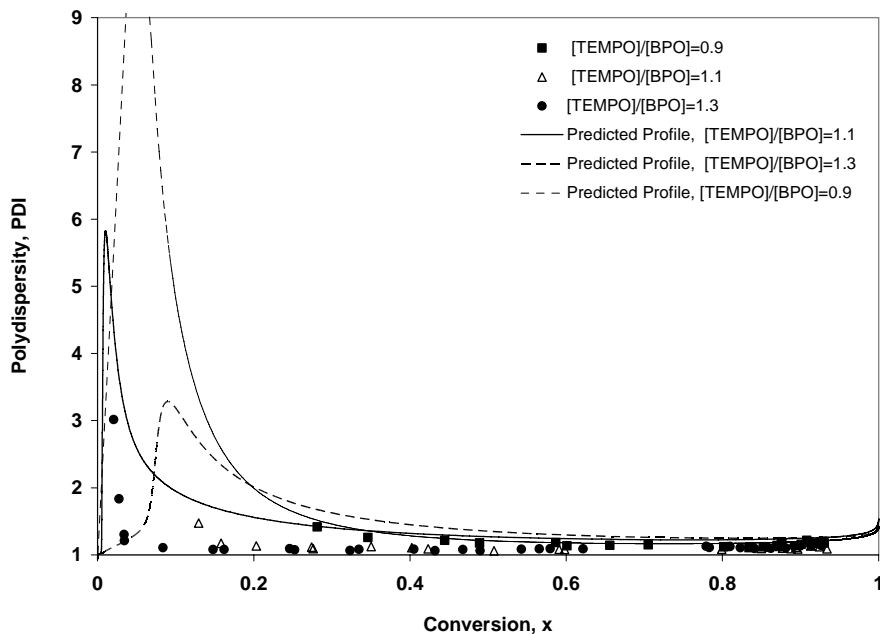


Figure B.30 Effect of $[\text{TEMPO}]/[\text{BPO}]$ ratio on polydispersity at 130 °C; comparison of experimental data and model predictions